Sr^{87}/Sr^{86} RATIOS, K/Rb RATIOS, AND RARE-EARTH ELEMENT ABUNDANCES IN PYROXENE GRANULITES

by

CHARLES MARTIN SPOONER

B.Sc. McMaster University, Hamilton, Ontario, Canada

(1965)

S.M. Massachusetts Institute of Technology, Cambridge, Massachusetts

(1967)

SUBMITTED IN PARTIAL FULFILLMENT

OF THE REQUIREMENTS FOR THE

DEGREE OF DOCTOR OF

PHILOSOPHY

at the

MASSACHUSETTS INSTITUTE OF TECHNOLOGY

June, 1969

Signature of Author.... .....
Department of Earth and Planetary Sciences,
May 16, 1969

Certified by.....
Thesis Supervisor

Accepted by.....
Chairman, Departmental Committee
on Graduate Studies

ABSTRACT

Rubidium-Strontium whole rock isotopic relationships are reported below for pyroxene granulites and charnockitic rocks from ten granulite facies terrains of world-wide distribution. The range in the Sr^{87}/Sr^{86} initial ratios is similar that that of anorthosites and continental basalts (0.703 to 0.706) and is lower than values common to granitic rocks. Published values for this ratio from Madras, and the Nilgiri charnockites, India; the Lewisian gneiss of Scotland; and the Ivory Coast, are 0.7059, 0.7023, 0.7042, and 0.7070 respectively.

LOCALITY	AGE (m.y.)*	$(Sr^{87}/Sr^{86})_o$
Kushalnagar, Mysore State, India	2618 ± 46	0.7039 ± 0.0005
Pallavaram, Madras State, India	1980 ± 124	0.7037 ± 0.0007
Salem, Madras State, India	2476 ± 115	0.7042 ± 0.0002
Okollo and Rakosi, Uganda	2629 ± 117	0.7054 ± 0.001
Pare Mountains, Tanzania	927 ± 63	0.7056 ± 0.0011
Labor Serrit, Tanzania	724 ± 8	0.7064 ± 0.0001
Kanuku Complex, Guyana	2182 ± 95	0.7018 ± 0.0011
Crane Mountain, New York	1336 ± 71	0.7025 ± 0.0025
Indian Lake, Blue Mountain, and West Canada Lakes, New York	1465 ± 85	0.7014 ± 0.0013
Westport, Ontario	1338 ± 47	0.7057 ± 0.0009

* $\lambda = 1.39 \times 10^{-11}\ y^{-1}$.

The K/Rb ratio is determined for thirty-two specimens from the localities listed above. The average K/Rb ratio is 354 for potassium contents between 0.15% and 5.0%. Compared with the Main Trend for igneous and quasi-igneous rocks previously defined, the pyroxene granulites appear to be depleted in rubidium for a given potassium content.

The rare-earth element abundance pattern is determined by instrumental neutron activation analysis for a composite of sixteen specimens of pyroxene granulite (charnockite) from the type localities in Madras and Mysore States. When normalized to the chondrite abundances, the composite shows a light rare-earth element enrichment and total rare-earth content, yttrium included, (91 ppm) which is similar to that found in gabbros and diabases. The composite has a bulk mineralogy approximating a diorite.

The results suggest that these rocks were initially of igneous origin, and subsequently underwent high grade regional metamorphism which depleted rubidium with respect to potassium.

Thesis Supervisor: Harold W. Fairbairn
Title: Professor of Geology

PART A

(Intended for Publication)

Sr^{87}/Sr^{86} Initial Ratios and Whole Rock Ages of Pyroxene Granulite

Charles M. Spooner

Massachusetts Institute of Technology
Department of Earth and Planetary Sciences
Cambridge, Massachusetts 02139

ABSTRACT

Rubidium-strontium whole-rock isotopic relationships are reported below for pyroxene granulites and charnockitic rocks from ten granulite facies terrains of world-wide distribution. The range in the Sr^{87}/Sr^{86} initial ratios is 0.701 to 0.706, similar to that of anorthosites and continental basalts, and is lower than values commonly encountered in granitic rocks. Published values for this ratio from Madras, the Nilgiri charnockites, India; the Lewisian gneiss of Scotland; and the Ivory Coast, are 0.7059, 0.7023, 0.7042, and 0.7070, respectively.

LOCALITY	AGE (m.y.)*	$(Sr^{87}/Sr^{86})_o$
Kushalnagar, Mysore State, India	2618 ± 46	0.7039 ± 0.0005
Pallavaram, Madras State, India	1980 ± 124	0.7037 ± 0.0007
Salem, Madras State, India	2476 ± 115	0.7042 ± 0.0002
Okollo and Rakosi, Uganda	2629 ± 117	0.7054 ± 0.001
Pare Mountains, Tanzania	927 ± 63	0.7056 ± 0.0011
Labor Serrit, Tanzania	724 ± 8	0.7064 ± 0.0001
Kanuku Complex, Guyana, S.A.	2182 ± 95	0.7018 ± 0.0011
Crane Mountain, New York	1336 ± 71	0.7025 ± 0.0025
Indian Lake, Blue Mountain and West Canada Lakes, N.Y.	1465 ± 85	0.7014 ± 0.0013
Westport, Ontario	1338 ± 47	0.7057 ± 0.0009

*$\lambda = 1.39 \times 10^{-11} y^{-1}$

The results suggest that these rocks were initially of igneous origin and subsequently underwent high grade regional metamorphism at the granulite facies level. The consistently low initial ratios and the relatively narrow range from 0.701 to 0.708 suggest a common source region with anorthosites in a deep-seated environment having a low Rb:Sr ratio.

INTRODUCTION

Recent studies of the rubidium-strontium isotopic variations and trace element content of material presumably of deep crustal origin have suggested that these regions may have low Sr^{87}/Sr^{86} initial ratios and are depleted in certain trace level lithophile elements [1], [2]. The widespread occurrence of rocks of the granulite facies, specifically pyroxene granulite, is being recognized with increasing frequency in the deeply eroded Precambrian shield areas throughout the world. The "dry" mineralogical assemblage, density (ca. 3.0 gm/cm^3), and association in terrains having undergone high grade regional metamorphism have suggested that pyroxene granulites and related members of the so-called charnockite series originate at deep crustal levels or perhaps in the upper mantle.

Correlations of the compressional-wave velocities of igneous rocks with their compositions indicate that about 55% of the average continental crust has a density of about 3.0 gm/cm^3 and the remaining 45% has a density of about 2.8 gm/cm^3, [3]. Inasmuch as pyroxene granulites and anorthosites have seismic velocities similar to those of mafic rocks, [4], and the velocity cannot be used to distinguish between igneous and metamorphic rocks unless high-pressure phase transformations are involved, significant quantities of these relatively dense rocks could exist at depth in the crust. If these rocks form significant portions of the lower continental crust, an investigation into the variations in their Rb:Sr ratios and Sr^{87}/Sr^{86} initial ratios is needed for an understanding of the rubidium and strontium inventory in the total crust, [5]. Collections of material

from the pyroxene granulite facies and terrains mapped as members of the charnockite series have been assembled and analyzed by isotope dilution methods for their rubidium and strontium contents and their Sr^{87}/Sr^{86} ratio. Ten localities of world-wide distribution have been studied. These include: Kushalnagar, Mysore State; Pallavaram and Salem in Madras State, India; Okollo and Rakosi, West Nile District, Uganda; Pare Mountains, Labor Serrit and Msagali, Tanzania; Kanuku complex, Guyana, South America; Crane Mountain, Indian Lake, Blue Mountain and West Canada Lake Quadrangles, New York; and the Westport map-area of Ontario.

ANALYTICAL TECHNIQUE

All the analyses were performed using a 6-inch, 60° sector, single filament, Nier-type mass spectrometer. All the strontium isotopic measurements are normalized to $Sr^{86}/Sr^{88} = 0.1194$ and all the Sr^{87}/Sr^{86} measurements are expressed relative to a value of 0.7082 ± 0.0008 (2σ at the 95% confidence level) for the Eimer and Amend $SrCO_3$ standard (see Table I). Isotopically enriched Sr^{84} and Rb^{87} spike solutions were used in the isotope dilution analyses. Seven analyses were made of the Rb^{85}/Rb^{87} ratio for unspiked rubidium extracted from the whole rock to evaluate the extent of mass spectrometer fractionation during analysis. A mean of 2.5770 ± 0.0706 (2σ at the 95% confidence level) was obtained. This value differs by about 0.8% from the value found by Shields, et al.[6]. The Rb^{87} decay constant (λ) used in calculating ages is $1.39 \times 10^{-11} y^{-1}$. All the isochrons in this study have been defined in terms of a

TABLE I

Replicate Analyses of E and A Isotopic Standard

Date	$(Sr^{86}/Sr^{88})_{measured}$	$(Sr^{87}/Sr^{86})_{normalized}$
29 Nov/67	0.1187	0.7083
30 Jan/68	0.1204	0.7085
10 Aug/68	0.1198	0.7086
7 Nov/68	0.1207	0.7088
22 Nov/68	0.1202	0.7082
20 Jan/69	0.1199	0.7076
8 May/69	0.1188	0.7082

$(Sr^{86}/Sr^{88})_{mean}$	$(Sr^{87}/Sr^{86})_{mean}$
0.1199	$0.7083 \pm 0.0004^{2} \pm 0.0008^{4}$*

* these are the σ and 2σ (i.e., 68.27% and 95.45% confidence levels)

least-squares regression method following York [7].

ANALYTICAL RESULTS

Madras and Mysore States, India

The geology and petrography of these type localities is presented in the classic memoir of Sir Thomas Holland [8]. Since his original description of the charnockite series, numerous reinterpretations for the origin of these rocks have appeared, and those prior to 1950 are summarized by Quensel [9].

At Salem in Madras State, the specimens analyzed correspond closely in mineralogy and location originally described by Holland, op.cit., p. 181. The results are shown in Figure 1. An age of 2476 $\pm$ 115 m.y. is obtained with an initial ratio of 0.7042 $\pm$ 0.0002.

At Kushalnagar, nine specimens were analyzed (Figure 2) and a Sr^{87}/Sr^{86} initial ratio of 0.7039 $\pm$ 0.0005 was obtained. Although the specimens from this locality did not have sufficient variation in the Rb/Sr ratio to construct a satisfactory isochron, the present results, which define the initial ratio, have been included with those previously determined by Crawford [10], and an age of 2618 $\pm$ 46 is obtained for a total of fifteen analytical points. Two specimens from Pallavaram (R7205 and R7240) give a younger age of 1980 $\pm$ 124 m.y. assuming the same initial ratio of 0.7039 $\pm$ 0.0005 found for the Kushalnagar specimens.

These analyses confirm the general grouping of ages in this region around 2500 m.y. as reported in recent studies by Crawford [10] and Aswathanarayana [11] and others.

FIGURE 1

SALEM, MADRAS

ISOCHRON

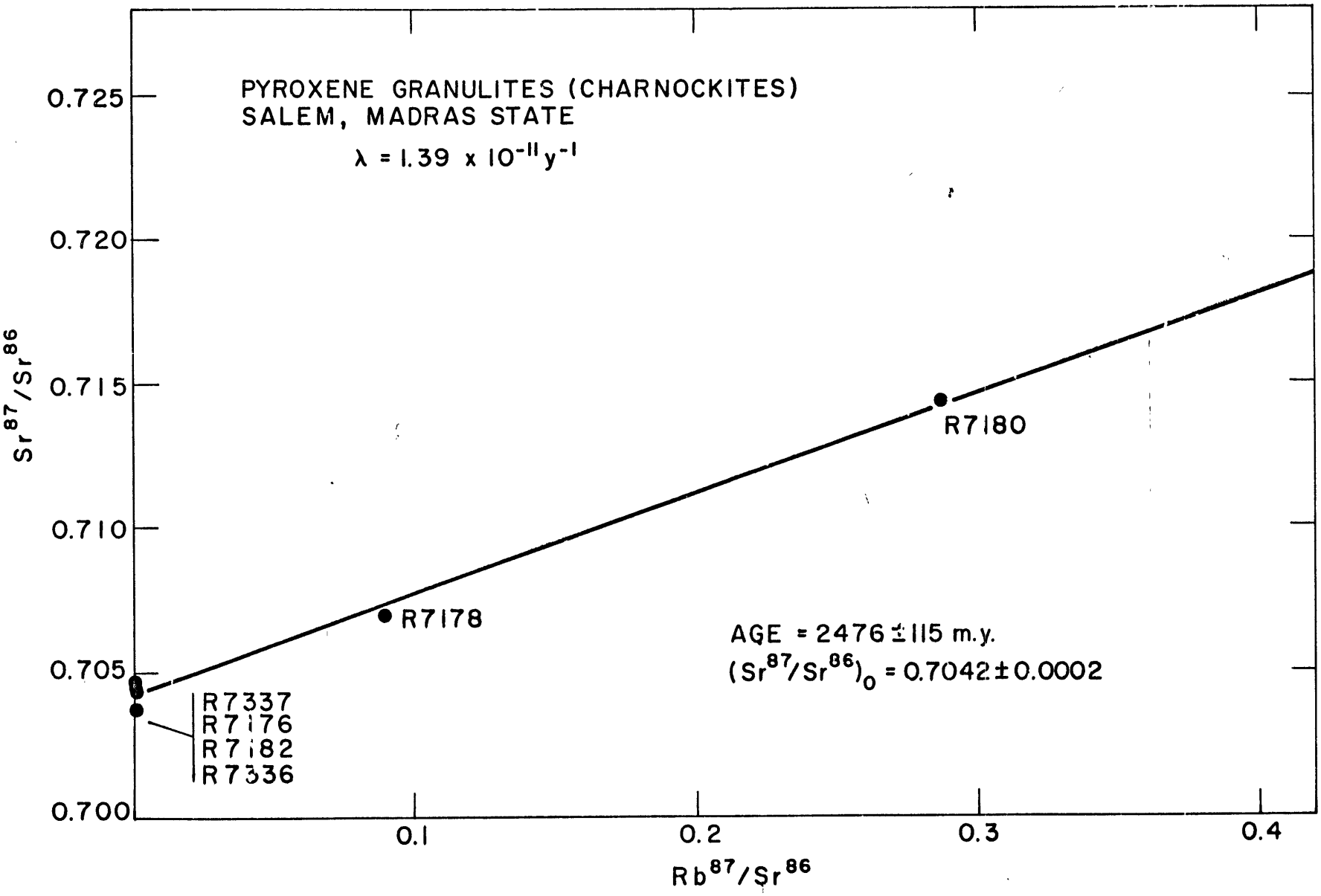
PYROXENE GRANULITES (CHARNOCKITES)
SALEM, MADRAS STATE
λ = 1.39 x 10⁻¹¹ y⁻¹
0.725
0.720
0.715
0.710
0.705
0.700
Sr⁸⁷/Sr⁸⁶
R7180
R7178
R7337
R7176
R7182
R7336
AGE = 2476 ± 115 m.y.
(Sr⁸⁷/Sr⁸⁶)₀ = 0.7042 ± 0.0002
0.1
0.2
0.3
0.4
Rb⁸⁷/Sr⁸⁶

FIGURE 2

KUSHALNAGAR, MYSORE

STATE

ISOCHRON

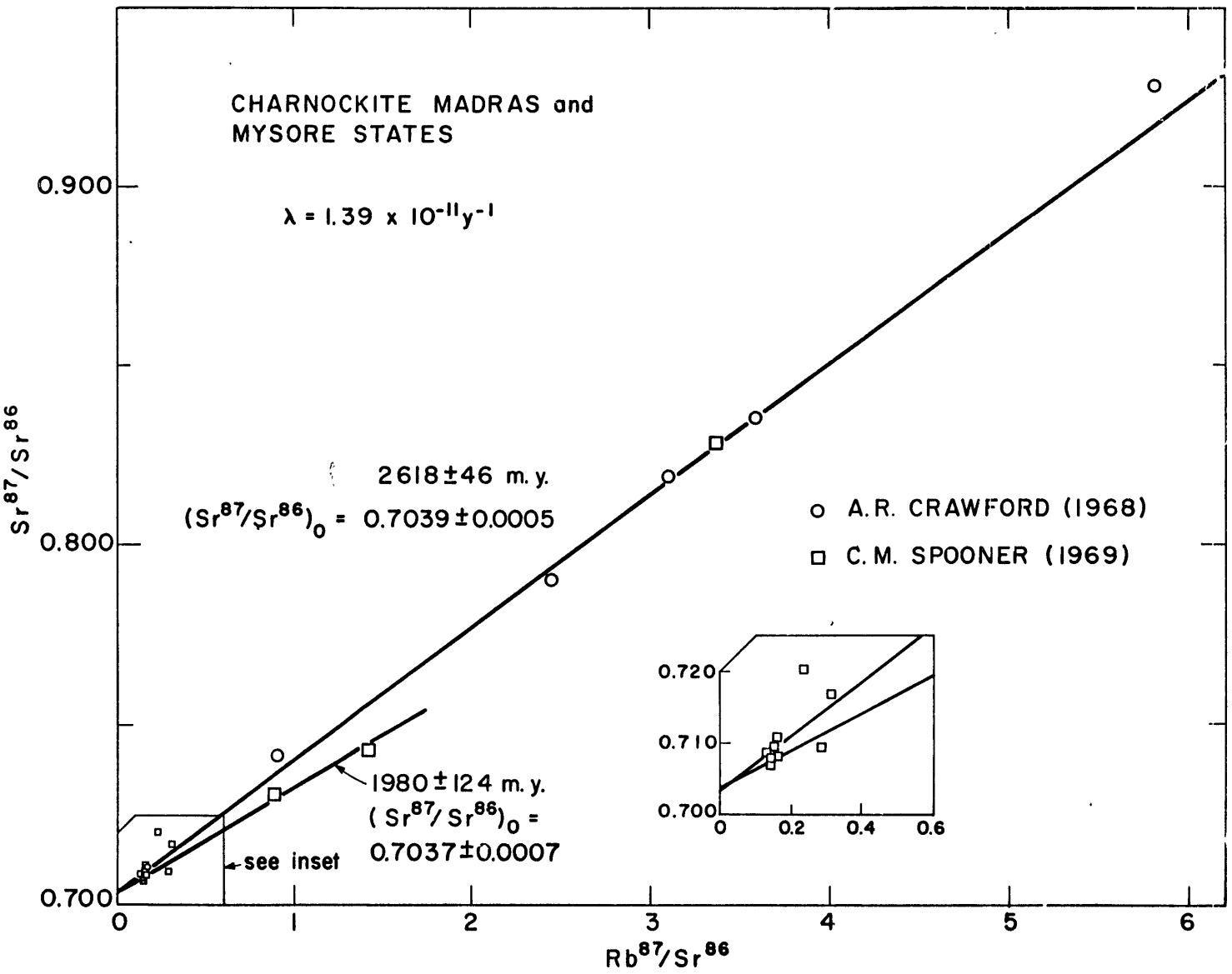
CHARNOCKITE MADRAS and
MYSORE STATES
λ = 1.39 x 10⁻¹¹y⁻¹
2618±46 m.y.
(Sr87/Sr86)0 = 0.7039±0.0005
A.R. CRAWFORD (1968)
C.M. SPOONER (1969)
1980±124 m.y.
(Sr87/Sr86)0 =
0.7037±0.0007
see inset
0.900
0.800
0.700
0
1
2
3
4
5
6
Sr87/Sr86
Rb87/Sr86
0.720
0.710
0.700
0
0.2
0.4
0.6

FIGURE 3

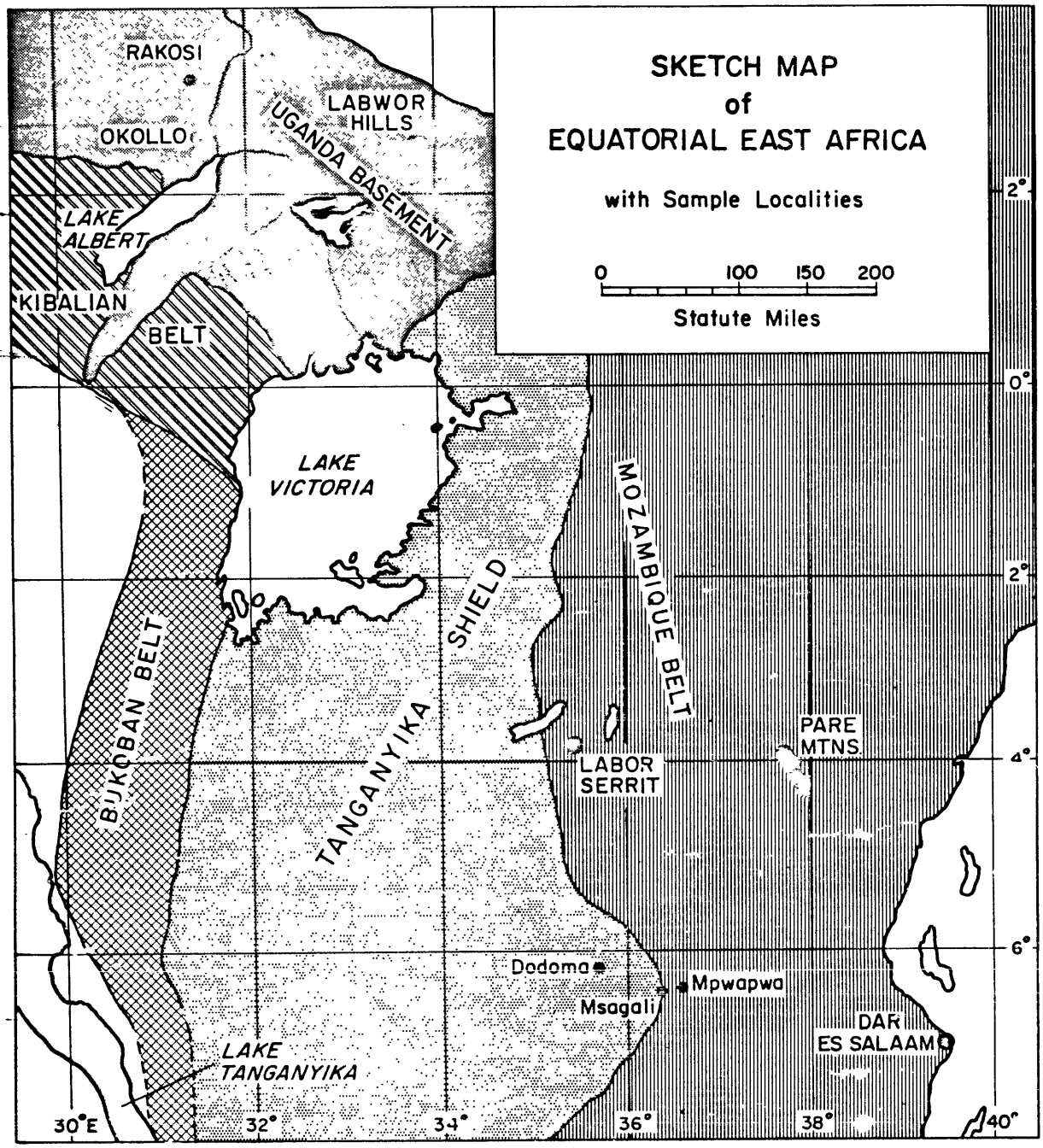
SKETCH MAP
of
EQUATORIAL EAST AFRICA
with Sample Localities
0 100 150 200
Statute Miles
RAKOSI
OKOLLO
LABWOR HILLS
UGANDA BASEMENT
LAKE ALBERT
KIBALIAN
BELT
LAKE VICTORIA
MOZAMBIQUE BELT
SHIELD
BUKOBAN BELT
TANGANYIKA
LABOR SERRIT
PARE MTNS
Dodoma
Mpwapwa
Msagali
DAR ES SALAAM
LAKE TANGANYIKA
2°
0°
2°
4°
6°
30°E
32°
34°
36°
38°
40°

An analysis of a composite of sixteen specimens described in the field as intermediate-to-acid "charnockites" from Madras and Mysore States for the rare-earth elements shows an enrichment of the light rare-earth elements when each is normalized to its chondrite abundance. The total rare-earth content, including yttrium, is 91 ppm. The details of this rare-earth pattern will be published elsewhere.

Okollo and Rakosi, West Nile District, Uganda, and the Pare Mountains and Labor Serrit Areas of Tanzania

The granulite facies rocks of Okollo and Rakosi were assigned originally to the "Basement Complex" by Groves [12]. Recent field studies by Hepworth [13] have suggested a tripartition of these ancient rocks into the amphibolite grade Western Grey Gneiss, the Eastern Grey Gneiss and the higher grade Granulite Group. These names are synonomous with Macdonald's [21] subdivisions: "Aruan", "Mirian", and "Watian". On the basis of photo-geological interpretation, these groups appear to extent throughout northeast and north-central Uganda. The Granulite Group is recognized in this region on the basis of the typomorphic mineral assemblage peculiar to the granulite facies. To the north, at Rakosi, an aplitic granulite, characterized by a leucocratic medium-to fine-grained texture, is included as an integral part of the Granulite Group. Similar associations of this rock type with more intermediate charnockitic granulites have been found in other localities throughout the world (i.e., the Madras, India charnockite series).

A suite of firty-five specimens was collected by Dr. H. W.

FIGURE 4

OKOLLO & RAKOSI

WEST NILE DISTRICT, UGANDA

ISOCHRON

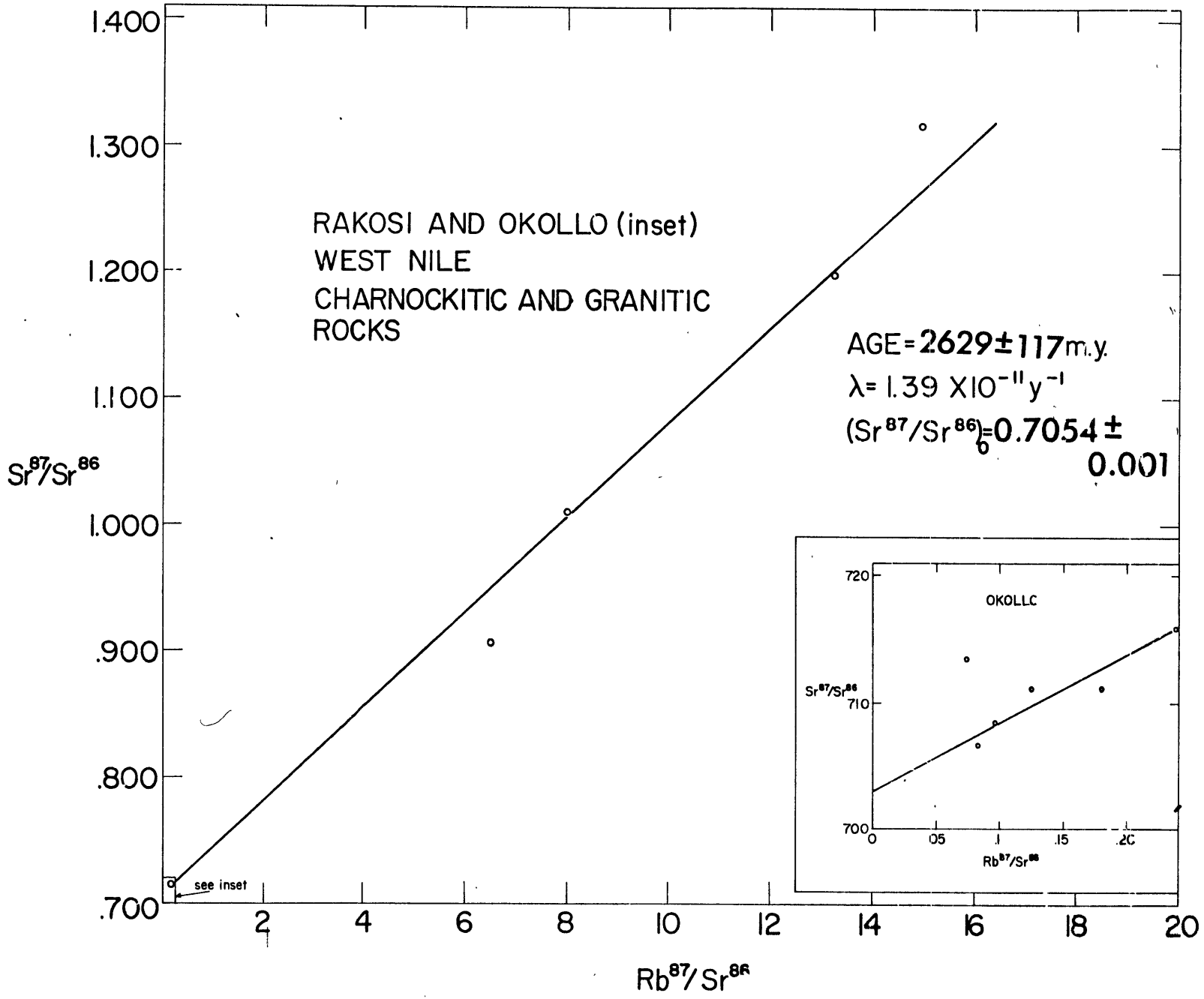
RAKOSI AND OKOLLO (inset)
WEST NILE
CHARNOCKITIC AND GRANITIC ROCKS
AGE = 2629 ± 117 m.y.
λ = 1.39 X10⁻¹¹ y⁻¹
(Sr87/Sr86)o = 0.7054 ± 0.001
see inset
OKOLLC
Sr87/Sr86
Rb87/Sr86
1.400
1.300
1.200
1.100
1.000
.900
.800
.700
2
4
6
8
10
12
14
16
18
20
720
710
700
0
05
1
15
2C

FIGURE 5

MSAGALI, TANZANIA

ISOCHRON

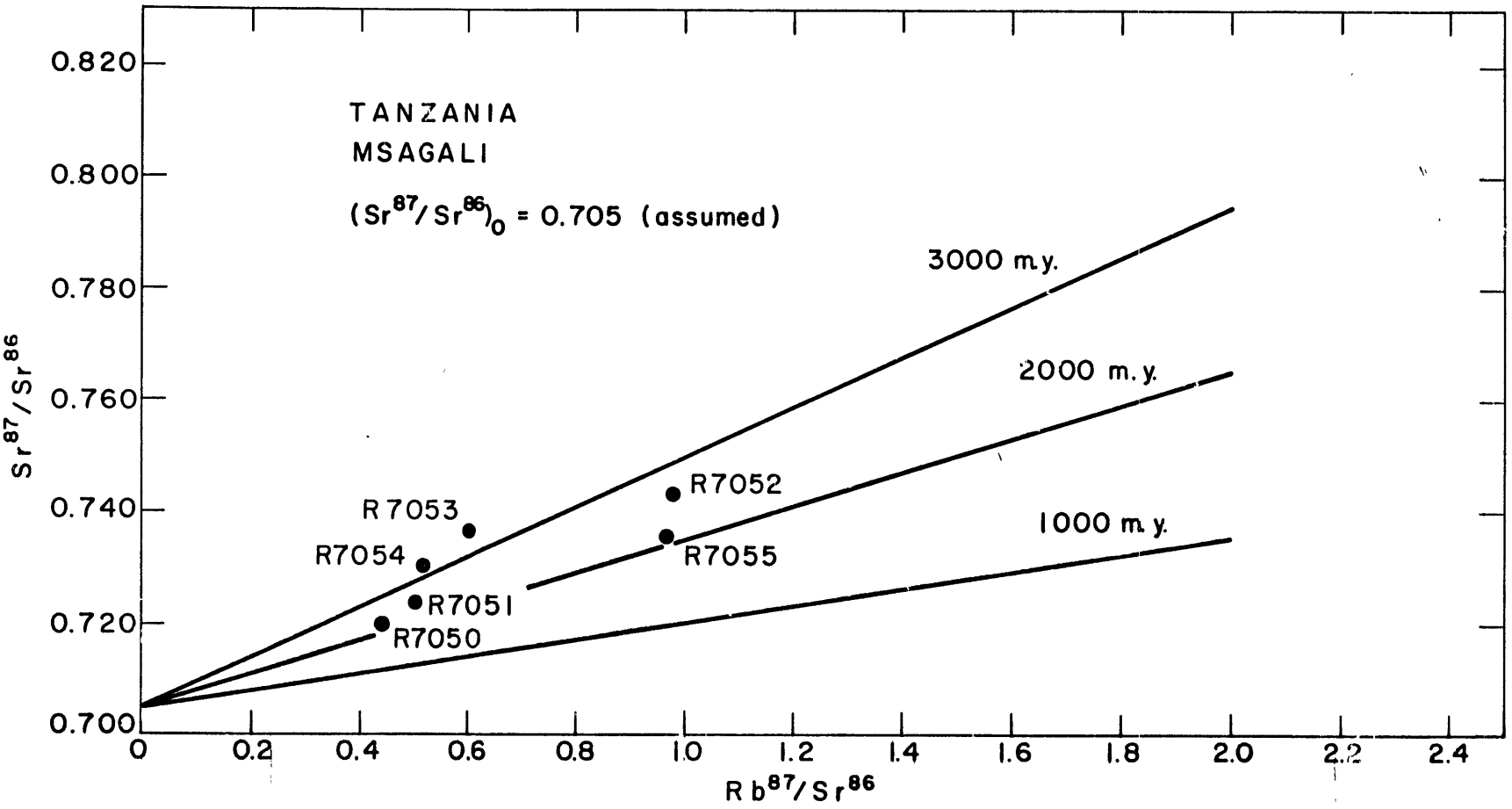
TANZANIA
MSAGALI
$(Sr^{87}/Sr^{86})_0$ = 0.705 (assumed)
3000 m.y.
2000 m.y.
1000 m.y.
R7052
R7053
R7055
R7054
R7051
R7050
0.820
0.800
0.780
0.760
0.740
0.720
0.700
Sr^{87}/Sr^{86}
0
0.2
0.4
0.6
0.8
1.0
1.2
1.4
1.6
1.8
2.0
2.2
2.4
Rb^{87}/Sr^{86}

Fairbairn during the summer of 1967, from which ten were chosen for isotopic analysis on the basis of their Rb/Sr ratios.

An isochron plot of the analyses gives an age of 2629 ± 117 m.y. with an initial ratio of 0.7054 ± 0.001 (Figure 4). Hepworth [13] has reported some retrograde metamorphism which is especially evident in the aplitic granulites and may explain the scatter in the Rakosi analytical points. A biotite age (K:Ar) of 660 ± 25 m.y has been reported by Cahen and Snelling [14] from Okollo.

Mpwapwa is situated in central Tanzania between Dar es Salaam and Dodoma in the south-central portion of Quarter Degree Sheet 163 (see Figure 3). The area has been restudied by J. V. Hepworth, Institute of Geological Sciences, London, during the course of an investigation into the nature of the boundary between the Mozambique Orogenic Belt and the Tanganyika Shield. The specimens analyzed were taken from a disused railway ballast quarry located in a transitional region between the Shield and the generally north-south trending Unsagaran System of the Mozambique Belt, that is, between the sheared edge of the batholithic granite and the fairly high-grade metasedimentary rocks (epi[?]-amphibolite facies) of Unsagaran System.

All six samples submitted were analyzed isotopically (Figure 5) and it is apparent that these specimens do not define an isotopically closed system. If an initial ratio of 0.705 is assumed, then a rather crude "age" of about 2500 m.y. is indicated. Two previous age determinations reported previously from this same quarry give disparate results also. Kulp and Engels [15], using biotite separates, obtained

ages of 475 ± 80 m.y. (Rb:Sr) and 3600 ± 100 m.y. (K:Ar).

The Pare Mountains and the Labor Serrit area (see map, Figure 3) form part of a vast complex of granulite that has only been partially mapped. The granulites, which are surrounded by lower grade biotite and hornblende gneisses and volcanic rocks, are a major structural unit consisting of gently plunging and dipping stratiform-like sheets that appear to have undergone only minimal deformation and metamorphism [16].

The granulites have been regarded as members of the "Mozambique Orogenic Belt" and age determinations were expected to be in the neighborhood of 450 to 600 m.y. Recently, however, there has been speculation that these rocks may be related to the older Tanganyikan Shield to the west. Five specimens were provided by J. V. Hepworth from the Pare Mountains and three from Labor Serrit:

	Age (m.y.)	$(Sr^{87}/Sr^{86})_o$
Pare Mountains	927 ± 63	0.7056 ± 0.0011
Labor Serrit	724 ± 8	0.7064 ± 0.0001

Admittedly, there are too few analyses over this vast area to arrive at any firm conclusion. The minimum age, however, is greater than the Mozambiquian Orogeny (450 to 600 m.y.). The possibility exists that the granulite analyzed here may be an eastern extension of the granulite and amphibolite facies of the Tanganyikan Shield that was affected by a later episode of metamorphism.

Kanuku Complex, Guyana, South America

The Kanuku Complex and adjacent South Savanna Group occupy a major portion of the southern half of Guyana and are part of the Guiana Shield which covers a large part of northern Brazil and Venezuela (see Figure 6). The major rock types of the Kanuku Complex are a variety of high-grade acid biotite gneisses in which are found enclaves of acid and basic granulite. The regional geology of this and adjacent groups is discussed by Williams et al. [16]. Singh [17] has demonstrated an intrusive relation of the presumably younger South Savanna granites with both the Kanuku Complex and the lower grade Marudi Group of metasedimentary rock of the greenschist and amphibolite facies. The emplacement also involved extensive assimilation and contact metamorphism followed by a phase of post-crystalline shearing along northeast-southwest zones. Though of low abundance, orthopyroxene-bearing acid granulites (distinct from the gneisses above) occur in association with quartzo-feldspathic granulites, acid garnet-granulites, acid cordierite-granulites, and alaskites. Singh ascribes the origin of the highest grade assemblage to the strong recrystallization of the acid biotite gneisses at high temperatures and pressures. Hybridization by norite granulites is thought to have been responsible for the random occurrence of the pyroxene-rich acid granulites in the acid granulite terrain.

Despite the difficulty of access and the reconnaissance nature of mapping in this geologically complex region, numerous age determinations have been made by K:Ar, Rb:Sr, and U:Th:Pb methods. A

FIGURE 6

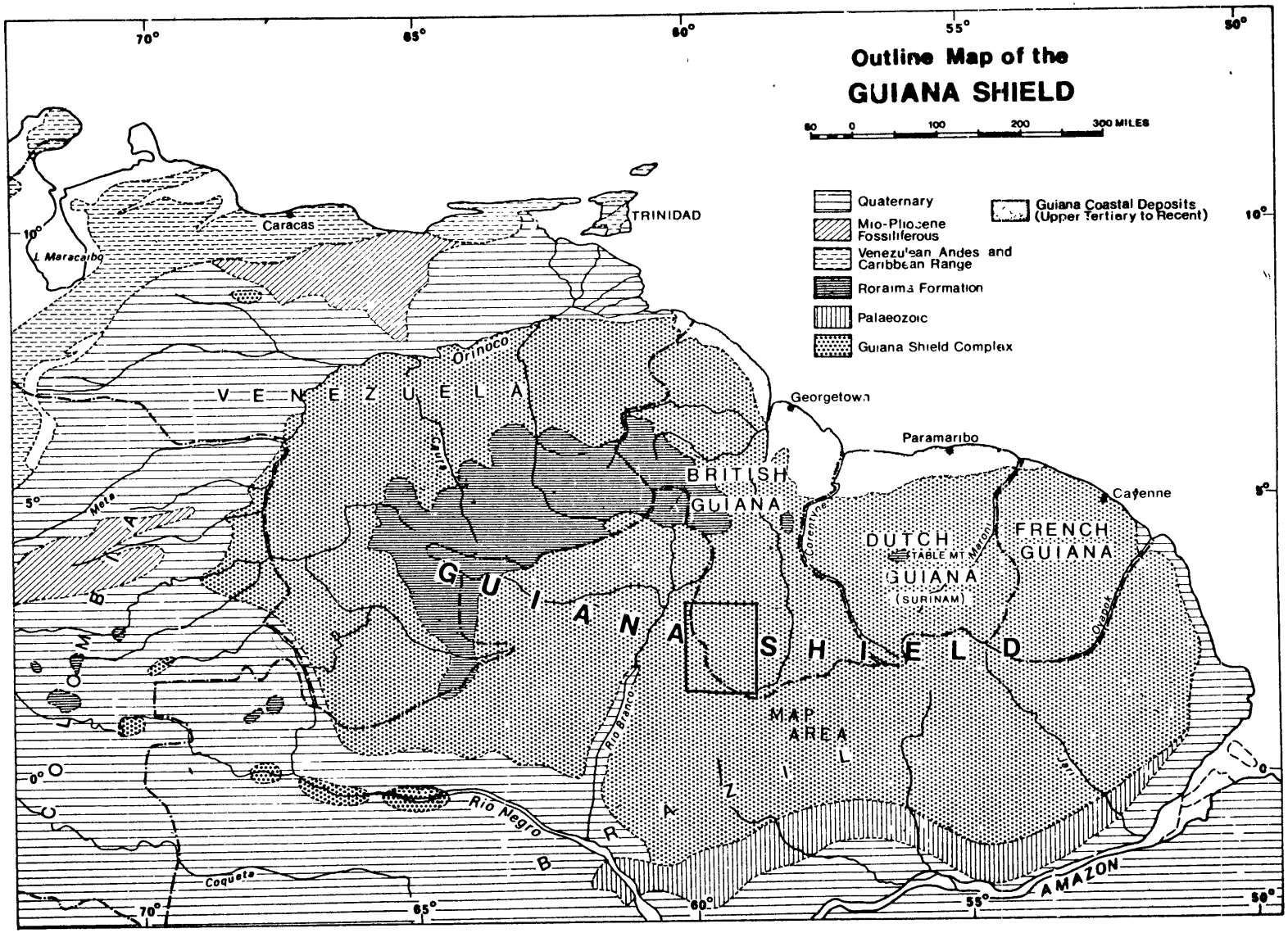
Outline Map of the
GUIANA SHIELD
80 0 100 200 300 MILES
Quaternary
Mio-Pliocene Fossiliferous
Venezuelan Andes and Caribbean Range
Roraima Formation
Palaeozoic
Guiana Shield Complex
Guiana Coastal Deposits (Upper Tertiary to Recent)
70°
65°
60°
55°
50°
10°
5°
0°
Caracas
TRINIDAD
L. Maracaibo
Orinoco
VENEZUELA
Georgetown
Paramaribo
Cayenne
BRITISH GUIANA
DUTCH GUIANA (SURINAM)
FRENCH GUIANA
TABLE MT
Courantyne
Maroni
Oyapock
GUIANA SHIELD
MAP AREA
COLOMBIA
Meta
Rio Branco
Rio Negro
BRAZIL
Coquete
AMAZON

TABLE II

Age Determinations on the Kanuku Complex and South Savanna Group, Guyana, South America*

Sample	Rock Type and Locality	Age (m.y.)
Biotite	South Savanna Granite, 1 mile SE of Shiwirtau, South Savanna	1190 ± 45, K:Ar
Biotite	South Savanna Granite, Tabtau facies, Tabtau Mountain, South Savanna	1300 ± 50, K:Ar
Biotite	South Savanna Granite, strongly cataclased biotite porphyry	1256 ± 50, K:Ar
Muscovite	South Savanna Granite, Rewa River	1720 ± 70, K:Ar
Biotite	South Savanna Granite, same locality	1685 ± 70, K:Ar
Biotite	Biotite schist in S. Savanna Granite	1545 ± 60, K:Ar
Biotite	South Savanna Granite, near Awariwau	1355 ± 55, K:Ar
Biotite	South Savanna Granite, Bat Mountain	1320 ± 50, K:Ar
Plagioclase	Diabase dike cutting South	450 ± 25, K:Ar
Pyroxene	Savanna Granite	450 ± 40, K:Ar
Whole Rock	South Savanna Granite, seven analyses Initial ratio 0.7073 [Snelling and McConnell, in press]	1880 ± 100, Rb:Sr
Monazite	South Savanna Granite, eluvial origin [A. G. Darnley, Geological Survey of Great Britain]	2270 ± 185, U:Th:Pb

*by Age Determination Unit, Institute of Geological Science, at Department of Geology and Mineralogy, Oxford University.

summary of available data is given below. Williams et al. [16] have placed the Kanuku and South Savanna Groups as well as the lower metamorphic grade Marudi Group into the Rapununi Assemblage to form a Southern structural province. An east-west rift valley about 100 miles long and 30 miles wide provides a profound structural break separating the northern structural province from the south. As this rift, which continues as a fault zone to the east-northeast into Surinam, precludes field correlations of the north and south portions of Guyana, age determinations are essential to relate the two regions.

In the present study, six samples were analyzed, and an age of 2182 $\pm$ 95 m.y. was obtained with an initial ratio of 0.7018 $\pm$ 0.0011. This age for the Kanuku complex, and the age of 1880 $\pm$ 100 m.y. for the South Savanna granite, is consistent with the intrusive relation proposed for the latter by Singh [17], (Figure 7).

Adirondack Highlands, New York and the Westport Map-area, Ontario

In this study suites of pyroxene granulites were collected by the author from two localities in the Grenville province (Figure 8). Although the rocks in each of these areas have developed the requisite mineralogy for classification in the pyroxene granulite subfacies, totally different origins have been proposed for them. Simply stated, the anorthosites and pyroxene granulites of the central Adirondacks have been interpreted by Buddington [18] and others to be of igneous origin, whereas the granulite terrain of the Westport area has been interpreted by Wynne-Edwards [19] to be of sedimentary origin, resulting

FIGURE 7

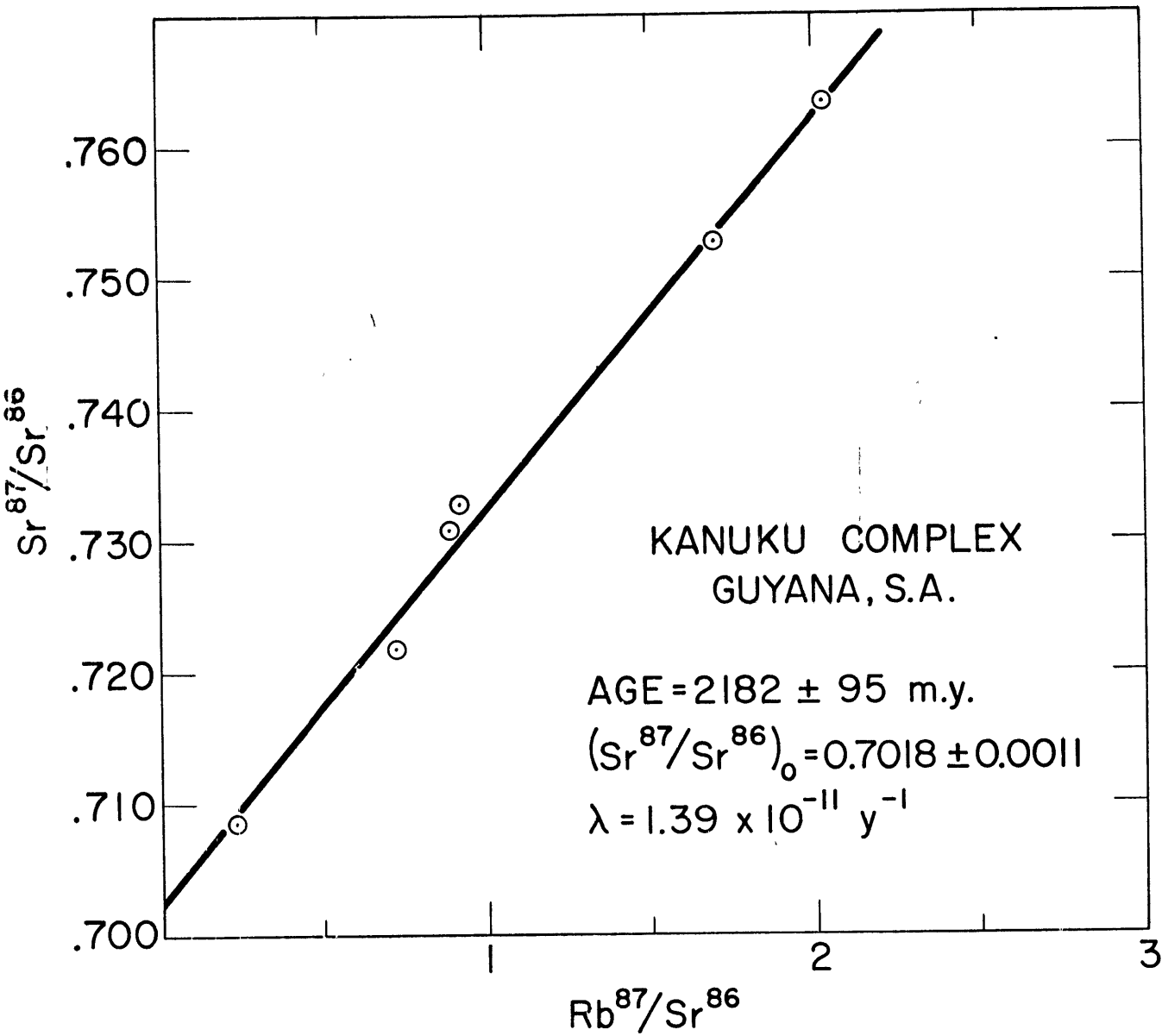
.760
.750
.740
.730
.720
.710
.700
Sr^{87}/Sr^{86}
1
2
3
Rb^{87}/Sr^{86}
KANUKU COMPLEX
GUYANA, S.A.
AGE = 2182 ± 95 m.y.
$(Sr^{87}/Sr^{86})_0 = 0.7018 \pm 0.0011$
$\lambda = 1.39 \times 10^{-11}\ y^{-1}$

from the metamorphism of a sequence of greywackes. Buddington [18] p. 197 et seq. and earlier workers favor an intrusive origin for the plutonic complex into the older Grenville metasediments, followed by later regional high-grade metamorphism during the Grenville orogeny.

Walton and deWaard [20] on the other hand, have observed remarkable continuity of a single marble unit in contact with the anorthosite, and "charnockitic"-quartz-syenite-gneisses which persists for over 80% of the exposed contact. They propose that this continuity is the result of the deposition of the marble as a basal supracrustal unit followed by the succeeding units which show a similar stratigraphic coherence upon a complex older basement of meta-igneous rock. Subsequently, both basement and cover rocks were involved in an intensive deformation involving plastic remobilization, giving rise to the complex structural picture now observed. Walton and deWaard propose that this later metamorphic event, the Grenville orogeny, gave rise to the pyroxene granulite (subfacies) assemblage.

Relatively few age determinations are available for this large, complex area. Hills and Gast [21] have reported a Rb-Sr whole rock age of 1092 $\pm$ 20 m.y. for pyroxene-hornblende granite gneisses from the Lake George Village pluton. An analysis of two feldspars from a pegmatite in aluminous paragneiss gave an age of 1060 $\pm$ 75 m.y. with an initial ratio of 0.7159. These ages are in agreement with both K:Ar and Rb:Sr ages reported by Doe [22] and Lowden et al. [23] for other areas of the Grenville province. Heath [1] reports an age of 1055 $\pm$ 31 m.y. for a large pyroxene-hornblende quartz syenite body north of the main Adirondack anorthosite massif.

FIGURE 8

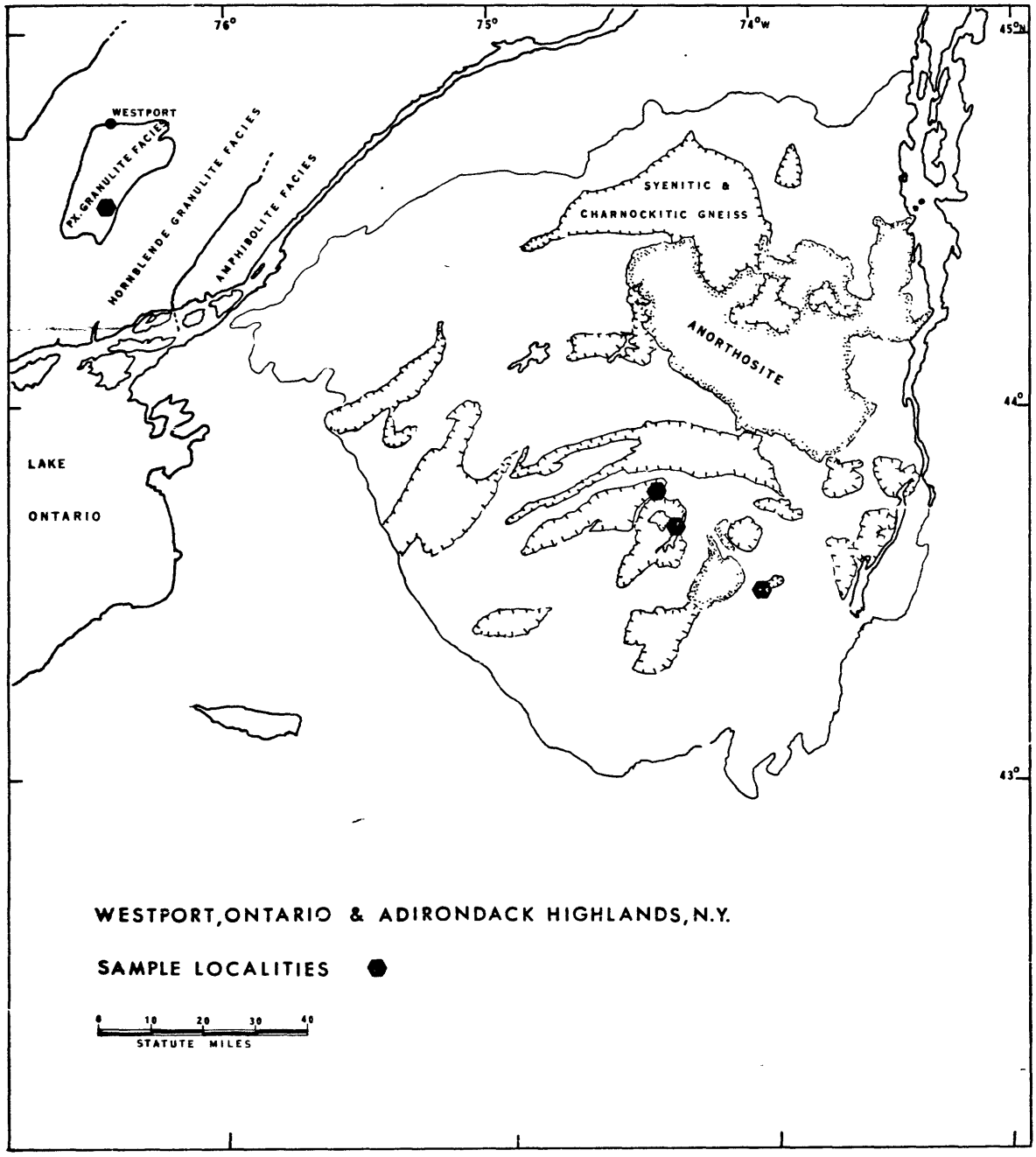
76°
75°
74°W
45°N
44°
43°
WESTPORT
PX. GRANULITE FACIES
HORNBLENDE GRANULITE FACIES
AMPHIBOLITE FACIES
SYENITIC &
CHARNOCKITIC GNEISS
ANORTHOSITE
LAKE
ONTARIO
WESTPORT, ONTARIO & ADIRONDACK HIGHLANDS, N.Y.
SAMPLE LOCALITIES
0 10 20 30 40
STATUTE MILES

FIGURE 9

CRANE MOUNTAIN, NEW YORK

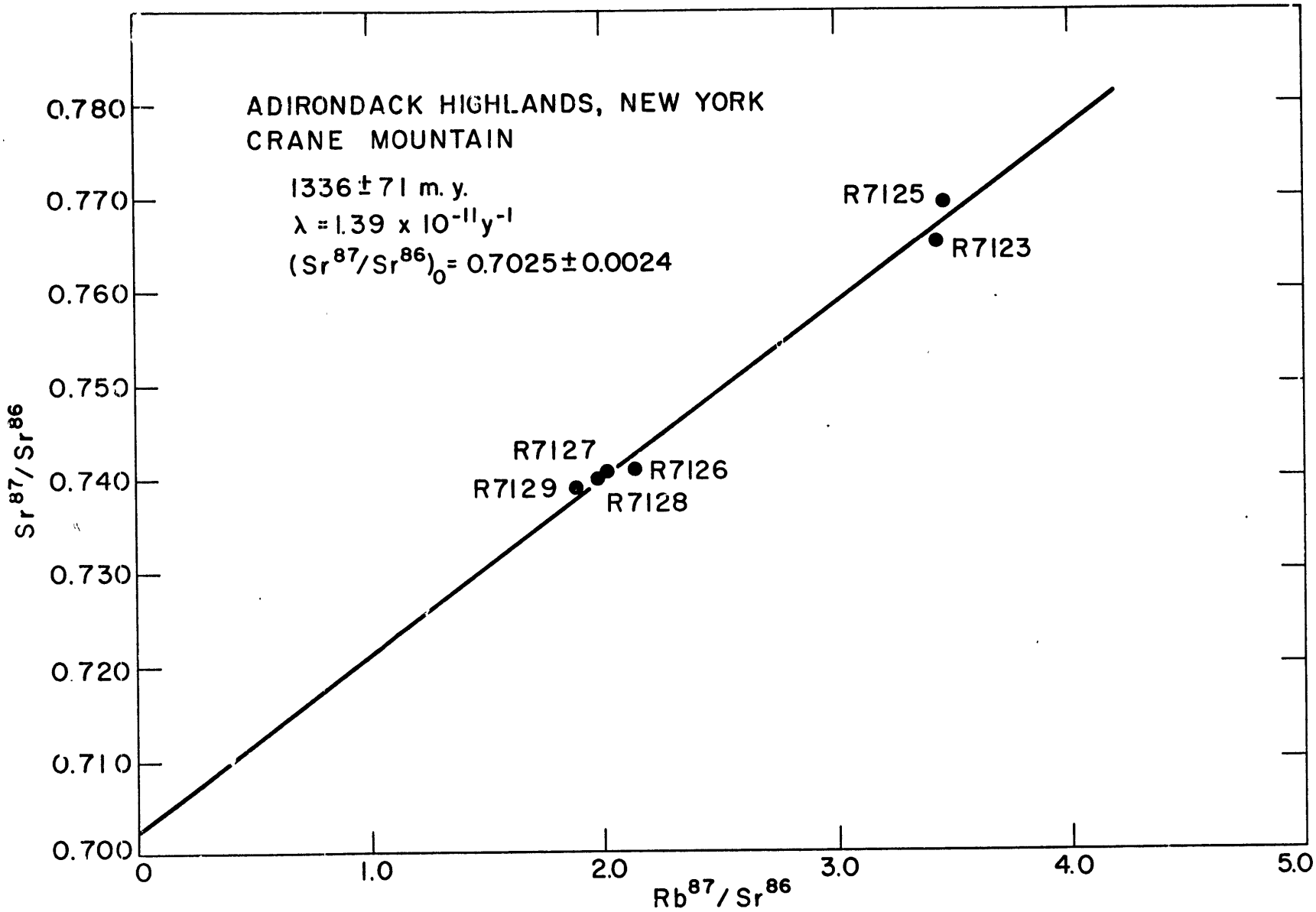
ADIRONDACK HIGHLANDS, NEW YORK
CRANE MOUNTAIN
1336 ± 71 m. y.
λ = 1.39 x 10⁻¹¹ y⁻¹
(Sr87/Sr86)0 = 0.7025 ± 0.0024
R7125
R7123
R7127
R7126
R7129
R7128
0.780
0.770
0.760
0.750
0.740
0.730
0.720
0.710
0.700
Sr87/Sr86
0
1.0
2.0
3.0
4.0
5.0
Rb87/Sr86

FIGURE 10

INDIAN LAKE, BLUE MOUNTAIN

AND

WEST CANADA LAKES

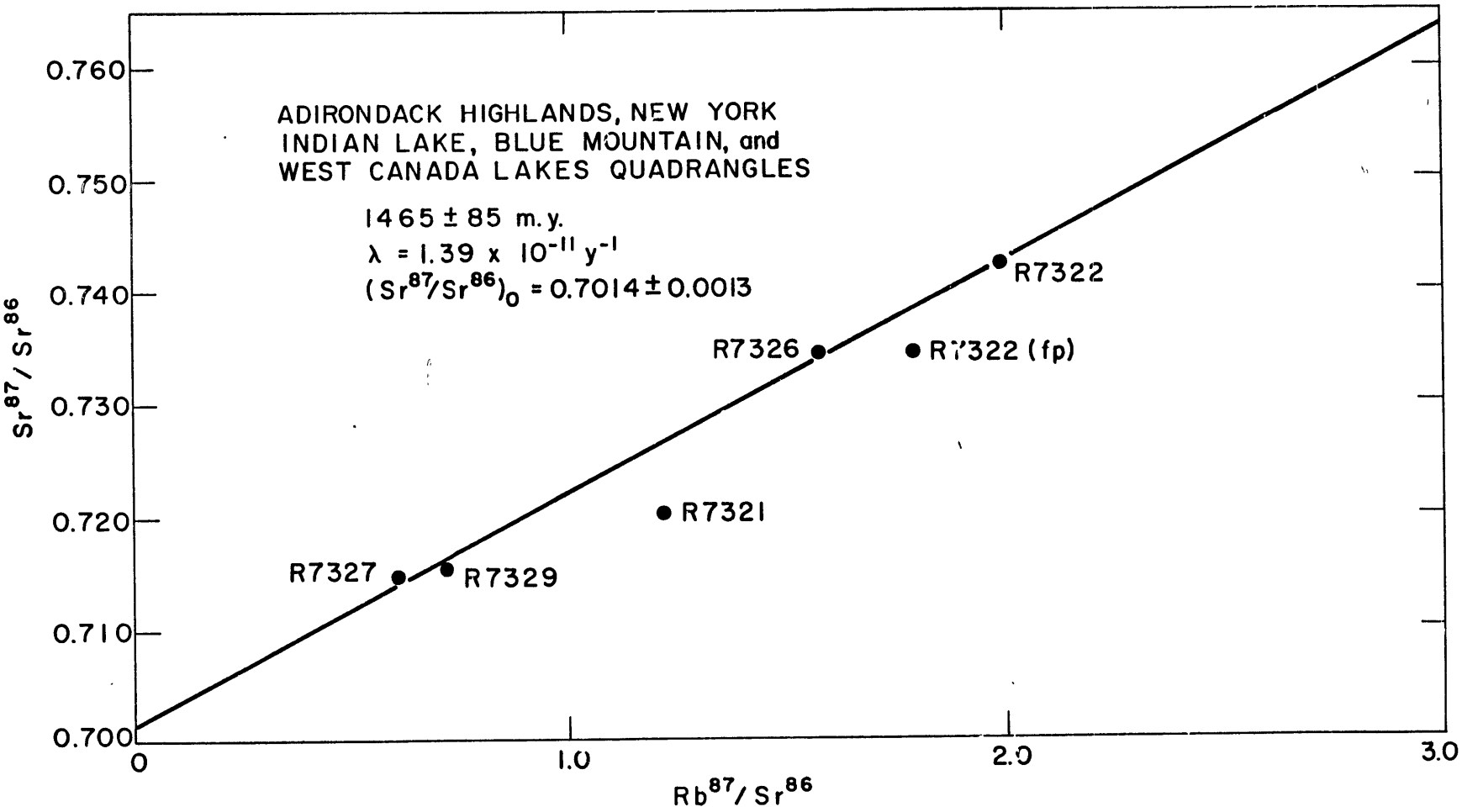
ADIRONDACK HIGHLANDS, NEW YORK
INDIAN LAKE, BLUE MOUNTAIN, and
WEST CANADA LAKES QUADRANGLES
1465 ± 85 m.y.
λ = 1.39 x 10^-11 y^-1
(Sr87/Sr86)0 = 0.7014 ± 0.0013
R7322
R7326
R7322 (fp)
R7321
R7327
R7329
0.760
0.750
0.740
0.730
0.720
0.710
0.700
Sr87 / Sr86
0
1.0
2.0
3.0
Rb87 / Sr86

At Crane Mountain, six specimens from a differentiated and overturned sill have been analyzed. An age of 1336 $\pm$ 71 m.y. was obtained with an initial Sr^{87}/Sr^{86} ratio of 0.7025 $\pm$ 0.0024. Unfortunately, the specimens fell into two groups on the plot, which resulted in a relatively large uncertainty in the initial ratio determination (Figure 9).

Five whole rock analyses and one mineral (potash feldspar) analysis have been made on pyroxene granulites from Indian Lake, Blue Mountain, and West Canada Lakes Quadrangles. Specimens R7321 and R7322 have been mapped as part of the supracrustal sequence by Walton and deWaard (personal communication) and specimens R7326, R7327, and R7329 are mapped as part of the basement complex. Four of the analyses define a reasonably good isochron with an age of 1465 $\pm$ 85 m.y., with an initial ratio of 0.7014 $\pm$ 0.0013. Whole rock R7321 was excluded from the regressional analysis. Assuming the same initial ratio found above, this one specimen gives a slope of 0.01527 corresponding to an age of 1087 m.y.

These ages appear to be the oldest reported for the central Adirondacks and suggest a period of intrusion pre-dating the 1100 m.y. reported by Hills and Gast [21] and Heath [1]. The low initial ratios measured for both these localities indicates that there was no extensive pre-Grenville history and that the age determination closely represents the age of intrusion.

Westport, Ontario Map-Area

The Westport map-area is about 30 miles northeast of Kingston, Ontario and 70 miles southwest of Ottawa, and comprises parts of

Leeds, Lanark and Frontenac counties.

The metamorphic rocks are dominantly marbles, quartzites and quartzo-feldspathic gneisses typical of the Grenville province of southeastern Ontario. Pyroxene granulites are the highest metamorphic grade rocks exposed and occur in the Clear Lake anticline surrounded by hornblende granulites and lower grade amphibolites.

Fifty specimens were collected by the writer from the pyroxene granulite horizon and of these, eight were analyzed isotopically. An age of 1320 $\pm$ 59 m.y. was found with an initial ratio of 0.7059 $\pm$ 0.0009. Using five points only, omitting R7070, R7071, and R7091, an age of 1334 $\pm$ 34 m.y. is obtained, with an initial ratio of 0.7065 $\pm$ 0.0004 (Figure 11).

Krogh and Hurley [22] report an age of 1016 $\pm$ 39 m.y. for the Westport quartz monzonite based on seven analyses with an initial ratio of 0.704 (no error limits quoted). Their results were analyzed using York's [7] method and an initial ratio of 0.7035 $\pm$ 0.0004 and an age of 1044 $\pm$ 17 m.y. was found, based on an error of 3% in Rb^{87}/Sr^{86}. Krogh et al. propose an upper mantle origin for this intrusive body on account of the low initial ratio. On the basis of analytical error only, the initial ratios for the quartz monzonite and pyroxene granulites do not overlap, lending credence to Wynne-Edward's hypothesis that the pyroxene granulites formed through high-grade regional metamorphism of a sequence of greywackes. In support of this, the Sr^{87}/Sr^{86} ratio of a specimen of chondrodite marble in the vicinity of the pyroxene granulite yielded a value of 0.7066 $\pm$ 0,001 (2 at the 95% confidence level). This value, if taken to represent the Sr^{87}/Sr^{86} ratio in

FIGURE 11

WESTPORT, ONTARIO

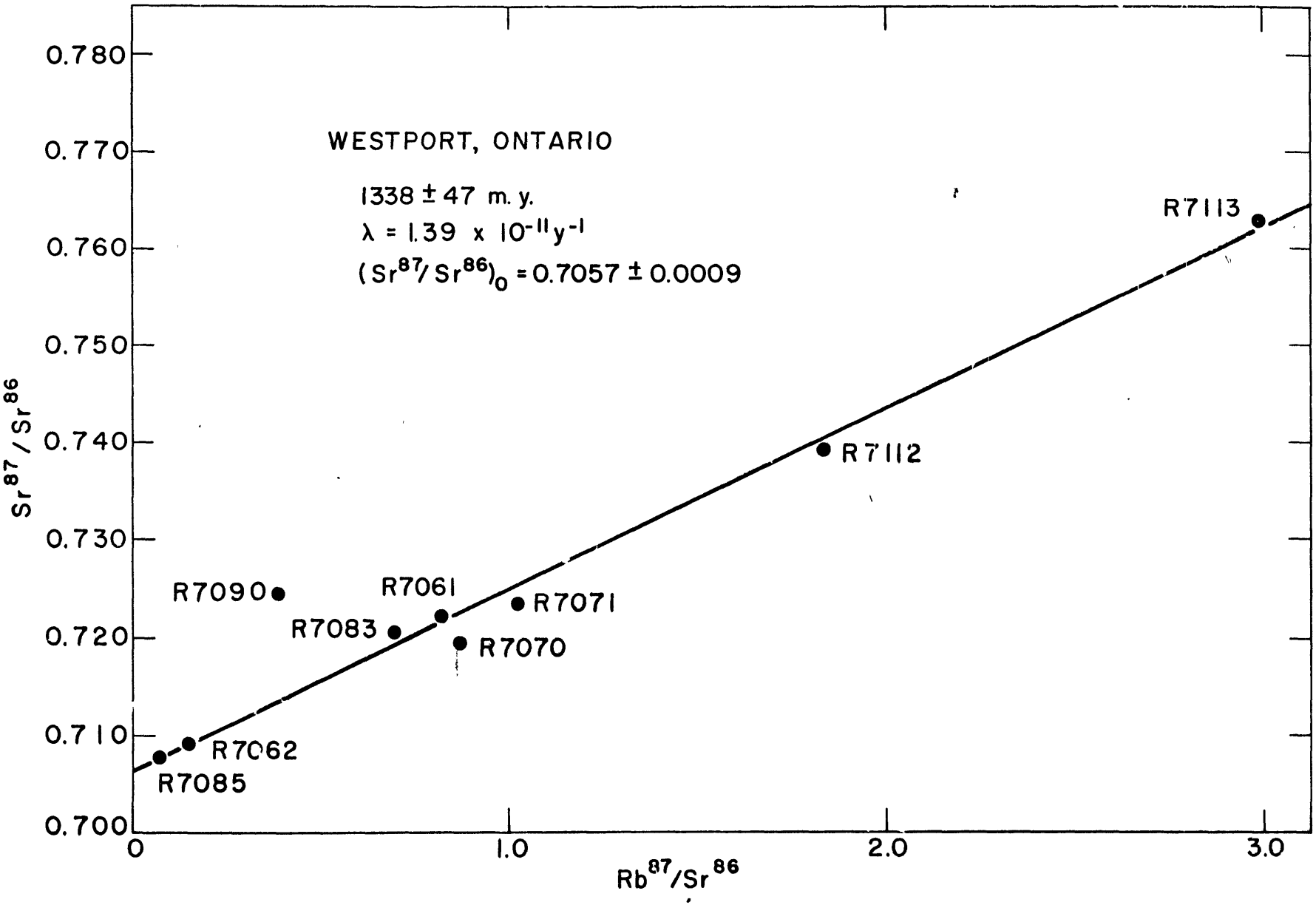
WESTPORT, ONTARIO
1338 ± 47 m. y.
λ = 1.39 x 10⁻¹¹ y⁻¹
(Sr⁸⁷/Sr⁸⁶)₀ = 0.7057 ± 0.0009
R7113
R7112
R7090
R7061
R7071
R7083
R7070
R7062
R7085
0.780
0.770
0.760
0.750
0.740
0.730
0.720
0.710
0.700
Sr⁸⁷/Sr⁸⁶
0
1.0
2.0
3.0
Rb⁸⁷/Sr⁸⁶

ancient sea water, lies on the Marine Geochron [23] about 1000 m.y. ago. Although the difference in initial ratio between the Westport quartz monzonite and the pyroxene granulites is not great, it is larger than that between the pyroxene granulite and the chondrodite marble, which is presumably of marine origin. On the basis of the isotopic evidence, it is proposed that these high-grade rocks had an association with a marine environment prior to metamorphism and only small additions of common strontium from lower crustal or upper mantle regions were made.

SUMMARY AND CONCLUSIONS

This rubidium-strontium isotopic study of the granulite facies is based on material from ten localities from four continents. The total range in Sr^{87}/Sr^{86} initial ratio is from 0.701 to 0.708 with an arithmetic mean of 0.7042.

A range from 0.702 to 0.705 has been established by Faure and Hurley [24] for oceanic basalts and a range from 0.703 to 0.711 for continental basalts by Hedge and Walthall [25] and Hamilton [26]. Heath [1] has found a relatively narrow range from 0.703 to 0.706 for anorthosites.

The similarity in initial Sr^{87}/Sr^{86} ratio of both the anorthosites and the pyroxene granulites (Table III) of this study suggests a common origin in a deep-seated environment having a low Rb:Sr ratio. This general survey suggests that the lowermost regions of the continental crust have had a low Rb:Sr ratio throughout much of geological time and that separation of rubidium from strontium must have occurred early during the evolution of the crust.

TABLE III

SUMMARY OF Sr^{87}/Sr^{86} INITIAL RATIOS IN PYROXENE GRANULITES

	Age (m.y.)	$(Sr^{87}/Sr^{86})_o$
Range of 54 Anorthosites (Heath, 1967)		0.703 to 0.706
Man Charnockite Series, Ivory Coast, Papon et al., 1968.	2750 ± 107	0.707 ± 0.001
Granodioritic migmatite series	2701 ± 135	0.699 ± 0.001
Lewisian Basement Gneisses, Lochinver, Sutherland, Scotland (Evans, 1965)	2600	0.7065
Inverian and Laxfordian Amphibolite Gneiss (Evans,1965)	2100 to 1560	0.7053
Nilgiri Charnockite Series and Gneiss,(Crawford, 1968)	2616 ± 80	0.7023 ± 0.0012
Madras City Charnockite (Crawford, 1968)	2580 ± 95	0.7059 ± 0.0042
PRESENT STUDY		
Kushalnagar, Mysore State (13)	2618 ± 46	0.7039 ± 0.0005
Pallavaram, Madras State (8)	1980 ± 124	0.7037 ± 0.0007
Okollo and Rakosi, West Nile District Uganda (9)	2629 ± 117	0.7054 ± 0.001
Crane Mountain, New York (6)	1336 ± 71	0.7025 ± 0.0025
Indian Lake, Blue Mtn. and West Canada Lake Quadrangles (6)	1465 ± 85	0.7014 ± 0.0013
Westport, Ontario (8)	1338 ± 47	0.7057 ± 0.0009
Kanuku Complex, Guyana South America (6)	2182 ± 95	0.7018 ± 0.0011
Pare Mountains (3)	927 ± 63	0.7056 ± 0.0011
Labor Serrit (3)	724 ± 8	0.7064 ± 0.0001
Salem, Madras State (6)	2476 ± 115	0.7042 ± 0.0002

BIBLIOGRAPHY

[1] Heath,S.A. (1967) Sr^{87}/Sr^{86} ratios in anorthosites and some associated rocks in Origin of Anorthosites-- a symposium, N.Y. State Mus. and Sci. Serv.,I.W. Isachsen,Ed. in press

[2] Lambert,I.B. and Heier,K.S. (1967) Geochemical investigation of deep-seated rocks in the Australian shield. Lithos.1,no. 1, 30-53.

[3] Pakiser,L.C. and Robinson,R.(1967) Composition of the continental crust as estimated from seismic observations in The Earth Beneath the Continents. Steinhart,J.S. and Smith T.J.(eds.) American Geophysical Union, 10,620-626.

[4] Birch,F.(1961) The V_p in rocks to 10 kb. 2, Jour. Geophys. Res., 66,2199-2224.

[5] Hurley, P.M.(1968) Absolute abundances and distribution of Rb, K and Sr in the Earth. Geochim.Cosmochim.Acta.,32,273-283.

[6] Shields,R. et al. (1963) Survey of Rb^{85}/Rb^{87} ratios in minerals. Jour. Geophys. Res.,68,2331-2334.

[7] York,Derek (1966) Least-squares fitting of a straight line. Canad. Jour. Phys. 44, 1079-1086.

[8] Holland,T.H.(1900) The charnockite series, a group of hypersthenic rocks in Peninsular India. Mem. Geol. Surv. India. 28,pt. 2.

[9] Quensel,Percy (1950) The charnockitic series of the Varberg District on the south-western coast of Sweden. Arkiv. för Mineralogi och Geologi. 1, no. 10, 229-329.

[10] Crawford,A.R.(1968) Geochronology of the Precambrian rocks of peninsular India and Ceylon. Unpub. Ph.D. Thesis,Australian National University.

[11] Aswathanarayana,U.(1968) Precambrian geochronology of peninsular India and Ceylon:an interpretation. Bull. Geol. Soc. India., 5,591.

[12] Groves,A.W.(1935) The charnockite series of Uganda. Quart. Jour. Geol. Soc. London. 91, 150.

[13] Hepworth,J.V. (1964) Explanation of the geology of sheets 19,20, 28, and 29 (Southern West Nile). Geological Surv. of Uganda Report no. 10.

[14] Cahen,L. and Snelling, N.J.(1966) The Geochronology of Equatorial Africa. North-Holland Publishing Company.

[15] Kulp,J.L. and Engels,J. (1963) Discordances in K:Ar and Rb:Sr isotopic ages. Radioactive dating 219-235, Proc. Symp. Intern. Atomic Energy Agency Joint Comm. Appl. Radioactivity, Athens, 1962 (Intern. Atomic Energy Agency, Vienna).

[16] Williams,E.,etal.(1967)Records of the Geological Survey of Guyana,5.

[17] Singh,S. (1966) Orthopyroxene-bearing rocks of charnockitic affinity in the South-Savanna-Kanuku Complex of British Guiana. Jour. Pet.,7, no. 2, 171-194.

[18] Buddington,A.F.(1939) Adirondack igneous rocks and their metamorphism. Geol. Soc. Am. Mem. 7, 201-230.

[19] Wynne-Edwards,H.R.(1967) Westport map-area, Ontario, with special emphasis on the Precambrian rocks. Geol. Sur. Canad. Mem. 346.

[20] Walton,M.S. and Waard,D. de (1963) Orogenic evolution of the Precambrian in the Adirondack Highlands, a new synthesis. Koninkl. Nederlandse. Akad. Wetensch. Proc.,ser. B, 66, 98-106.

[21] Hills,A. and Gast,P.W.(1964) Age of pyroxene-hornblende granitic gneiss of the eastern Adirondacks by the rubidium-strontium whole-rock method. Geol. Soc. Am. Bull. 75, 759-766.

[22] Krogh,T.E. and Hurley,P.M. (1968) Strontium isotope variation and whole-rock isochron studies, Grenville province of Ontario. Jour. Geophys. Res. 73, no. 22, 7107-7125.

[23] Hurley,P.M. and Fairbairn,H.W. (1965) Evidence from western Ontario of the isotopic composition of strontium in Archean seas. M.I.T. Thirteenth Annual Report, 145-147.

[24] Faure,G. et al. (1963) The isotopic composition of strontium in oceanic and continental basalts: Application to the origin of igneous rocks. Jour. Pet.,4, 31.

[25] Hedge,C.E. and Walthall,F.G. (1963) Radiogenic strontium-87 as an index of geologic processes. Science. 140, 1214.

[26] Hamilton,E.I.(1963) Jour. Pet.,4,pt. 3, 383.

PART B

Fronticepiece

Tomb

of

Job Charnock

Founder of Calcutta

Died 1692

TABLE OF CONTENTS

TABLE OF CONTENTS (cont.)

LIST OF TABLES

LIST OF TABLES (cont.)

LIST OF FIGURES

ACKNOWLEDGEMENTS

I wish to express my sincerest appreciation to Professor H. W. Fairbairn for his sound advice and encouragement throughout this investigation. His constructive and valuable criticism is most gratefully appreciated. I wish to thank Professor P. M. Hurley for his support and for providing much useful information for this investigation. Professor W. H. Pinson aided the writer in solving some of the problems associated with the chemical preparation of the samples for mass spectrometric analysis. I would especially like to thank Professor F. A. Frey for his material aid in the radiochemical preparation of the composite sample for rare-earth element analysis and Dr. P. A. Baedecker for introducing me to the techniques of instrumental neutron activation analysis.

My thanks are also extended to Dr. R. H. Reesman who instructed me in the technique of isotope dilution analysis using a Sr^{84} spike and to Mr. T. M. Gates who kindly performed the potassium analyses by atomic absorption spectrophotometry. Mrs. Veronica Posadas aided the writer greatly in preparative chemistry in the last stages of this study. Mr. T. Mariano of the Ledgemont Laboratory, Kennecott Copper, Lexington, Massachusetts, kindly provided the spark source mass spectrometric analysis of the charnockite composite.

The writer benefited from many fruitful discussions with his fellow graduate students, Mr. J. B. Reid and Mr. Y. J. A. Pelletier.

Professor Bernhard Kummel, Harvard University, was instrumental in obtaining the fronticepiece to this study and his efforts are appreciated.

I wish to extend my sincere thanks to the numerous field geologists who so kindly provided me with collections of pyroxene granulites and charnoclites from all over the world. My thanks go to:

Dr. J. P. Berrangé, Institute of Geological Sciences, London, England.

Dr. D. deWaard, Department of Geology, Syracuse University, Syracuse, New York.

Dr. J. V. Hepworth, Institute of Geological Sciences, London, England.

Professor P. R. J. Naidu, Honorary Director, The Mineralogical Institute, University of Mysore, Mysore, India.

Professor S. Subramanian, Department of Geology, Government College, Salem, Madras, India.

Dr. P. R. Whitney, Department of Geology, Rensselaer Polytechnic Institute, Troy, New York.

Professor H. R. Wynne-Edwards, Department of Geology, Queen's University, Kingston, Ontario.

I extend my sincerest appreciation to my Father and my Mother for their encouragement, and to my fiancée, Miss Judith R. Lang, for her unstinting devotion to the final presentation of this study.

The computational aspects of this investigation were carried out using the facilities of the Computation Center at the Massachusetts Institute of Technology.

This study received support through a grant to Professor P. M. Hurley from the United States Atomic Energy Commission, Division of Research.

INTRODUCTION

For many years it has been the goal of geochemists to sample adequately the exposed surface of the earth's crust to determine an average composition for material presumably common in the deeper levels of the crust (for example: Goldschmidt, 1933; Reilly and Shaw, 1967). A basic assumption underlying these studies is that the high grade regional metamorphic rocks exposed at the surface, especially of the granulite facies, are also abundant at depth. The principal constraint to this assumption is the extent to which the limited exposures of granulites and charnockites in the older deeply eroded high grade metamorphic terraines represent deep crustal material. That is, in these regions of the crust, estimates of chemical zoning with depth must be made and this extrapolation is hazardous.

Modern techniques of geophysics and geochemistry have become available that will do much to map out the areal extent and depth of deep crustal rocks and elucidate their history and origin. By means of remote sensing methods,such as seismic refraction, the structure of the continental crust at depth has been delineated (Pakiser and Robinson, 1966). Compressional wave velocities of rocks can be measured directly in the laboratory or they can be computed from a knowledge of the volume percent of the mineral phase present and its velocity. Christensen (1965) has found that silicic igneous rocks average about 6.2 km/sec. and velocities for mafic igneous rocks average about 7.0 km/sec. It would be expected, therefore, that rock velocities could serve as a general guide to rock composition.

The velocity, however, cannot be used to distinguish igneous from metamorphic rocks unless high pressure phase transformations are involved. Birch (1960, in Pakiser and Robinson, 1966) has noted that anorthosites and some altered dunites have seismic velocities similar to those of many mafic rocks despite their widely differing chemistry. This method alone has inherent difficulties since it would not be correct to state simply on the basis of seismic data alone that the upper crust is composed of 'granite' and the lower crust of 'gabbro' or 'basalt'. Interpretations based on this technique must be supplemented with geochemical studies.

In the recent geochemical literature, increasing attention has been paid to the significance of certain elemental ratios such as K/Rb, K/Ba, K/U, K/Th, and K/Sr in crustal and oceanic rocks (Shaw, 1968, Lambert and Heier, 1967). In the case of the K/Rb ratio, Shaw (1968) has delineated three distinct trends for igneous and quasi-igneous rocks. Oceanic tholeiitic basalts have higher K/Rb ratios than crustal rocks and pegmatitic and hydrothermal types are found to have even lower K/Rb ratios despite higher absolute abundances of potassium and rubidium.

The recent introduction of neutron activation analysis for the rare-earth elements (REE) in geological materials has revealed startling differences in abundance patterns of crustal, oceanic rocks and rocks presumably of mantle origin when expressed relative to a chondritic meteorite REE abundance. One very important aspect in the understanding of crustal evolution is the REE abundance pattern of lower crustal materials. In studies of continental basalts, there

always exists some doubt to the extent of contamination of these mafic rocks as they pass through the sialic crust. Studies of REE distribution coefficients of coexisting phases (Frey, 1968, and Haskin et al., 1966) and also phenocryst-matrix pairs (Schnetzler and Philpotts, 1968) show a pronounced mineralogical control over the fractionation of the REE. For example, it is found that some pyroxenes concentrate the light lanthanides and that garnets concentrate the heavy REE. Thus, it would be expected that the REE distribution in a magma produced in an environment containing this mineral pair would strongly depend upon the sequence of crystalization of pyroxene and garnet as well as their relative proportions, total rare-earth content, and degree of equilibration among the mineral phases.

Following important papers by Hedge and Walthall (1963) and Faure and Hurley (1963) on the significance of Sr^{87}/Sr^{86} initial ratios as indicators of the separation of rubidium and strontium between the crust and mantle, numerous rubidium-strontium isotopic measurements have been made on a variety of rock types both from the oceanic and continental environments. These studies have been of profound importance in the development of theories regarding the origin of the crust and the nature of crustal processes.

This investigation is concerned for the most part with the variations in the Sr^{87}/Sr^{86} initial ratios encountered in high grade regionally metamorphosed pyroxene granulites and charnockitic rocks. In some respects this work follows that of Heath (1967) who analyzed for these isotopic variations in anorthosites. This association of

anorthosites and charnockites is well known and in some localities the two are considered to be cogenetic (Buddington, 1939).

The type locality for the charnockite series in Madras State, India was described in detail in a classic memoir of the Geological Survey of India by Sir Thomas Holland (1900). Sir Lewis Fermor, onetime director of the Geological Survey of India, remarked that no final judgement on the origin of these rocks could be made unless based on a study of Holland's original occurrence. A composite of the charnockitic rocks from the Pallavaram type locality in Madras State was therefore made and analyzed for the rare-earth element abundance pattern by neutron activation. In addition, K/Rb ratios from this and several other localities were determined by atomic absorption spectrophotometry (K) and isotope dilution (Rb) and their variations compared with previous studies of this parameter.

CHAPTER I

OCCURRENCE AND THEORIES OF ORIGIN OF CHARNOCKITES AND PYROXENE GRANULITES

Since Sir Thomas Holland published his classic memoir in 1900, descriptions of rocks of similar appearance to the Madras Charnockite Series have appeared with increasing frequency in the literature and occurrences of similar rocks have been recorded from every Precambrian shield area. Although there has been continual controversy concerning the origin(s) of these rocks, to which this investigation adds its share, there are features peculiar to all the localities suggesting that these rocks are found invariably in high grade metamorphic terraines of the granulite facies wherever the older Precambrian basement complexes are exposed. Specimens from various localities are remarkably similar in chemistry, color and texture, mineralogy, and field relations to such an extent that there are many instances in the literature where workers have drawn comparisons between the Madras area in India and their own area of study (Quensel, 1950, p. 237; Heier, 1960; Singh, 1966).

The voluminous literature prior to about 1950 has been discussed in an excellent review paper by P. Quensel (1950, pp. 291-311) which he combines with the petrology of a similar suite of rocks from the southwestern coast of Sweden in the Varberg district. Only a brief discussion of these early papers will be given to show the evolution of the various arguments concerning the charnockite suite.

In Holland's day, it was common to regard the highly banded and foliated gneisses, because of their resemblance to stratified sediments,

as younger than the more granitoid crystalline varieties. This sequence was later reversed by others who found the granitoid rocks to be intrusive into the gneisses. This latter view was prompted particularly by Holland in his interpretation of the origin of the Charnockite Series.

The Charnockite suite in Peninsular India is confined almost entirely to a band having a northeasterly strike along the east and south coasts of the Peninsula and central Ceylon. The charnockitic rocks are differentiated from the non-charnockitic schists and gneisses by the higher temperature and pressure mineral assemblage of the former. Fermor (1936) concluded that this was the result of deeper burial, with later emplacement into its lower grade neighbors either through intrusion, large scale faulting and uplift of the whole series, or through tilting of the Peninsula. Since only two localized areas in Madras State have shown any evidence in favor of large scale faulting, a plutonic, igneous origin was advocated. The intrusion of the Charnockite Series into the surrounding non-charnockite schists and gneisses has been held to account for the aureole of slightly higher metamorphic grade adjacent to the Series.

When Holland examined the old crystalline rocks of Peninsular India, he noted a distinct set of characteristics and a relation of the group to the underlying older gneisses that was so invariable that he conferred upon the Charnockite Series the status of a petrographic province:

> The name Charnockite Series, which we now commonly employ for these rocks in India, expresses the fact that we group together in one petrogenetic province a number of lithical

> types genetically related to charnockite (defined below) and to one another. Within this petrographical province there are petrical and lithical forms which vary from the acid charnockite to the ultra-basic pyroxenite; but any one who has studied the group in the field would readily recognize the consanguinity of the different members....[1]

Quite apart from the use of the term "charnockite" to designate a series of diversified rock types, Holland also applied it as a convenient name for a "quartz-feldspar-hypersthene-iron-ore rock"[2] and not the name for any hypersthene-bearing rock. At the time, he expressed the hope that the term not be used outside India unless all features between the localities compared were identical.

Despite the partial obliteration of field evidence that would be expected with rocks of such great antiquity, Holland considered the Charnockite Series to be igneous in origin. In addition to the relation of the Charnockite Series to the country rock, he noted the following internal features which he considered to be indicative of an igneous origin:

(a) Mountain masses such as the Nilgiris, the Palnis, and the Shevaroys are quite uniform internally, retaining internal characteristics faithfully but sharply marked off from the surrounding schists and gneisses.

(b) Internal structural features common to igneous massifs are also present in the Madras charnockites, such as basic fine-grained segregative schlieren, coarse-grained, acid, contemporaneous veins, apophyses of the basic charnockite protruding into crushed and altered biotite-gneiss, and the occurrence of well-defined dikes with chilled

---

1. Holland, T. H. (1900), p. 128.
2. Ibid., p. 131.

contacts with the older gneiss.

(c) The chemical composition and mineralogy of the common members of the series have their nearest equivalents in igneous petrology.

Variations on the magmatic theme have been proposed by Washington (1916), on the basis of extensive chemical analyses of the Series, and by Goldschmidt (1922) who suggested direct crystallization from a primary magma. Rosenbusch (1932) grouped the charnockites with the anorthosites, as in eastern Canada and in the Adirondacks of New York, proposing a "Charnockit-Anorthositereihe". Suter (1922) also supported this view and believed the charnockites and anorthosites to be genetically related and suggested that in localities where the association is lacking, it would eventually be found. Groves (1935) has noted, however, that no anorthosite has been found in any of the charnockite terraines anywhere in Africa.

In the Adirondacks, the characteristic feature of the charnockite series is the presence of hypersthene throughout the acid, intermediate, and basic members. Although augite is present in the Adirondack syenite series, so also is hypersthene, though in minor amounts (Buddington, 1939, p. 229).

For the Adirondack association, Buddington (1939, p. 237) proposed a parent magma approximating a gabbro-anorthosite. He suggested that the small volume of olivine gabbro that is observed could be produced provided that a small amount of early olivine settled into the gabbroic liquid following crystallization of the plagioclase (forming the anorthosite). Following consolidation of the anorthosite, the olivine-

bearing gabbroic magma could be emplaced around it. Assimilation at depth of some pre-existing basement gabbroic rock and some anorthosite followed by differentiation to a more granitic composition could give rise to the quartz syenite magma. This type of mechanism would explain the association of charnockites with anorthosites.

A sudden swing to a metamorphic approach was heralded by Stillwell (1918) and Vrendenburg (1918) and elaborated by Groves (1935).

The Uganda charnockite series described by Groves (1935) includes nearly all the rock types found in the type locality in India, and as in India, the sub-acid to basic variants predominate in about equal proportions of quartz-diorite and norite. The surrounding country rock consists of gneiss which, in the Mt. Wati area, appear to grade into normal types in the charnockite series nearby. In the Karamojo district, the charnockites are associated with numerous plugs and flows of sodic lavas and masses of nepheline-syenite which are believed to be Tertiary in age. Groves appealed to plutonic metamorphism in Tyrrell's sense for the origin of these rocks. The changes produced in these rocks are the result of great heat and uniform pressure involving changes in rock chemistry through diffusion in the solid state. Tyrrell did not intend this term to include anatexis or palingenesis as all the changes take place in a dry environment.[3] Criteria used by Groves in favor of a plutonic metamorphic rather than an igneous origin are:

---

[3]. Tyrrell, G. W. (1948) The Principles of Petrology, London, p. 313.

(a) Geological setting of the charnockite series among ortho- and para-gneisses.

(b) Lack of zircon and apatite which are common in igneous rocks. Others, notably Subramaniam (1959, p. 338), have observed apatite, zircon, and ores as occasional accessories, however.

(c) Absence of observed contacts and evidence of assimilation of the charnockites and the neighboring gneisses.

(d) The abundant myrmekite and lack of twinning and clarity of the feldspars are characteristic of rocks having undergone metamorphism.

(e) The petrography and mineralogy of the series is abnormal in view of the normal calc-alkali chemical composition.

A similar opinion has been advanced by Ramberg (1948) in the case of a charnockite-mangerite-anorthosite association in a granulite facies complex in West Greenland on the coast south of Disko Island. To the north and south of the high grade rocks, gneisses occur belonging to the amphibolite and epidote amphibolite facies. Anorthosite is rare in this setting, as in India, Ceylon and Uganda, but, when present, occurs exclusively with the charnockite suite. The main rock in this area is an enderbite (hypersthene-bearing quartz diorite) which has approximately equal proportions of massive and gneissic variants. In this vast complex of enderbitic gneisses, there are also basic norites and a few hypersthene granites. Ramberg refutes the idea that this suite of rocks is primary magmatic in origin because the formation of a differentiated series requires a gradual decrease in temperature and consequent increase in acidity of the younger rocks. Instead, the characteristic mineralogical assemblage is the result of granulite

facies metamorphism under the same pressure and temperature conditions throughout the world without regard to the variations in whole rock chemistry within an individual locality. In the Greenland locality, the chemical and structural inhomogeneity is presumably pre-metamorphic. Syn-metamorphic rearrangement of many of the mafic minerals due to the differential crystalline plasticity as well as solid state diffusion between different rock types is presumed to have taken place. He points out that the temperature of metamorphism was not high enough to produce partial melting except in the case of pegmatitic veins which fill cross-cutting fractures in the country rock.

J. A. Evans is the only worker to suggest a direct sedimentary origin for the charnockite series. In a discussion of C. E. Tilley's paper dealing with the enderbite members of the charnockite series of Enderby Land in Antarctica (Evans, 1921) it was suggested that argillite when metamorphosed would undergo mineralogical changes such that feldspar would combine with the excess Al_2O_3 and SiO_2, thus removing CaO from further reaction by forming anorthite. As the CaO would be insufficient for formation of diopside, hypersthene would be the only major pyroxene.

Quensel (1950) reviewed the literature pertinent to the genesis of the charnockite series and discussed the varied suggestions in the light of the charnockite series of the Varberg district, Sweden. He found that chemical analyses of the charnockite suite of the district are similar to rocks of the surrounding lower metamorphic grade gneiss complex. Since the basic charnockites were similar in composition to the amphibolites and the felsic members to the

orthogneiss, he concluded that the high grade assemblage was the result of deep-seated plutonic metamorphism of the surrounding heterogeneous gneiss formations. He encountered a problem with the intermediate members, however, and like Ghosh (1941), found no neighboring rock of appropriate composition, and concluded that these are hybrid rocks formed as a result of a composite series of reactions between rocks of divergent chemical composition. He postulated that these hybrid rocks resulted from an intermingling followed by appropriate reactions of the orthogneiss and the basic charnockite. The transformation to the intermediate rock supposedly took place in situ.

Howie (1955), in an important paper on the geochemistry of the charnockite series in Madras, presents evidence in favor of an igneous genesis which involves igneous rocks subsequently subjected to high grade regional metamorphism. The distinction is difficult to make, especially on the basis of chemistry alone, because the stability fields of the constituent phases, especially in the acid and intermediate members, approach or coincide under magmatic or plutonic matamorphic conditions. The best evidence in favor of the latter is textural: although the order of crystallization is difficult to determine, the persistent granular texture of the rock and the embayed or corroded borders of hypersthene in the acid members point to a metamorphic alteration. The chemical analyses presented in this paper are considered in detail in Chapter II.

In 1959 A. P. Subramaniam examined the Madras type area and many of the same specimens described in Holland's original work on this area. He gives a clear account of the petrology and mode of occurrence

of the charnockites and their relation to the basement rocks. One of the major points that he makes in this paper is the misuse and resulting confusion in the literature of the term "charnockite" and "charnockite series". Holland anticipated this when he wrote (Holland, 1900, p. 131):

> The much complained of burdens of petrographical nomenclature are not due to the creation of specific names for local types, but to irresponsible and unwarranted extension of such names to include unrelated members of different and widely separated petrographic provinces, in which the accidents of differentiation and segregative consolidation may have produced by chance similar mineral aggregates.

In the worst of cases, the term has been taken to include amphibolites, pyroxene granulites, pyroxene gneisses, pyroxene syenites, norites, gabbros, diorites, granodiorites, and dark colored granites--all of which are referred to as charnockite (A. P. Subramaniam, 1959, p. 328). In addition to the characteristic minerals identified by Holland, A. P. Subramaniam found almandine garnet and redefined charnockite as: a hypersthene quartz feldspar rock with or without garnet, characterized by greenish blue feldspars, and greyish blue quartz, the dominant feldspar being a microperthite. (A. P. Subramaniam, 1959, p. 328).

As a result of this re-interpretation of the type area, Subramaniam concluded that (A. P. Subramaniam, 1959, pp. 345-346):

(a) Charnockite is redefined as a hypersthene quartz feldspar rock with or without garnet, characterized by greenish blue feldspars and greyish blue quartz, the dominant feldspar being a microperthite. This redefinition is justified as the paratype (Charnock's tombstone)

is found to be garnetiferous, and this facies is prevalent in the type area.

(b) The term "charnockite suite" is suggested for a group of genetically related alaskites, charnockites (birkremites), enderbites and hypersthene-quartz syenites, all of which are partly garnetiferous. This will correspond to the 'Acid' division of Holland's Charnockite Series. If it be considered desirable to retain the term Charnockite Series, it should be restricted to mean only the above suite of rocks.

(c) The 'Intermediate' division of Holland consists of an assemblage of hybrid rocks, derived by interaction of charnockite magma on pyroxene granulites of the basement.

(d) The occurrences of norite with related pyroxenitic layers and schlieren at Pammal Hill and at a few other points in the type area are considered syntectonic lenses, unrelated to the charnockite suite.

(e) The 'Basic' division of Holland is largely made up of pyroxene granulites and variants, which are interstratified with quartzo-feldspathic garnetiferous sillimanite gneisses (khondalite).

(f) The 'Ultrabasic' division of Holland is represented by the pyroxenitic schlieren referred to in paragraph (d) above.

(g) Holland's leptynite is considered a highly metamorphosed and reconstituted facies of khondalite, referred to in paragraph (e) above.

(h) The charnockite suite of rocks is thought to have been emplaced as thick sheets and lenses in gently folded basement rocks; all the rock units have subsequently suffered intense regional deformation.

(i) The charnockite suite or rocks and hybrid types are, as

exposed at present, interstratified with the basement rocks with which they are structurally conformable. The rock units in the type area represent a series of tight isoclinal folds plunging gently to the north, and overturned to the west.

(j) The charnockite suite of rocks is considered of primary igneous origin based on the following lines of evidence:

(i) The rocks carry mesoperthitic feldspars which indicate their having consolidated at magmatic temperatures.

(ii) The high barium content of the potash feldspars in these rocks point to a high temperature of formation.

(iii) The occurrence of pyrrhotite as an accessory mineral also points to high temperatures of consolidation.

(iv) The orthopyroxenes in these rocks show a systematic variation in composition. Some of them show lamellar structure while others show schiller inclusions, both of which are regarded as characteristic of igneous orthopyroxenes.

(v) The plagioclases in these rocks exhibit a rare complex twin law, which may be regarded as suggestive of a magmatic origin for these rocks.

(vi) The rocks of the charnockite suite carry inclusions of older pyroxene granulites.

(vii) The absence of amphiboles in these rocks point to their consolidation at elevated temperatures [or low activity of water].

Naidu (1963) in a presidential address to the Indian Science Congress has completed the circle regarding the origin of these rocks. While admitting that metamorphism has taken place on a regional scale, like Holland (1900), he places a special emphasis on the igneous nature of the series and has proposed that the "charnockite problem" is not simply one relegated to high grade metamorphic terraines of India, but should include the "granite problem" also, so that acid members of the series are simply hypersthene-granites rather than charnockite.

On the basis of volume representation of the various rock types in the Madras area, Naidu concludes that the intermediate and acid group on one hand and the basic and ultrabasic group on the other have not differentiated from the same magma. He is in agreement with Howie (1955) in choosing a norite parental magma for the hypersthene-eclogites, pyroxenites, basic granulites, and noritic dikes. However, for the acid and intermediate charnockites, he appeals to contamination and mixing through migmatisation between the very widespread potassic granites of Southern India and the older noritic rocks and Peninsular gneisses.

Since descriptions of rocks of charnockitic kindred are so widespread for localities throughout the world, Naidu's suggestion for dropping Fermor's designation of a "charnockitic province" in Southern India alone seems sound, especially in the context of the present study. Of basic importance is the fact that these rocks have remarkable constancy in mineralogy and setting that links them to rocks forming the lowermost regions of the earth's crust. Certain

mineralogical criteria such as the presence of hypersthene fall down in many instances even in the type locality in Madras State, for Holland has noted that certain horizons lack the definitive assemblage. This has been noted in other localities also, as for example in the Westport map area, Ontario (Wynne-Edwards, 1967) where this writer visited in 1967. Units mapped as pyroxene granulite and charnockite often lack hypersthene locally in the hand specimen, but upon examination on the larger outcrop scale, a rhombic pyroxene with biotite, or an amphibole can be distinguished. Clearly many geologists use the petrological name as a field convenience using hypersthene as an index mineral characteristic of that grade of metamorphism. Much confusion resulted, especially in the early literature, because of the mistaken identity of hypersthene for an amphibole (Holland, op.cit., p. 123), especially when both are present in the same specimen and there is no recourse to a petrographic microscope. In this study, a specimen sent to the writer identified as an "hypersthenite" was found to be an "amphibolite" on thin section examination.

Problems also arise in the interpretation of chemical analyses. Groves (1935), for example, analyzed a specimen considered by him representative of the acid charnockite in the West Nile District of Uganda and compared it with an analysis of an orthogneiss some four miles away. He concluded, on the basis of similarity of their compositions, that the two had the same origin and differed mineralogically only because of the higher metamorphic grade imposed upon the former. Quensel (1950) presents a similar line of reasoning for the origin of the charnockite series in the Varberg district of Sweden. Recently,

methods of surface trend analysis (E. H. Timothy Whitten, in Shaw, 1963) have shown the extent of compositional variability within granite and other igneous massifs. Studies of this nature show the extremely tenuous nature of the conclusions that may be drawn from one analysis which may not represent the outcrop from which it was taken.

To avoid placing a false perspective upon the specific distinctions between rock types of a particular grade of metamorphism, recent studies in geochemistry have begun to emphasize the broad areal and compositional relationships of rock types to interpret their origin and the part they have played in the evolution of the crust.

In the present work it would seem desirable to adopt a policy regarding the meaning intended for the term "charnockite". It must be remembered that this term was in use before the introduction of Eskola's facies concept of regional metamorphism and in Holland's day there was a tendency to propose new petrographic names for unusual rock types. In the case of the "charnockite problem", individual specimens commonly do not possess all the required features, but may qualify for inclusion in the suite if they have some of the features or, more commonly, they are clearly related to outcrops showing all the defined characteristics. Thus, these rocks do not have one clearly defined characteristic, but a number of more or less incidental features, i.e.: a rhombic pyroxene, clouded salic minerals, and a xenomorphic granular texture. These features are easily recognized in the acid

and intermediate types. They are so ill-defined, however, in the basic and ultrabasic variants that Subramaniam (1959) has proposed the removal of the basic and ultrabasic from the more acid types. Buddington (in Poldervaart, Geol. Soc. South Africa, 1966) states: "Who the devil knows what and when mafic rocks are associated with intermediate and felsic charnockitic rocks?".

In terms of this investigation, the author has restricted the study to the acid and intermediate varieties. From the field descriptions for many of these localities, it is apparent that these rocks have undergone high grade regional metamorphism up to granulite grade. The development of an orthopyroxene either in hand specimen or thin section or as an index mineral within a particular outcrop has been chosen as the prerequisite for analysis. In some cases, alaskitic gneisses were included since they were in gradational association with pyroxene-bearing types (at Okollo, West Nile District, for example). In view of the dual use made of the term "charnockite", it is felt that the general term "pyroxene granulite" is to be preferred.

For the descriptions of the localities studied, however, the nomenclature used in the field study has been kept, particularly in the case of the Indian type localities. Finally, it would appear worthwhile to adopt Subramaniam's (1959) suggestion that the term "charnockite" be restricted to the particular mineralogy given above, and not to the series which involves a variety of rock types.

TABLE I

SUMMARY OF THEORIES OF ORIGIN OF CHARNOCKITIC ROCKS

AUTHOR	PRINCIPAL VIEWS PROPOSED
Magmatic or Magmatic + later Metamorphism Interpretations:	
Holland (1900)	Original description of charnockite series in Madras State. Conclusions based largely on field relationships and similarity in chemical composition to igneous rocks.
Washington (1916)	Whole rock chemistry similar to that found in igneous rocks.
Goldschmidt (1922)	Chemical similarity to igneous rocks.
Rosenbusch (1923)	Grouped charnockite series with anorthosites.
Suter (1922)	Incorporation of the charnockite-anorthosite province into the calcalkali suite or circumpacific province.
Buddington (1939)	Proposed a parent magma approximating a gabbro-anorthosite in composition. Possible igneous differentiation following.
Quensel (1951)	Basic charnockites are primary igneous rocks later affected by profound metamorphism. Intermediate charnockites are hybrid since there is no similar country rock. Felsic charnockites represent direct plutonic metamorphism of surrounding orthogneiss.
Howie (1955)	Based on variation diagrams and on trace element geochemistry of the whole rock and minerals, he considers the series to be of igneous derivation with possible later high grade metamorphism.
Naidu (1963)	Equates "charnockite problem" with "granite problem". Basic and ultrabasic members formed from a norite parent magma. The "charnockite province" is more properly called a "granite-gneiss-schist" province since khondalites and calcsilicate rocks occur also.

TABLE I (cont.)

AUTHOR	PRINCIPAL VIEWS PROPOSED
Stillwell (1918)	In Antarctica, charnockite series is believed to be the metamorphosed equivalent of diabase (basic members) and granites (acid members).
Metamorphic Interpretation:	
Vredenburg (1918)	Dhawars and charnockite series mutually exclusive. Charnockite series a more intensely metamorphosed facies of the Dhawars. The adjacent khondalites are regarded as equally highly metamorphosed sediments originally belonging to the Dhawars.
Groves (1935)	Based on chemical comparison of charnockite series and lower grade rocks of similar composition surrounding the high grade complex at Mount Wati, Uganda.
J. Bugge (1940)	Arendal Norway charnockites formed from reaction and diffusion in the solid state. Similar argument to Groves (1935).
Ghosh (1941)	Basic and ultrabasic members are due to high heat and pressure subsequent to intrusion but the acid and intermediate members are formed by assimilation.
Rama Rao (1945)	Suggests rather than an igneous province (Holland) a metamorphic province produced under varying metamorphism of diverse ages.
Ramberg (1949)	Similar mechanism as proposed by J. Bugge (1940). Since charnockites are so similar over the world, he proposes that they all formed under the same P - T environment.
Sedimentary + later Metamorphism Interpretation:	
J. W. Evans (1921)	Subsequent metamorphism of argillites caused Al_2O_3 to combine with all CaO available so that there remained insufficient lime to form diopside so that hypersthene was the resulting pyroxene.
J. A. Dunn (1942) and others	Various other authors suggest that a melange of igneous and sedimentary rocks was hybridized through deep-seated metamorphism, giving rise to the wide variety of rocks observed.

CHAPTER II

SOME ASPECTS OF THE CHEMISTRY OF THE PYROXENE GRANULITE SERIES

2.1 Introduction

Experimental studies regarding the constitution of the lower crust have been based upon phase equilibria studies on various appropriate bulk compositions thought to represent lower crustal material. At this stage it is pertinent to discuss various aspects of the dispersed element geochemistry to attempt to establish restrictions or relationships between lower crustal and upper mantle material. Variations in certain trace element pairs, especially those having slightly different geochemical behavior, are also useful when used in conjunction with the inferences that may be made from Rb-Sr isotopic studies. In addition to a general survey of the whole rock chemistry of the pyroxene granulite facies in this chapter, the K/Rb, La/Yb, and rare-earth abundance data have been used to characterize some features of these rocks. These data complement a more general survey of Sr^{87}/Sr^{86} initial ratios from diverse localities over the earth discussed in Chapter III.

2.2 Conditions of Granulite Facies Metamorphism

Before consideration is given to the total rock chemistry of this environment, a brief discussion will be given regarding the pressure and temperature conditions that prevailed to give the characteristic assemblages of this facies.

There is no doubt on the basis of structural and mineralogical evidence that the granulite facies, or, more specifically in this study, the pyroxene granulite subfacies mineral paragenesis is indicative of high temperatures and pressures. The general lack of hydrous phases suggests crystallization in an environment with a low activity of water, or one in which temperatures were high enough to prohibit crystallization of hydrous phases. It does not appear that any one granulite facies terrain was completely anhydrous through time or space, as many of the localities studied by the writer contained variants of pyroxene granulites and charnockites sensu stricto containing significant quantities of either hornblende or biotite or both. Alaskitic granites, and normal biotite and hornblende granites have been recognized with these high grade metamorphic rocks, and their association could be the result of cooling of a pyroxene granulite migmatite with the concentration of water during crystallization. The presence of a condensed phase that does not leave the system could account for the retrograde reaction of pyroxene to biotite and hornblende. The granulite grade overlaps with the domain of partial melting and palingenesis and since the temperature of fusion of material of granitic composition is strongly dependent upon the partial pressure of water, it is not surprising to find granites associated in this terrain.

On the low temperature side of the granulite facies field there is considerable overlap with the almandine amphibolite facies via the

hornblende granulite subfacies, also termed the biotite granulite subfacies by Hsu (1955). In many of the terrains of this study, there seems to be some overlap of the pyroxene granulite and hornblende granulite subfacies. It is not known, however, to what extent polymetamorphism is responsible for the association of the two subfacies assemblages. In some localities, the Westport area of Ontario, for example, there is a banding of the hornblende granulite and pyroxene granulite subfacies on the scale of an outcrop which is reasonably attributed to variations in water activity during metamorphism. It has been suggested by Fyfe et al. (1958) that partial pressures of fluorine may be related to the incidence of hornblende and biotite. The breakdown of biotite and hornblende is gradual and would occur over a significant temperature interval at any given pressure. The prevailing fugacity of oxygen would also affect the temperature of breakdown.

The completely anhydrous assemblages which conform strictly to the granulite facies are:

1. Khondalite assemblage: quartz + perthite + garnet (+ plagioclase + kyanite or sillimanite). This assemblage is recognized to be the result of metamorphism of aluminous sediment and is commonly associated with charnockite terrains.

2. Charnockite assemblage: quartz + perthite + hypersthene (+ garnet + plagioclase). This assemblage is characteristic of the acid charnockite series.

3. Basic and intermediate assemblages: plagioclase + hypersthene + garnet + (quartz + perthite). Also plagioclase + hypersthene + diopside + (quartz + orthoclase).

4. Silica deficient basic assemblage: plagioclase + hypersthene + diopside + garnet.

5. Diverse calc-silicate assemblages: (a) diopside + plagioclase + calcite + quartz, (b) diopside + scapolite + calcite + quartz, (c) calcite + diopside + forsterite, (d) dolomite + calcite + forsterite.

6. The names birkremite and enderbite (C. E. Tilley, 1936) have been proposed for the potash-feldspar and plagioclase end-members of the series, respectively.

In addition, cordierite has also been recorded in some low temperature assemblages. Among the minor accessories apatite and zircon have variable abundance and are entirely absent in some localities (Groves, 1935). Rutile and ilmenite or ilmenomagnetite are the titanium-bearing phases of note, apart from minor amounts of Ti in the mafic phases. These rocks are generally silica saturated to the extent that spinel (ulvöspinel) does not occur except possibly in the most basic members of the series. Further details of the mineralogy of the Madras charnockites and their analyses are given by Howie (1955).

Experimental studies on the system $KAlSiO_4$-SiO_2-H_2O by Luth (1967) are of specific importance to the study of the charnockite problem since the appropriate phase relationships approximating the acid charnockite assemblage differ widely in P-T space depending on whether a vapor phase was present or whether the system consisted of condensed phases during crystallization. If the assemblage quartz + potash feldspar +

enstatite is an adequate representation for the natural assemblage quartz + alkali feldspar + hypersthene, then two possibilities exist for the P-T conditions during crystallization of these rocks depending upon whether an aqueous vapor phase is present or not (see Figure 1).

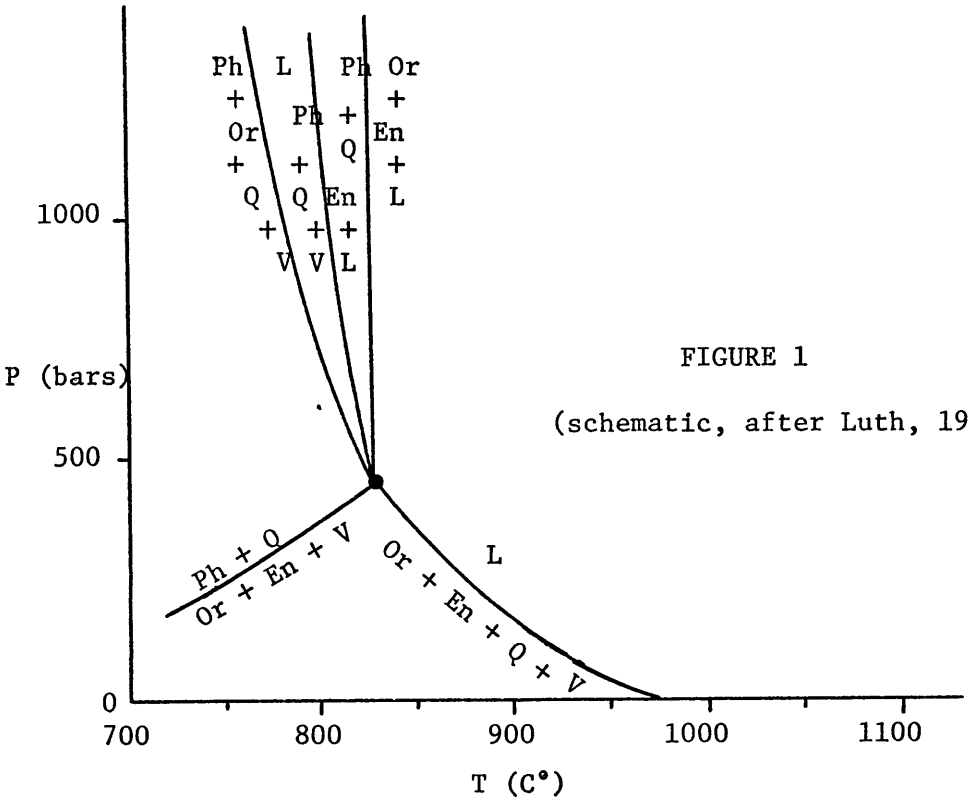

FIGURE 1

(schematic, after Luth, 1967)

If the natural assemblage can be treated as a simple quaternary system, then the coexistence of potash feldspar and enstatite with an aqueous vapor phase is restricted by the two pertinent invariant reactions below the quaternary invariant point. If the existence of a vapor phase could be demonstrated petrographically, then near surface crystallization (about 1.5 to 2 kilometers depth) would be indicated. In the case of a condensed system, however, no restriction can be placed upon the depth of crystallization since a near-infinite slope is indicated for the appropriate invariant reaction which continued

beyond the range of 3 kb. in Luth's study. The high slope for this reaction (Ph + Q = Or + En + L) is the result of the very small change in ΔV for this reaction.

Miarolitic cavities and other evidences for a vapor phase are notably absent in rocks of the charnockite suite and, to this writer's knowledge, there are no recorded instances in the charnockite literature of their being such cavities. In addition, there are other mineralogical criteria that support a deep-seated environment of crystallization. Boyd and England (1964) have noted considerable coupled substitution of Al-Al for Mg-Si in enstatite and monoclinic diopside with increasing temperature and pressure. The most aluminous enstatite found under equilibrium conditions with pyrope had 16 weight percent Al_2O_3 maximum at about 1650°C. and 30 kb pressure. Although temperatures and pressures would not be this high during granulite facies metamorphism, high alumina contents in hypersthenes have been noted by Groves (1935, p. 156-157) and Howie (1955, p. 751-756). In the Madras Charnockites, Howie (ibid.) found bronzites from ultrabasic members to have Al_2O_3 contents ranging from 4.40 to 4.55% and in an analysis of hypersthenes from two neighboring rocks from the South Savanna complex (see Chapter III) he found a range from 2.52% to 9.48% by weight Al_2O_3 (Howie, in Pitcher and Flinn, 1965, p. 319).

White (1964) presents criteria for distinguishing eclogitic and basic granulitic clinopyroxenes on the basis of the molecular percentages of the various clinopyroxene end members: Ac, Jd, Ts, Hd, and Di. Thompson (1947) suggested that the amount of aluminum in four-fold coordination increases with temperature while that in six-fold

coordination increases with pressure. This suggestion is evaluated by plotting the percentage of Tschermak's molecule, the measure of aluminum in four-fold coordination versus the percentage of jadeite, a measure of aluminum in six-fold coordination coupled with soda. White found a distinct separation of the two clinopyroxenes when plotted on this basis,thus allowing a distinction,which is otherwise difficult, between the higher pressure eclogite suite and the lower pressure basic granulite suite.

Hubbard (1966) has described the petrography and mineralogy of perthite and myrmekite from charnockitic rocks of the Ikerre Group of southwest Nigeria. The development of myrmekite is considered to be the result of local exsolution processes associated and contemporaneous with the development of perthite in the alkali feldspar. A high temperature would allow significant solution of Ca, as the fictive Schwankte's molecule: $Ca(AlSi_3O_8)_2$, to take place which would exsolve to "normal" anorthite on slow cooling with the release of excess SiO_2. Hubbard suggests that such local readjustments would be in keeping with a system subjected to high confining pressures with slow cooling in a relatively volatile-free environment.

2.3 Chemical Analyses of Pyroxene Granulites

A number of papers discussed in the preceding chapter have included both whole rock and mineral analyses of various members of the charnockite series from a variety of localities. Quensel (1950) and Howie (1955) provide extensive compilations, the former including the analytical data given by Groves (1935). Naidu (1963 has also presented sixty-eight analyses of hypersthene-bearing rocks from

Madras State.

Howie (1955) gives a detailed examination of the trends in the analytical results through the series. Plotting the weight percent of the cation versus its "position" given by (1/3 Si + K) + (Ca + Mg) following the method of Larsen (1938)[1] and modified by Nockolds and Allen (1953)[2], a continuous variation is observed that corresponds very closely with the elemental variations in igneous rock series. When the alkalies: Ca, K, and Na are plotted on a triangular diagram, two trends are apparent. One trend curves upward to higher potassium values, Howie (1955, p. 736), and the other has a lesser curvature toward potassium, more closely approaching sodium, and representing the enderbitic types. Howie (1955) has pointed out the similarity of this and the Fe + Mg + alkali trend with those of the Crater Lake series and the Lassen Peak volcanics. This last trend in particular is only slightly more curved than the trend of typical calc-alkali igneous series.

A computer program, originally written by Diness and Luth and later re-written by the author for the IBM OS/360 computer at the M.I.T. Computation Center, has been used to calculate the C.I.P.W. norm for the fifty-four analyses presented in Howie (1955, 1965) and Quensel (1950). The program is listed in Appendix C and is designed to calculate the weight norm as originally proposed by Cross, Iddings,

---

1. Larsen, E. S. (1938) Jour. of Geology, Some new variation diagrams for groups of igneous rocks, 46, pp. 505-520.

2. Nockolds, S. R. and Allen, R. (1953), The geochemistry of some igneous rock series, Geochim. et Cosmochim Acta, 4, pp. 105-142.

FIGURE 2

Charnockite Series

Differentiation Index vs. SiO_2

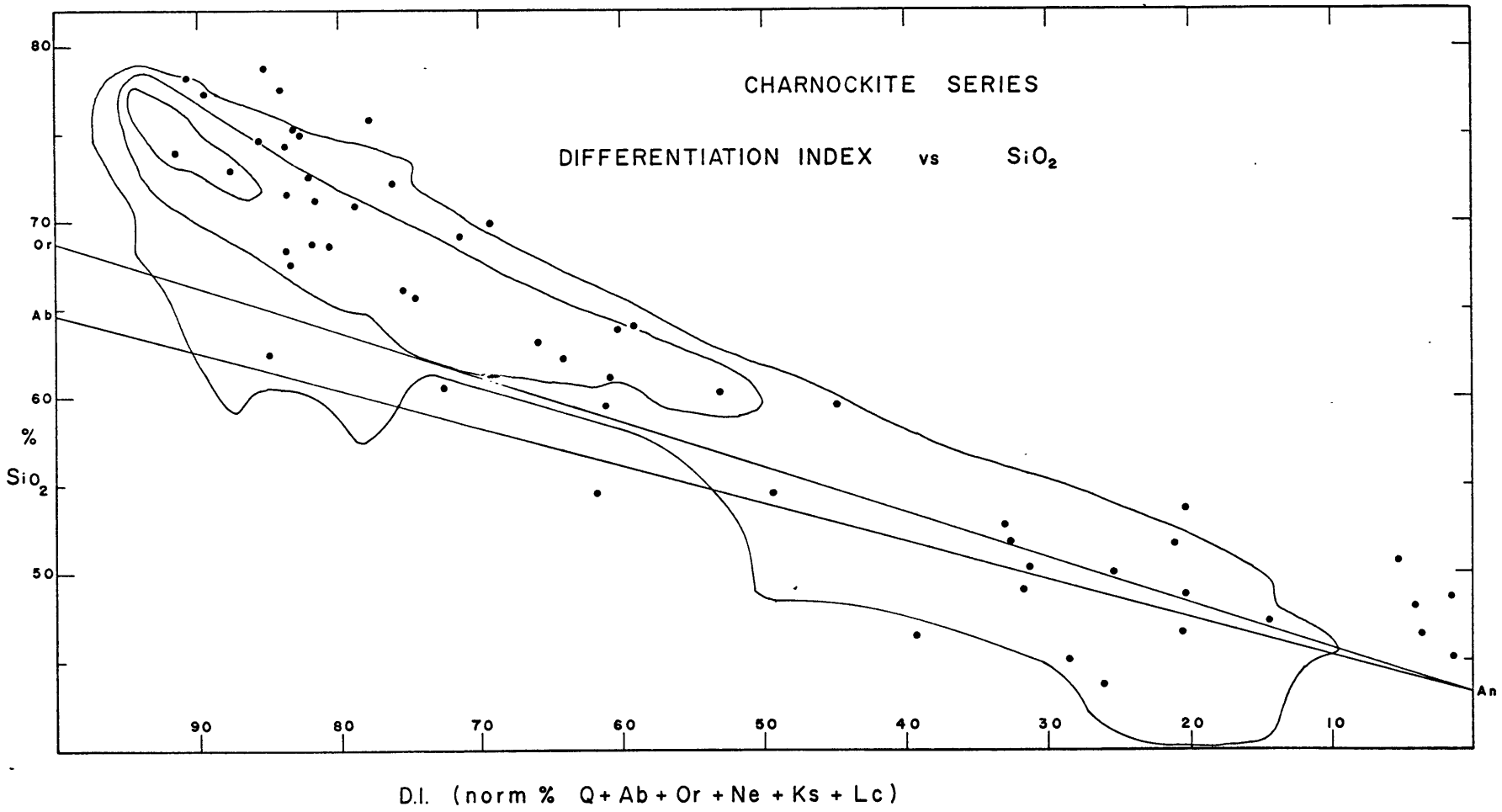
CHARNOCKITE SERIES
DIFFERENTIATION INDEX vs SiO_2
80
70
Or
Ab
60
%
SiO_2
50
An
90
80
70
60
50
40
30
20
10
D.I. (norm % Q + Ab + Or + Ne + Ks + Lc)

Pirsson, and Washington. It is modified only to the extent that Li_2O, if reported in the analysis, is added with MgO and when SO_3 is reported it is calculated as thenardite (Na_2SO_4). In addition, the MgO/FeO ratio in olivine, hypersthene, or diopside is given when the norm contains that mineral. Also reported are the fractions of Or, An, and Ab and Or, Ab, and Q. The extent of deficiency of Al_2O_3 which would be required to form corundum is indicated by (-C). Ab, Or, Lc, Ne, and kaliophyllite ($KAlSiO_4$) are recalculated to 1.00 in terms of the "granite system": Ne, Ks, and Q. The oxidation ratio is calculated according to Chinner (1960) and finally the Differentiation Index (D.I.) as proposed by Thornton and Tuttle (1960) is calculated.

Despite the shortcomings of a weight norm compared with a molecular norm, the variation within the charnockite series as well as other characteristics of the series is still apparent.

In Figure 2, the Differentiation Index is plotted against the weight percentage SiO_2 in the rock analysis. The Differentiation Index as defined by Thornton and Tuttle is the sum of the weight percentages of normative quartz + orthoclase + albite + nepheline + leucite + kalsilite. Obviously only three of these minerals will occur depending upon the degree of silica saturation; vis: Q + Or + Ab or Ne + Lc + Ks. The two groups are considered the salic constituents of the C.I.P.W. norm with the exception of anorthite which in Thornton and Tuttle's study is considered a femic constituent. They also consider zircon and corundum as femic although with less justification than in the case of anorthite. The Differentiation Index

is a measure of the degree to which a rock has approached "petrogeny's residua system": SiO_2 - $NaAlSiO_4$ - $KAlSiO_4$ as proposed by N. L. Bowen (1937). If a tetrahedron is constructed with Q - Ne - Ks forming the base and the femic constituents summed to form the apex, the distance from the apex to where the rock plots within the tetrahedron is a measure of the basicity of the rock. The Differentiation Index may be the same whether the rock is acid or alkaline and is not a measure of silica saturation. Figure 2 does show the degree of silica saturation throughout the series, however. Points that fall above the Or-An line are generally over-saturated and those analyses falling within the Ab-An-Or triangle would be expected to be rich in these phases and would be anorthosites, or syenites. Undersaturated rocks would fall below the Ab-An line in this figure. Superimposed on this diagram are the three highest frequency contours for points as shown in Thornton and Tuttle's (op. cit.) work. The contours show the number of points in a 1.6% area rather than the usual 1.0% area commonly used in petrofabric work. Shown in Figure 2 are the contours for the 1.6% areas containing 151-175, 126-150, and 101-125 points. The majority of the charnockite analyses fall in the oversaturated region occupied by dacite and rhyodacite and trends upward and somewhat to the right of the calc-alkali rhyolite area, indicating that the charnockites are a little less mafic and probably are very close or coincident to where many granites would plot. In the low SiO_2, D.I. end of the diagram, the analyses plot near the tholeiitic and tholeiitic olivine basalt region as delineated by Thornton and Tuttle.

Since the standard norm calculation gives preference in all cases to the more silica saturated minerals (i.e. feldspars instead of feldspathoids, and hypersthene instead of olivine), there will usually be more free quartz in the mode than in the norm. Also titanium in various valence states can proxy for silicon in many minerals further increasing modal quartz. All the points that fall above the Ab-Or line represent analyses that contain quartz in the norm. Alumina, expressed as excess (+C) or deficient (-C) corundum in the norm, shows an excess only in rocks having SiO_2 greater than about 70% in which case the excess corundum does not exceed about 6%. There is one exception in a garnet granulite from Proclamation Island, Antarctica where (+C) is 8.44%. The average (-C) of these analyses is about 3.4%. It is generally regarded that argillaceous rocks show an excess of Al_2O_3 over that required to form feldspar and the excess should be greater than that found in igneous rocks. Bastin (1909) has studied the extent of these differences and has found that over 60% of schists and gneisses of argillaceous origin contain an excess of normative corundum greater than 5% and in half of these the excess is greater than 10%. The corresponding proportions for igneous rocks are less than 3% and 0.6% respectively. In the present study the pattern of excess alumina supports an igneous affinity in the light of Bastin's work since the average excess corundum is only about 1.7%, and probably can be accounted for by the formation of biotite in the rock. This has been accepted as an explanation for a similar situation in Ceylon as noted by F. D. Adams (1929).

2.4 Regional Trace Element Trends with Regional Metamorphism

Recent advances in methods of rapid chemical analysis combined with appropriate statistical techniques are finding increasing application to problems involving regional compositional differences in crustal materials. In the case of the radiogenic elements, such data are prerequisite to studies of the heat budget of the crust and mantle. Also, detailed analyses of deep-seated Precambrian terrains will show the extent of compositional zoning with depth in the crust.

Reilly and Shaw (1967) have discussed the assumptions that must be recognized in estimating crustal abundances of elements by any direct method. The concentration and variation of an element may not be the same over the surface as in the vertical sense. Also, the sampled area must be weighted proportionately to each rock type that outcrops within the area, assuming further that the surface area of a particular rock type is directly proportional to its volume. In addition, the sample population may be biased because of surficial control over outcrop. For example, effects of glaciation or differential erosion may interfere with sampling.

An increasing number of papers have appeared proposing a depletion with depth of potassium, rubidium, and other strongly lithophile elements in the crust due to a fractionating effect during regional metamorphism: (Heier, 1964; Heier and Adams, 1965; Eade, et al., 1966; Heier and Lambert, 1967, 1968; and Shaw, 1968).

Heier (1964)has proposed a mechanism whereby the transport of major and trace lithophile elements could take place during progressive

regional metamorphism. As lower grade rocks are subjected to increasingly higher temperatures and pressures, mineral transitions such as the breakdown of micas would occur which would give rise to product phases less favorable to the inclusion of rubidium. For example, in rocks such as granulites containing excess quartz, Heier proposes the reaction:

$$K(Mg,Fe)_3AlSi_3O_{10}(OH)_2 + 3SiO_2 \longrightarrow KAlSi_3O_8 + 3(Mg,Fe)SiO_3 + H_2O$$

From crystallochemical considerations, then, it would be expected that rubidium would become concentrated in a volatile phase,depleting the higher grade rocks in rubidium. Strontium,on the other hand, would not be expected to behave in this manner because of its ability to proxy for calcium. During progressive high grade metamorphism, then, one would expect a progressive decrease in the Rb: Sr ratio. A plot of %K vs. Rb/Sr of granulites would be expected, in light of the discussion above, to show a lower Rb/Sr ratio for a given potassium concentration than in amphibolites and lower grade rocks. There is a suggestion for such a trend for amphibolites and granulites from Langøy, Norway (Heier, op.cit., Figure 1) though many more analyses would be needed for statistical proof. In Figure 3, a similar plot for the charnockitic types from a variety of localities is given, and these show a much greater range in both ordinate and abscissa than in Heier's work. The results of Figure 3 are not strictly comparable to Heier's results, since his work was restricted to a single locality and coexisting amphibolites and pyroxene granulites were being compared. On the other hand, the results show the variation in an approximate sense that one would expect for the charnockite series considered as

FIGURE 3

%, K vs. Rb/Sr

in

Pyroxene Granulites and Charnockites

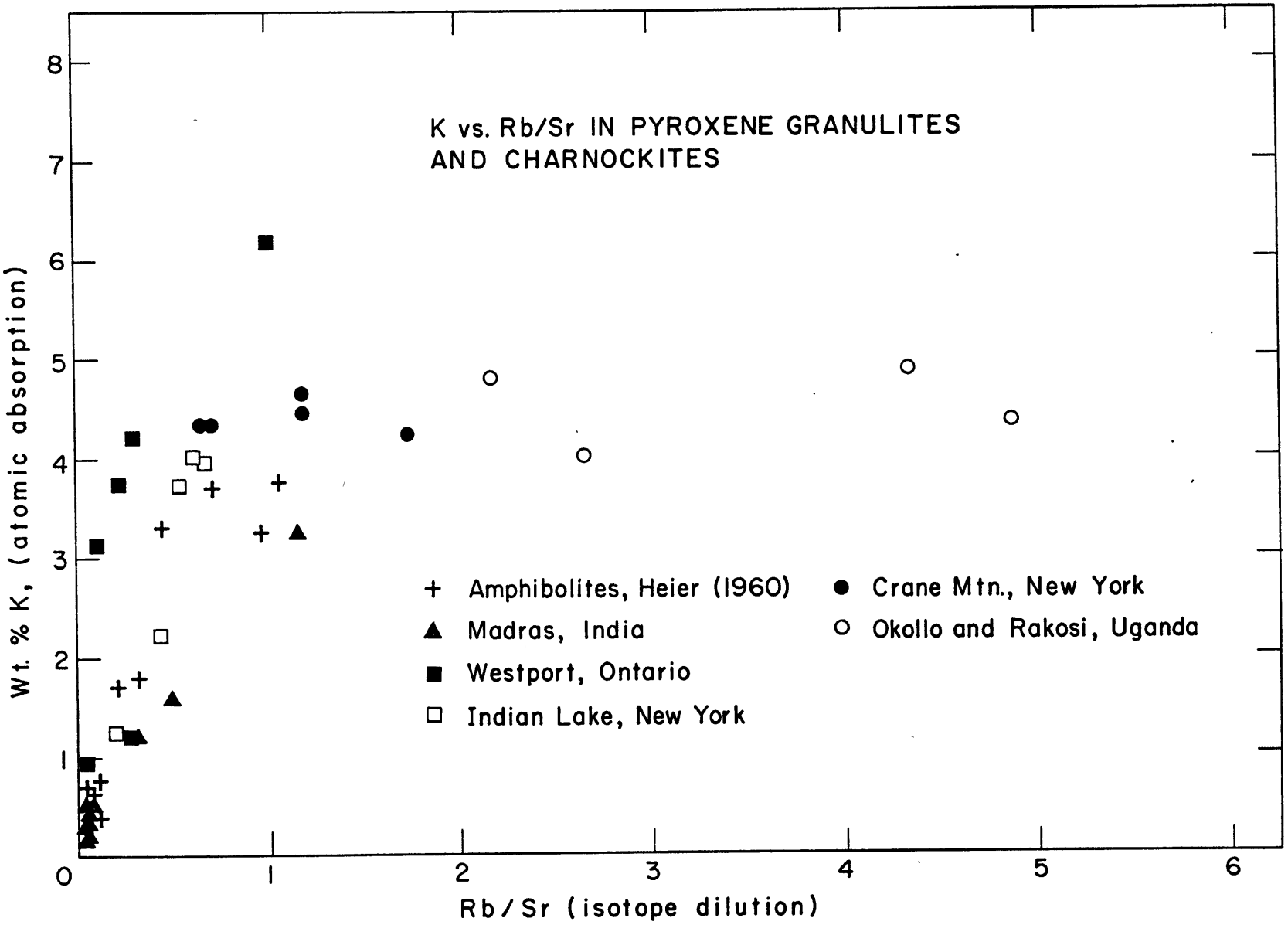
K vs. Rb/Sr IN PYROXENE GRANULITES
AND CHARNOCKITES
Wt. % K, (atomic absorption)
Rb / Sr (isotope dilution)
0
1
2
3
4
5
6
7
8
+ Amphibolites, Heier (1960)
▲ Madras, India
■ Westport, Ontario
□ Indian Lake, New York
● Crane Mtn., New York
○ Okollo and Rakosi, Uganda

a group. Also, many of the rocks analyzed in this study contain small amounts of an amphibole so that if two populations really exist, small degrees of mixing of either end-member would only obscure the bimodal nature of the distribution in spite of the inherent accuracy of each analytical point.

Heier made a further proposal regarding the possibility of natural fractionation of radiogenic strontium as a result of regional metamorphism. Heier believes that during anatectic melting of silicate rocks containing potassic phases, these potassic phases corresponding to a granitic melt would be the first to break down. Since these are the host phases for rubidium, they will also be the sites of Sr^{87} built up after the last isotopic homogenization. Since biotite is fairly common in this facies, and is also low in common strontium, anatectic melting could presumably lead to a residual rock with a low Sr^{87}/Sr^{86} ratio.

It is difficult to envisage a mechanism whereby this reaction could take place without having the radiogenic strontium, released from the biotite, incorporated into the strontium acceptor phases on the right hand side of the equation. In addition, it must be assumed that there be no common strontium available to mix with this radiogenic strontium, which would render the effect immeasurable. The implications of this model are considered further in Chapter IV in the light of the Rb-Sr isotopic data.

In a study of Precambrian medium to high-grade rocks of the Australian sheild, Lambert and Heier (1967) have demonstrated distinct differences in the total rock content of potassium, uranium and thorium

between the gneisses of the felsic amphibolite facies and hornblende granulite subfacies and the more deeply seated pyroxene granulite subfacies. As a result of approximately 400 analyses for U, Th, and K the concentrations in pyroxene granulite subfacies rocks show a marked depletion when compared to lower grade metamorphic gneisses, granites and greenstones of the sheild areas, and the granites and shales of younger mountain regions. The pyroxene granulites generally have consistently low values of K and U and Th, which are much less when compared with the lower grade rocks. In magmatic series and in sedimentary rocks, it is common to observe an increase in the U/K and Th/K ratios with increasing K content of the rock (Heier and Rogers, 1963); in this respect the pyroxene granulites show a reverse trend.

Compared with the common surface rocks of appropriate bulk composition, the acid and intermediate pyroxene granulite subfacies rocks are depleted in Th and U by factors of 9 and 5 respectively.

In a sequel to the paper above, Lambert and Heier (1968) consider these elemental variations further and also present additional data on Rb, Sr, Pb, and Ba determined by X-ray fluorescence. In this more recent paper, they divide the pyroxene granulite subfacies into low, medium, and high pressure variants on the basis of mineralogical assemblage:

(i) Low pressure: Cordierite, andalusite and the mineral pair: olivine + plagioclase and characteristic. Also present are brownish hornblende $\pm$ biotite, $\pm$ almandine garnet. Hypersthene is widespread in the mafic types.

(ii) Medium pressure: Plagioclase + hypersthene $\pm$ clinopyroxene,

± quartz. Stable aluminosilicates are sillimanite or kyanite. Olivine and plagioclase are incompatible and cordierite is unstable.

(iii) High pressure granulite subfacies: The mineral association developed with increasing pressure is garnet + clinopyroxene + hypersthene + plagioclase first in silica undersaturated rocks then in silica saturated rocks. At higher pressures plagioclase disappears, marking the beginning of the eclogite facies. When the activity of water is high enough, hydrous phases such as biotite or hornblende form. Anorthosites are exclusively developed in the medium to high pressure granulite terrains.

Their results show a decrease in K, Rb, Th, U, Pb and Si and related elements in the highest granulite grade rocks analyzed (Table II-A). There appears to be a corresponding increase in Ca, Mg, Fe, Mn, and Ti. The high grade rocks show lower Rb/Sr, (Th/K) x 10^4 and (U/K) x 10^4 ratios and higher K/Rb ratios than in the low pressure granulites and amphibolites. That is, for a given potassium content, there is a relative depletion of Rb, Th, and U compared with the lower grade rocks.

TABLE II-A

Average K and Trace Element Compositions, Australian Shield
(from Lambert and Heier, 1968)

	Musgrave Range		Fraser Range	Cape Naturaliste		Eyre Peninsula		SW
	G	A	G	G	A	G	A	Shield*
K	2.2	2.8	1.4	3.7	3.8	3.6	3.7	2.6
Rb	70	140	45	190	180	175	200	115
Pb	20	25	15	30	35	30	30	35
Ba	1090	990	420	625	780	630	610	610
Sr	340	400	170	160	190	140	120	135
U	0.4	1	0.3	2.5	1.5	2.0	4.5	3.0
Th	2.1	11	1.8	35	23	23	30	20
Zr	310	250	115	525	400	185	195	220

*Average for all rocks G = granulite facies A = amphibolite facies

Heier and Rodgers (1963) have found an average (U/K) x 10^4 ratio of about 1.2 in granitic rocks. All the ratios recorded in Lambert and Heier's work are significantly lower than this value, the lowest values being found in the high and medium pressure granulites. The values for the (Th/U) x 10^4 ratios show a much greater degree of variability. Although values of about 4 have been recorded for this ratio in a variety of rock types, this ratio is generally higher than 4 in lower pressure granulites, and lower than 4 in the high and medium pressure granulites. Lambert and Heier (1968) interpret the depletion of lithophile elements and the higher K/Rb ratios and lower Rb/Sr, (Th/K) x 10^4, and (U/K) x 10^4 in high to medium pressure granulites as the result of a series of dehydration reactions involving partial melting under the P-T conditions of the upper amphibolite facies discussed previously in this chapter. Studies of similar nature carried out on lower grade rocks (up to the high amphibolite facies) have revealed that there is no change in bulk chemistry apart from loss of volatiles (Shaw, 1954, 1956; Phinney, 1963; Chinner, 1960). Eade et al. (1966) found minor changes in bulk chemistry in medium pressure granulite facies rocks of the Canadian shield but major changes in chemistry seemingly do not occur until the highest metamorphic grades are attained (Heier and Adams, 1965; Heier, 1965; Lambert and Heier, 1967, 1968).

In the present investigation, thirty-two specimens from various localities (Table II-B) were analyzed for potassium by atomic absorption spectrophotometer by the addition method and were combined with rubidium values determined by isotope dilution. The accuracy of the potassium

TABLE II-B

M.I.T. #	$\%K_2O$	%K	Rb(ppm)	Sr(ppm)	K/Rb	Rb/Sr
Pallavaram Area, Madras, India:						
R7220	0.315	0.262	4.3	94	609	0.045
R7215	0.346	0.287	6.5	123	442	0.053
R7219	0.611	0.507	11.5	143	441	0.081
R7216	0.561	0.466	12.6	116	370	0.109
R7221	0.624	0.518	20.2	203	256	0.100
R7242	1.897	1.574	210	427	75	0.492
R7241	0.487	0.404	7.6	---	527	---
R7218	0.445	0.369	11	192	335	0.056
R7214	0.241	0.200	6.3	110	383	0.057
R7205	3.92	3.25	134	116	243	1.152
R7217	0.241	0.200	3.9	76	513	0.051
R7240	1.45	1.20	146	473	82	0.309
Westport, Ontario:						
R7070	5.09	4.23	140	466	364	0.301
R7083	4.52	3.75	85	359	532	0.236
R7090	3.76	3.12	57	417	660	0.136
R7112	4.82	4.00	88	142	454	0.616
R7113	7.45	6.18	125	121	494	1.030
R7061	1.45	1.20	28	99	428	0.284
R7062	1.19	0.99	24	454	413	0.053
Indian Lake, West Canada Lake, New York:						
R7321	2.70	2.24	93	220	241	0.425
R7322	4.78	3.97	135	197	354	0.682
R7326	4.49	3.73	121	223	371	0.543
R7327	1.50	1.25	53	255	283	0.208
Crane Mountain, New York:						
R7125**	5.30	4.42	151	126	293	1.195
R7123	5.58	4.65	165	140	282	1.181
R7126	5.09	4.24	138	187	307	1.740
R7127	5.21	4.33	126	180	344	0.702
R7128	5.21	4.33	122	187	355	0.654

TABLE II-B (cont.)

M.I.T. #	$\%K_2O$	%K	Rb(ppm)	Sr(ppm)	K/Rb	Rb/Sr
Rakosi and Okollo, West Nile District, Uganda:						
R7011	5.82	4.83	163	74	296	2.191
R7012	5.88	4.88	135	31	362	4.366
R7018	5.24	4.35	303	62	147	4.879
R7020	4.81	4.00	207	78	196	2.668

* to accompany Figures 3 and 4 .

** Samples R7125 to R7128 inclusive: potassium analyzed by X-ray Fluorescence, (Whitney, 1967). Rubidium analyzed by isotope dilution, this study.

analyses was confirmed by frequent analysis of G-1 and W-1 throughout the period of analysis. The values obtained agreed to within 1.5% of the recommended values of Fleischer (1965). The rubidium determinations by isotope dilution are of similar precision. The errors in the mass spectrometry are considered in Chapter III. These values, plotted in Figure 4, are compared with the trends found by Shaw (1968) for twenty-one suites of igneous and quasi-igneous rocks whose potassium and rubidium values have been reported with sufficient accuracy in the literature. In view of the geographic diversity, there exists a marked trend in the K/Rb ratio. For the data presented here, the mean K/Rb ratio appears to be about 300 to 400. Considering the Madras charnockite suite alone, there appears to be a slightly higher K/Rb ratio of about 400 (see Table II-C) for specimens having lower potassium contents. The trend for all the samples is somewhat sigmoidal with the axis of symmetry parallel to Shaw's Main Trend at about K/Rb = 300. This Main Trend is defined by 12 of the 21 suites of rocks mentioned

TABLE II-C

Summary of K/Rb Ratios of Charnockitic Rocks (Figure 4)

Locality	n	Average K/Rb Ratio
Madras	10	412
Madras	12	356
Westport	7	478
Indian Lake	4	312
Crane Mtn.	5	316
Rakosi & Okollo	4	250
Total	32	354

above having nearly identical regression coefficients described by

FIGURE 4

K-Rb Trends in Charnockites

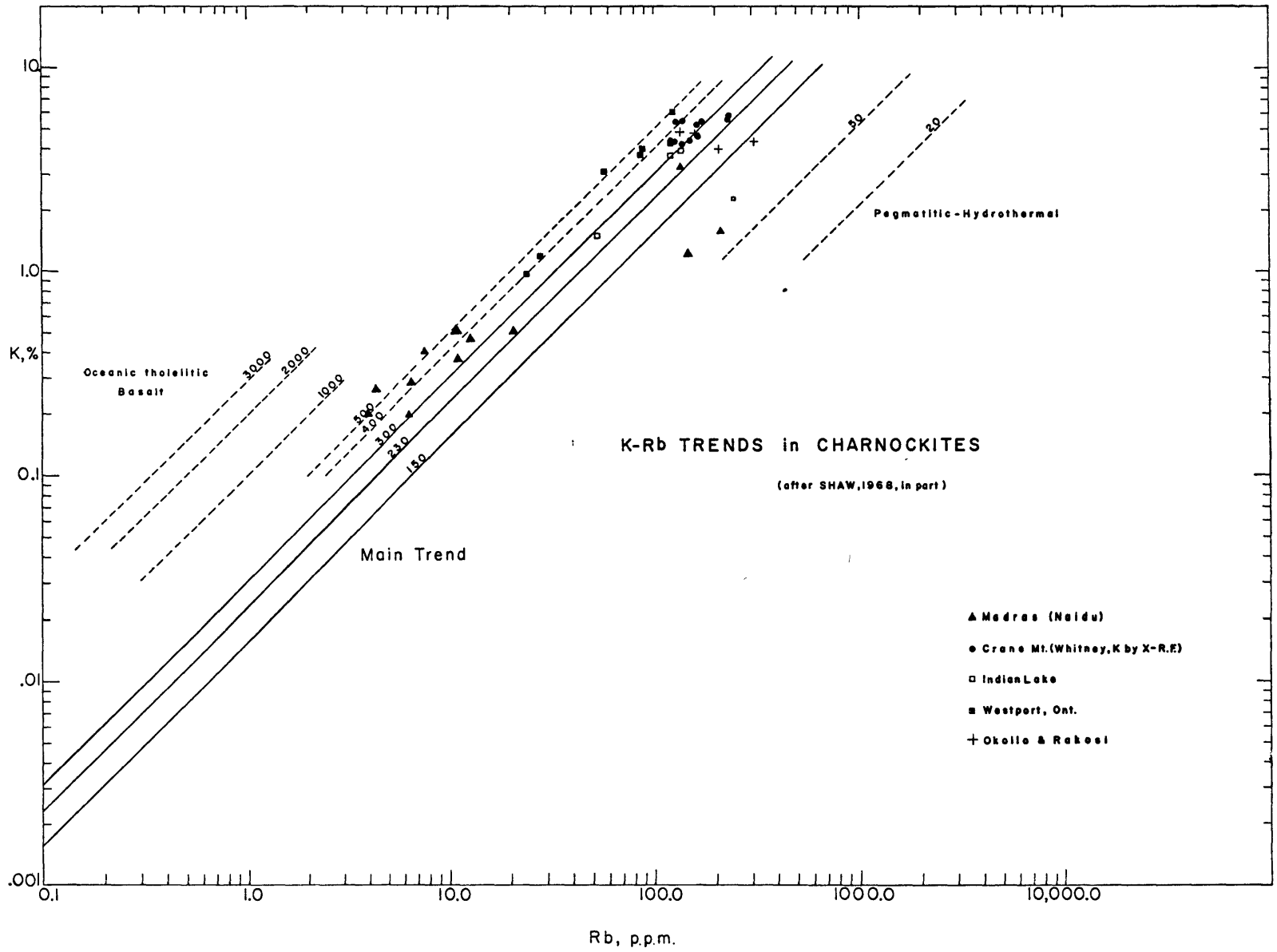
K-Rb TRENDS in CHARNOCKITES
(after SHAW, 1968, in part)
Oceanic tholeiitic Basalt
3000
2000
1000
500
400
300
250
150
Main Trend
50
20
Pegmatitic-Hydrothermal
▲ Madras (Naidu)
● Crane Mt. (Whitney, K by X-R.F.)
□ Indian Lake
■ Westport, Ont.
+ Okolio & Rakosi
K, %
10
1.0
0.1
.01
.001
0.1
1.0
10.0
100.0
1000.0
10,000.0
Rb, p.p.m.

the equation:

$$\%K = 0.0369 \text{ (ppm Rb)}^{0.897}$$

The line of constant R** (= 263) is taken as the overall average Main Trend in igneous differentiation for the 12 sub-parallel suites used in Shaw's study which include the following rock types:

New England Granites (29)
Skaergaard Complex (8)
Slieve Gullion Granites (19)
Continental Tholeiites (41)
Hawaiian Basalts (35)
Ultramafic rocks (23)
Diabases (42)
Banks Peninsula Volcanics (30)
Various Composite Igneous Rocks (9)
Continental Alkalic Basalts (11)
Composite Basalts and Granites (5)
Eclogites (19)

Number of analyses given in parentheses.

The trend in K/Rb is not constant throughout the range in potassium values. Shaw found the following values:

%K	K/Rb
0.01	433
0.1	332
1.0	254
10.0	195

It Is apparent from Table II-C and Figure 4 that the majority of the new analyses fall above the Main Trend for igneous rocks. The results also confirm Shaw's observation that the relation is not linear for all values of potassium but shows a decrease in value of R with increasing potassium: "It should be noticed that the decrease in R

** $R = (\%K/\text{ppm Rb}) \times 10^4$.

observed in these studies was accompanied either by a trend towards younger petrological age or by increased content of K."[3]

Although this investigation was carried out in a different manner from that of Lambert and Heier (1968), both in analytical technique and regional extent of sampling, the results presented here tend to substantiate their results based on a regional scale. That is, there appears to be a tendency for slightly higher K/Rb ratios in these rocks relative to many igneous rock types that Shaw (1968) included in his Main Trend. Additional restraints can be placed on the interpretations of these results in the light of the Rb-Sr isotopic determinations in each suite of rocks. These results are considered in the last chapter.

2.5 Rare-Earth Element Studies

Rare-earth abundances, normalized to the chondrite abundance for each element, have been published now for a variety of rock types from both oceanic and continental areas. Reviews of the older literature are given by Haskin et al.,(1966) and more recent aspects of research in this field are considered by Haskin and Schmitt (1967). Only a brief discussion of the geochemistry of the rare-earth elements will be given here.

The lanthanide elements include the fourteen elements from La (Z = 57) to Lu (Z = 71) and include Y (Z = 39) because both the atomic and M^{+3} ionic radii for this element lie between those values for Tb and Dy despite the fact that yttrium lies above lanthanum in transition element Group III. Although a rare-earth, $_{61}Pm$ is not

---

[3]. Shaw (1968), p. 577.

considered in this work because of its vanishingly low abundance, it is found only in nature as a spontaneous fission fragment of uranium having a maximum half-life of about 30 years for its longest-lived isotope (Pm^{145}). Lanthanum has a ground state configuration of $6s^2$ 5d and the thirteen elements following it are formed by the addition of up to fourteen electrons to the 4f shell which is slightly more stable than the 5d shell. As the nuclear charge and number of 4f electrons are increased by unit increments through the series, there is a reduction in size of the entire $4f^n$ shell, giving rise to the so-called lanthanide contraction. Owing to the shape of the 4f orbitals which are unable to shield to the same degree as the 5d orbitals, the addition of one 4f electron increases the effective nuclear charge of each electron, reducing the size of the orbital. All of the lanthanides form M^{+3} ions. In addition, Nd, Sm, Eu, Tm, and Tb form M^{+2} species and Pr, Nd, Tb, and Dy form M^{+4} ions though these two states are less stable than the characteristic group valency of M^{+3}. The stability of the M^{+3} state may be related to a special stability associated with empty ($4f^{\circ}$), half-filled ($4f^7$), or filled ($4f^{14}$) f shells as is observed to a lesser degree in the regular transition series. Thus La and Y form M^{+3} ions only since the removal of three electrons leaves the inert-gas configuration. Eu and Yb can attain the f^7 and f^{14} configurations respectively in the M^{+2} state. Although there appear to be valid theoretical reasons for the various valence states to occur, the M^{+3} state is thought to be prevalent in nature because fairly rigorous conditions are required (extremes of pH, for example) to attain other valence states in the laboratory.

TABLE II-D

SAMPLE COMPOSITE FOR RARE-EARTH ANALYSIS

MYSORE AND MADRAS STATES, INDIA

M.I.T. #	Sample Wt. (gms.)	Sample Description and Locality
Pallavaram		
R7239/AS-4	10.9	Basic Charnockite (Hb-Bio-rich), Pammal
R7240/AS-5	10.4	Basic Charnockite, Thattangannu
R7241/AS-7	11.6	Basic Charnockite (Hb-rich), Pammal
R7242/AS-10	10.5	Basic Charnockite (Bio-rich) Cherimalai
R7205/AS-12	11.6	Basic Charnockite, St. Thomas Mount
Kushalnagar		
R7214/A-85	10.8	Charnockite, Dindgad
R7215/A-95	10.6	Charnockite, Chikkamarahalli
R7216-A-110	10.8	Charnockite, Kudige-Kanive
R7217/A-115	10.7	Charnockite, Kanive Hill (left)
R7218/A-117	10.7	Charnockite, Kanive-Jainkal Betta
R7219/A-121	11.1	Charnockite, Marur
R7220/A-124	10.6	Charnockite, Kanive Temple Hill (right)
R7221/A-126	10.7	Charnockite, Near Adinadur Tribal Colony
R7248/A-142	10.6	Charnockite, garnetiferous, Doddakamarahalli
R7244/A-148	10.7	Charnockite, Cauvery River Bed, Hulse
R7246/A-150	10.1	Charnockite, Cauvery River Bed, Shanbhoganahalli

TABLE II-E

RARE-EARTH ABUNDANCES IN CHARNOCKITE COMPOSITE, MYSORE AND MADRAS STATES, INDIA

ELEMENT	CHARNOCKITE COMPOSITE	CHARNOCKITE COMPOSITE CHONDRITE*
(Y)	(22.70)	(11.35)
La	12.90	39.1
Ce	16.47	18.7
Pr	4.59	40.8
Nd	17.26	28.8
Sm	4.20	23.2
Eu	1.37	19.9
Gd	4.63	18.6
Tb	0.75	16.0
Ho	0.97	13.9
Er	2.70	13.5
Tm	0.37	12.3
Yb	1.86	9.3+
Lu	0.36	10.6++

* Chondrite R.E.E. values from Haskin, et al., (1967) given in Table II-F

\+ value obtained by γ counting taken because of slight contamination in Yb fraction for β counting by Lu.

++ identical value obtained by both γ and β counting.

TABLE II-F

RARE-EARTH ELEMENT ABUNDANCES IN CHONDRITES
(after Haskin et al., 1967)

ELEMENT	ABUNDANCE
Y	1.96 ± 0.09
La	0.330 ± 0.013
Ce	0.88 ± 0.01
Pr	0.112 ± 0.005
Nd	0.60 ± 0.01
Sm	0.181 ± 0.006
Eu	0.069 ± 0.001
Gd	0.249 ± 0.011
Tb	0.047 ± 0.001
Ho	0.070 ± 0.001
Er	0.200 ± 0.005
Tm	0.030 ± 0.002
Yb	0.200 ± 0.007
Lu	0.034 ± 0.002

TABLE II-G

ELEMENT ABUNDANCES BY SPARK SOURCE MASS SPECTROMETRY, CHARNOCKITE COMPOSITE

Element	ppm Atomic	ppm Weight
B	2	1
F	200	170
Na	2500	2500
Mg	major	major
Al	major	major
Si	major	major
P	3000	4000
Cl	100	150
K	major	major
Ca	major	major
Sc	50	100
Ti	3000	6300
V	800	1800
Cr	1000	2300
Mn	3000	7200
Fe	major	major
Co	75	190
Ni	50	130
Cu	100	280
Zn	120	330
Rb	10	37
Sr	75	290
Ba	50	300
La	<2	12
remaining REE	<2 each	10 each

* This analysis was kindly provided by Mr. T. Mariano, Ledgemont Laboratories, Kennecott Copper Company.

** the 'ppm weight' was calculated from the 'ppm atomic' by taking an 'average' composition for charnockite from the literature (Mariano, personal communication).

TABLE II-H

La, Yb, and Total REE Contents of Igneous Rocks

Rock Type	La*	Yb*	La/Yb	ΣREE*
Gabbros and Diabases (Haskin et al., 1966, p. 224)**				
Ironton, Mo.	12.8	2.7	4.7	123
Bushveldt, Norite	4.8	0.54	8.9	28
San Marcos	4.0	1.70	2.4	59
W-1	9.3	2.2	4.2	96
W-1	11.7	2.1	5.6	100
Finnish, Gabbro + Diabase	1.7	0.8	2.1	22
Eclogites (Ibid., p. 229)				
Delegate	3.6	2.0	1.8	82
Roberts Victor	4.2	1.6	2.6	40
Dutoitspan	7.4	2.3	3.2	116
Japan	1.8	1.13	1.6	34
Granites (Ibid., p. 232)				
Composite, 70% SiO_2	55	4.0	13.8	220
Composite, 60-70% SiO_2	84	4.0	21.0	320
Composite, 60% SiO_2	68	3.0	22.7	250
Composite, Finnish	47	3.0	15.7	260
Finnish, Archean	43	1.8	23.9	200
Finnish, Granite-gneiss	19	2.6	7.3	120
E. Tuva, Radyros	130	1.7	76.5	480
E. Tuva, Nizh-Kad	53	10	5.3	370
E. Tuva, Agash	22	5.5	4.0	230

TABLE II-H (cont.)

Rock Type	La*	Yb*	La/Yb	ΣREE*
Granites (cont.)				
Ukraine, Rapakivi	90	3.2	28.1	230
G-1	92	0.94	97.9	340
G-1	102	0.63	161.9	350
Wisconsin, Red	31	2.3	13.5	180
Wisconsin, Ruby	36	4.3	8.4	220
Basalts (Ibid., p. 223)				
Columbia Plateau	25	3.9	6.4	230
Linz, Prussia	41	3.5	11.7	310
Jefferson Co., Colorado	79	2.6	30.4	530
Composite of 213 basalts	17	2.7	6.3	170
Composite Sediments (Ibid., p. 270)				
European and Japanese Shales	18	2.7	6.7	148
Finnish Sediments	13.6	1.31	10.4	77
40 North American Shales	39	3.4	11.5	240
Russian Platform Average	50	4.2	11.9	280

* in ppm

** All data from compilation from Haskin, et al. (1966), Meteoric, Solar, and Terrestrial Rare-Earth Distributions, in Physics and Chemistry of the Earth, Pergamon Press, Volume 7.

FIGURE 5

Composite of Sixteen Charnockites

(Mysore and Madras States)

India

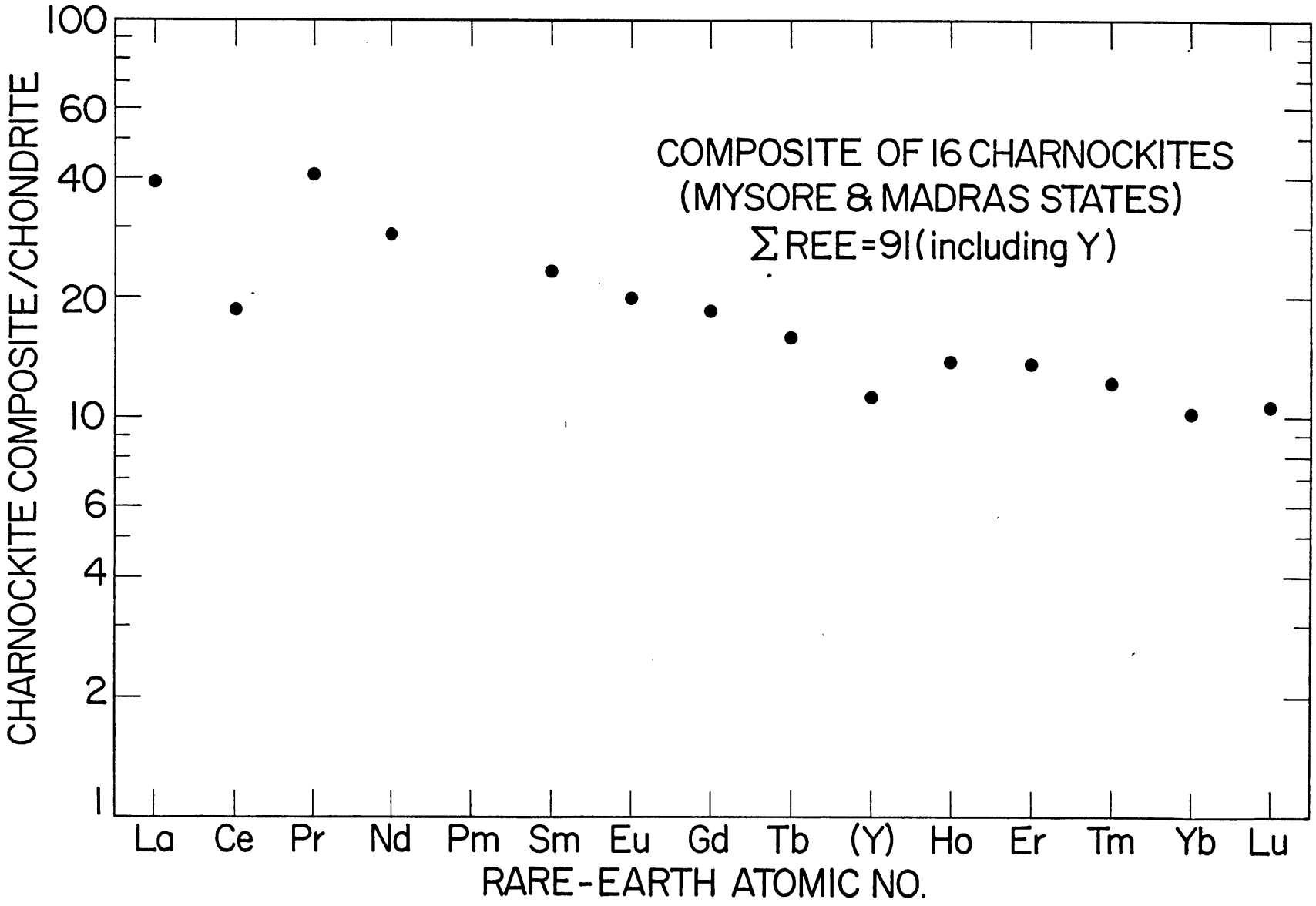
100
60
40
20
10
6
4
2
1
CHARNOCKITE COMPOSITE/CHONDRITE
COMPOSITE OF 16 CHARNOCKITES
(MYSORE & MADRAS STATES)
ΣREE=91 (including Y)
La
Ce
Pr
Nd
Pm
Sm
Eu
Gd
Tb
(Y)
Ho
Er
Tm
Yb
Lu
RARE-EARTH ATOMIC NO.

FIGURE 6

La/Yb versus Total REE

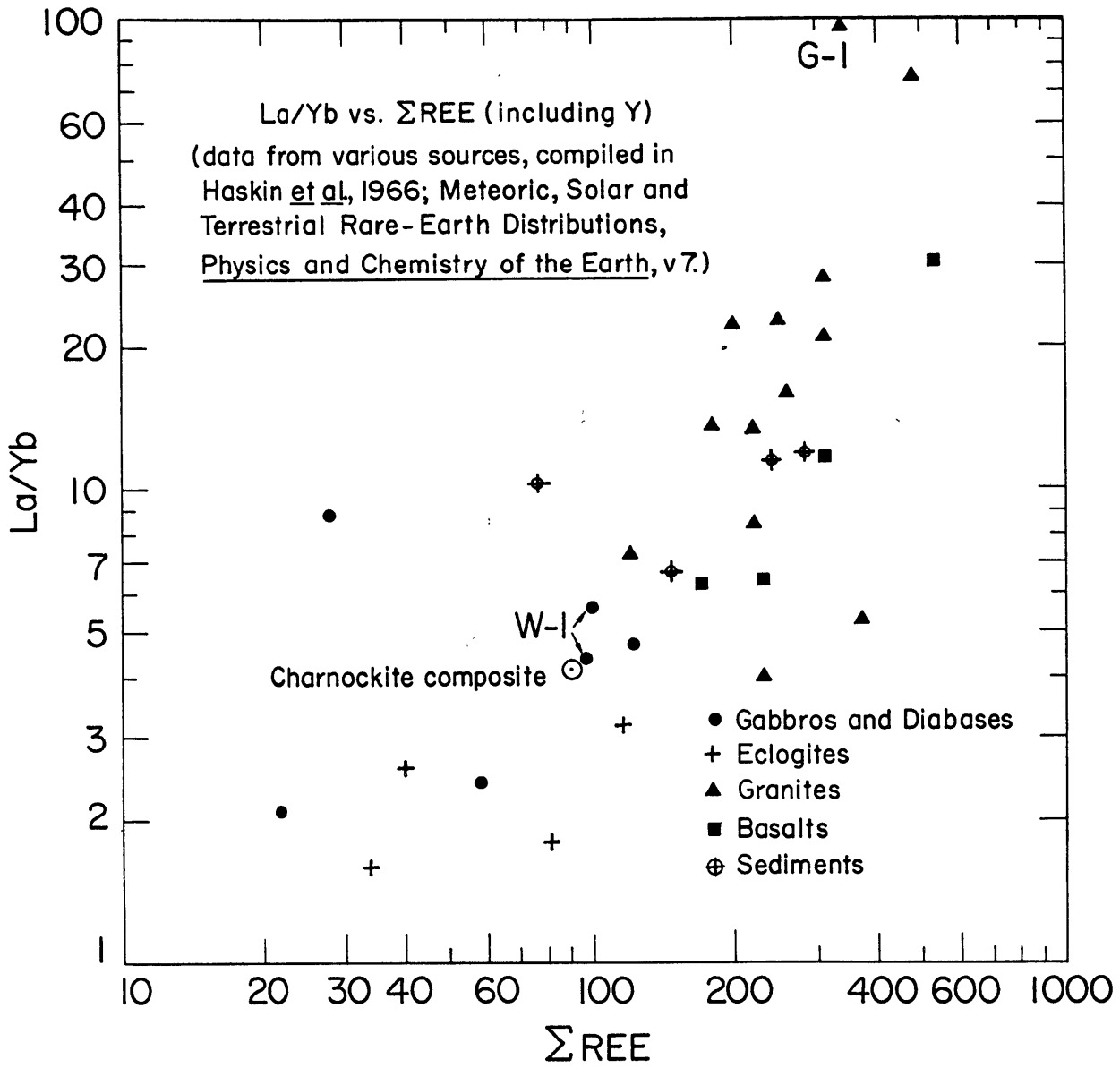
La/Yb vs. ΣREE (including Y)
(data from various sources, compiled in
Haskin et al., 1966; Meteoric, Solar and
Terrestrial Rare-Earth Distributions,
Physics and Chemistry of the Earth, v 7.)
G-1
W-1
Charnockite composite
Gabbros and Diabases
Eclogites
Granites
Basalts
Sediments
La/Yb
ΣREE
100
60
40
30
20
10
7
5
3
2
1
10
20
30
40
60
100
200
400
600
1000

The chemical coherence of this group has always made individual analysis of the rare-earth elements by classical wet chemistry involving fractional crystallization inaccurate,often masking real differences in geochemical abundances. Neutron activation and X-ray spectrographic techniques are routinely used at present to obtain most of the data. Isotope dilution and atomic adborption spectrophotometric methods, however, are now being developed to the required sensitivity for this work.

In the present study, the REE abundances have been determined by a neutron activation technique developed by Haskin et al. (1968). Briefly, the method entails the irradiation of the powdered rock sample along with a standard solution containing a mixture of rare-earth nitrates. The rock powder is dissolved by means of a Na_2O_2 fusion in the presence of a rare-earth carrier. The rare-earth group is separated from the silicate residue by hydroxide and oxalate precipitations and the individual rare-earths in both sample and standard are separated by means of an ion-exchange column. A radioassay is made by both γ and β counting and then corrected by a chemical yield determination by EDTA titrations. The method is found to have an average precision for duplicate analyses by different analysts of better than $\pm$.4% mean deviation (for a shale having a total REE content of 200 ppm). The mean deviation varies from element to element and since there was only a single determination made in this study, such a high degree of accuracy cannot be claimed, though comparable precision is likely. The analytical procedure has been presented in detail by Haskin et al.[4]

---

[4]. Jour. Radioanalytical Chemistry (1968), 1, pp. 337-348.

A composite of sixteen samples of charnockite from Madras and Mysore States, India, weighing about 10-11 grams each was prepared (Table II-D) in the same fashion as used in the Rb-Sr analyses. This composite was analyzed as in the method above and the concentrations are shown in Table II-E. These values, when normalized to the currently accepted REE chondrite abundances (Table II-F) give a REE abundance pattern as shown in Table II-E, column 3, and Figure 5.

Twenty-five element abundances were determined by Spark Source Mass Spectrometry (Table II-G) for the Indian Charnockite composite. This analysis was kindly provided by Mr. T. Mariano of the Ledgemont Laboratories, Kennecott Copper Company, Lexington, Massachusetts. The 'ppm Atomic' concentration was converted to 'ppm Weight' by dividing each element concentration by the 'molecular weight' of an 'average' charnockite taken from the literature (T. Mariano, personal communication). The precision in each determination is about 300 atomic percent.

2.6 Discussion of Results of Rare-Earth Element Studies

In Figure 5 the chondrite normalized rare-earth abundances for the charnockite composite are plotted, including yttrium. The outstanding feature in this pattern is the enrichment of the light REE relative to the heavy REE when normalized to the chondrite values. The trend, with minor exceptions, is remarkably smooth with no apparent anomalies. Europium shows no depletion with respect to gadolinium and samarium as is commonly the case if granitic rocks. Cerium appears to be somewhat depleted. Owing to analytical difficulties with this element, replicate determinations are needed to verify its

apparent lower abundance. Yttrium also appears to be slightly depleted in these rocks. This element is not a rare-earth and is included because it commonly behaves in a similar fashion to dysprosium. Depending upon the ion exchange resin and the eluent used, yttrium may separate between terbium and holmium or ytterbium and lutecium.

The total rare-earth element content is 91 ppm (including Y). This value is compared with a measure of enrichment of the light REE/heavy REE approximated by the La/Yb ratio (Figure 6). Since lanthanum shows greater variability than ytterbium, especially in granitic rocks, there are certain drawbacks to using this ratio alone. While there is no consensus on which elements to use, some Russian workers use a parameter such as La+...+Gd/Er+...+Lu as a measure of enrichment. Despite the scatter, there is a pronounced tendency for the enrichment of the light REE with increase in total REE as has been pointed out previously by Haskin et al. (1966, p. 221).

The detailed rare-earth distribution pattern (Figure 5) and the comparison of La/Yb vs. total REE enrichment (Figure 6) suggests that the charnockite composite from Madras and Mysore States is most nearly like patterns found for gabbroic rocks. This pattern is in keeping with the intermediate nature of the rock composite. Examination of thin sections of all the specimens of this composite show a quartz content of about 10% and a composition approximating a quartz diorite.

In addition to the individual rare-earth determinations involving prior chemical preparation, four single specimens of pyroxene granulite--three from Madras State, and one from Westport, Ontario--were analyzed

after irradiation as powders (-200 mesh) without prior chemical treatment or separation following a method outlined by Gordon et al. (1968).

From 0.1 to 0.8 grams of the aliquots of the powdered samples were weighed into clean 2-dram vials and were irradiated three-at-a-time along with a flux monitor of similar rare-earth content (Table II-I) in the M.I.T. Research Reactor with a flux of 2×10^{13} n cm^{-2} sec^{-1}. To measure the short-lived species, an irradiation time of ten minutes was used and in the case of longer lived species, five hours' irradiation time elapsed followed by five days' "cooling" to allow the activity to decrease to about 0.5 microcuries.

Radioassay was made by means of a 30 cm^2 Ge(Li) detector. A sample holder consisting of fifteen milled depressions was provided in front of the crystal for counting and a position was chosen such that the dead time of the detector was below 30%. Lead shielding was used sparingly to reduce background, yet was not placed so close to the sample to interfere with the spectrum through backscattered electrons. The detector signal was amplified by a Tennelec TC 130 field effect transistor preamplifier and a TC 200 main amplifier. The amplified signal was stored in a Packard 4096 channel analyzer and the spectrum was placed on computer compatible magnetic tape via an ADC (analog to digital converter) unit.

The computer program, written by Dr. P. A. Baedecker, searches out the photopeaks, calculates their area, centroid and energy. A correction to the area is also made for detector efficiency. A Cs

spectrum must be provided if the energies are to be determined and if the γ-ray energy of the standard photopeak is greater than 1836 keV, a Y^{88} spectrum must also be provided. The following spectra were used in each counting experiment: Hg^{203}, 279.1 keV; Y^{88}, 1836.1 keV; Na^{22}, 1274.5 keV; Cs^{137}, 661.6 keV; Co^{60}, 1332.4 keV.

TABLE II-I

Flux Monitors

Long-Lived				Short-Lived	
	u gm/ml		u gm/ml		u gm/ml
Ce	171.17	Cs	9.70	V	35.26
Nd	183.4	Cr	101.0	Mg	15.68
Gd	51.94	Co	48.88	Na	576.0
Tb	1.019	Th	102.2	Mn	2 56.82
Tm	1.145	Sb	24.48	Al	4.77
			mg/ml		
Yb	2.83	Rb	1.046	K	7 .56
Lu	5.69	Ba	1.34	La	7 5.55
Sc	10.4	Hf	10.29	Sm	9.32
		Fe	20	Eu	2.21
				Dy	5.17
				Ho	5.05

In the table below (Table II-J) the abundances of the individual rock analyses are shown in ppm unless otherwise indicated. The peaks chosen for analysis are those indicated by Gordon et al.(1968) which are relatively free from interference from other elements of high

TABLE II-J

Some Elemental Abundances by Neutron Activation for Pyroxene Granulites

M.I.T.#	Tm	Gd(+Sm+Ta)	Hf	Ce	Lu	Nd	Sc	Co	Th	Fe
R7120/ACS-40 Crane Mountain, New York	--	19*	19	343**	7	50	11	9	53	3.3%
R7121/ACS-41 Crane Mountain, New York	--	1	15	216**	4	28	7	9	13	2.8%
R7129/ACS-48a Crane Mountain, New York	1	17	15	200**	5	48	11	8	--	4.3%
R7091/32 Westport, Ontario	0.1	4	9	179**	3	38	25	14	--	3.8%

* abundances in ppm unless indicated otherwise.

** probable interference of Fe^{59} (E = 145 keV) with Ce^{141} (E = 145.43 keV).

Precision based on replicate analysis is about ± 25%.

abundance. The worst interference was found to be from 45^{d} Fe^{59} with a photopeak at E_{γ} = 142.5 keV with 33^{d} Ce^{141} E_{γ} = 145.43 keV. This interference invariably resulted in an unreasonably high value of about 200 ppm for this element.

The abundances of Co and Sc reported here are of a similar magnitude reported by Howie (1955) for the Madras Charnockite Series. In the case of Co, the values range from 100 ppm to less than 5 ppm and Sc has a reported variation from 30 ppm to 10 ppm. The values determined by Spark Source Mass Spectrometry on the charnockite composite at Co = 190 ppm and Sc = 50 ppm seem to be in rough agreement with the values found by Howie for individual specimens.

Conclusions based on so few analyses can only be tentative and though this aspect of the study is far from complete, the technique of instrumental activation analysis (INAA) holds great promise for trace element analysis, especially with the increase in resolution with Ge(Li) detectors.

2.7 Summary of Chapter

In this chapter, three geochemically useful parameters have been used to investigate the variations found in the "charnockite series".

The differentiation index defined by Thornton and Tuttle (1960) has been calculated for fifty-four analyses taken from the literature, and when plotted against the weight percent SiO_2 in the rock, the trends outlined by these analyses coincide with those found by Thornton and Tuttle for igneous rocks.

The K/Rb trends determined for thirty-two specimens from the collections available for this study show a trend that is parallel to the Main Trend found by Shaw (1968) for igneous and quasi-igneous rocks. There is a suggestion that the pyroxene granulites analyzed in this study may be depleted in Rb with respect to potassium when compared to this Main Trend. The extent of depletion is discussed in Chapter IV. The details of the pyroxene granulite trend seem to parallel Shaw's Main Trend closely, showing a degrease in the K/Rb ratio as potassium and rubidium both increase.

A study of the rare-earth element abundance pattern for a composite of sixteen samples of pyroxene granulite (charnockite) from the type localities in Madras and Mysore States of India, shows an enrichment of the light rare-earth elements when each element is normalized to its chondrite abundance. The rare-earth pattern coincides almost exactly, element for element, with the pattern found for the Duluth gabbro. The total mineralogy of the composite analyzed is in agreement with the observed rare-earth pattern.

On the basis of these three aspects of total rock chemistry of this series, an igneous origin for these rocks is possible. The mineralogical assemblages observed in these rocks point to a later metamorphic episode that was of such intensity to give rise to high grade assemblages consisting of garnet, hypersthene and myrmekite.

CHAPTER III

RUBIDIUM-STRONTIUM ISOTOPIC VARIATIONS IN THE PYROXENE GRANULITE FACIES

3.1 General

An hypothesis of wide acceptance in geochemical investigations of crust-mantle systems is that the total earth is similar in composition to that of Type I carbonaceous chondrites (Urey, 1953; Mason, 1960; Ringwood, 1961) which are more primitive in their chemical composition than any other class of meteorites. These volatile-rich and highly oxidized bodies are suggestive of a primordial material which accreted into a small body and was subjected to only mild thermal metamorphism, less than 200°C, so that the more volatile elements were largely retained. The present day differences in element abundances and isotopic ratios in the crust are the result of an early differentiation of the core, mantle and crust.

Gast (1962), Faure et al. (1962), and Hedge and Walthall (1963) have suggested that the initial ratio of 0.698 ± 0.001 determined for stony meteorites by Gast (1962) and Pinson et al.(1965), and Shields (1965) be adopted as the initial ratio for the primordial earth 4.5 b.y. (billion years) ago. Early development of the continental plates involving upward movement of strongly lithophile elements such as K, Rb, U, Th, Pb, and Ba from the upper mantle has strongly depleted this region with respect to these elements. Further redistribution of these elements through the geological cycle involving erosional processes and possibly regional metamorphism has given rise to large variations in certain elemental ratios. Pertinent to this discussion are the

variations in the Rb/Sr ratio in the crust and mantle.

In magmatic processes, Rb^{+} (1.48 Å, Pauling) and Sr^{++} (1.13 Å, Pauling) are concentrated in the silicate melt phase during partial melting or differentiation. Similarity of ionic charge and size allows Sr to follow Ca by diadochic substitution into calcium-bearing phases and likewise Rb follows K into potassic phases such as potash feldspar or biotite so that during magmatic crystallization there is an increase in the Rb/Sr ratio as crystallization proceeds.

Various compilations of data for the $(Sr^{87}/Sr^{86})_o$ ratio have been given by Faure and Hurley (1963), Hedge and Walthall (1963), Tatsumoto et al. (1965), and Bence (1966) for oceanic and continental basalts. The measured Sr^{87}/Sr^{86} ratios are remarkably uniform varying by less than 2%. The range in Sr^{87}/Sr^{86} for oceanic basalts is rather narrow from 0.700 to 0.706 whereas continental basalts have higher values generally from 0.703 to 0.705 with occasional values as high as 0.710 (Steuber and Murthy, 1966). Ultramafic inclusions have a similar range as found in continental rocks of similar bulk chemistry Steuber et al. (op.cit.). Hedge and Walthall (op.cit.) have interpreted older continental basalts as having come from the upper mantle and postulate a straight line growth of Sr^{87}/Sr^{86} in this region from the primordial 0.698 value to a present day ratio of about 0.703. This would require a Rb/Sr = 0.03 approximately for the upper mantle basalt source region. Many oceanic tholeiitic basalts have Rb/Sr ratios of about 0.01 and Tatsumoto et al. (1965) and Bence (1966) suggest that the source region had a higher Rb/Sr ratio (to give rise to the observed Sr^{87}/Sr^{86} ratios) but underwent differentiation

ca. 1 b.y. or more ago.

Granitic rocks show much greater variability in Sr^{87}/Sr^{86} initial ratios with values overlapping with basalts and as high as 0.734 and 0.741 recorded in the Heemskirk granite (Heier and Brooks, 1966). The majority of the initial ratios, however, are about 0.710 or less (Hedge and Walthall, op.cit.; Hurley et al. 1965; Fairbairn et al. 1964a, 1964b). In view of the higher ratios encountered in sediments (see below), Hurley et al. (1965) conclude that granitic rocks are not formed entirely by selective fusion of reworked sedimentary material in a geosyncline.

Sedimentary rocks commonly have high Rb/Sr ratios so that high Sr^{87}/Sr^{86} ratios are developed with time. Whitney (1964) and Compston and Pidgeon (1962) report values between 0.710 and 0.720 for shales and Faure and Hurley (1963) have found a value of about 0.720 for a composite of Paleozoic shales from both the east and west coast with a Rb/Sr ratio of 0.4. In recent oceanic sediments the detrital component ranges from 0.709, the value of present day sea water, to about 0.730, (Dasch et al., 1966). Faure et al. (1963) estimate a Sr^{87}/Sr^{86} ratio of about 0.720 for the Canadian shield from determinations on fresh water calcareous shales.

Hurley and Fairbairn (1965) have presented additional data for the marine geochron which shows a non-linear smooth growth in the Sr^{87}/Sr^{86} ratio with time to the present day value of 0.7093 for modern sea water. This growth from the primordial value is only 1.55% over 4.5 billion years. Recently Peterman et al. (1967) have shown that the primary strontium composition of sea water as preserved in

marine limestones may be altered by diagenesis of the carbonate or inclusion of varying amounts of clay minerals. Dasch et al. (1966) have found values as high as 0.7394. Variations in this value in limestones are also strongly affected by the average Sr^{87}/Sr^{86} value in the surrounding source regions of sediment. Hoefs et al. (1968) have recorded the following variations in marine limestones of Europe:

TABLE III-A

Sr^{87}/Sr^{86} Ratios from European Limestones*

Composite of 32 Devonian Limestones	0.7174
Composite of 45 Jurassic Limestones	0.7129
Composite of 16 Cretaceous Limestones	0.7141
Recent fresh water Limestones (Westerhof, Northeim)	0.7113

*Hoefs, J. and Wedepohl, K. H. (1968) Sr Isotope Studies on Young Volcanic Rocks from Germany and Italy, Contr. Mineral. and Petrol., 19, pp. 328-338.

The results of the Sr^{87}/Sr^{86} variations in limestones have important implications in the interpretation of the initial Sr^{87}/Sr^{86} ratio of the Westport, Ontario pyroxene granulites discussed below.

3.2 Initial Ratios in Anorthosites and Pyroxene Granulites

Heath (1967) determined the strontium isotopic relationships for specimens from fifteen anorthosite bodies in North America and Norway, giving special attention to the Adirondack Massif in New York State. The total range in Sr^{87}/Sr^{86} initial ratios found by Heath was from 0.703 to 0.706. A summary of individual anorthosite bodies is given in Table III-B.

TABLE III-B

Summary of $(Sr^{87}/Sr^{86})_o$ for Anorthosites (after Heath, 1967)

Area	No. of Samples	$(Sr^{87}/Sr^{86})_o$	Range
Adirondacks	13	.7049 ± .0003	.7043-.7056
Larami, Wy.	8	.7052 ± .0002	.7048-.7054
Boehls Butte, Ida.	5	.7046 ± .0005	.7039-.7049
Honeybrook, Penna.	2	.7040	.7038-.7041
Nain, Labrador	3	.7055	.7052-.7059
Michikamau, Labrador	3	.7036	.7024-.7048
Morin, Quebec	2	.7052	.7050-.7054
Sept.-Isles,Quebec	2	.7041	.7039-.7043
Penticote, Quebec	1	.7031	
Lake St. John, Quebec	2	.7033	.7029-.7036
San Gabriel, Cal.	1	.7032	
Ekersund-Sojndal, Southern Norway	2	.7059	.7056-.7061
Naero Fjord, Central Norway	3	.7031	.7031-.7032
Pluma Hidalgo, Mex.	3	.7040	.7038-.7042
Roseland, Va.	4	.7052	.7047-.7056

The narrow range in initial ratios, the absence of high Sr^{87}/Sr^{86} ratios, and the fact that most of the measured ratios have a lower value than that for sea water at their time of origin suggests a derivation from the upper mantle or an even lower crustal level rather than a generative process involving anatexis, metamorphism or metasomatism.

Man Charnockite Series, Ivory Coast:

The geochronology of this region has been described recently by Papon et al. (1968). The area consists largely of norites and andesine

quartzites cut by leuco- and biotite granites partially transformed to charnockite. To the south there are hypersthene gneisses, charnockitic gneisses, and leucocratic and biotite migmatites in association with granodioritic orthogneisses. Papon et al. analyzed 14 whole rock specimens and their mineral separates of both the charnockitic and granodioritic series and found that both gave an isochron age of 2700 m.y. The two series, however, form two distinct groups:

Granodioritic Migmatite Series:	2701 ± 135 m.y.	0.699 ± 0.001*
Charnockite Series:	2750 ± 107 m.y.	0.707 ± 0.001

*based on a least squares regression method of McIntyre et al. (1966) $= 1.47 \times 10^{-11}\ y^{-1}$.

They propose that the higher initial ratio in the charnockite series indicates an origin in the sialic crust whereas the granodioritic series, while giving the same age, is of mantle origin. Since the initial ratios are not reported relative to the E & A Standard or an equivalent, the 0.699 value for the migmatite may be somewhat low.

Lewisian Basement Gneisses Near Lochinver, Sutherland:

The Lewisian on the northwest coast of Scotland was divided by Sutton and Watson (1951) into two chronological divisions: the 'Scourian' granulite facies metamorphic event and a later 'Laxfordian' amphibolite facies metamorphism. Evans (1965) has examined the strontium whole rock isotopic composition from each metamorphic facies from Lochinver, Sutherland (Table III-C).

Potassium-Argon dating of biotite and hornblende set the Scourian episode at a minimum age of at least 2600 m.y. The Inverian episode followed the intrusion of pegmatites at 2250 ± 50 m.y. (Evans, 1963) and is recognized as a period of almandine amphibolite facies metamorphism and structural deformation. Hornblende and biotite K-Ar

TABLE III-C

$(Sr^{87}/Sr^{86})_o$ ratios in Lewisian Gneiss, Lochinver

Scourian Pyroxene Gneiss	
Ultrabasic body	0.7105
Basic garnet gneiss	0.701
Basic gneiss	0.7070
Acid gneiss	0.7003
Acid gneiss	0.7083
Average Sr^{87}/Sr^{86} ratio weighted for strontium content:	0.7065
Inverian and Laxfordian Amphibolite Gneiss	
Ultrabasic body	0.7008
Basic garnet gneiss	0.7029
Acid gneiss	0.7073
Acid gneiss	0.7038
Average Sr^{87}/Sr^{86} ratio weighted for strontium content:	0.7053

determinations give an age between 2100 and 1560 m.y. with 2100 m.y. the preferred age for this event. The final Laxfordian episode consisted of relatively confined epidote amphibolite facies metamorphism dated at about 1580 m.y. by K-Ar, Giletti et al. (1961).

Evans concludes that the low $(Sr^{87}/Sr^{86})_o$ ratios for these rocks indicates a source region lower in Sr^{87}/Sr^{86} than most igneous rocks, and, further, if this complex ever contained normal crustal abundances of Rb, it was removed within a short time (about 300 m.y.) after differentiation from the mantle.

Mysore and Madras Charnockite Series:

Recently Crawford (1968) has presented chronological data by rubidium-strontium methods for the vast area of Peninsular India and Ceylon including several members of the charnockite suite from various localities in Mysore and Madras States:

Tamizhagam, Nilgiri Charnockites and Gneiss: 2615 ± 80(4), 0.7023 ± 0.0012
Madras City Charnockites: 2580 ± 95 m.y., 0.7059 ± 0.0042.

The charnockitic gneisses of the Nilgiri Hills region give an age slightly older than that of the Peninsular Gneisses of Bangalore (2585 ± 35 m.y.). The results obtained by Crawford (1968) will be discussed further in the light of the present study of Mysore and Madras States considered below.

3.3 Analytical Procedures

All rubidium and strontium determinations were made by mass spectrometry in the M.I.T. Geochronology Laboratory. In the case of strontium, isotopic ratios were obtained on both spiked and unspiked samples, the latter in cases where no rubidium was detected by X-ray fluorescence (detection limit 5 ppm).

In general, the standard analytical procedures of this laboratory were used throughout the investigation. The procedures used for sample preparation, calibration and use of spike solutions, and method of calculation of the isotope dilution ratios have been presented in detail recently by Reesman (1968).

Mass Spectrometry:

During the course of this investigation only one mass spectrometer, designated "Sally", was used for all the isotopic measurements. The instrument used was a 6-inch, 60° sector, solid-source, single filament, Nier-type mass spectrometer utilizing a Cary model 31 vibrating reed electrometer (VRE) to amplify the ion beam current. The VRE output was recorded on a Brown strip chart recorder. The vacuum for

the system was attained by means of a mercury diffusion pump backed by an oil-seal mechanical fore pump. A liquid nitrogen cold trap was provided for cryogenic pumping of condensibles between the diffusion pump and the mass spectrometer analyzer tube. Pressures of less than 5×10^{-6} mm Hg were found necessary for successful rubidium analyses and lower pressures of less than 1×10^{-6} mm Hg were needed for strontium runs. Throughout the study peak-hopping was used to obtain the isotopic ratios after continuous magnetic scanning over the appropriate mass range was made to check the base line to determine whether there was a pressure broadening effect which would seriously limit resolution. This scanning also provided a check for contamination by rubidium during strontium analyses since there should be no peak at m/e = 85.

Tantalum ribbon filaments 0.020" wide and 0.001 " thick were used in all the analyses. It was found that a thin layer of an aqueous slurry consisting of Ta + TaO + sucrose provided smoother emission during rubidium analyses and was used consistently throughout the investigation. Previous monitoring of the filament for cleanliness was made prior to addition of sample to the filament. Each sample, stored in a Vycor beaker, was nitrated with 1:1 HNO_3 (triply distilled) and a small portion (on the order of 0.5 ugm) was evaporated onto the heated filament using a fine Vycor capillary.

The calculation of the rubidium and strontium concentrations and the strontium isotopic ratios from spiked samples has been revised and brought up to date by Reesman (1968) following an earlier outline of the method by Van Schmus (1966) and reference should be made to these papers for the actual details of the calculations.

Isotope Dilution Analysis for Strontium and Rubidium:

During this investigation only one Sr^{84} spike was used for all determinations. The isotopic composition of this spike solution was measured several times by different analysts and using different mass spectrometers. Two different shelf solutions were used in the calibration of the rubidium and strontium spike solutions:

	RVS	CMS
Sr	60.74 ugm Sr/ml	68.16 ugm Sr/ml
Rb	101.8 ugm Rb/ml	80.35 ugm Rb/ml

Both shelf solutions were prepared from carefully dried and accurately weighed Johnson-Matthey 'Specpure' $RbCl_2$ and $Sr(NO_3)_2$.

The isotopically-enriched Sr^{84} spike obtained from Oak Ridge National Laboratory was found to have the following average isotopic composition:

$$Sr^{86}/Sr^{84} = 0.04685$$
$$Sr^{87}/Sr^{84} = 0.01574$$
$$Sr^{88}/Sr^{84} = 0.13875$$

The concentration of the spike was determined three times by different analysts prior to and during the course of this study:

ugm Sr^{84}/ml	Analyst and Date
1.948	P.M. Hurley, 6/29/67 (Connie)
1.94	C.M. Spooner, 7/12/68 (Sally)
1.941	R.S. Naylor, 1/68

Rubidium was determined by isotope dilution using three spike solutions isotopically enriched in Rb^{87} provided by Oak Ridge National Laboratory.

Spike Solution	ugm Rb/ml	ugm Rb^{87}/ml	Analyst & Date
65-A Rb^{87}Spike+	11.304	11.210	PMH 4/11/67*
65-A Rb^{87}Spike	11.458	11.363	CMS 6/20/68**
65-A Dilute Rb^{87} Spike+	3.467	3.438	CMS 6/19/68**
Rb^{87}Spike++	9.819	9.742	CMS **

+Rb^{85}/Rb^{87} = 0.00841 (PMH, Connie)
++Rb^{85}/Rb^{87} = 0.00789 (PMH, Connie, 9/19/68)
*analyzed on 12" mass spectrometer "Connie"
**analyzed on 6" mass spectrometer "Sally"

3.4 Analytical Precision

Replicate Analysis of the E & A Strontium Isotopic Standard:

In keeping with common practice in the M.I.T. Geochronology Laboratory, the operating characteristics of each mass spectrometer are monitored through frequent analysis of a strontium standard. Such analyses are of considerable importance when changes or adjustments have been made to the mass spectrometer source, for example, changing or re-positioning the filament posts. The standard used is the Eimer and Amend spec-pure $SrCO_3$ (Lot No. 492327) originally provided to this laboratory by Dr. S. R. Hart, of the Department of Terrestrial Magnetism, Carnegie Institute, Washington, D.C. Immediately prior to this investigation, the 6-inch mass spectrometer "Sally" was used extensively in

R. H. Reesman's study (1968) and his measurements for the E & A standard are presented in Table III-E along with subsequent measurements made during this study. It can be seen that good agreement was obtained over the period of analysis (Table III-D). The standard deviation for these analyses is compared with that found by Reesman (1968) on the same instrument. The standard deviation is calculated from the expression:

$$\sigma = \pm \sqrt{\frac{\sum(x_i - \bar{X})^2}{n - 1}}$$

where x_i is a value of the i th analysis, $\bar{X}$ is the arithmetic mean of all n analyses.

TABLE III-D

Standard Deviations of E & A Standard Replicate Analyses

Analyst	$(Sr^{86}/Sr^{88})_{mean}$	$(Sr^{87}/Sr^{86})_{mean}$	
R. H. Reesman	0.1191	0.7086	$\pm$ 0.0004 $\pm$ 0.0008
C. M. Spooner	0.1199	0.7083	$\pm$ 0.0004^2 $\pm$ 0.0008^4

Assuming the variation among analyses is normally distributed, σ gives the 68.27% confidence level and 2σ gives the 95.45% confidence level for these analyses over the period of investigation.

3.5 Blank Corrections:

Throughout the history of this laboratory the levels of contamination for rubidium and strontium have been demonstrably low, usually $\ll$1 ugm for each. In this study the concentrations of rubidium and strontium in the rock samples were such that the blank contamination

TABLE III-E

Replicate Analyses of E & A Isotopic Standard

Record	Date	$(Sr^{86}/Sr^{88})_{measured}$	$(Sr^{87}/Sr^{86})_{normalized}$
R. H. Reesman, Unpublished Ph.D. Thesis, M.I.T., p. 27:			
3372(L)*	2 Nov/63	0.1202	0.7083
3404(N)	29 Nov/63	0.1186	0.7080
3715(N)	11 May/64	0.1193	0.7087
3745(N)	22 May/64	0.1186	0.7085
3770(N)	4 Jun/64	0.1188	0.7086
3799(N)	24 Jun/64	0.1187	0.7089
3811(S)	29 Jun/64	0.1189	0.7085
4974(S)	3 Nov/66	0.1194	0.7091
4991(S)	19 Nov/66	0.1194	0.7090
5066(S)	12 Jan/67	0.1191	0.7091
5197(S)	30 Mar/67	0.1187	0.7081
5245(S)	3 May/67	0.1188	0.7084
5260(S)	10 May/67	0.1193	0.7085
5364(S)	22 Jun/67	0.1196	0.7081
5538(S)	8 Sep/67	0.1183	0.7083
5639(S)	20 Nov/67	0.1190	0.7085
5671(N)	11 Dec/67	0.1183	0.7083
5678(N)	14 Dec/67	0.1181	0.7083
5685(N)	22 Dec/67	0.1193	0.7091
5713(N)	15 Jan/68	0.1198	0.7084
5747(N)	31 Jan/68	0.1182	0.7084
This study:			
5654(S)	29 Nov/67	0.1187	0.7083
5746(S)	30 Jan/68	0.1204	0.7085
5942(S)	10 Aug/68	0.1198	0.7086
6038(S)	7 Nov/68	0.1207	0.7088
6055(S)	22 Nov/68	0.1202	0.7082
6137(S)	20 Jan/69	0.1199	0.7076
6237(S)	8 May/69	0.1188	0.7082

*M.I.T. Geochronology Laboratory mass spectrometer designation: Lulu = (L); Nancy = (N); Sally = (S).

was inconsequential. Blank runs made during this study verify the levels found by Reesman (1968) at about 0.03 ugm for rubidium and 0.032 ugm for strontium.

3.6 Mass Spectrometer Fractionation (Mass Discrimination):

In the mass spectrometric determination of strontium isotopic ratios it is assumed that the ratio of Sr^{86}/Sr^{88} is invariant in Nature. The value assumed for this ratio is 0.1194 as measured by Bainbridge and Nier (1950) and the measured Sr^{87}/Sr^{86} ratios are normalized to this value.

In the case of the isotopic measurement of rubidium, the analyst is plagued by variations in the measured Rb^{85}/Rb^{87} ratio resulting from fractionation. Unfortunately, the effect cannot be corrected for by normalization as in the case of strontium, since natural rubidium contains two isotopes only. Apart from uncertainties in the decay constant and inhomogeneities in the geological system, the error due to uncorrected fractionation of rubidium in the mass spectrometer accounts for the largest error in the determination of "absolute age" of a rock system. In any case, revision of present day determinations can be made simply when eventual consensus is achieved, if ever, on the present 6% disparity in the two values for the decay constant in common use. On the other hand, precise corrections for Rb^{85}/Rb^{87} mass spectrometer fractionation cannot be made at present and only an approximate indication of the extent of fractionation can be had by repeated runs on unspiked normal rubidium.

Shields et al.(1963) have repeatedly measured the Rb^{85}/Rb^{87} ratio in a rubidium sulfate standard obtained from geological material ranging

in age from 20 to 2600 m.y. The analyses were performed on a 12-inch mass spectrometer using triple-filament ionization yielding a value of 2.5995 $\pm$ 0.0015 at the 95% confidence level. The natural variation in the atomic abundance ratio of this element is less than the experimental error.

During the present study, the Rb^{85}/Rb^{87} ratios of the specpure Johnson and Matthey RbCl C.M.S. Shelf and six samples prepared following the normal chemical procedure were measured (Table III-F):

TABLE III-F

Measured Rb^{85}/Rb^{87} Ratios

Date	Sample	Rb^{85}/Rb^{87}
29 Mar/68	C.M.S. RbCl Shelf Solution	2.5006
10 Apr/68	C.M.S. RbCl Shelf Solution	2.5827
13 Feb/68	R7025, Okollo, Uganda	2.5760
13 Feb/68	R7042, Okollo, Uganda	2.6093
13 Feb/68	R7042, Okollo, Uganda	2.5938
22 Feb/68	R7120, Crane Mtn., N.Y.	2.5397
20 May/68	R7012, Rakosi, Uganda	2.6179
12 Jun/68	Uganda	2.5214
12 Jun/68	Uganda	2.5806
	Arithmetic mean =	2.5770

With the exception of the C.M.S. RbCl Shelf Solution analyses, the mean for these analyses is 2.5770 and using the statistic for the standard deviation discussed previously: $\sigma = \pm 0.0353$ and $2\sigma = \pm 0.0706$ at the 68.27% and 95.45% confidence levels respectively.

Of all the analyses, one of the C.M.S. RbCl Shelf Solution analyses appeared to show the greatest degree of fractionation at

about 4% maximum, whereas the mean of the Rb^{85}/Rb^{87} ratios determined on rubidium separated from rock samples,following the regular laboratory procedure used for all the samples,varied about 0.8% from the value found by Shields et al. (1963).

The extent of mass discrimination appears to be governed principally by two factors: (i) the filament temperature at which the isotopic ratios are measured, and (ii) the "matrix" through which the rubidium isotopes are to be emitted. The two effects are not mutually exclusive, for in one experiment (sample R7216) the spiked rubidium isotopic ratio was measured at a relatively low current (about 0.8 amperes) and again at about 1.3 amperes, a rather high current. The decay characteristics of both runs were about the same, but there was a difference of about 2% in the measured ratio. Assuming negligible depletion of Rb^{85} during the lower temperature run, the observed effect is likely due to a combination of the two effects above, for at higher filament temperatures the effect of mass discrimination tends to decrease. In the case of the RbCl spec-pure reagent, the temperature of thermionic emission is much lower than in samples that contain,in addition to rubidium, potassium and other alkali perchlorates and aluminum complexes. The isotopic ratio was measured at a very low filament current of about 0.2 or 0.3 amperes. In addition the behavior of the run is different between pure shelf and sample. In the former situation, the run tends to grow slowly or behave in a linear fashion over the half hour duration of the run, whereas samples containing impurities usually decay rather rapidly though there is no difficulty in extrapolating through the peaks during "peak-hopping".

At present, the extent of fractionation cannot be predicted with sufficient accuracy to apply suitable corrections to the measured Rb^{85}/Rb^{87} ratio. It seems that the largest mass discrimination would arise when calibrating spike solutions that are free of the cations present in the samples. Generally speaking, one would expect less fractionation at higher filament temperatures and less error would result if both sample and spike could be run under identical conditions of filament current and common matrix.

3.7 Sources of Error in Rb and Sr Analyses:

Both the random and systematic errors involved in the mass spectrometric determination of rubidium and strontium have been discussed by Reesman (1968, pp. 30-31).

3.8 Least Squares Regression Analysis:

All the isochrons in this study have been defined in terms of a least-squares fit method outlined by York (1966). A computer program provided by York based on this method was re-written by this investigator for use on the IBM/OS 360 computer at the M.I.T. Computation Center. The input data consist of the values of x and y, i.e., Sr^{87}/Sr^{86} and Rb^{87}/Sr^{86} with the appropriate uncertainties taken into consideration. An error of 0.1% was taken for Sr^{87}/Sr^{86} and 3% was taken for Rb^{87}/Sr^{86}. The weighting factor for each ratio is the inverse of the variance ($1/\sigma^2$). A listing of this program is given in Appendix C and is modified slightly from York's original program in that the age and error in age are also calculated.

While there are obvious advantages in this treatment over those

involving regressions of x on y and y on x, taking the mean value of the two, problems arise with higher values of Rb^{87}/Sr^{86}. With values for this variable higher than, say 2 or so, the residual for each analytical point decreases in the x direction, despite the same relative error for that point. The net effect is to give an age with a seemingly lower error than is actually the case. For example, in the determination of the Westport and Adirondack Composite isochron, an age of 1261 $\pm$ 32 m.y. was obtained using this program. Intuitively, one would not expect the age to be this precise in view of the scatter about this isochron (Figure 15). Also, the initial ratio quoted at 0.7063 $\pm$ 0.0007 does not seem realistic, for despite the scatter in the analyses, the error is less than the 2σ error for an individual analysis (based on replicate analysis of the E & A standard). In the literature there are examples of isochrons based on as few as four analyses quoting similarly small errors in age. It is usually the case that the precision of the age determination as determined by the slope of the isochron decreases with increasing number of analyses showing perhaps the fortuitous nature of the "lineup" of a small number of points. A more realistic approach, perhaps, would be to estimate the statistical variation (σ) one would expect in the target population based on the small number of samples analyzed using a statistical test such as the Student t distribution. The results of such calculations are rather sobering (S. R. Hart, personal communication), and reflect an increase in uncertainty in σ owing to the small sample population.

FIGURE 7

Sketch Map of Equatorial East Africa

with

Sample Localities

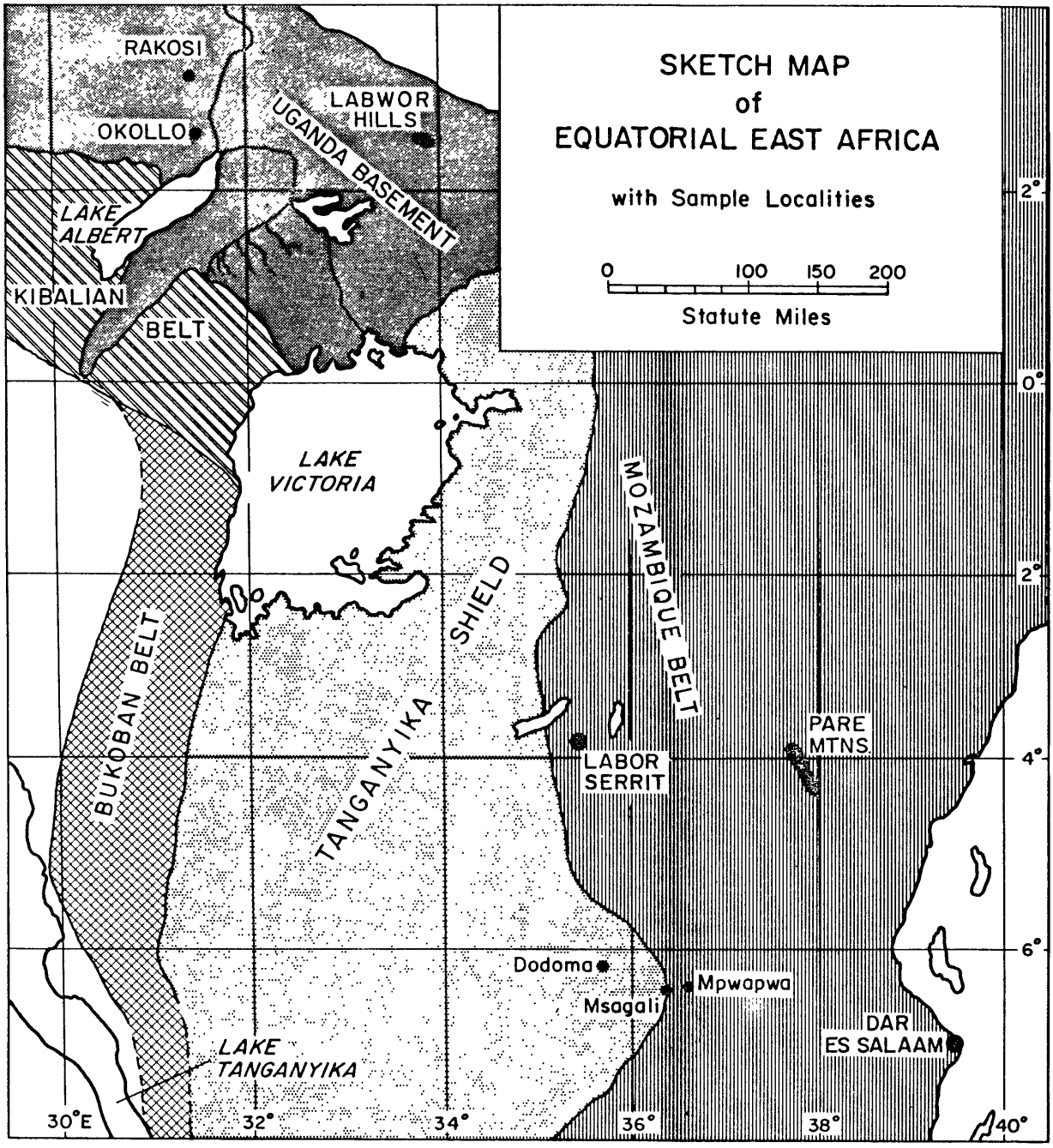
SKETCH MAP
of
EQUATORIAL EAST AFRICA
with Sample Localities
0 100 150 200
Statute Miles
RAKOSI
OKOLLO
LABWOR HILLS
UGANDA BASEMENT
LAKE ALBERT
KIBALIAN BELT
LAKE VICTORIA
BUKOBAN BELT
TANGANYIKA SHIELD
MOZAMBIQUE BELT
LABOR SERRIT
PARE MTNS.
Dodoma
Mpwapwa
Msagali
DAR ES SALAAM
LAKE TANGANYIKA
2°
0°
2°
4°
6°
30°E
32°
34°
36°
38°
40°

3.9 Msagali Charnockite Quarry, Tanzania (6° 22' S, 36° 17' E)

This locality, situated in central Tanzania between Dar es Salaam and Dodoma in the south central portion of Quarter Degree Sheet 163, has been restudied by J. V. Hepworth of the Institute of Geological Sciences, London, during the course of an investigation into the nature of the boundary between the Mozambique Orogenic Belt and the Granitoid Shield in Tanzania.

The term "Mozambique Belt" was introduced by Holmes (1948) to describe a younger series of biotite gneisses and migmatites containing later pegmatite phases which cut across older east-west striking rocks of the Nyanzian, Dodoman and Kauirondian Series. Holmes (1951) was of the opinion that the exposed rocks of this belt are the uplifted and deeply eroded core of an orogenic belt.

The disused railway ballast quarry is located in a transitional region between the Granitoid Shield and the generally north-south trending Unsagaran System of the Mozambique Belt, that is, between the sheared edge of the batholithic granite and the fairly high grade metasedimentary rocks (epi(?)-amphibolite facies) of the Unsagaran System which at this locality have an unusual east-west trend.

Within the quarry, the charnockite has been described by Hepworth (personal communication) as a "very dark-coloured, resinous-looking rock, either dark brownish grey or dark blue depending to some extent upon the light and the freshness of the surface.... In hand specimen it strongly resembles charnockite from the type locality in Madras." Specimens R7050 and R7051 are of this rock type. Above the charnockite

is a coarse-grained gneissose aplo-granite having a slight foliation similar to that of the charnockite.

Between the above lithologies is a "contact facies" (Temperley, 1938) where the foliation is much stronger as the concentration of closely-spaced biotite bands increases (R7053).

Hepworth points out that the magmatic intrusion of the gneissose aplo-granite is clearly separate from the metamorphic event which raised the charnockite to the present granulite metamorphic facies. The later intrusion and folding of the aplo-granite produced rods and mullions about a southeast plunging axis (see Figure 8) and imparted a foliation to the charnockite as well.

3.10 Discussion of Results

All six samples submitted from this quarry were analyzed for Rb and Sr by isotope dilution methods and the results are shown in Table III-G. The Sr^{87}/Sr^{86} - Rb^{87}/Sr^{86} plot is given in Figure 9.

It is evident from the scatter of points in Figure 9 that the specimens analyzed did not remain closed systems with respect to Rb and Sr throughout their history. This is not surprising in view of the extreme cataclasis and deformation to which these rocks have been subjected.

Two previous age determinations reported in Cahen and Snelling (1966) from this same quarry also give disparate results. Kulp and Engels (1963) using biotite separates for both determinations obtained an age of 475 $\pm$ 80 m.y. by the Rb-Sr method and an age of 3600 $\pm$ 100 m.y. by K-Ar analysis.

FIGURE 8

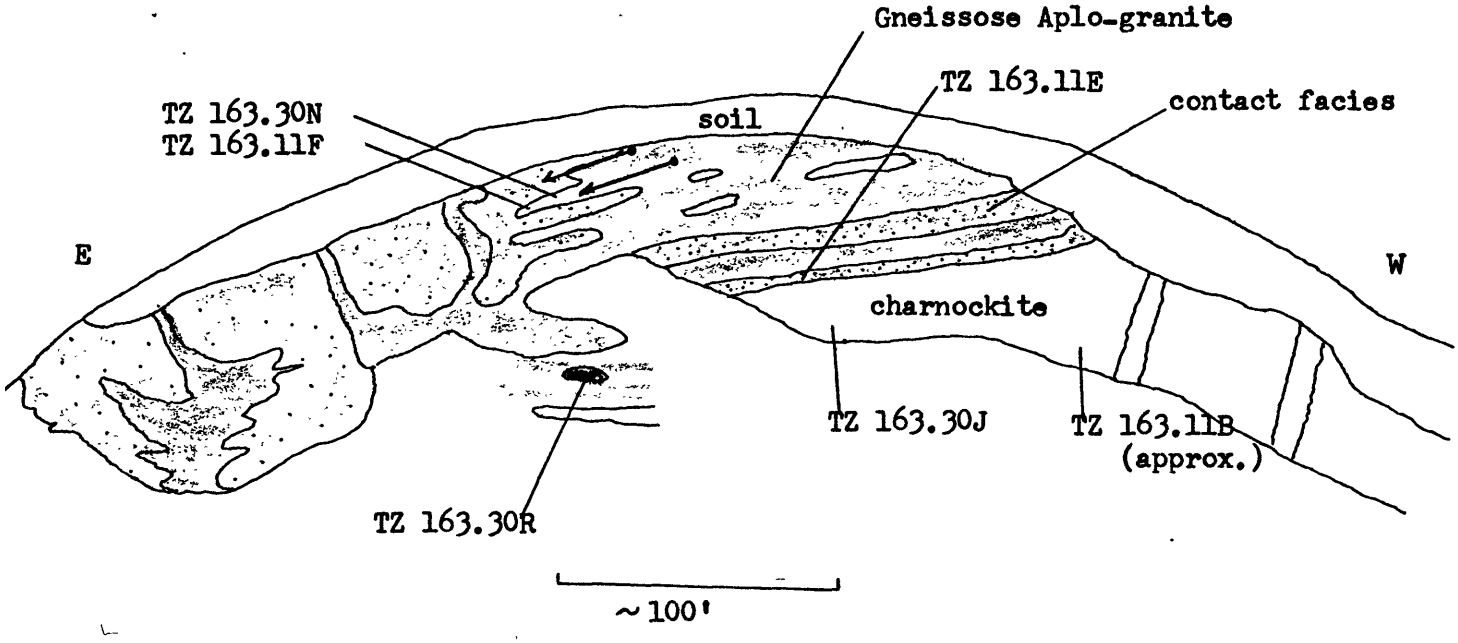

MSAGALI CHARNOCKITE QUARRY, TANZANIA

after Temperley (1938) with notes by J. V. Hepworth. Folding and rodding as a result of Mozambiquian deformation at top of section. Looking south.

TABLE III-G

MSAGALI CHARNOCKITE QUARRY

Sample	Rb^{87}/Sr^{86}	Sr^{86}/Sr^{88}	$(Sr^{87}/Sr^{86})_{normalized}$	Isotope Dilution Rb(ppm)	Sr(ppm)	Rb/Sr
R7050/ TZ 163.11B	0.4405	0.1181	0.7204	66	434	0.152
R7051/ TZ 163.30J	0.5039	0.1190	0.7237	71	410	0.174
R7052/ TZ 163.30R	0.9789	0.1195	0.7430	88	261	0.337
R7053/ TZ 163.11E	0.6056	0.1229	0.7367	78	376	0.209
R7054/ TZ 163.30N	0.5217	0.1190	0.7308	46	253	0.180
R7055/ TZ 163.11F	0.968	0.1195	0.7361	81	242	0.334
R7057/ TZ 163.73*				63		

* charnockite 5 miles west of Msagali.

FIGURE 9

Isochrons for Charnockitic Rocks

Msagali, Tanzania

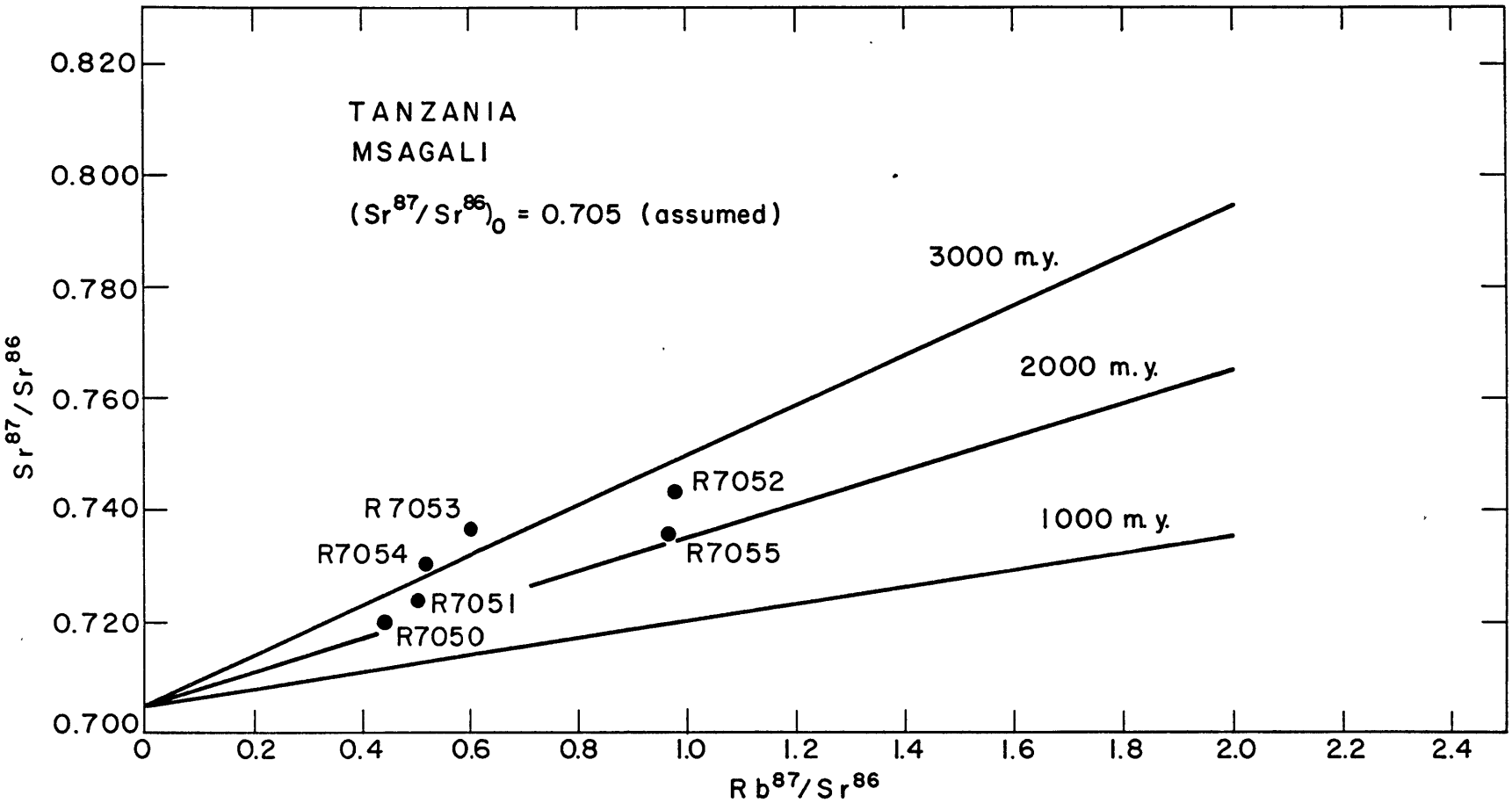
TANZANIA
MSAGALI
$(Sr^{87}/Sr^{86})_0$ = 0.705 (assumed)
3000 m.y.
2000 m.y.
1000 m.y.
R7052
R7053
R7054
R7055
R7051
R7050
0.820
0.800
0.780
0.760
0.740
0.720
0.700
Sr^{87}/Sr^{86}
0
0.2
0.4
0.6
0.8
1.0
1.2
1.4
1.6
1.8
2.0
2.2
2.4
Rb^{87}/Sr^{86}

From the array of time lines drawn (Figure 9), assuming an initial Sr^{87}/Sr^{86} ratio of .705, a crude "age" of about 2500 m.y. is obtained. It is interesting to note that there is a reversal in the usual trend of ages obtained by the two dating methods. The Rb-Sr Whole Rock analyses confirm the extremely old age found by K-Ar analysis and point to a disturbance of the system probably during the Mozambiquian Orogeny. The fact that a Precambrian age is hinted at may indicate that these rocks are in part material of the older Precambrian Massif to the west that have been caught up in the orogeny. As pointed out by Holmes, these rocks may well represent formerly deep-seated blocks brought to light as the result of orogenic activity and subsequent deep erosion.

3.11 Okollo and Rakosi, West Nile District, Uganda

These localities, 2° 30' N - 3° 00' N Latitude and 31° 00' - 31° 15' E Longitude, northwest of the headwaters of the Albert Nile, are part of a highland region resulting from Pliocene and Pleistocene rifting.

Originally assigned to the "Basement Complex" in A. W. Groves' (1935) original study of the crystalline gneisses of the region, a further division of these basement rocks into three main groups below the Kibalian Group has been proposed by Hepworth (1964). The highest metamorphic grade present is the Granulite Group which is considered to be the oldest exposed, and was affected by the earliest tectonic phase preserved now in blocks and cores unaffected by later tectonisms. Also present are the Western Grey Gneiss (amphibolite facies) and the Eastern Grey Gneiss, the latter being slightly lower in grade. On the basis of Macdonald's (1963) terminology in northern Uganda, Hepworth has accepted the terms "Watian", "Aruan", and "Mirian" as approximately synonomous with his "granulite Group", "Western Grey Gneiss Group", and "Eastern Grey Gneiss Group" in the West Nile District. By means of photogeological interpretation these groups appear to extent throughout northeast and north-central Uganda. The Eastern Grey Gneiss or Mirian has been folded and refolded during the same major structural event termed the Namarodo in this region. It has been suggested that this event may be correlated with the Mozambiquian event to the south. The Kibalian Group lies unconformably above the previous two groups and consists in the main of hornblende schists and amphibolite. The Kibalian Group represents

the lowest metamorphic grade mapped in this region (greenschist to epiamphibolite facies) and is the least affected by tectonic events. All the groups in the region have been subjected to pervasive retrogressive metamorphism involving the unmixing of the feldspars, conversion of the pyroxenes to biotite + garnet, amphibolitization, and recrystallization of the fabric of the original rock. The retrogressive event may be related to a later complex tectonism involving northwest-southeast structural belts such as the Aswa Zone in the southeast and the Madi Belt of the northern West Nile. The two are collectively placed in Holmes' (1951) "Chua Orogenic Belt". The complex structural relationships are discussed by Cahen and Snelling (1966, pp. 44-45).

The Granulite Group has been recognized in this region on the basis of the typomorphic mineral assemblage peculiar to the granulite facies defined by Eskola (1952), despite the retrogressive metamorphism that has obscured the primary texture. As in the type locality in Madras State, India, a wide compositional variety of charnockites, enderbites, and granodioritic charnockites are represented here. However, the compositional variation is expressed in the Group as a whole in the form of a large-scale layered series and not in a single outcrop, which tends to be rather massive, lacking compositional banding. Individual layers are generally several hundred yards across strike. In addition to the more massive charnockites mentioned above, more magmatic and mobilized types are present, especially in the southeast portion of the Luku Hills (Figure 10) where there has been apparent increased mobility of the felsic fraction, forming an incipient agmatite

FIGURE 10

Sample Locations, Okollo and Rakosi,

West Nile District, Uganda

(Geology from Geological Survey of Uganda, Report 10, Sheets 19 and 20 by J. V. Hepworth)

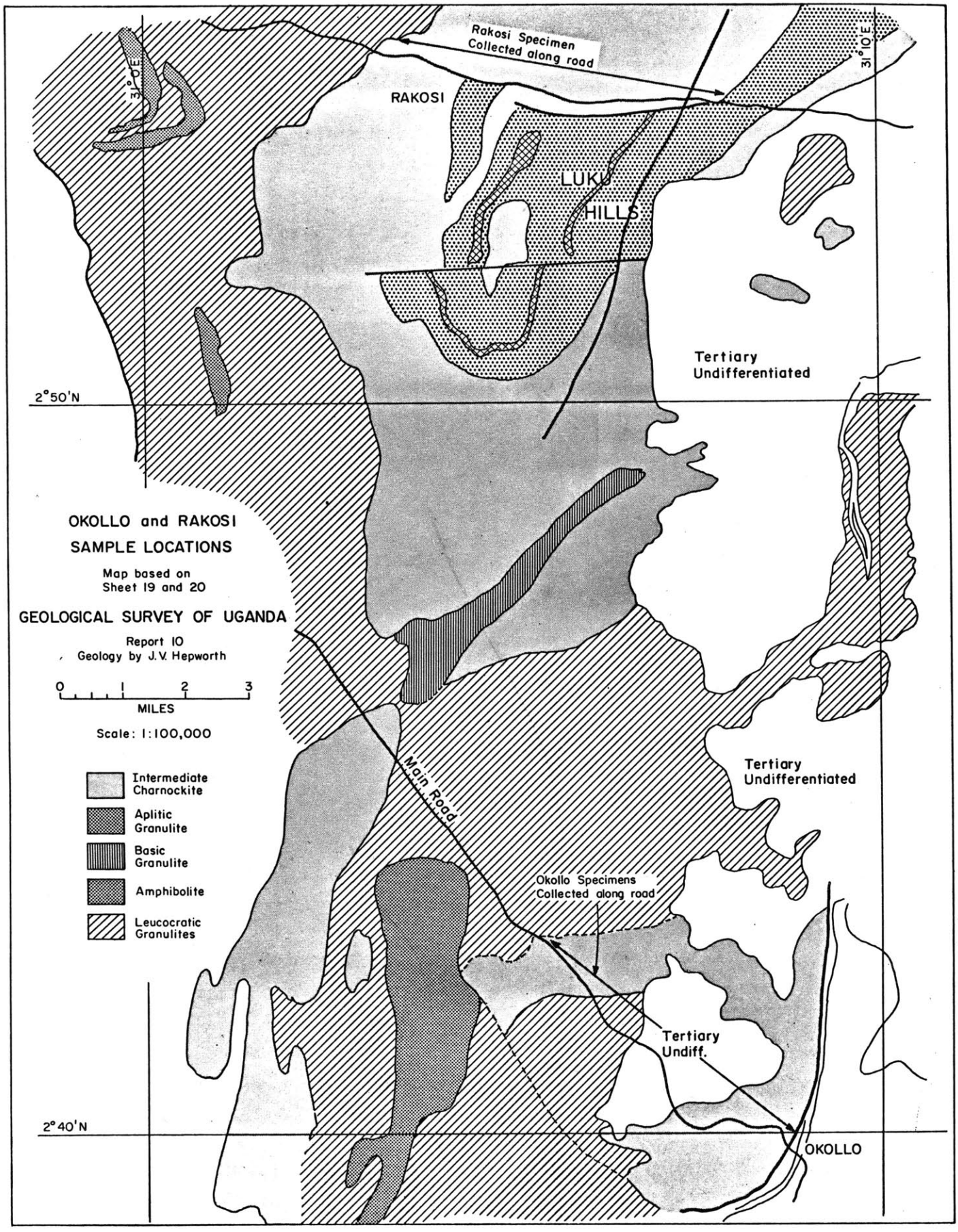
Rakosi Specimen
Collected along road
RAKOSI
LUKU
HILLS
31°10'E
31°E
Tertiary
Undifferentiated
2°50'N
OKOLLO and RAKOSI
SAMPLE LOCATIONS
Map based on
Sheet 19 and 20
GEOLOGICAL SURVEY OF UGANDA
Report 10
Geology by J.V. Hepworth
0 1 2 3
MILES
Scale: 1:100,000
Intermediate
Charnockite
Aplitic
Granulite
Basic
Granulite
Amphibolite
Leucocratic
Granulites
Main Road
Tertiary
Undifferentiated
Okollo Specimens
Collected along road
Tertiary
Undiff.
2°40'N
OKOLLO

mingling with angular blocks of dioritic charnockite.

In the north part of the region mapped, at Rakosi, an aplitic granulite characterized by a leucocratic medium to fine-grained texture and a flesh to pink color has been included as an integral part of the Granulite Group. Similar associations of this rock type with more intermediate charnockites have been found throughout the world (i.e., the Madras State Charnockite Series). The aplitic granulite is commonly interlayered with intermediate charnockite forming a distinct junction with a zone of transition less than an inch wide, suggesting that if their juxtaposition involved intrusion, the temperatures in the adjacent bodies was not widely different. In the Luku Hills, large and small scale, apparently conformable, layering of pink aplitic granulite and intermediate charnockite has been noted by Hepworth. Local variants of the aplitic granulite have been found to contain the assemblage hypersthene + diopside + garnet and is felt to unite the two major units within the group since it indicates that the aplitic granulite also underwent metamorphism up to granulite grade.

Hepworth noted that the aplitic granulites become relatively scarce where the associated charnockite becomes fine-grained and banded, approaching a pyroxene granulite or "para-charnockite" following Parras' (1958, p. 55) nomenclature. It has been suggested that the aplitic granulites occur in loci of higher temperature, involving partial melting. The absence of biotite in the aplitic granulites tends to support this since the partial pressure of water vapor in the high temperature regions would be lower.

The Acid Granulites comprise the remaining suite sampled in this study from the Granulite Group. These include rocks having a modal composition varying from quartz-rich microcline-oligoclase-biotite granulites and biotite-rich quartz-microcline-oligoclase granulites. These rocks present some difficulty in unambiguous assignment to the Granulite Group primarily because their chemistry precludes development of the granulite facies mineral assemblage so that at times it is difficult to distinguish them from the lower grade Grey Gneisses. At Goli Hill, about two miles northwest of Okollo, intermediate and basic charnockites are gradationally associated with the acid granulites and thus provide justification for their inclusion into the Granulite Group. At this locality there exists a gradation from basic charnockite through the brown to grey intermediate types to acid granulites and as the proportion of mafic minerals decreases, the rock assumes the typical aplitic granulite discussed above. Hepworth has suggested that this represents a differentiated series although this is impossible to show when mapping at a scale of 1:50,000.

3.12 Geochronology

The structural complexity of the region brought to light by field mapping shows that the relatively few ages available are at present insufficient to completely reveal the metamorphic and tectonic events that have taken place. A characteristic of many of the radiometric ages determined in this region is the surprisingly young age (see Table III-H) of about 575 m.y. for many of the intrusive rocks. Both K:Ar and Rb:Sr ages along the Uganda-Kenya border from micas and amphiboles of country rock gneisses are considered anomalously young (430-660 m.y.) since reliable ages of 655 m.y. and 620 m.y. have been obtained by the U:Pb method for the Morukong and Kokusan pegmatites in Kenya. These ages set an upper limit of ca. 650 m.y. for the enclosing gneisses. Although the interpretation of these anomalously young ages is still somewhat speculative, it appears likely that the ca. 650 m.y. age is the younger limit of deformation and metamorphism in the area and is roughly synchronous with the Katangan Orogeny of Central Africa. Ages younger than about 650 m.y. by both the K:Ar and Rb:Sr methods may represent blocks that remained isotopically open until emplaced by epirogenic uplift into cooler regions in the early Paleozoic.

To the west in the Congo, Kibalian Group granulites within greenschist to epi-amphibolite grade hornblende schists give ages within a range of 1725 to 2075 m.y. averaging 1840 m.y. by both the K:Ar and Rb:Sr methods. Complementary model lead ages have also been obtained from two galenas from the Kibalian. The age of about 1850 m.y. is considered to correspond roughly to the post-tectonic

stages of the major orogeny.

In the southern Congo, at Kasai, the Dibaya basement is considered to have undergone granitization about 2700 m.y. ago (Ledent and others, 1962; in Clifford, T. N., 1968, p. 383) and a Rb:Sr microcline age of ca. 3310 m.y. has been obtained from a pegmatite in the Luiza-type basement further south.

TABLE III-H

Age Determinations from the Basement of Uganda and Adjacent Parts of Kenya

(from Cahen and Snelling, 1966)

SAMPLE	LOCALITY	AGE (m.y.)
Biotite	Granite dike cutting basement acid granulites; 0.3 mi. E. of Kaabong rest camp, Uganda	515 ± 18 K:Ar
Whole Rock	Granite dike cutting basement acid granulite; Kaabong area	565 ± 20 Rb:Sr
Whole Rock	Granite dike cutting basement acid granulite; Kaabong area	565 ± 20 Rb:Sr
Whole Rock	Granite dike cutting basement acid granulite; Kaabong area	565 ± 20 Rb:Sr
Biotite	Pyroxene gneiss, Basement Complex; Nakothogwan Hill, Karamoja District, Uganda	575 ± 20 K:Ar
Biotite	Hornblende-biotite-pyroxene granulite, Basement Complex, Obongya River, E. Acholi, Uganda	540 ± 20 K:Ar
Biotite	Mesocratic sheared gneiss, Ogom (Basement) Complex, 1 mi. N. Gulu-Kitgum road, Acholi, Uganda	650 ± 25 K:Ar
Fuschite	Western Grey Gneiss quartzite, Basement Complex, Kango Hill, 2° 36' N; 30° 51' E.	540 ± 20 K:Ar

TABLE III-H (cont.)

SAMPLE	LOCALITY	AGE (m.y.)
Biotite	Charnockite, Granulite Group, Basement Complex, 1 mi. north of Okollo 2° 41' N; 31° 09' E.	660 ± 25 K:Ar
Biotite	Basement Gneiss; 20 mi. E. Fort Portal, 1 mi. W. Butiti quartzite, Uganda	1040 ± 40 K:Ar
Whole Rock	Rakosi and Okollo Charnockites (This Study), See Figure 10 for localities of specimens and Figure 11 for isochron.	2629 ± 117 Rb:Sr

TABLE III-I

OKOLLO AND RAKOSI, WEST NILE DISTRICT, UGANDA

Sample	Rb^{87}/Sr^{86}	Sr^{86}/Sr^{88}	$(Sr^{87}/Sr^{86})_{normalized}$	Isotope Dilution Rb(ppm)	Sr(ppm)	Rb/Sr
R7042/54	0.239	0.1207	0.7159	43	521	0.082
R7011/23	6.503	0.1202	0.9068	163	74	2.191
R7012/24	13.241	0.1199	1.1969	135	31	4.366
R7018/30	14.960	0.1192	1.3158	303	62	4.879
R7020/32	8.003	0.1220	1.0081	207	78	2.668
R7038/50	0.096	0.1199	0.7082	19	68	0.033
R7049/61	0.125	0.1189	0.7117	19	434	0.043
R7027/39	0.181	0.1212	0.7119	38	611	0.062
R7039/51	0.074	0.1220	0.7134	19	730	0.026
R7040/52	0.084	0.1191	0.7066	19	642	0.029
R7019/31*	16.024	0.1196	0.8008	371	68	5.486

*this alaskitic gneiss from the Rakosi area gave an anomalous result compared with the ten analyses above. The age obtained from this one specimen assuming the initial ratio of 0.7049 determined above gave an age of about 425 m.y.

FIGURE 11

Isochron for Rakosi and Okollo (inset)

Charnockitic and Granitic Rocks, West Nile District, Uganda

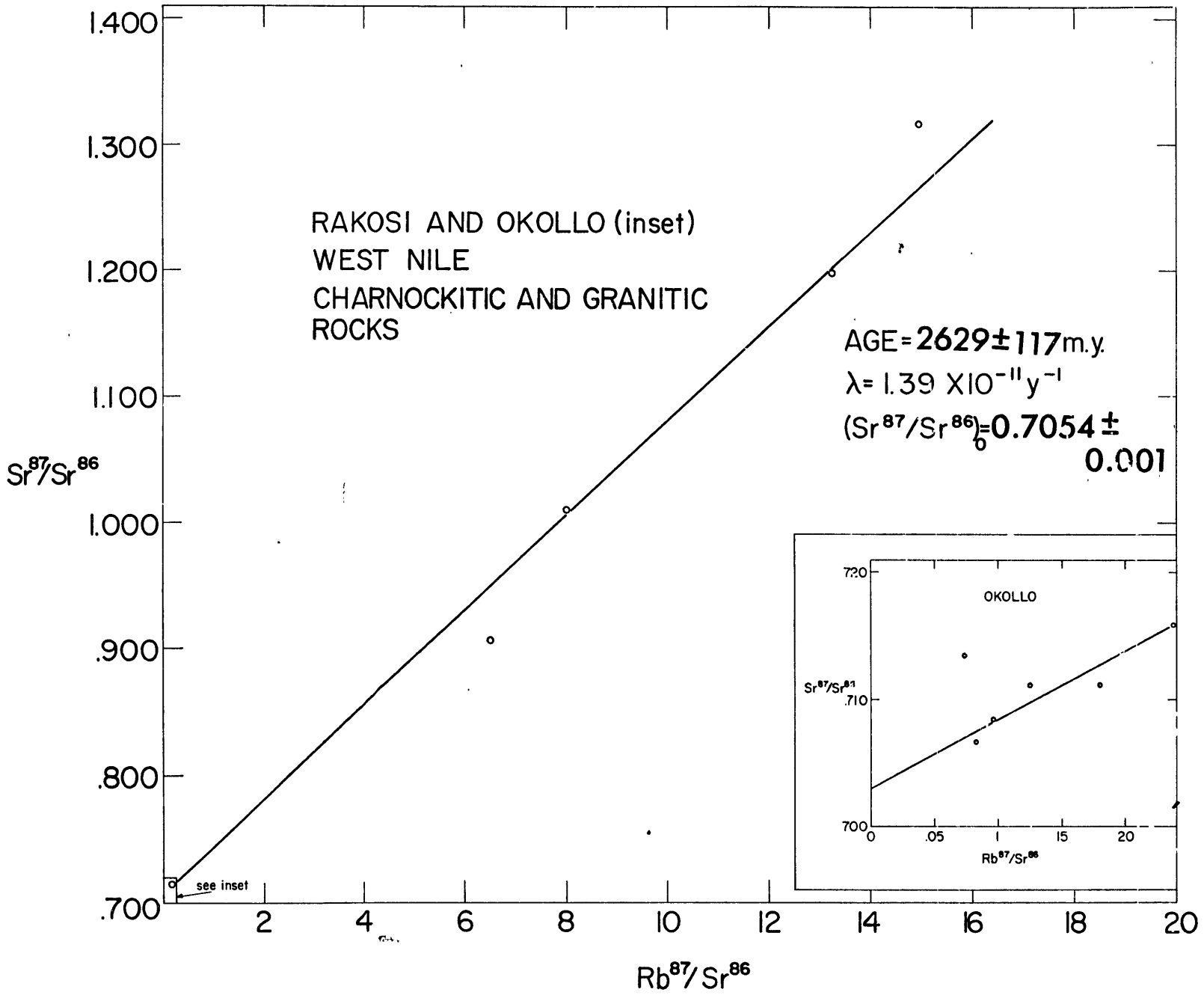
RAKOSI AND OKOLLO (inset)
WEST NILE
CHARNOCKITIC AND GRANITIC ROCKS
AGE = 2629 ± 117 m.y.
λ = 1.39 X 10⁻¹¹ y⁻¹
(Sr87/Sr86)o = 0.7054 ± 0.001
see inset
OKOLLO
Sr87/Sr86
Rb87/Sr86
1.400
1.300
1.200
1.100
1.000
.900
.800
.700
2
4
6
8
10
12
14
16
18
20
.05
15

3.13 Labor Serrit and Pare Mountains, Tanzania

Labor Serrit and the Pare Mountains are located in the northeast corner of Tanzania near 4° S Latitude at 36° E and 38° E Longitude respectively. These areas form part of a vast and poorly understood complex of granulites, which are surrounded by volcanics and amphibolite facies biotite and hornblende gneisses. The granulites form gently plunging and dipp ing stratiform-like sheets that form a major structural unit that appears to have undergone only a minimal amount of deformation or metamorphism. These granulites have been regarded as belonging to the "Mozambiquian" and ages in the range 450 to 600 m.y. were suspected (J. V. Hepworth, personal communication). Recently, however, there has been speculation that these rocks may be related to the older Tanganyikan Shield to the west.

In the present study, five specimens of pyroxene granulite from the Pare Mountains and three from the Labor Serrit area were provided for analysis by Dr. J. V. Hepworth, Institute of Geological Sciences, London. The results of these analyses are shown in Table III-J and Figure 12.

	Age	$(Sr^{87}/Sr^{86})_o$
Pare Mountains	927 $\pm$ 63 m.y.	0.7056 $\pm$ 0.0011
Labor Serrit	724 $\pm$ 8 m.y.	0.7064 $\pm$ 0.0001

The data are too few to come to any firm conclusion regarding the meaning of these two ages. It would appear, however, that these results indicate an age older than the "Mozambiquian" orogeny that took place between 450 and 600 m.y. The possibility exists that the

granulite belt studied here may be an eastern extension of the granulite and amphibolite facies rocks of the Tanganyikan Shield that underwent a later episode of metamorphism.

TABLE III-J

PARE MOUNTAINS AND LABOR SERRIT, TANZANIA

Sample	Rb^{87}/Sr^{86}	Sr^{86}/Sr^{88}	$(Sr^{87}/Sr^{86})_{normalized}$	Isotope Dilution Rb (ppm)	Sr (ppm)	Rb/Sr
Pare Mountains, Sheet 73:						
R7224/73 1	----	0.1209	0.7054	nd*	----	----
R7225/73 2	1.473	0.1194	0.7259	51.7	101.8	0.5078
R7228/73 11	0.0201	0.1200	0.7083	2.55	366.6	0.0070
R7229/73 14	2.335	0.1192	0.7347	59.4	73.8	0.8046
R7230/73 15	0.9397	0.1201	0.7111	42.9	132.2	0.3245
Labor Serrit:						
R7231/86 24		0.1208	0.7065		721.6	
R7233/86 27	1.0734	0.1202	0.7173	82.4	222.5	0.3705
R7236/86 32	0.0525	0.1201	0.7069	7.28	401.1	0.0182

*not detected at 5 ppm level by X-ray fluorescence.

FIGURE 12

Pare Mountains and Labor Serrit

Tanzania

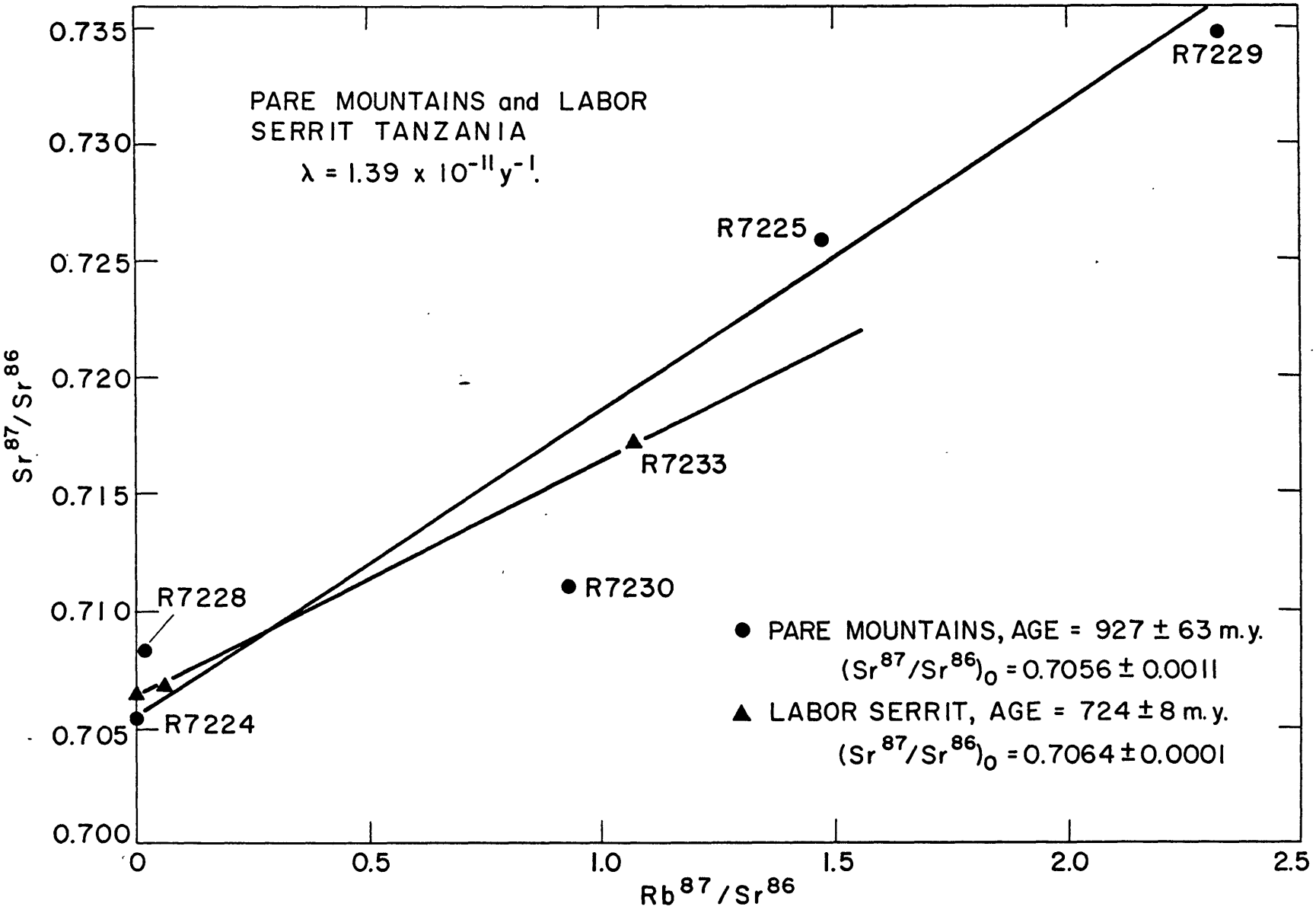
PARE MOUNTAINS and LABOR
SERRIT TANZANIA
λ = 1.39 x 10⁻¹¹ y⁻¹.
R7229
R7225
R7233
R7230
R7228
R7224
● PARE MOUNTAINS, AGE = 927 ± 63 m.y.
(Sr⁸⁷/Sr⁸⁶)₀ = 0.7056 ± 0.0011
▲ LABOR SERRIT, AGE = 724 ± 8 m.y.
(Sr⁸⁷/Sr⁸⁶)₀ = 0.7064 ± 0.0001
Sr⁸⁷/Sr⁸⁶
Rb⁸⁷/Sr⁸⁶
0.735
0.730
0.725
0.720
0.715
0.710
0.705
0.700
0
0.5
1.0
1.5
2.0
2.5

3.14 Adirondack Highlands, New York

In the present study, suites of pyroxene granulites were collected from two localities in the Grenville province (Figure 13). Although the rocks in each of these areas have developed the requisite mineralogy for classification in the pyroxene granulite sub-facies, totally different origins have been suggested for them. Simply stated, the anorthosites and pyroxene granulites of the central Adirondacks have been interpreted by Buddington (see below) and others to be of igneous origin, whereas the granulite terrain of the Westport area has been interpreted by Wynne-Edwards (1967) to be of sedimentary origin, that is, the granulites are a sequence of metamorphosed greywackes. A comparison of the Sr^{87}/Sr^{86} initial ratios have been made to see whether a distinction between the two suites can be made.

The Adirondack Highlands which form the southern extension of the Grenville province of the Canadian shield occupy a central massif covering about 1200 square miles. The highland region itself consists of an anorthosite core associated with pyroxene granulite, granitic, syenitic, and gabbroic variants. The gabbro and anorthosite account for about a third of the rocks which were classified as igneous by Buddington (1939). A review of the literature pertaining to the origin of the anorthosites in the Adirondacks and other localities has been given by Heath (1967) who, in addition, has also commented on the various hypotheses in the light of Sr^{87}/Sr^{86} initial ratios.

In close association with the anorthosite is an extensive series of syenite and granite belonging to the hornblende or pyroxene granulite sub-facies. It is generally agreed (Buddington, 1939; Walton

and deWaard, 1963) that the rocks of this area are of plutonic igneous origin but have undergone subsequent metamorphism which culminated in the Grenville orogeny. The relationship of the "supracrustal" Grenville metasediments to the underlying igneous rocks has received various interpretations.

Buddington (1939, p. 197 et seq.) and earlier workers (Cushing, 1917, p. 507) favor an intrusive origin of the plutonic complex into the older Grenville metasediments, followed by later regional high-grade metamorphism during the Grenville orogeny. An opposing view regarding the intrusive character of the plutonic rocks is considered below.

On the basis of extensive mapping of the relationships between the meta-igneous series and the supracrustal units, Walton and deWaard (1963) have observed remarkable continuity of a single marble unit in contact with the anorthosite, "charnockitic"-quartz-syenite-gneisses and granite gneisses. This continuity persists for over 80% of the exposed length where the contact between the two units is exposed. They account for this remarkable continuity as the result of the deposition of the marble as a basal supracrustal unit followed by the succeeding units which also show a similar stratigraphic coherence upon a complex older basement of the meta-igneous rocks. Subsequently, both basement and cover rocks were involved in an intensive deformation involving plastic remobilization giving rise to the complex structural picture now observed. It appears that this later regional metamorphic event, the Grenville orogeny, gave rise to the pyroxene granulite sub-facies assemblage.

FIGURE 13

Westport, Ontario and Adirondack Highlands

Sample Localities

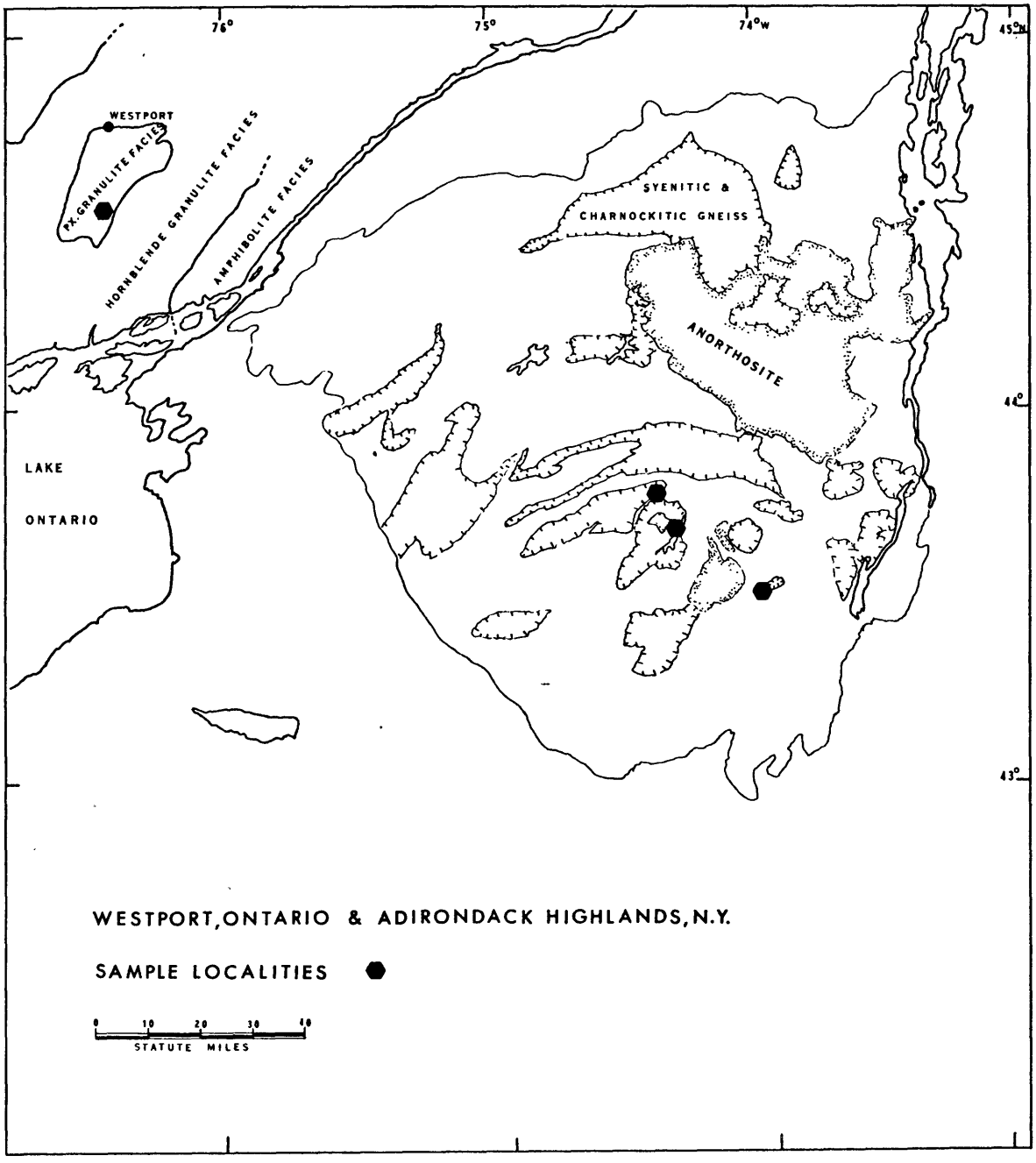
76°
75°
74°W
45°N
WESTPORT
PX. GRANULITE FACIES
HORNBLENDE GRANULITE FACIES
AMPHIBOLITE FACIES
SYENITIC &
CHARNOCKITIC GNEISS
ANORTHOSITE
LAKE
ONTARIO
44°
43°
WESTPORT, ONTARIO & ADIRONDACK HIGHLANDS, N.Y.
SAMPLE LOCALITIES
0 10 20 30 40
STATUTE MILES

3.15 Geochronology

Considering the vastness and geological complexity of this area, there are relatively few age determinations available. Such information, however, may prove extremely useful in the interpretation of the pre-Grenville history as well as later metamorphic overprints that may have occurred.

U-Pb determinations on zircons from two Grenville basement syenites in the Adirondack Highlands (Silver, 1966) give an age of 1125 m.y.

Hills and Gast (1964) have reported a Rb-Sr whole rock age of 1092 ± 20 m.y. ($\lambda = 1.39 \times 10^{-11} y^{-1}$) for pyroxene-hornblende granite gneisses from the Lake George Village pluton. Also included in the isochron were two samples from the Ticonderoga area which have a similar mineralogy and are presumably related to one another. An analysis of two feldspars from a pegmatite in aluminous paragneiss gave an age of 1060 ± 75 m.y. with an initial ratio of 0.7159. They noted the similarity of these ages with both K/Ar and Rb/Sr ages reported by Doe (1962) from other areas of the Adirondacks, and from the Grenville province of Canada (Lowden *et al.*, 1963). Since the initial ratio of the granite gneisses is well within the range expected for granitic rocks (0.7058 ± 0.0010), Hills and Gast conclude that the age represents the age of emplacement or if this is indeed a metamorphic age, the body did not have an extensive pre-Grenville history because on isotopic re-homogenization a higher initial ratio would be expected.

Heath (1967) has determined a Rb-Sr whole rock isochron on seven specimens from a large pyroxene-hornblende quartz syenite body north of the main Adirondack anorthosite massif (Figure 16). An age of 1055 $\pm$ 31 m.y. ($\lambda = 1.39 \times 10^{-11} y^{-1}$) was obtained with an initial ratio of 0.7060 $\pm$ 0.0004. The age and initial ratio are in good agreement with the determination by Hills and Gast discussed above, and Heath has suggested that these may be comagmatic.

In the present study, specimens from the central Adirondacks, Crane Mountain, Indian Lake, West Canada Lake and Blue Mountain, have been analyzed.

The Crane Mountain suite, kindly supplied by Dr. P. R. Whitney, Rensselaer Polytechnic Institute, was collected from a postulated overturned and differentiated 900' thick sill. Reynolds et al. (1967) suggest a common origin for these pyroxene granulites and the adjacent Snowy Mountain anorthosite body on the basis of K/Rb ratios, Niggli values and the Differentiation Index (discussed in Chapter II). Later it became apparent that within the pyroxene granulite itself there was a "dark" and a "light" group which differed from each other in chemistry as well as mineralogy (P. R. Whitney, personal communication). The present study of the Rb and Sr isotopic ratios confirmed the presence of two distinct populations. The analytical results for six specimens are given in Table III-K. Based on the six analyses, an age of 1336 $\pm$ 71 m.y. was obtained with an initial ratio of 0.7025 $\pm$ 0.0024. The close grouping of the analyses about two points (at Rb^{87}/Sr^{86} = 2 and 3.5 approximately) accounts for the relatively large uncertainty in the initial ratio. These values are

TABLE III-K

CRANE MOUNTAIN, NEW YORK

Sample	Rb^{87}/Sr^{86}	Sr^{86}/Sr^{88}	$(Sr^{87}/Sr^{86})_{normalized}$	Isotope Dilution Rb(ppm)	Sr(ppm)	Rb/Sr
R7123/ ACS 43	3.438	0.1198	0.7653	165	140	1.181
R7125/ ACS 44	3.479	0.1205	0.7695	151	126	1.195
R7126/ ACS 45	2.148	0.1197	0.7411	138	187	0.739
R7127/ ACS 46	2.038	0.1198	0.7408	126	180	0.702
R7128/ ACS 47	1.997	0.1203	0.7404	130	189	0.688
R7129/ ACS 48	1.899	0.1201	0.7390	122	187	0.654

TABLE III-L

MODES OF CRANE MOUNTAIN SAMPLES ANALYZED (P. R. Whitney, personal communication)

Sample	Number of Sections	Points Counted	Volume Percents Qtz	Plag	Orth	Hornblende	Pyroxene	Gt	Bio	Other**
R7123/ ACS 43	1	842	31.4	22.3	39.2	4.8	----	--	2.4	---
R7125/ ACS 44	1	720	29.6	17.5	46.7	4.2	----	--	1.9	0.1
R7126/ ACS 45	3	2857	22.7	22.2	41.3	10.6	2.6	xx*	---	0.6
R7127/ ACS 46	2	1831	19.6	23.6	45.9	7.8	1.7	0.5	---	0.9
R7128/ ACS 47	2	1588	16.3	30.7	42.1	3.1	6.2	0.8	---	0.8
R7129/ ACS 48	2	1818	24.0	23.2	40.9	1.7	8.3	1.3	---	0.7

* xx= garnet visible in hand specimen but not present in thin section.

** Other= apatite, zircon and ore minerals.

The "dark" group was found to contain pyroxene (hypersthene) and no biotite, whereas the "light" group contained biotite and no pyroxene.

FIGURE 14

Adirondack Highlands, New York

Crane Mountain

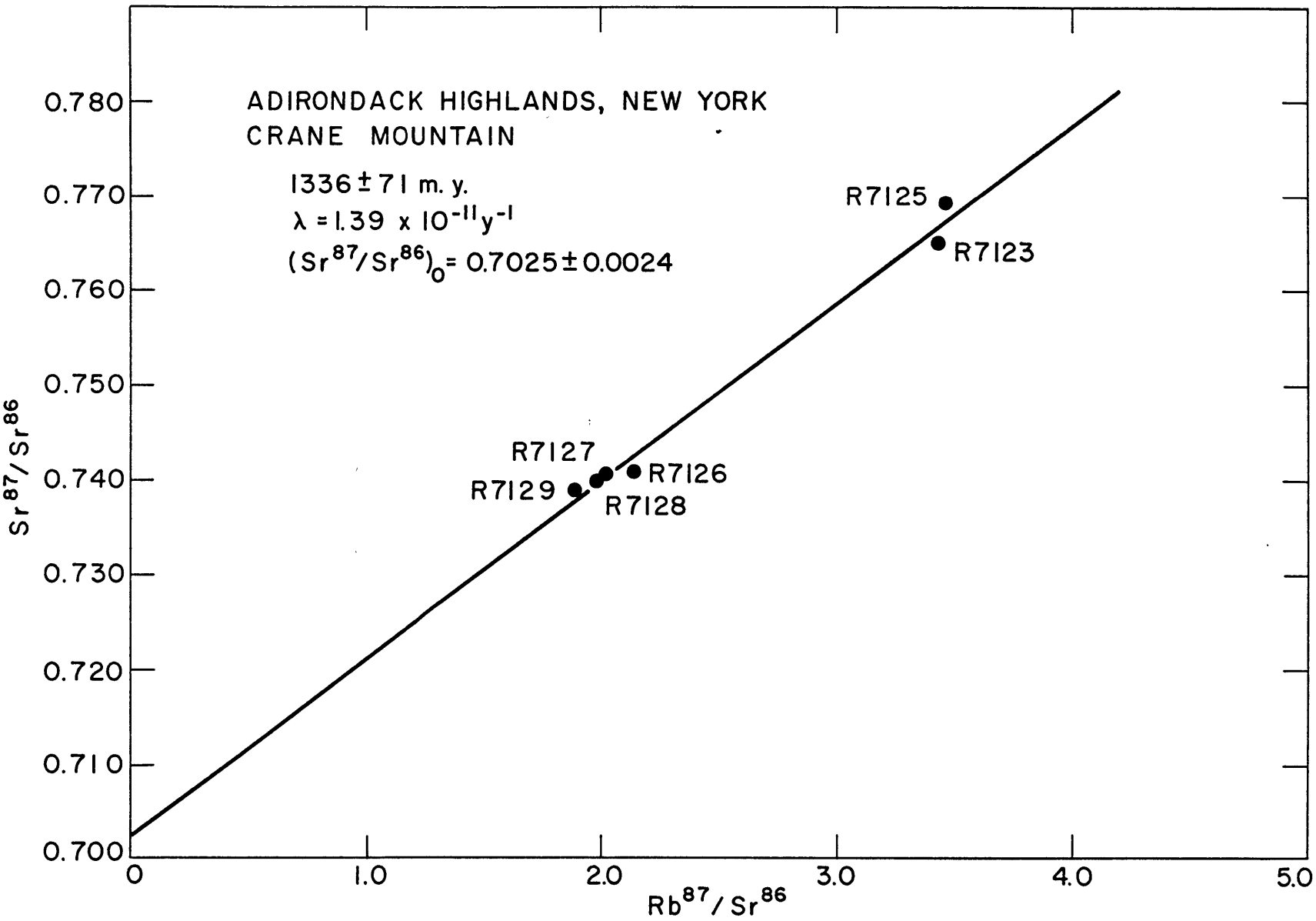
ADIRONDACK HIGHLANDS, NEW YORK
CRANE MOUNTAIN
1336 ± 71 m. y.
λ = 1.39 x 10⁻¹¹ y⁻¹
(Sr⁸⁷/Sr⁸⁶)₀ = 0.7025 ± 0.0024
R7125
R7123
R7127
R7126
R7129
R7128
0.780
0.770
0.760
0.750
0.740
0.730
0.720
0.710
0.700
Sr⁸⁷/Sr⁸⁶
0
1.0
2.0
3.0
4.0
5.0
Rb⁸⁷/Sr⁸⁶

presented in the isochron in Figure 14.

Ten specimens from the Indian Lake, Blue Mountain, and West Canada Lakes Quadrangles were collected and submitted for analysis by Professor Dirk deWaard, Department of Geology, Syracuse University, Syracuse, New York. This area has been under extensive field investigation recently since it is a critical area for the recognition of the basement and supracrustal sequence outlined briefly above from the paper by Walton and deWaard (1963).

Five whole rock analyses have been made and an analysis of a potash feldspar separate from specimen R7322 has also been made (Table III-M and Figure 15). Specimen R7321 from Blue Mountain and R7322 from West Canada Lakes quadrangles have been mapped as part of the supracrustal sequence by deWaard (personal communication) and specimens R7326, R7327, and R7329 from Indian Lake have been interpreted as members of the basement complex.

Four of the analyses define a reasonably good isochron with an age of 1465 $\pm$ 85 m.y. with an initial ratio of 0.7014 $\pm$ 0.0013. Whole rock R7321 has been rather arbitrarily excluded from the regression analysis. Assuming the same initial ratio found above, this one specimen gives a slope of 0.01527 corresponding to an age of 1087 m.y.

These ages appear to be the oldest reported for the central Adirondacks and suggest a period of intrusion pre-dating the events reported by Hills and Gast and Heath at about 1100 m.y. The low initial ratio for both the Crane Mountain and the Indian Lake - Blue Mountain - West Canada Lakes isochrons indicates that there was not an extensive pre-Grenville history and that the age determination

closely represents the age of intrusion. A later metamorphism of lower intensity could possibly be recorded in specimen R7321 and it would be interesting to investigate further to see if two ages can be distinguished. An attempt should be made to see if a distinction between the supracrustal sequence and the basement can be made.

TABLE III-M

INDIAN LAKE, BLUE MOUNTAIN, AND WEST CANADA LAKES QUADRANGLES

Sample	Rb^{87}/Sr^{86}	Sr^{86}/Sr^{88}	$(Sr^{87}/Sr^{86})_{normalized}$	Isotope Dilution Rb(ppm)	Isotope Dilution Sr(ppm)	Rb/Sr
R7321/ W-15(b)	1.231	0.1207	0.7202	93	220	0.425
R7322/ 2(a)	1.984	0.1200	0.7417	135	197	0.682
R7326/ W-126(a)	1.576	0.1195	0.7344	121	223	0.543
R7327/ W-126(b)	0.6032	0.1178	0.7147	53	255	0,208
R7329/ W-124	0.7225	0.1198	0.7153	101	403	0.249

Specimens submitted by Dr. D. deWaard, Department of Geology, Syracuse University, Syracuse, New York

FIGURE 15

Adirondack Highlands, New York

Indian Lake, Blue Mountain, and West Canada Lakes Quadrangles

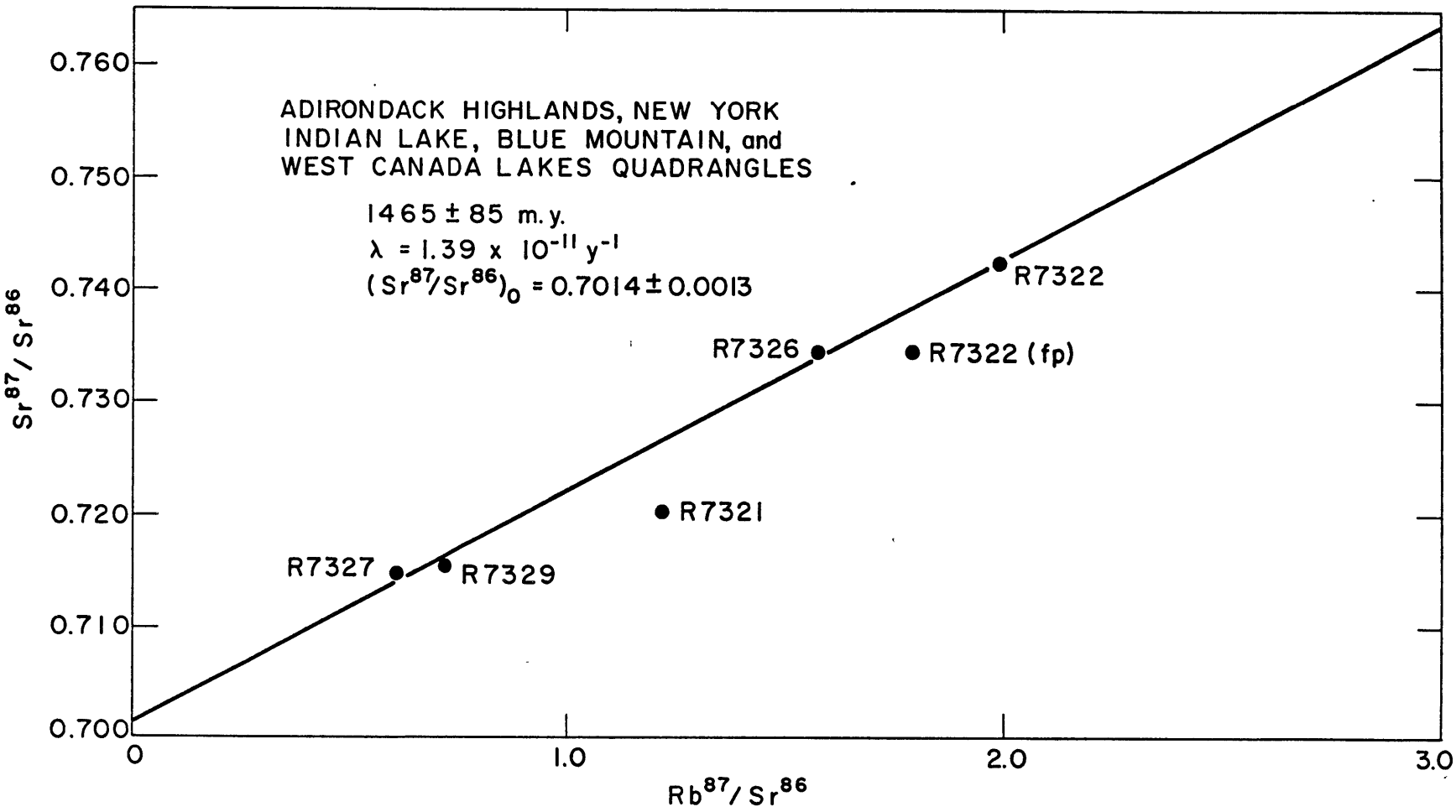
ADIRONDACK HIGHLANDS, NEW YORK
INDIAN LAKE, BLUE MOUNTAIN, and
WEST CANADA LAKES QUADRANGLES
1465 ± 85 m.y.
λ = 1.39 x 10^-11 y^-1
(Sr87/Sr86)0 = 0.7014 ± 0.0013
R7322
R7326
R7322 (fp)
R7321
R7327
R7329
0.760
0.750
0.740
0.730
0.720
0.710
0.700
Sr87/Sr86
0
1.0
2.0
3.0
Rb87/Sr86

FIGURE 16

Adirondack Highlands, New York

Sample Localities (Geology Simplified)

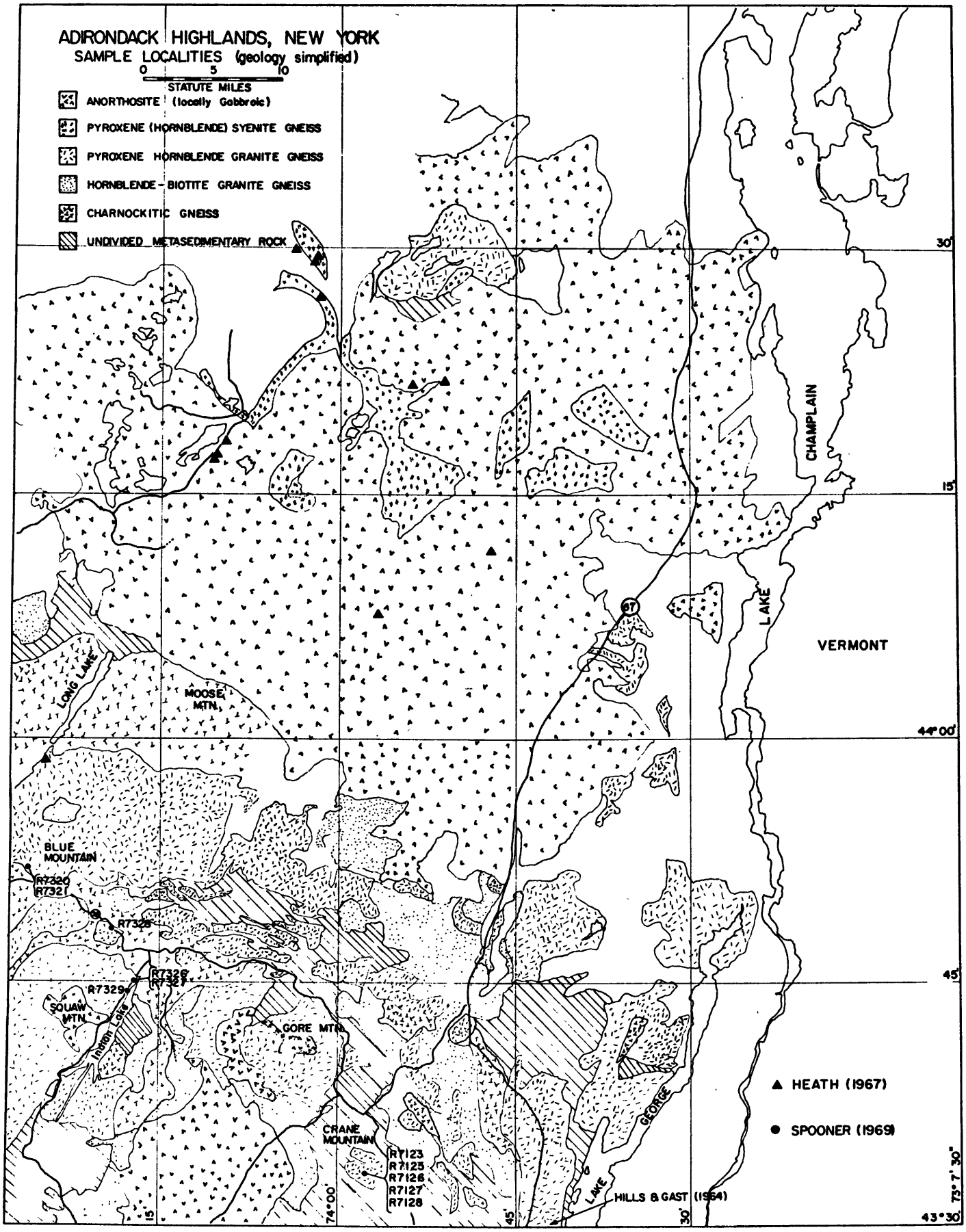
ADIRONDACK HIGHLANDS, NEW YORK
SAMPLE LOCALITIES (geology simplified)
0 5 10
STATUTE MILES
ANORTHOSITE (locally Gabbroic)
PYROXENE (HORNBLENDE) SYENITE GNEISS
PYROXENE HORNBLENDE GRANITE GNEISS
HORNBLENDE-BIOTITE GRANITE GNEISS
CHARNOCKITIC GNEISS
UNDIVIDED METASEDIMENTARY ROCK
CHAMPLAIN
LAKE
VERMONT
LONG LAKE
MOOSE MTN.
BLUE MOUNTAIN
R7320
R7321
R7328
R7329
R7327
SQUAW MTN.
INDIAN LAKE
GORE MTN.
CRANE MOUNTAIN
R7123
R7125
R7126
R7127
R7128
GEORGE
LAKE
HILLS & GAST (1964)
HEATH (1967)
SPOONER (1969)
30'
15'
44°00'
45'
74°00'
45'
30'
73°7'30"
43°30'

3.16 Westport, Ontario Map-Area

The Westport map-area is located about 30 miles northeast of Kingston, Ontario and 70 miles southwest of Ottawa, and comprises parts of Leeds, Lanark and Frontenac counties.

The most recent geological study of this area was undertaken by Wynne-Edwards (1967) who mapped the area at one inch to one mile, special emphasis being paid to the Precambrian rocks which outcrop in two-thirds of the mapped area.

On a regional scale the metamorphic rocks exposed are dominantly marbles, quartzites and quartzo-feldspathic gneisses typical of the Grenville province of southeastern Ontario. The highest metamorphic grade exposed in the region is attained in the Westport map-area in the Clear Lake anticline where characteristic assemblages of the pyroxene granulite facies occur. This high grade core (Figure 17) is surrounded by rocks of the hornblende granulite subfacies and these, in turn, by the amphibolite facies. The lowest grade present, the greenschist facies, lies adjacent to the amphibolite facies and forms the Hastings Basin to the northwest.

The granulite horizon (Wynne-Edwards, op.cit., map unit 8) forms an almost structureless unit throughout the area and is distinguished from the adjacent gneisses by a lower abundance of mafic minerals and an almost complete absence of foliation.

The mineralogical assemblages observed are characteristic of the granulite facies described by Eskola (1952):

1. sillimanite-garnet-biotite-plag.-quartz
   sillimanite-garnet-potash feldspar-plag.-quartz

FIGURE 17

Westport, Ontario Map Area (Geology Simplified)

Showing Sample Localities

(after H. R. Wynne-Edwards, 1967)

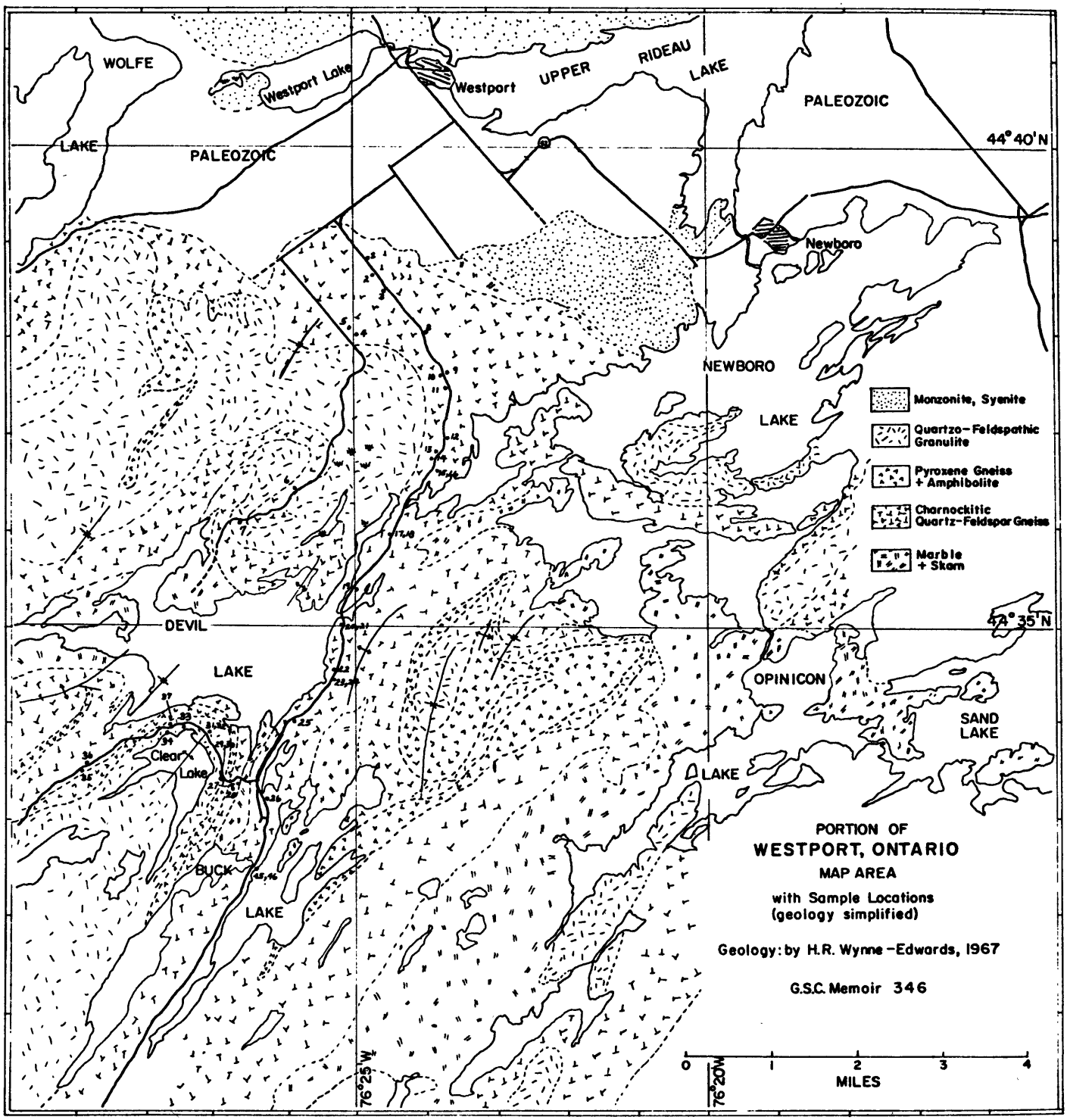
WOLFE
LAKE
Westport Lake
Westport
UPPER
RIDEAU
LAKE
PALEOZOIC
PALEOZOIC
44°40'N
Newboro
NEWBORO
LAKE
Monzonite, Syenite
Quartzo-Feldspathic Granulite
Pyroxene Gneiss + Amphibolite
Charnockitic Quartz-Feldspar Gneiss
Marble + Skarn
44°35'N
DEVIL
LAKE
OPINICON
LAKE
SAND LAKE
Clear Lake
BUCK
LAKE
PORTION OF
WESTPORT, ONTARIO
MAP AREA
with Sample Locations
(geology simplified)
Geology: by H.R. Wynne-Edwards, 1967
G.S.C. Memoir 346
76°25'W
76°20'W
0
1
2
3
4
MILES

2. garnet-biotite-plag.-quartz
   garnet-potash feldspar-plag.-quartz

3. garnet-hypersthene-biotite-plag.-quartz
   garnet-hypersthene-potash feldspar-plag.-quartz

4. hypersthene-biotite-plag.-quartz
   hypersthene-potash feldspar-plag.-quartz

The textures shown in the specimens analyzed in this study show many features in common with those from Madras State. For example, in many of the specimens the characteristic blue-grey color and greasy texture of the quartz is apparent. The potash feldspar is dominantly mesoperthitic although antiperthite is also common. Biotite and hornblende are also present and in some cases are the predominant mafic mineral present, the latter present especially in quartz-poor rocks. In the area adjacent to Devil Lake and Clear Lake the highest metamorphic grade was attained and hydrous phases are virtually absent. It is suggested that the following reaction took place:

biotite = hypersthene + potash feldspar + water

The presence of these hydrous phases does not disqualify membership in the granulite facies, however. Although the use of this term is somewhat of a field convenience (Wynne-Edwards, personal communication) it appears that its use is justified in that the addition of water vapor as another component must be considered. Also the partial pressure of CO_2 may be an important control since this component would exert a control over the activity of water in the system. Further, despite the usual "definition" of charnockite from the type locality in India, biotite and hornblende do occur there, although in relatively minor abundance (Subramanian, 1959). In like fashion, the

same may be said about the occurrence of hypersthene. Although this was an important part of the definition, hypersthene does not occur in every hand specimen or in every outcrop. When considered on the scale of the geological unit, however, it is a characteristic index mineral.

Toward the northern edge of the map-area, there are three major plutons of quartz monzonite roughly four miles in diameter and concordant with the metamorphic rocks enclosing them. The cores of the plutons are relatively homogeneous, whereas the borders contain numerous inclusions and in places the gneissic country rock is altered to monzonite, the original gneissic texture being only faintly preserved. Wynne-Edwards has suggested that these three plutons were emplaced late in the tectonic sequence of events that took place in the region and that these represent remobilized pre-Grenville basement.

Petrographic and analytical results from the various rock units are discussed at length by Wynne-Edwards.

3.17 Geochronology

In the Fall of 1967, the writer visited the Westport map-area and with the aid of Professor H. R. Wynne-Edwards some fifty specimens were collected with emphasis on the charnockitic quartzo-feldspathic gneisses. Eight specimens were selected on the basis of characteristic granulite facies mineralogy and range in the rubidium-strontium ratio,and were analyzed isotopically. The petrographic descriptions are given in Appendix A and the analytical results are presented in Table III-N and Figure 18.

A least squares regression analysis (after York, 1966) on the eight Westport, Ontario analyses gives an age of 1320 $\pm$ 59 m.y. with an initial Sr^{87}/Sr^{86} ratio of 0.7059 $\pm$ 0.0009. Using five points only (omitting R7070, R7071, and R7091) an age of 1334 $\pm$ 24 m.y. is obtained with an initial Sr^{87}/Sr^{86} ratio of 0.7065 $\pm$ 0.0004. Each analytical point used in the least squares regression was weighted using an error in Sr^{87}/Sr^{86} of 0.1% and in Rb^{87}/Sr^{86} of 3%.

Krogh and Hurley (1968) have recently published whole-rock isochron data from various localities in the Grenville Province including results on the Westport granite (quartz monzonite) and the Ridge granite which has a similar geological setting and occurs in the greenschist region to the northeast of Westport in the Hastings area. The whole-rock age reported in their study is 1016 $\pm$ 39 m.y. based on seven analyses with an initial Sr^{87}/Sr^{86} initial ratio of 0.704 (no error limits quoted).

It is interesting to note that the ages obtained for the pyroxene granulites of the present study and the adjacent quartz monzonites

TABLE III-N

WESTPORT MAP AREA, ONTARIO

Sample	Rb^{87}/Sr^{86}	Sr^{86}/Sr^{88}	$(Sr^{87}/Sr^{86})_{normalized}$	Isotope Dilution Rb(ppm)	Sr(ppm)	Rb/Sr
R7085/27	0.079	0.1207	0.7078	15	530	0.027
R7083/25	0.684	0.1202	0.7203	85	359	0.236
R7070/13	0.873	0.1208	0.7193	140	466	0.301
R7090/31	0.394	0.1205	0.7245	57	417	0.136
R7113/49(2)	2.998	0.1189	0.7628	125	121	1.030
R7062/5	0.154	0.1200	0.7091	24	454	0.053
R7061/4	0.822	0.1195	0.7219	28	99	0.284
R7112/49(1)	1.789	0.1210	0.7393	88	142	0.616
R7071/14	1.023	0.1210	0.7234	63	180	0.353
Chondrodite Marble: Isotopic ratio						
R7106/44	--	0.1204	0.7066 $\pm$ 0.001 at 95% C.L. (2σ)			

FIGURE 18

Isochron

Westport, Ontario

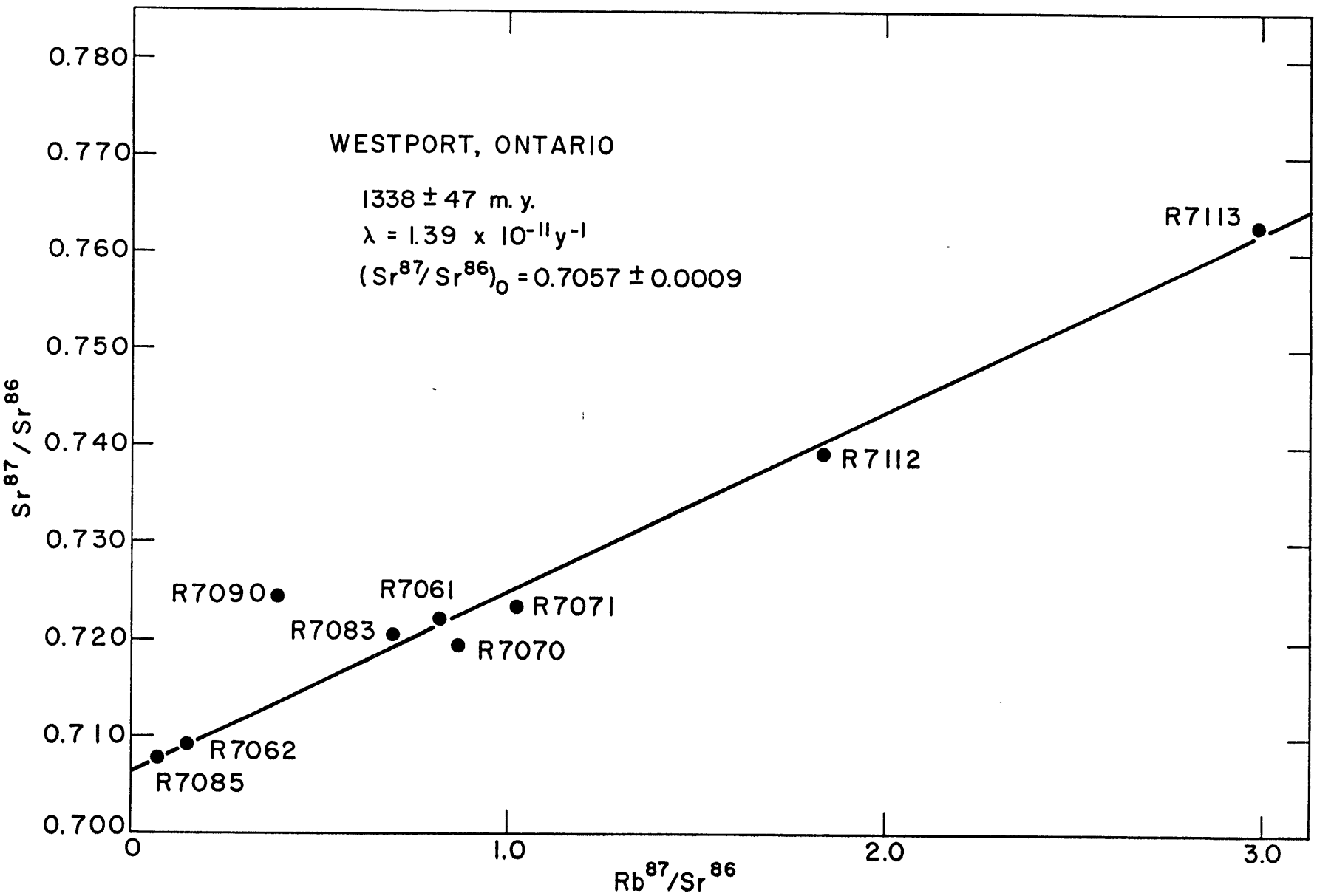
WESTPORT, ONTARIO
1338 ± 47 m. y.
λ = 1.39 x 10⁻¹¹ y⁻¹
(Sr⁸⁷/Sr⁸⁶)₀ = 0.7057 ± 0.0009
R7113
R7112
R7090
R7061
R7071
R7083
R7070
R7062
R7085
0.780
0.770
0.760
0.750
0.740
0.730
0.720
0.710
0.700
0
1.0
2.0
3.0
Sr⁸⁷/Sr⁸⁶
Rb⁸⁷/Sr⁸⁶

support the sequence of events inferred from the field relationships. Wynne-Edwards has pointed out the distinct stratigraphic position that the granulites occupy in the sequence of rock types represented in the area. The quartzo-feldspathic and dioritic pyroxene granulite constituting the highest grade represented in the region and the one most closely approaching the type charnockite mineralogical assemblage, is localized in the Clear Lake anticline and is placed at the bottom of the sequence. Stratigraphically above this unit are interbedded major units of marble, quartzite, and gneiss.

The initial Sr^{87}/Sr^{86} ratio obtained for the pyroxene granulite (0.7059 ± 0.0009 or 0.7065 ± 0.0004) is measurably higher than the value obtained by Krogh et al. (1968) for the combined Westport and Ridge quartz monzonite bodies. The values for the initial ratios and ages with 3 and 5% errors for the standard deviation of the mean for the Rb^{87}/Sr^{86} ratios of the Westport quartz monzonites are:

Error in (Rb^{87}/Sr^{86})	$(Sr^{87}/Sr^{86})_o$	AGE (m.y.)*
5%	0.7034 ± 0.0005	1047 ± 17
3%	0.7035 ± 0.0004	1044 ± 17

*Calculated from York's (1966) method of regression analysis.

This slightly higher value in initial ratio for the pyroxene granulites suggests that they were derived from a source region having a slightly higher Rb/Sr ratio than in the source region for the quartz monzonite which is intrusive into them. Krogh et al. (1968) suggest an upper mantle origin for these intrusive rocks on account of the low

initial ratio. On the basis of analytical error only, the initial ratios for the quartz monzonites and pyroxene granulites do not overlap, and this lends credence to Wynne-Edward's hypothesis that the pyroxene granulites formed through high-grade regional metamorphism of a sequence of greywackes. Further, the Sr^{87}/Sr^{86} isotopic ratio of a specimen of chondrodite marble (R7106/44) interpreted as being stratigraphically above the granulites yielded a value of 0.7066 ± 0.001 (at the 95%, 2σ Confidence Limits). This value, if taken to represent the Sr^{87}/Sr^{86} ratio in sea water, lies on the Marine Geochron (M.I.T. Annual Report, 1965, p. 147) at about 1000 m.y. ago. Peterman et al. (1967) have found significant variations in the isotopic composition of sea water strontium during Phanerozoic time which may reflect the changes in isotopic composition of strontium as the chemistry of sea water changed perhaps due to increased volcanism or changes in provenance of sediment introduced into the oceanic system.

Admittedly, the difference in initial ratios for the Westport and Ridge quartz monzonite and the pyroxene granulites is not great. There is, however, less difference between the pyroxene granulite initial ratio and that of the chondrodite marble which is presumably of marine origin. On the basis of the isotopic evidence, it is suggested that these high-grade rocks had an association with a marine environment prior to metamorphism and only small additions of common strontium from lower crustal or upper mantle regions were made.

3.18 Kanuku and South Savanna Groups, Guyana, South America

The Kanuku Complex and adjacent South Savanna Group occupy a major portion of the southern half of Guyana and are part of the Guiana Shield which covers a large part of northern Brazil and Venezuela. The map area and pertinent geology are presented in Figures 19 and 20. The major rock types of the Kanuku Complex are a variety of high-grade acid biotite gneisses in which are found enclaves of acid and basic granulite. The regional geology of this and adjacent groups has been presented in a report by the Geological Survey of Guyana by Williams, Cannon and McConnell (1967). In a paper dealing primarily with the charnockitic affinities of the South Savanna-Kanuku Groups, Singh (1966) has demonstrated an intrusive relation of the presumably younger South Savanna granites with both the Kanuku Complex and the lower grade Marudi Group of metasediments of the greenschist and amphibolite facies. The emplacement also involved extensive assimilation and contact metamorphism followed by a phase of post-crystalline shearing along northeast-southwest zones. This granite complex also contains many enclaves bearing a resemblance to rocks of both groups, roughly maintaining their regional structural trends.

Though preferring to avoid the terms 'charnockite' and 'charnockitic' in his description of the Kanuku Complex, Singh draws out many points of similarity between this and the Madras type lithology. His explanation for the origin of some of the rocks of the Group closely parallels the proposals set forth by Howie (1955) for the Indian locality.

In the case of the basic granulites, the dike and sill-like

FIGURE 19

Outline Map of the Guiana Shield Showing Map Area of Kanuku Complex and South Savanna Granite

(from Records of the Geological Survey of Guyana, Volume 5, 1967, by E. Williams, R. T. Cannon and R. B. McConnell)

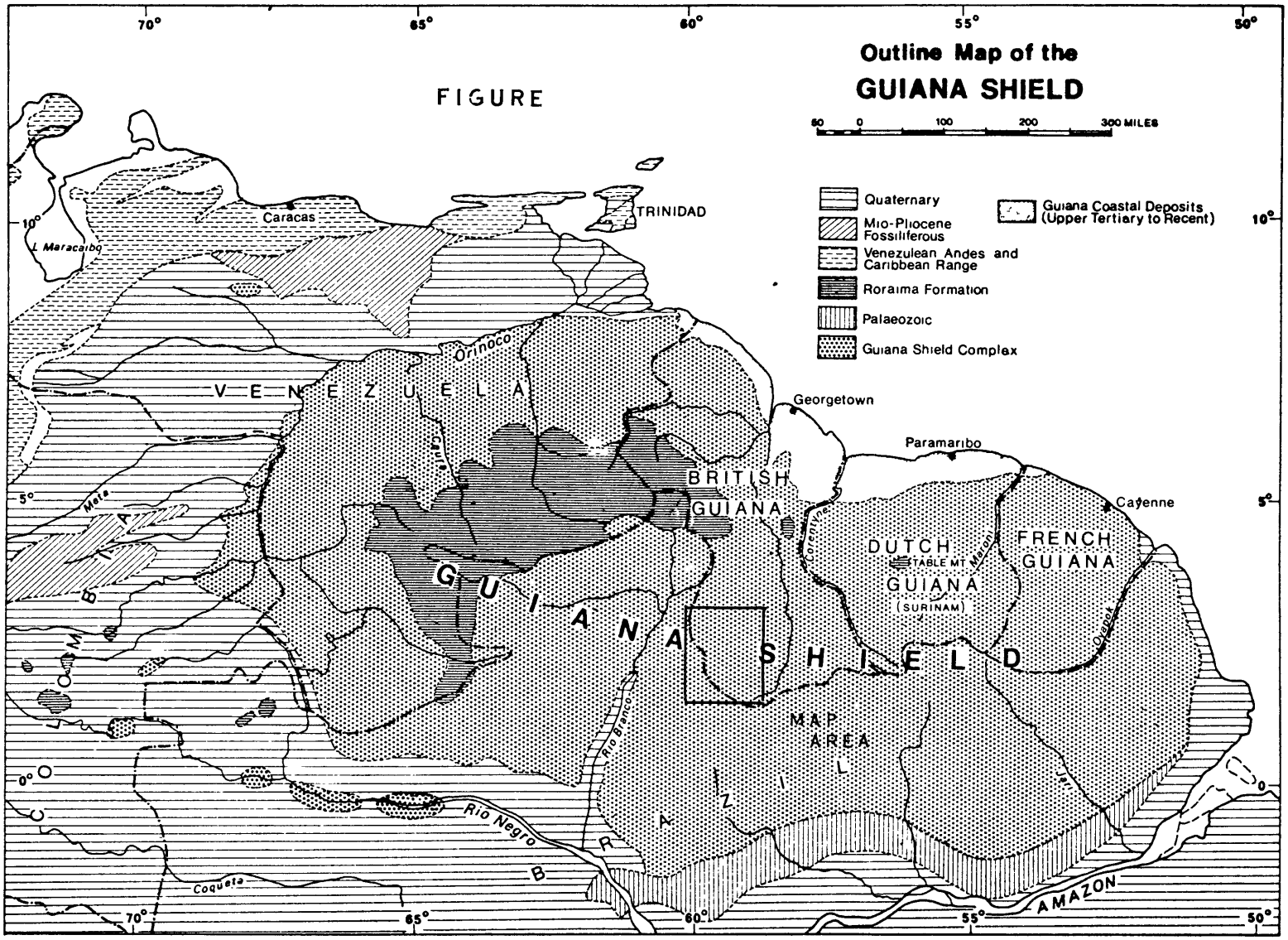
FIGURE
Outline Map of the
GUIANA SHIELD
80 0 100 200 300 MILES
Quaternary
Mio-Pliocene Fossiliferous
Venezulean Andes and Caribbean Range
Roraima Formation
Palaeozoic
Guiana Shield Complex
Guiana Coastal Deposits (Upper Tertiary to Recent)
70°
65°
60°
55°
50°
10°
5°
0°
Caracas
TRINIDAD
L. Maracaibo
Orinoco
VENEZUELA
Georgetown
Paramaribo
Cayenne
BRITISH GUIANA
DUTCH GUIANA (SURINAM)
FRENCH GUIANA
TABLE MT
GUIANA SHIELD
MAP AREA
Mato
Caura
Caroni
Cuyuni
Marowijne
Oyapock
Rio Branco
Rio Negro
Coquetá
AMAZON
COLOMBIA
BRAZIL

FIGURE 20

Kanuku-South Savanna Complex, Guyana

(from Records of the Geological Survey of Guyana,
Volume 5, 1967, by
E. Williams, R. T. Cannon and R. B. McConnell)

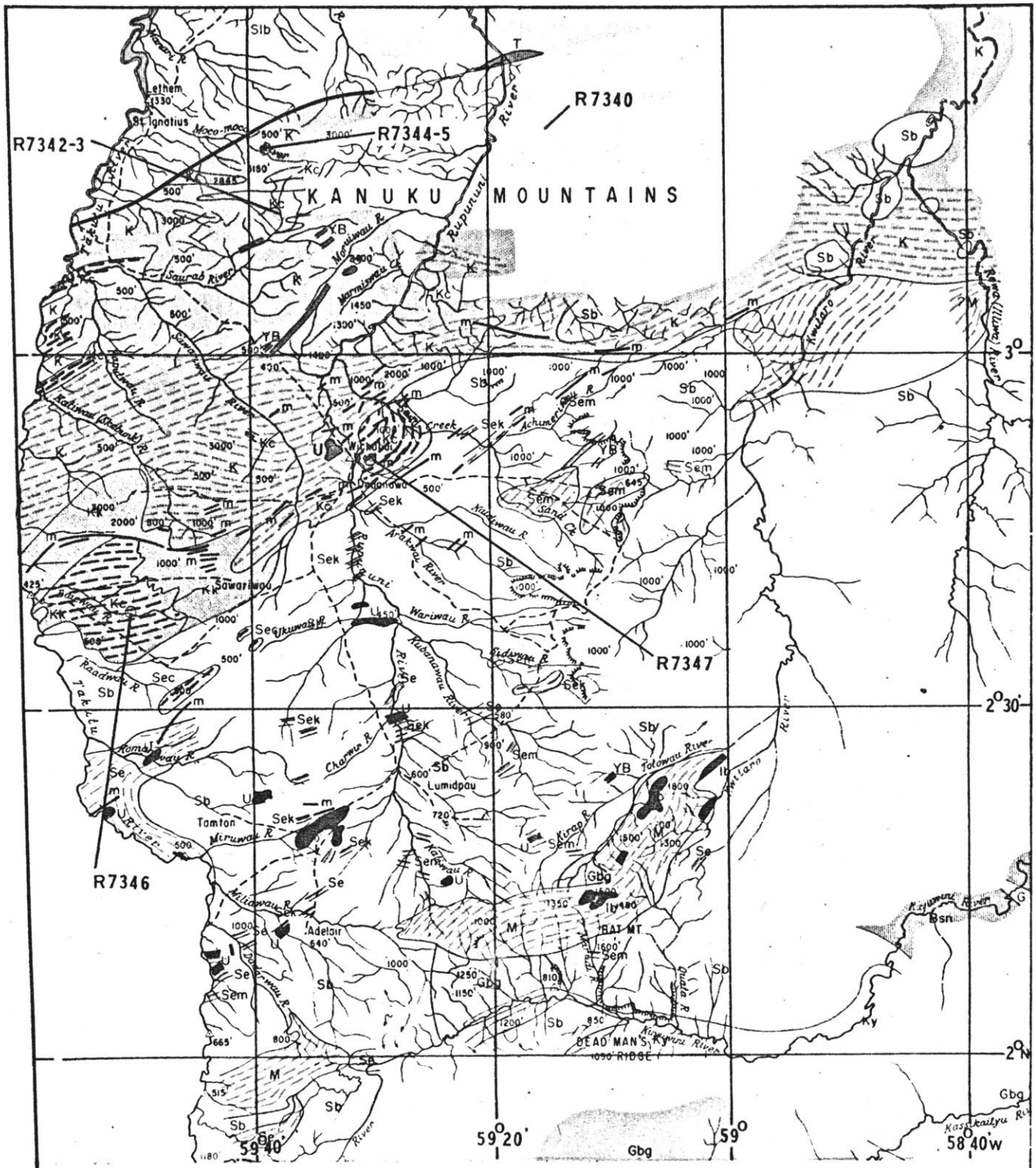

KANUKU - SOUTH SAVANNA COMPLEX

GUYANA

Sb	Biotite Granite	S. SAVANNA GP.
Se, Sek	Gneiss	S. SAVANNA GP.
Sec	Charnockitic Gneiss	S. SAVANNA GP.
K	Bio.-gt. Gneiss	KANUKU GP.
Kc	Charnockitic Gneiss & hypersthene Granite	KANUKU GP.
Kk	Granodiorite Gneisses	KANUKU GP.

attitude suggests that these were originally of igneous origin, probably gabbroic or diabasic in composition. The gabbro-granulites preserve the original ophitic texture, composition and zoning of the plagioclase appropriate for an igneous origin. Apatite was also noted as an accessory. It would appear that these rocks, originally igneous, subsequently underwent high-grade regional metamorphism and metasomatism with the host gneisses (discussed below).

The orthopyroxene-bearing acid biotite gneisses account for a significant portion of the map area and are characterized by assemblages of the sillimanite-almandite subfacies of the almandine-amphibolite facies of regional metamorphism. Where orthopyroxene occurs, it is found as small anhedra in biotite flakes. On the basis of field and petrographic criteria, Singh proposes that these rocks formed by contamination by basic norite granulites which presently occur as boudins, lenses and bands within the acid gneisses.

Though of low abundance, orthopyroxene-bearing acid granulites (distinct from the gneisses above) occur in association with quartzo-feldspathic granulites, acid garnet-granulites, acid cordierite-granulites, and alaskites. This association is suggestive of the low to medium pressure assemblage suggested by Lambert and Heier (1968) for rocks of a similar setting in Australia. Singh has also noted the strained aspect of quartz with sutured margins and extensive development of myrmekite. Similar findings for the suite of specimens analyzed here are reported in Appendix A on petrographic descriptions.

Singh ascribes their origin to the strong recrystallization of

the acid biotite gneisses at high temperatures and pressures. Hybridization by norite granulites is thought to have been responsible for the random occurrence of the pyroxene-rich acid granulites in the acid granulite terrain.

TABLE III-O

Compilation of Age Determinations by Potassium-Argon on South Savanna Group and Kanuku Group by Age Determination Unit, Institute of Geological Science, at Department of Geology and Mineralogy, Oxford University (modified from Table 3, p.40, Williams et al.(1967)

Sample	Rock Type and Locality	K:Ar Age (m.y.)
Biotite	South Savanna Granite, strongly porphyritic type, 1 mi. SE of Shiwirtau, South Savanna, 2° 52' N, 59° 16' W.	1190 ± 45
Biotite	South Savanna Granite, Tabtau facies, Tabtau Mountain, South Savanna, 2° 52' N, 59° 16' W.	1300 ± 50
Biotite	South Savanna Granite, strongly cataclased porphyritic biotite type. Biotite thought to have undergone complete recrystallization during shearing. -Sand Creed bed, 1/2 mi. S. of Cheppirariwau mouth, 2° 55' N, 59° 18' W	1256 ± 50
Muscovite	South Savanna Granite, strongly porphyritic biotite type, Rewa River, 3° 02' N, 58° 40' W	1720 ± 70
Biotite	South Savanna Granite, same locality	1685 ± 70
Biotite	Low-grade unmigmatized biotite schists forming an enclave in South Savanna granite: tentatively equated with Marudi Group. 3° 03' N, 58° 55' W.	1545 ± 60
Biotite	South Savanna Granite; near Awariwau, 2° 38' N; 59° 13' W.	1355 ± 55
Biotite	South Savanna Granite ?; Bat Mountain 2° 10' N, 59° 10' W.	1320 ± 50
Plagioclase pyroxene	Fresh diabase dike cutting South Savanna Granite, near Arakwai mouth, 3 mi. S. of Dadanawa, 2° 47' N, 59° 32' W.	450 ± 25 450 ± 40

TABLE III-O (cont.)

Rb-Sr isochron of South Savanna Granite based on 7 whole-rock analyses and 2 potash feldspar mineral separates. Initial ratio: 0.7073. (Snelling and McConnell, in press). 1880 ± 100 m.y.

Monazite (eluvial origin but from the South Savanna Granite), Discordant U/Th/Rb Age determined by A. G. Darnley of the Atomic Energy Division, Geological Survey of Great Britain.

Pb^{208}/Th^{232} age=2270 ± 185 m.y.

This study:

Whole Rock Rb:Sr on six samples from the Kanuku Complex, see Table III-P. Isochron age 2182 ± 95 m.y.

Initial ratio: 0.7018 ± 0.0011. See Figure 22 for isochron.

3.19 Geochronology

Despite the difficulties of access and the reconnaissance nature of mapping in this geologically complex region, numerous age determinations have been made by K:Ar, Rb:Sr and U:Th:Pb methods. A summary of data pertaining to the South Savanna and Kanuku Groups is given in Table III-O. Williams et al., (1967) have placed the Kanuku and South Savanna Groups as well as the lower metamorphic grade Marudi Group into the Rapununi Assemblage to form a Southern structural province. An east-west rift valley about 100 miles long and 30 wide provides a profound structural break separating the northern structural province from the south. This rift, which continues as a fault zone to the east-northeast into Surinam, precludes field correlations of the north and south portions of Guyana so that age determinations are essential to relate the two regions.

Snelling and McConnell (in press) have analyzed six specimens of the South Savanna Granite by Rb:Sr techniques (see Table III-O) and arrive at 1880 $\pm$ 100 m.y. as the significant age of emplacement of the granite. A discordant age on eluvial monazite from the South Savanna Granite gave a Pb^{208}/Th^{232} age of 2270 $\pm$ 185 m.y. (A. G. Darnley, in Barron, 1962a) which was later revised to 2075 m.y. by Snelling on the basis of uranium leaching. This revised age does not differ significantly from the Rb;Sr isochron age. Although the two have different structural styles, the age for the South Savanna Complex approaches that of the Younger Granites of the Northern province which have ages in the 1900-2000 m.y. range.

TABLE III-P

KANUKU COMPLEX, GUYANA, SOUTH AMERICA*

Sample	Rb^{87}/Sr^{86}	Sr^{86}/Sr^{88}	$(Sr^{87}/Sr^{86})_{normalized}$	Isotope Dilution Rb(ppm)	Sr(ppm)	Rb/Sr
R7340/ JPB 156	0.7203	0.1195	0.7217	57	230	0.248
R7341/ JPB 157	0.8849	0.1193	0.7308	68	222	0.306
R7345/ JPB 177	2.030	0.1193	0.7633	120	172	0.698
R7346/ JPB 216	1.6976	0.1200	0.7526	138	236	0.585
R7347/ JPB 300	0.2272 0.2237	0.1208	0.7086	16 16	205	0.078 0.078
R7344/ JPB 177	0.9187	0.1194	0.7327	71	223	0.318

*Samples submitted by Dr. J. P. Berrangé, Institute of Geological Sciences, Overseas Geological Surveys; 5, Princes Gate, London S.W. 7.

FIGURE 21

Isochron for Kanuku Complex, Guyana

South America

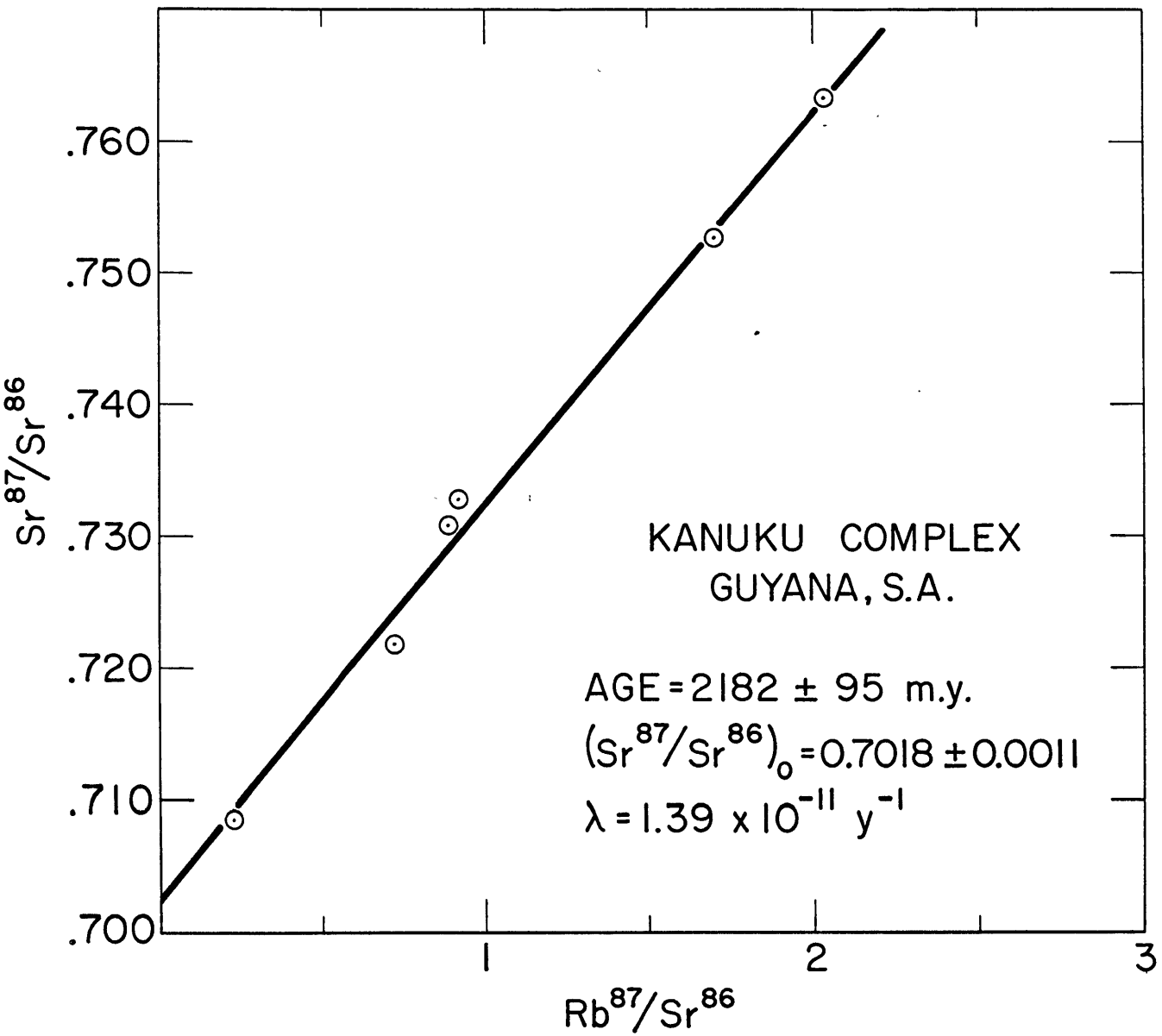
.760
.750
.740
.730
.720
.710
.700
Sr^{87}/Sr^{86}
1
2
3
Rb^{87}/Sr^{86}
KANUKU COMPLEX
GUYANA, S.A.
AGE = 2182 ± 95 m.y.
$(Sr^{87}/Sr^{86})_0 = 0.7018 \pm 0.0011$
$\lambda = 1.39 \times 10^{-11}\ y^{-1}$

3.20 The Granulite Facies of Pallavaram and Salem, Madras State and Kushalnagar, Mysore State, India

> "But nothing in India is identifiable, the mere asking of a question causes it to disappear or to merge into something else."
>
> E. M. Forster, A Passage to India

The granulite facies rocks forming the Archean of Peninsular India have received attention continuously since the late nineteenth century, particularly following Holland's (1900) descriptions of the so-called charnockite series in southern Madras State. The controversy concerning the origin of the "charnockite series" is discussed in Chapter I where reference is made to papers dealing with the field relations of these high grade rocks with their neighbors.

The three areas studied in the present investigation form part of the Eastern Ghats and Nilgiri Mountains of Peninsular India. Specimens from the type localities near Madras City which figure prominently in Holland's studies were kindly provided by Dr. P. R. J. Naidu, Honorary Director of the Mineralogical Institute, University of Mysore. He also provided the writer with an extensive suite from the Kushalnagar area, Mysore State. In addition, fifteen specimens from the Salem area of Madras State were kindly provided by Professor S. Subramanian, Government College, Salem, Madras State. The collections are listed in Appendix B.

At St. Thomas' Mount, about eight miles south of Madras City, a central portion of "charnockite" occurs with an augite-norite on the northeast and southwest sides (Holland, 1900, p. 172).

Both rock types are transected by contemporaneous charnockite pegmatites. About three miles further south, at Pallavaram, low rounded hills of charnockite are associated with a garnetiferous leptynite and norite. At Pammal, two miles west of Pallavaram, a hornblende-augite norite, locally biotite-rich, forms a hill rising about 200 feet above an alluvial plain. The regional foliation of these rocks strikes roughly northeast-southwest parallel to the Coromandel coast.

At Salem, the specimens provided by Dr. Subramanian correspond almost exactly with Holland's (1900, p. 181) detailed descriptions of the charnockite occurrences in this area. At Nagara Malai (malai = hill) which forms the southwest end of the Shevaroy Hills, the coarse-grained garnetiferous basic members are widely represented, R7336/14 and R7337/15. Locally, the garnet is fist-sized and is associated with marginal lenses of pyroxenite.

On the road to Trichinopoly (see Figure 22) about 3 1/2 miles south of Salem, transgressive tongues of the charnockite series in the older biotite-gneisses have been described by Holland (Ibid., p. 181, and p. 225). These descriptions appear to apply to specimens R7182/7 and R7330/8 to R7335/13 inclusive. The great mass of the charnockite series forming Jarugumalai protrudes into the biotite-gneisses which form a topographic low in the region about Salem. Holland (Ibid.) discusses several points of evidence in favor of an intrusive relation of the younger charnockites into the biotite gneiss.

The specimens from the Kushalnagar area of Mysore State are listed in Appendix B and are taken from various localities from the

FIGURE 22

Map of Specimen Localities, Salem Area,

Madras State, India

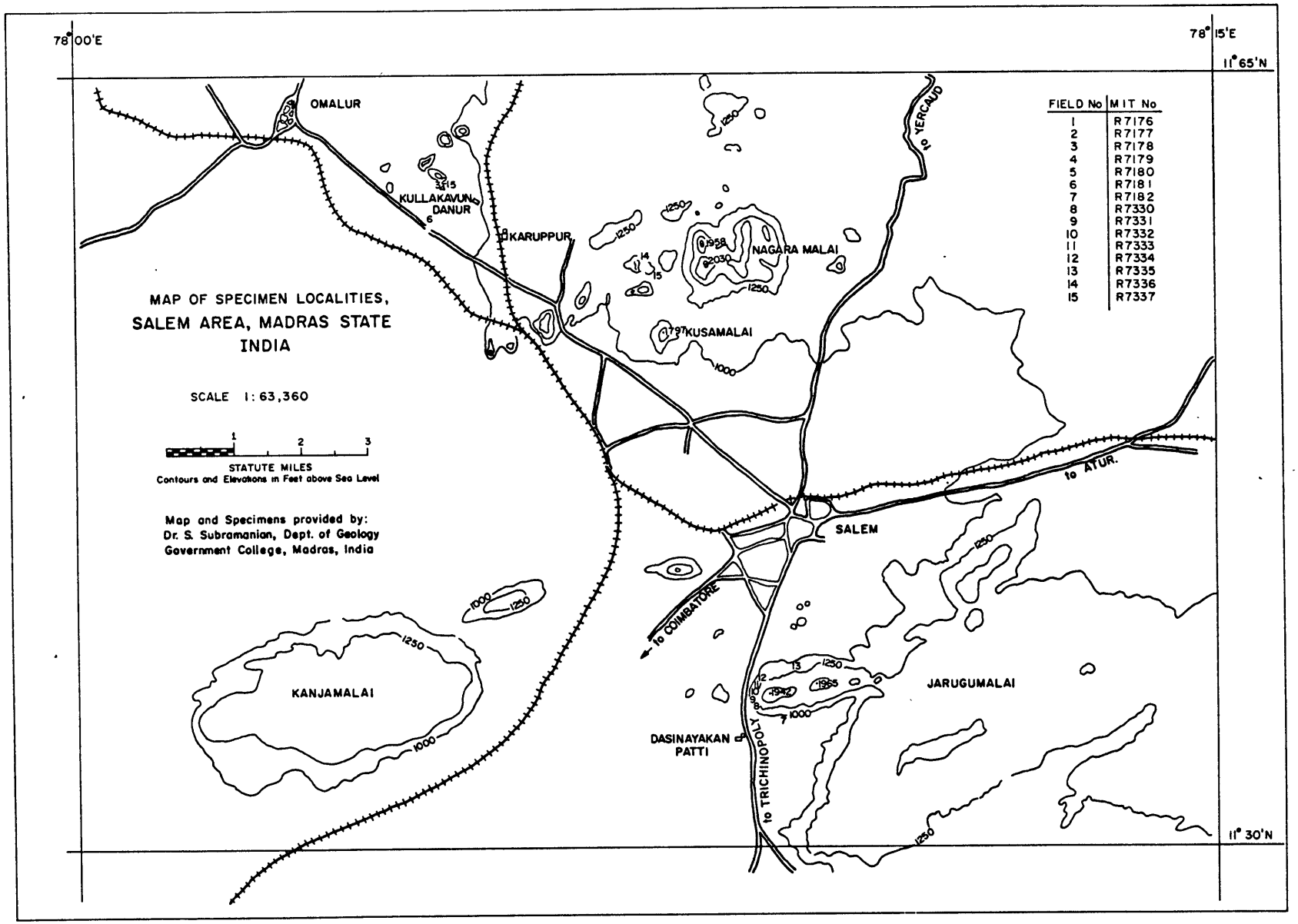
78°00'E
78°15'E
11°65'N
11° 30'N
OMALUR
KULLAKAVUNDANUR
KARUPPUR
NAGARA MALAI
KUSAMALAI
SALEM
KANJAMALAI
JARUGUMALAI
DASINAYAKAN PATTI
to YERCAUD
to ATUR.
to COIMBATORE
to TRICHINOPOLY
MAP OF SPECIMEN LOCALITIES,
SALEM AREA, MADRAS STATE
INDIA
SCALE 1:63,360
STATUTE MILES
Contours and Elevations in Feet above Sea Level
Map and Specimens provided by:
Dr. S. Subramanian, Dept. of Geology
Government College, Madras, India
FIELD No | MIT No
1 R7176
2 R7177
3 R7178
4 R7179
5 R7180
6 R7181
7 R7182
8 R7330
9 R7331
10 R7332
11 R7333
12 R7334
13 R7335
14 R7336
15 R7337

Nilgiris Mountains and the districts of Coimbatore. These two areas form the western extremities of the Eastern Ghats Belt which maintains the granulite facies grade throughout its length.

The problems associated with unravelling the complex sequence of intrusion and multiple episodes of regional metamorphism in Peninsular India have been partly resolved by the use of the various techniques of radiometric dating, but there still remains the necessity of detailed investigations within each area to completely understand the metamorphic and tectonic sequence in these ancient rocks.

3.21 Geochronology

Pichamuthu (1967) gives a brief account of the general geology and geochronology of Precambrian India in the broadest regional terms. Though this is by no means the most comprehensive account of Indian geology, it clearly demonstrates the relations among the various metamorphic belts exposed. Aswathanarayana (1968a, 1968b) and Crawford (1968) give possibly the most up to date account of both the overall age pattern in Peninsular India and of the granulite facies of Madras and Mysore States, which are of immediate concern in terms of this investigation. The following is in no way an exhaustive attempt at an extensive compilation of age data for the whole of Peninsular India, except insofar as it bears on the specimens analyzed in this work.

Crawford (1968) presents an isochron based on six analyses from St. Thomas' Mount and the Pallavaram area. An age of 2580 $\pm$ 90 m.y. was obtained with an initial Sr^{87}/Sr^{86} ratio of 0.7056 $\pm$ 0.0040,

though he points out that this determination was of insufficient accuracy to distinguish these rocks from the Peninsular Gneisses which outcrop further west at Bangalore. Since the two suites appear to fit the same isochron equally well, it was not possible to distinguish any difference in age between the charnockitic and non-charnockitic gneisses. Aswathanarayana (1968a) reports an age of 2650 $\pm$ 275 m.y. for the Madras locality and suggests that these may be consanguinous with the gneissic charnockites of Mysore. For these rocks, located in the Nilgiri Hills area, Crawford obtained a maximum indicated age of 2670 m.y. and an isochron age of 2615 $\pm$ 80 m.y. with an initial ratio of 0.7023 $\pm$ 0.0012 based on four analyses. Although Aswathanarayana suggests a derivation of the Madras and Mysore charnockites from the Peninsular Gneisses, Crawford (op.cit., p. 145) suggests with reservations that the Mysore (Nilgiri Hills) rocks may be slightly older than the Peninsular Gneisses from the neighboring Bangalore area.

The main contribution of this study to an understanding of these areas lies in the accurate determination of the initial Sr^{87}/Sr^{86} ratio. Nine of the specimens analyzed (Tables III-Q and III-R) did not have a sufficiently wide range in Rb/Sr ratio to construct an isochron. Using the analytical data presented by Crawford (1968) (Table III-S) for the Pallavaram and St. Thomas' Mount areas, however, along with the analytical data for specimen R7205, an age of 2618 $\pm$ 46 m.y. was obtained. The initial ratio for these analyses, including the seven specimens from Mysore State (a total of thirteen analyses), is 0.7039 $\pm$ 0.0005. In view of the low Rb/Sr ratio (about 0.2) for the seven analyses, the error in regression back to about 2600 m.y. ago

TABLE III-Q

PYROXENE GRANULITES (CHARNOCKITES) FROM SALEM, MADRAS STATE*

Sample	Rb^{87}/Sr^{86}	Sr^{87}/Sr^{86}	$(Sr^{87}/Sr^{86})_{normalized}$	Isotope Dilution Rb(ppm)	Sr(ppm)	Rb/Sr
R7176/1	----	0.1199	0.7045	nd**	----	----
R7178/3	0.0898	0.1198	0.7071	14.68	473.0	0.031
R7180/5	0.2877	0.1209	0.7143	40.5	407.7	0.099
R7182/7	----	0.1172	0.7044	nd	----	----
R7336/14	----	0.1174	0.7037+	nd	----	----
R7337/15	----	0.1188	0.7048+	nd	----	----

*Samples provided by Dr. S. Subramaniam, Government College, Salem, Madras State, India

**not detected at the 5 ppm level by X-ray fluorescence.

+Analyzed on mass spectrometer "Iris": value 0.003 low (from currently "accepted" value of 0.7082) for E & A Standard. A correction of 0.003+ applied (Dr. H. W. Fairbairn, personal communication).

FIGURE 23

Pyroxene Granulites (Charnockites)

Salem, Madras State

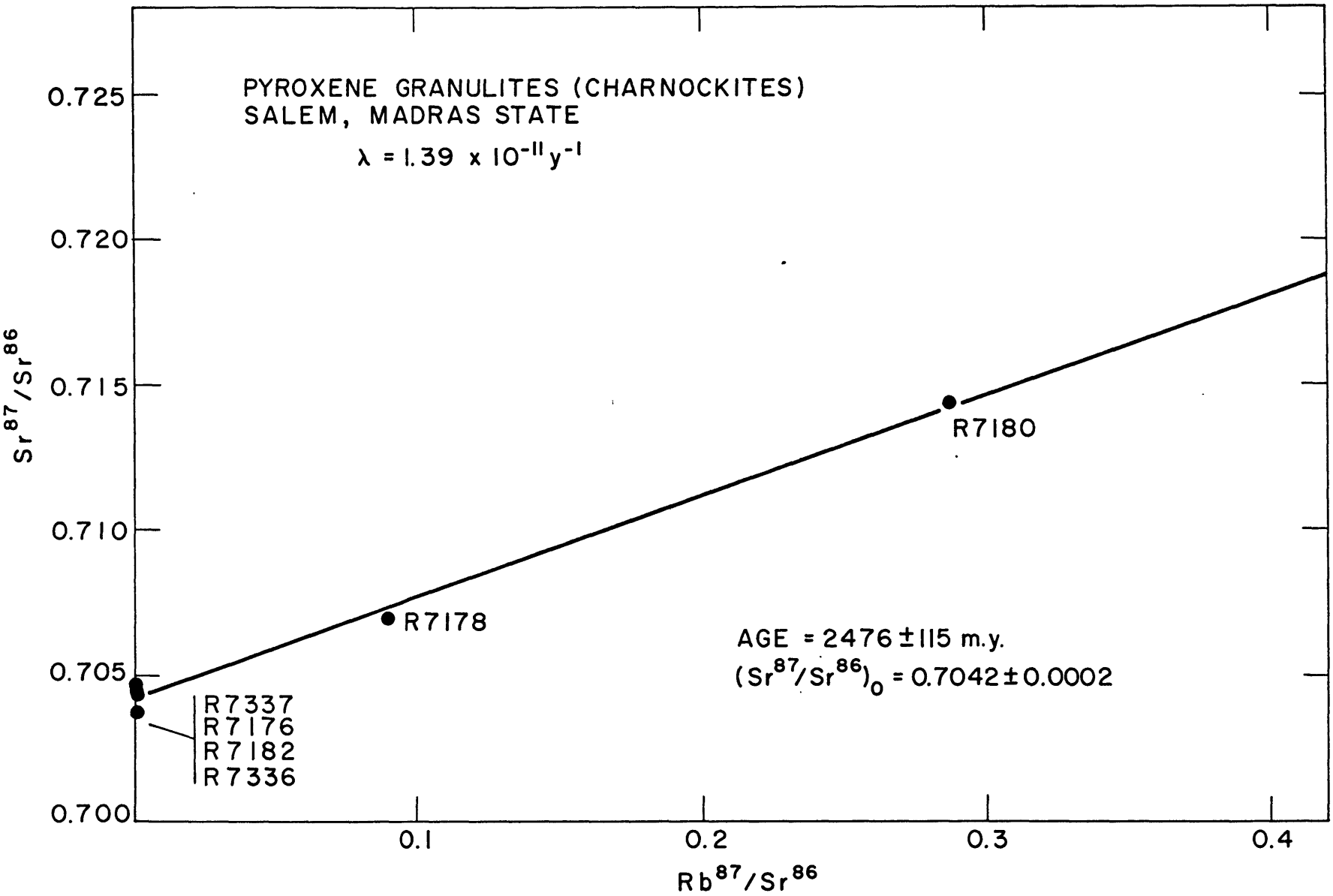
PYROXENE GRANULITES (CHARNOCKITES)
SALEM, MADRAS STATE
λ = 1.39 x 10⁻¹¹ y⁻¹
0.725
0.720
0.715
0.710
0.705
0.700
Sr87/Sr86
R7180
R7178
AGE = 2476 ± 115 m.y.
(Sr87/Sr86)0 = 0.7042 ± 0.0002
R7337
R7176
R7182
R7336
0.1
0.2
0.3
0.4
Rb87/Sr86

TABLE III-R

CHARNOCKITES FROM PALLAVARAM (TYPE AREA), MADRAS STATE
Latitude 12° 55' N, Longitude 80° 10' E

Sample and Locality	Rb^{87}/Sr^{86}	Sr^{86}/Sr^{88}	$(Sr^{87}/Sr^{86})_{normalized}$	Isotope Dilution Rb(ppm)	Sr(ppm)	Rb/Sr
Basic Charnockite St. Thomas Mount R7205/AS-12	3.373	0.1206	0.8282	134	116	1.152
Basic Charnockite Thattangannu R7240/AS-5	0.896	0.1203	0.7301	146	473	0.309
Basic Charnockite Biotite-rich, Cherimalai R7242/AS-10	1.429	0.1203	0.7430	210	427	0.492

TABLE III-S

CHARNOCKITES FROM KUSHALNAGAR AREA, MYSORE STATE

Latitude 12° 26' 45", Longitude 75° 56' 36"

Sample and Locality	Rb^{87}/Sr^{86}	Sr^{86}/Sr^{88}	$(Sr^{87}/Sr^{86})_{normalized}$	Isotope Dilution Rb(ppm)	Isotope Dilution Sr(ppm)	Rb/Sr
Charnockite, Dindgad R7214/A-85	0.165	0.1185	0.7083	6.3	110	0.057
Charnockite, Chikkamarahalli R7215/A-95	0.154	0.1200	0.7094	6.5	123	0.053
Charnockite, Kudige-Kanive R7216/A-110	0.312	0.1202	0.7167	13	116	0.108
Charnockite, Kanive Hill (left) R7217/A-115	0.147	0.1200	0.7077	3.9	76	0.051
Charnockite, Kanive-Jainkal Betta R7218/A-117	0.161	0.1205	0.7107	11	192	0.056
Charnockite, Marur R7219/A-121	0.234	0.1195	0.7203	12	143	0.081

TABLE III-S (cont.)

Sample and Locality	Rb^{87}/Sr^{86}	Sr^{86}/Sr^{88}	$(Sr^{87}/Sr^{86})_{normalized}$	Isotope Dilution Rb(ppm)	Sr(ppm)	Rb/Sr
Charnockite, Kanive Temple Hill (right) R7220/A-124	0.131	0.1205	0.7087	4.3	94	0.045
Charnockite, near Adinadur Tribal Colony R7221/A-126	0.288	0.1202	0.7094	20	203	0.099[6]
Charnockite, Cauvery River Bed, Hulse R7244/A-148	0.144	0.1197	0.7068	9.5	191	0.050

TABLE III-T

ISOTOPIC ANALYSES BY A. R. CRAWFORD (1968) FOR MADRAS STATE PYROXENE GRANULITES

from A. R. Crawford (1968) Table 24, p. 147

Sample Number and Locality	Rb^{87}/Sr^{86}	Sr^{87}/Sr^{86}	Isotope Dilution Rb ppm	Isotope Dilution Sr ppm
Pallavaram				
1867, Acid Charnockite N side saddle	0.9051	0.7412	44.2	140.9
1868, Acid Charnockite Port Trust Quarry	3.1046	0.8190	107.3	99.7
1869, Coarse grained vein in 1868	2.4519	0.7904	201.5	237.1
1870, Intermediate-basic Charnockite, Port Trust Quarry	0.1742	0.7105	11.4	189.0
1871, Leptynite, Total Rock	3.5838 3.5869	0.8356 0.8358	98.7	79.4 79.4
St. Thomas' Mount				
1874, Acid Charnockite St.Thomas' Mount proper, Total Rock	5.8134	0.9182	127.2	63.1

FIGURE 24

Charnockite

Madras and Mysore States

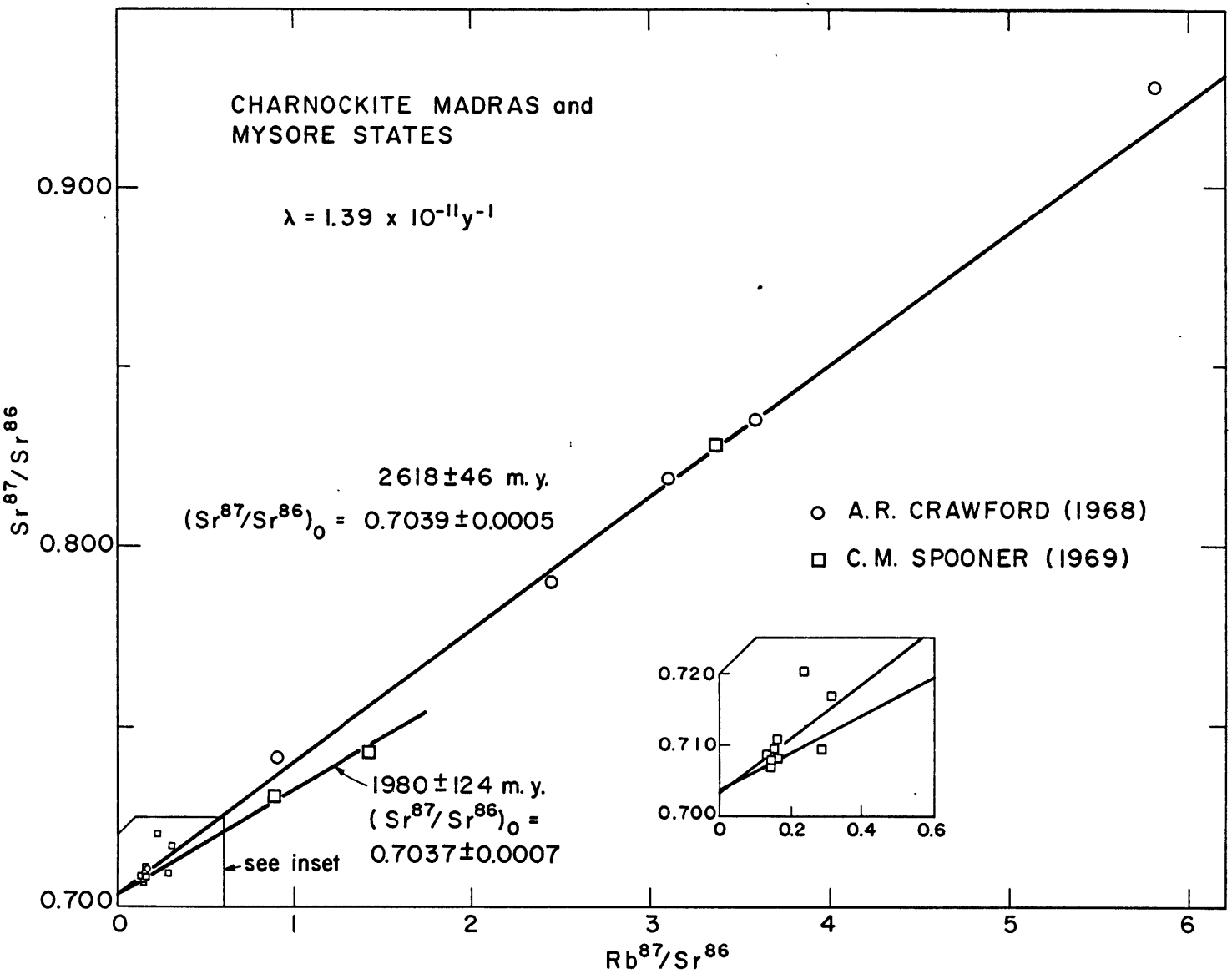
CHARNOCKITE MADRAS and
MYSORE STATES
λ = 1.39 x 10⁻¹¹y⁻¹
2618±46 m.y.
(Sr87/Sr86)0 = 0.7039±0.0005
1980±124 m.y.
(Sr87/Sr86)0 =
0.7037±0.0007
see inset
A.R. CRAWFORD (1968)
C.M. SPOONER (1969)
Sr87/Sr86
Rb87/Sr86
0.900
0.800
0.700
0
1
2
3
4
5
6
0.720
0.710
0.700
0
0.2
0.4
0.6

is not great and would appear to be justifiable in view of the discussion above concerning the similarity in age of both the Madras and Mysore charnockites. Two specimens (R7240 and R7242) from Pallavaram give an apparently younger age of about 1980 $\pm$ 124 m.y. including the seven analyses having low Rb/Sr ratios, providing an anchor point for the initial ratios at 0.7037 $\pm$ 0.0007.

CHAPTER IV

DISCUSSION OF RESULTS AND CONCLUSIONS

This rubidium-strontium isotopic study of the granulite facies is based on material from ten localities from four continents. In the majority of cases, these terrains have been interpreted to be of igneous origin, possibly affected by a later episode of metamorphism. In one case, however, a sedimentary origin has been proposed. The field relationships for the Westport map area of Ontario have been interpreted as a sequence of greywackes transformed to pyroxene granulite through deep-seated metamorphism. The isotopic study of this locality suggests that these rocks have indeed formed through the metamorphism of a material having a higher Rb/Sr ratio than was encountered in any other locality studied. Secondly, the pyroxene granulite gave a higher initial Sr^{87}/Sr^{86} initial ratio than the younger Westport quartz monzonite pluton. In addition, the granulites have an initial ratio which overlaps with a nearby chondrodite marble sequence and which is slightly higher stratigraphically and is presumed to be of marine origin.

The Sr^{87}/Sr^{86} initial ratios determined in this study are compiled in Table IV-A along with data available in the literature. A graphical presentation of this data is given in Figure 26 for comparison purposes. Also, a comparison of the initial ratio data and age data from this study is made with similar data for igneous, volcanic, sedimentary and metamorphic rocks available in the literature. This compilation was made available to the author by Professor P. M. Hurley.

TABLE IV-A

SUMMARY OF Sr^{87}/Sr^{86} INITIAL RATIOS IN PYROXENE GRANULITES

	Age (m.y.)	$(Sr^{87}/Sr^{86})_o$
Range of 54 Anorthosites (Heath, 1967)		0.703 to 0.706
Man Charnockite Series, Ivory Coast, Papon et al., 1968.	2750 ± 107	0.707 ± 0.001
Granodioritic migmatite series	2701 ± 135	0.699 ± 0.001
Lewisian Basement Gneisses, Lochinver, Sutherland, Scotland (Evans, 1965)	2600	0.7065
Inverian and Laxfordian Amphibolite Gneiss (Evans,1965)	2100 to 1560	0.7053
Nilgiri Charnockite Series and Gneiss,(Crawford, 1968)	2616 ± 80	0.7023 ± 0.0012
Madras City Charnockite (Crawford, 1968)	2580 ± 95	0.7059 ± 0.0042
PRESENT STUDY		
Kushalnagar, Mysore State (13)	2618 ± 46	0.7039 ± 0.0005
Pallavaram, Madras State (8)	1980 ± 124	0.7037 ± 0.0007
Okollo and Rakosi, West Nile District Uganda (9)	2629 ± 117	0.7054 ± 0.001
Crane Mountain, New York (6)	1336 ± 71	0.7025 ± 0.0025
Indian Lake, Blue Mtn. and West Canada Lake Quadrangles (6)	1465 ± 85	0.7014 ± 0.0013
Westport, Ontario (8)	1338 ± 47	0.7057 ± 0.0009
Kanuku Complex, Guyana South America (6)	2182 ± 95	0.7018 ± 0.0011
Pare Mountains (3)	927 ± 63	0.7056 ± 0.0011
Labor Serrit (3)	724 ± 8	0.7064 ± 0.0001
Salem, Madras State (6)	2476 ± 115	0.7042 ± 0.0002

FIGURE 25

Initial Sr^{87}/Sr^{86} Ratios in –

Continental Rocks Including Pyroxene Granulites

(after P. M. Hurley [1968] in part)

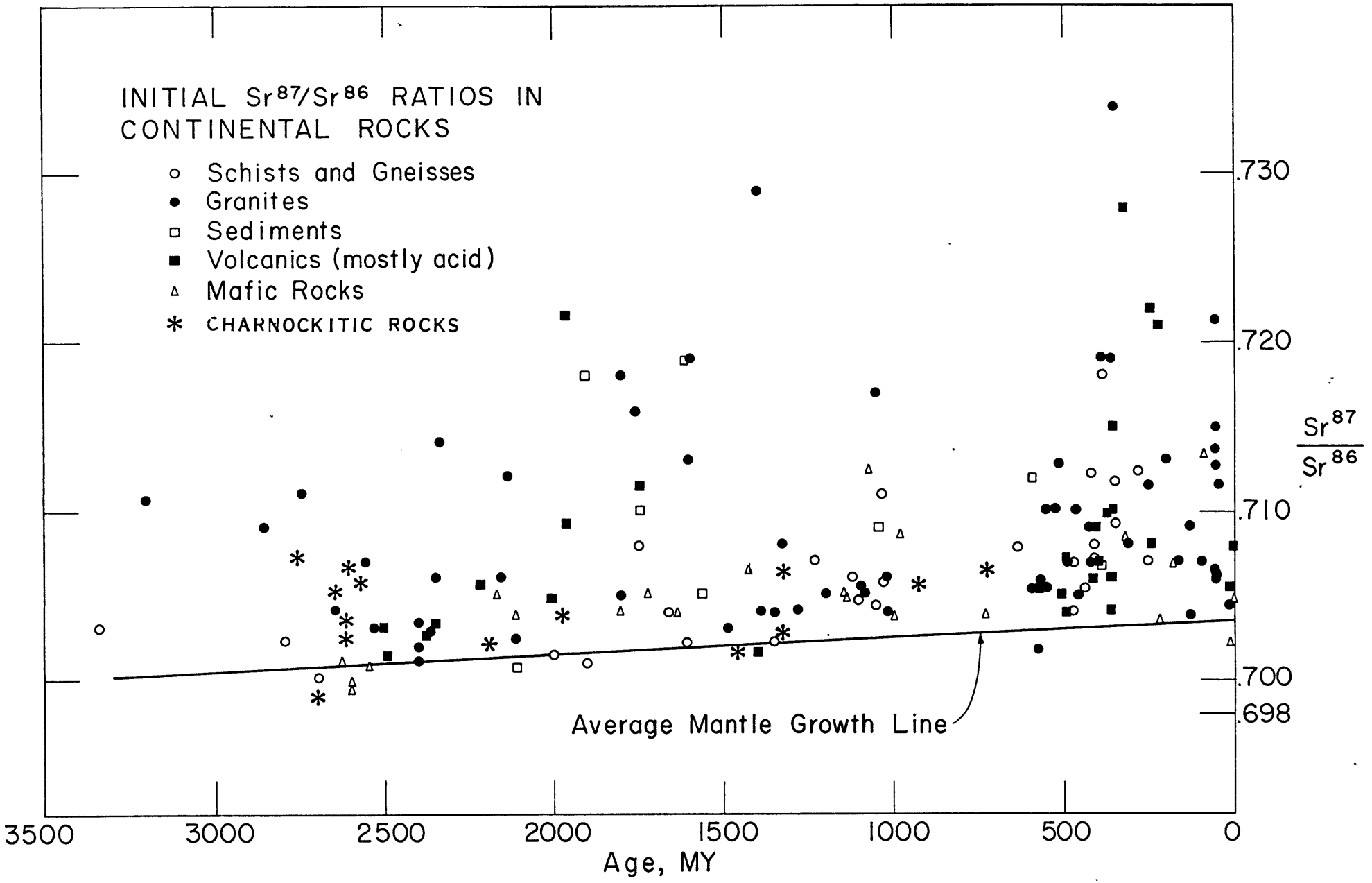
INITIAL Sr^{87}/Sr^{86} RATIOS IN CONTINENTAL ROCKS
Schists and Gneisses
Granites
Sediments
Volcanics (mostly acid)
Mafic Rocks
CHARNOCKITIC ROCKS
.730
.720
.710
.700
.698
$\frac{Sr^{87}}{Sr^{86}}$
Average Mantle Growth Line
3500
3000
2500
2000
1500
1000
500
0
Age, MY

FIGURE 26

Summary of Sr^{87}/Sr^{86} Initial Ratios

in Pyroxene Granulites

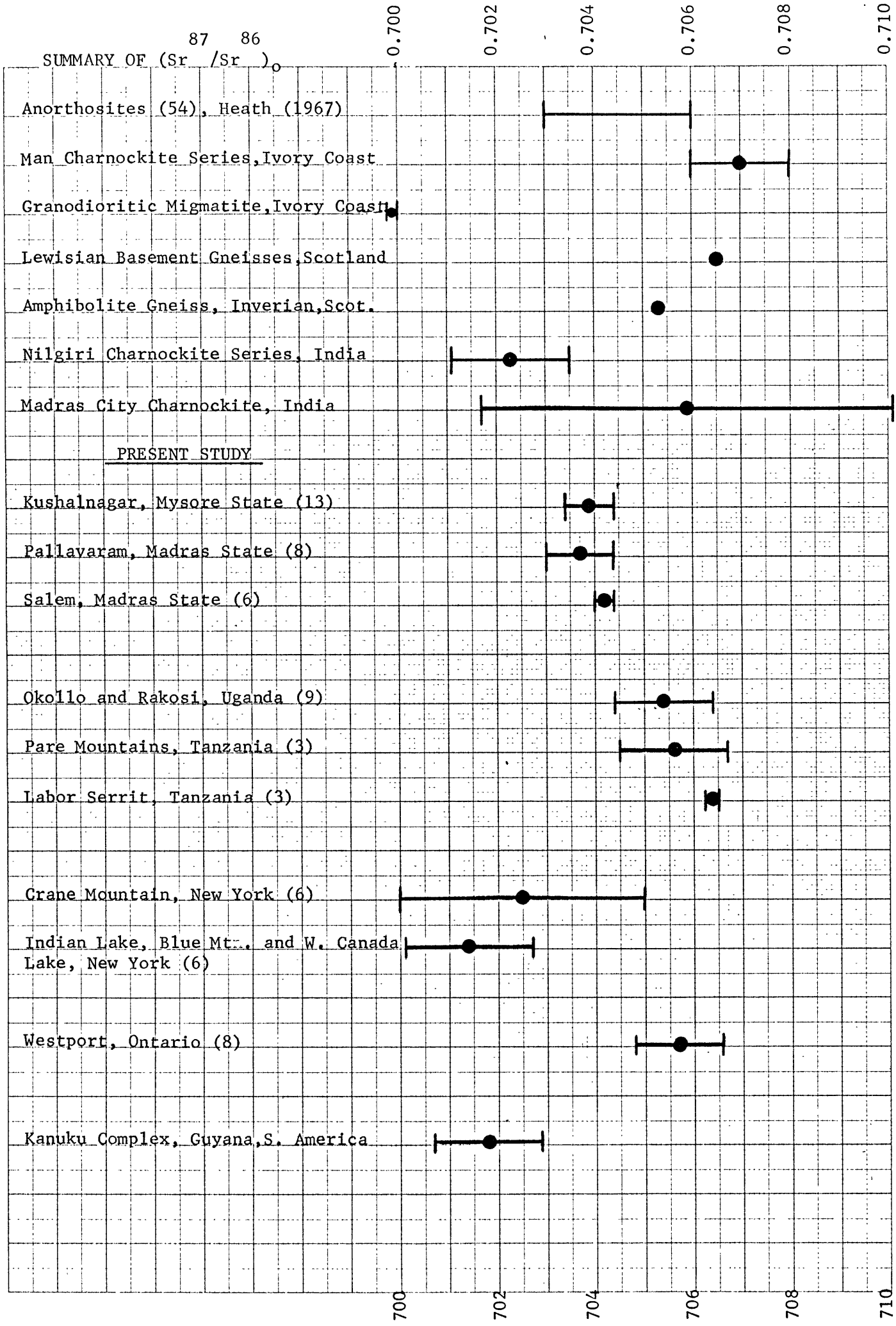
SUMMARY OF $(Sr^{87}/Sr^{86})_o$
0.700
0.702
0.704
0.706
0.708
0.710
Anorthosites (54), Heath (1967)
Man Charnockite Series, Ivory Coast
Granodioritic Migmatite, Ivory Coast
Lewisian Basement Gneisses, Scotland
Amphibolite Gneiss, Inverian, Scot.
Nilgiri Charnockite Series, India
Madras City Charnockite, India
PRESENT STUDY
Kushalnagar, Mysore State (13)
Pallavaram, Madras State (8)
Salem, Madras State (6)
Okollo and Rakosi, Uganda (9)
Pare Mountains, Tanzania (3)
Labor Serrit, Tanzania (3)
Crane Mountain, New York (6)
Indian Lake, Blue Mt. and W. Canada Lake, New York (6)
Westport, Ontario (8)
Kanuku Complex, Guyana, S. America
700
702
704
706
708
710

FIGURE 27

% K vs ppm Rb

with Shaw's (1968) Main Trend between

K = 0.1% and K = 1.0%

and

Madras and Mysore State Granulites

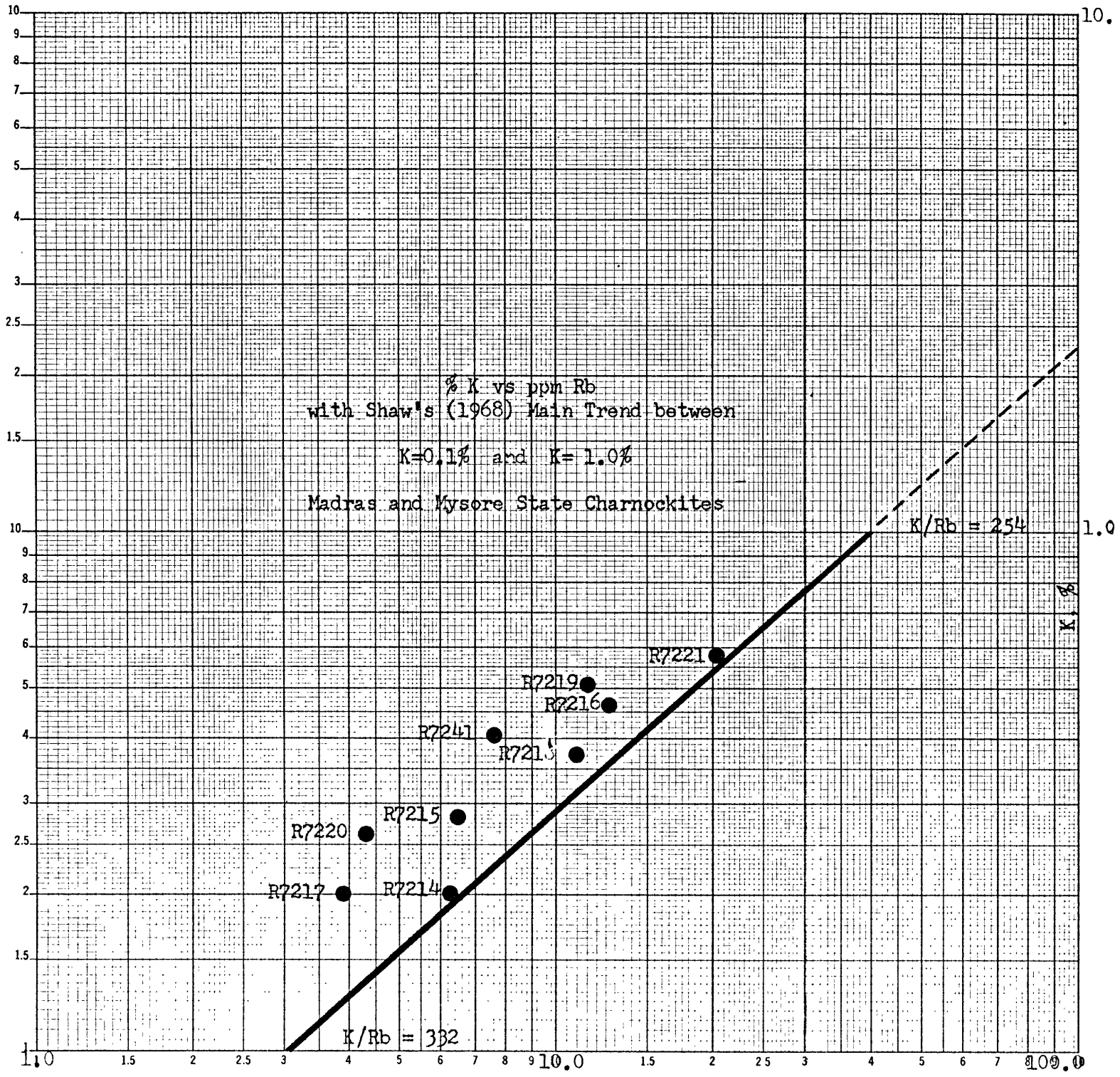
% K vs ppm Rb
with Shaw's (1968) Main Trend between
K=0.1% and K= 1.0%
Madras and Mysore State Charnockites
K/Rb = 254
K/Rb = 332
R7221
R7219
R7216
R7241
R7213
R7215
R7220
R7217
R7214
10.
1.0
K, %
10
9
8
7
6
5
4
3
2.5
2
1.5
1
1.0
1.5
2
2.5
3
4
5
6
7
8
9
10.0
1.5
2
2.5
3
4
5
6
7
100.0
Rb, parts per million

TABLE IV-B

M.I.T.#	(Sr,ppm)	$(Rb/Sr)_p$	Rb + ΔRb	$(Rb/Sr)_{orig}$	Δ%	$(Sr^{87}/Sr^{86})_p$	$(Sr^{87}/Sr^{86})_p^{orig}$	$\Delta(Sr^{87}/Sr^{86})$	Δ%
R7214	110	0.057	6.6	0.600	5	0.7083	0.7087	0.0004	0.1
R7215	123	0.053	9.8	0.080	51	0.7094	0.7112	0.0028	0.4
R7216	116	0.109	16.9	0.146	34	0.7167	0.7206	0.0039	0.6
R7217	76	0.051	6.6	0.087	71	0.7077	0.7115	0.0038	0.5
R7218	192	0.056	13.4	0.070	25	0.7107	0.7122	0.0015	0.2
R7219	143	0.081	18.5	0.129	59	0.7203	0.7254	0.0051	0.7
R7220	94	0.045	9.0	0.096	113	0.7087	0.7140	0.0053	0.8
R7221	203	0.100	21.5	0.106	6	0.7094	0.7101	0.0007	0.1

p = present day measured value
orig = original value of ratio before metamorphism
ΔRb = value of increment loss in Rb assuming Shaw's relationship for K/Rb

$(Sr^{87}/Sr^{86})_p^{orig}$ = value of present day Sr^{87}/Sr^{86} if there had been no loss of Rb through metamorphism.

The total range in Sr^{87}/Sr^{86} initial ratios is found to vary from 0.701 to 0.708 for the pyroxene granulite facies rocks considered here. The arithmetic mean for these analyses is 0.7042. Since the majority of the initial ratio determinations fall within the narrow range of 0.703 to 0.706 previously established for anorthosites by Heath (1967), a common source region at depth in the crust is postulated for these rocks. Although further work would be required to demonstrate whether the two rock types are consanguinous, the strontium isotopic data suggest a common source in a deep-seated, low Rb/Sr ratio environment.

This general survey of the initial ratios encountered in these deep-seated crustal rocks suggests that the lowermost regions of the continental crust are depleted in rubidium with respect to strontium; further, that the consistently low values found to date suggest that, if these rocks ever had higher Rb/Sr ratios and low K/Rb ratios, corresponding to the K/Rb trend established for crustal igneous and quasi-igneous rocks by Shaw (1968), the rubidium must have been lost soon after emplacement otherwise higher Sr^{87}/Sr^{86} initial ratios would result.

An approximate calculation may be made to find what the present day Sr^{87}/Sr^{86} ratio would have been if rubidium had not been lost from the system. It must be assumed that the K/Rb ratio varies linearly from 332 at 0.1% K to 254 at 1.0% K on the basis of Shaw's (1968) work. To test for this effect, loss of rubidium alone is assumed. If potassium is accounted for in the migration along with rubidium, then the effect will be greater since the "tie-line" between the present-day

potassium-rubidium plot and that before metamorphism will have a positive slope. This calculation is carried out for the Madras and Mysore State specimens. A plot of % K vs ppm Rb (Figure 27) for the Indian specimens shows clearly a deviation from the Main Trend defined by Shaw. For each specimen analyzed, an increment of rubidium is added to the present day rubidium content so that its K/Rb ratio coincides with the Main Trend. Assuming that strontium is fixed in the system, a new Rb/Sr ratio is obtained which is taken to represent the Rb/Sr ratio after emplacement and before the high grade metamorphic event. The average percentage change in Rb/Sr would be about 46%. Taking the initial Sr^{87}/Sr^{86} ratio found for these rocks at 0.7039, and an age of approximately 2600 m.y., one can calculate what the present-day Sr^{87}/Sr^{86} ratio would have been had there been no migration of rubidium. Using the power series expansion for $e^{\lambda t}$, the Sr^{87}/Sr^{86} ratio can be calculated approximately from the relation:

$$(Sr^{87}/Sr^{86})_t = (Sr^{87}/Sr^{86})_o + (Rb^{87}/Sr^{86})_t \, (\lambda t)$$

The appropriate calculations are given in Table IV-B. The percentage change in $(Sr^{87}/Sr^{86})_{meas}$ resulting from the depletion of rubidium is about 0.4% and amounts to a change of about 0.003 in the strontium isotopic ratio, well within the capability of measurement. In summary, assuming Shaw's (1968) relationship to be valid, the episode of high grade regional metamorphism up to granulite grade in India has resulted in a decrease in the Rb/Sr ratio of about 46% This gives a present-day Sr^{87}/Sr^{86} ratio about 0.4% lower than would result had there been no depletion.

Earlier mention was made of Heier's (1964) paper, wherein he proposes that mineral transitions in the deep crust, arising from progressive regional metamorphism up to the granulite facies, produce phases which are increasingly less favorable to the diadochic incorporation of rubidium. He suggests mineral transitions such as the breakdown of biotite at the beginning stage of granulite development that would be characterized, in the case of excess SiO_2, by the reaction:

$$K(Mg,Fe)_3AlSi_3O_{10}(OH)_2 + 3SiO_2 \longrightarrow KAlSi_3O_8 + 3(Mg,Fe)SiO_3 + H_2O$$

Since the phases produced on the right hand side of the equation are less favorable hosts to rubidium, Heier proposes that it becomes concentrated in a fluid phase resulting in a decrease in the Rb/Sr ratio in the deep-seated rocks with increasing metamorphic grade. As a consequence of the concentration of rubidium in the mica, he proposes further a mechanism for the natural fractionation of Sr^{87} from common strontium in a geological system. Anatectic melting under granulite facies conditions would be initiated by a granitic melt rich in potassium-bearing phases such as biotite and potash feldspar. Daughter Sr^{87} produced by the decay of the parent Rb^{87} in the mica would be in a less favorable site than its parent isotope and presumably would be easily removed from its lattice site into the melt.

The concentrations of rubidium and strontium in the coexisting phases of a pyroxene granulite have been determined by Howie (1965). Using these data, calculations will be made to see if such a fractionation would be observable.

The most serious objection to the above hypothesis lies in the nature of the reactions producing the anhydrous phases. As Heier recognizes, the whole mechanism of Sr^{87} fractionation rests upon the assumption that there is no exchange of radiogenic strontium produced in the biotite with common strontium in the other phases. As seen in Table IV-B, the other phases all have Rb/Sr<1 and an additional dehydration reaction involving hornblende would also be expected in

TABLE IV-C

Rb and Sr Distributions in an Intermediate Charnockite and its Phases, Mount Wati, West Nile District, Uganda. (after R. A. Howie,1965)

	Whole rock	Orthoclase	Andesine	Hornblende	Biotite
Rb	75**	300	nd	10	1000
Sr	800	800	1000	30	tr*
Rb/Sr	0.094	0.38	--	0.33	1000 ca.

* = ppm assumed
** = all values in parts per million.

view of the significant quantities of amphibole in many of these rocks. Expressed in its simplest form, the hornblende breakdown reaction could be expressed as:

$$Ca_2(Mg_4,Al)(AlSi_7O_{22})(OH)_2 \longrightarrow CaAl_2Si_2O_6 + CaMgSi_2O_6 + 3MgSiO_3 + H_2O$$

tschermakitic hornblende — anorthite — diopside — enstatite

As an example of the change in Sr^{87}/Sr^{86} of the system with the breakdown of both biotite and hornblende, consider a rock containing

10% by volume of both biotite and hornblende with the above distribution of rubidium and strontium. Allowing a liberal increment of time to elapse between homogenizations of the system, say 500 m.y., the growth in Sr^{87}/Sr^{86} after time (=500 x 10^6 y) in the biotite would be given by:

$$(Sr^{87}/Sr^{86})_{t=500} = (Sr^{87}/Sr^{86})_o + Rb^{87}/Sr^{86}(e^{\lambda t} - 1)$$

where:

$$(Sr^{87}/Sr^{86})_o = 0.705$$

from Table IV-B, $(Rb/Sr)_{bio} = 1000$, and $Rb^{87}/Sr^{86} = 3000$ approximately.

$= 1.39 \times 10^{-11} y^{-1}$.

so that:

$$(Sr^{87}/Sr^{86})_{bio.,t = 500\ m.y.} = 21.705$$

Of the 1000 ppm Rb originally present in the mica, 27.85% is Rb^{87} and about 1000 x 0.2785 x 0.01 = 2.785 ppm Sr^{87} would be produced during t = 500 m.y. due to the decay of Rb^{87}. Sr^{87} comprises 7.02% of common strontium and if the hornblende were to break down too, some 30 ppm common strontium or 0.0702 x 30 = 2.11 ppm Sr^{87} would be released to mix with the radiogenic Sr^{87} from the mica. This would reduce the $(Sr^{87}/Sr^{86})_{mica}$ to about one half of its former value of 21.705. It would be more realistic to expect several hundred ppm common strontium to be released since the feldspars have higher strontium concentrations and are likely to undergo some chemical change during metamorphism. Such a release and subsequent mixing would completely obscure the increase in the Sr^{87}/Sr^{86} ratio produced in the mica. If such a process could take place, then one would expect

it to occur in lithium pegmatites. In many cases, however, extremely high Sr^{87}/Sr^{86} ratios measured in lepidolites on the order of Sr^{87}/Sr^{86} = ca. 10^4 regress back to values between 0.705 and 0.710. These figures of Rb = 1000 ppm, and Sr = 1 ppm for the biotite and an interval of Sr^{87} growth of 500 m.y. are greatly weighted in favor of the separation process proposed by Heier and are not likely to be so extreme in nature. For example, in a study of the age of Nova Scotian granites by Fairbairn et al., (1960),the biotite with both the highest Rb and the lowest Sr was as follows:

	Rb ppm	Sr ppm	Rb/Sr	Sr^{87}/Sr^{86}	age
B2100	1666	4.9	340	4.49	330 m.y.

With these levels of concentration, it would take far less common strontium to completely obliterate the effect of buildup in the Sr^{87}/Sr^{86} ratio in the mica.

In summary, the results of this investigation indicate a source region for these deep-seated rocks which has a low Rb/Sr ratio similar to that of continental basalts and anorthosites. The rare-earth data show these rocks to have an enriched pattern of light rare-earths when the individual rare-earth elements are divided by their abundance in chondritic meteorites. This pattern of light enrichment is commonly observed in crustal rocks. The actual abundances are almost identical, element for element, to patterns found for gabbros and diabases. The similarity is extended to mineralogy also, since petrographic analysis indicates the composite sample to be approximately a diorite to quartz diorite in composition. The K/Rb data for thirty-two specimens show

a parallel trend with Shaw's (1968) Main Tend and details such as the curvature to lower K/Rb at higher K and Rb values are maintained. The results suggest that there may have been a depletion of rubidium with respect to potassium. This depletion may have occurred continuously after original emplacement into the deep-seated crustal environment or it may have been lost in a single episode or repeated episodes of high grade thermal metamorphism on a regional scale. The isotopic ages of these ancient rocks indicate that the K/Rb ratios typical of crustal rocks were established early in the evolution of the crust. The crustal rare-earth pattern for the ca. 2600 m.y. type locality of Madras indicates that this trend was also established at an early date. These data support the hypothesis put forward by Bence and Hurley (1967) that the light rare-earth elements, and lithophile elements such as K and Rb became enriched in the first differentiation product that formed the continental crust.

A plot of Thornton and Tuttle's (1960) differentiation index (D.I.) vs SiO_2 for fifty-four analyses taken from the literature shows that the various rock types collectively placed into the "charnockite series" fall well within the contours defining the various igneous rock series considered in this study.

The results discussed above indicate that the majority of pyroxene granulites that are now seen in the high grade cores of deeply-eroded shield areas are very likely of igneous origin, although possible exceptions exist (i.e., Westport, Ontario), indicating that "There are charnockites and charnockites" (Pichamuthu, 1950). Subsequent metamorphism of these rocks up to granulite grade has imparted a

metamorphic overprint involving changes in texture, mineralogy, chemistry, and isotopic age.

CHAPTER V

SUGGESTIONS FOR FURTHER STUDY

It is felt that further study of the trace element content and distribution between phases could be profitably undertaken in order to estblish whether there are additional depletions of lithophile elements at depth in the crust. For instance, it would be useful to establish the concentration of uranium and thorium in these rocks to complement the potassium determinations thus enabling one to calculate the heat production of these rocks. Actually, an attempt was made to determine Th and U in some of these rocks. Thorium is not difficult to determine by instrumental neutron activation (INAA) especially when using a Ge(Li) γ-detector. Gordon *et al.* (1968) have suggested the use of the 311.9 keV γ-ray 27^{d} Pa^{233} produced by the reaction $Th^{232}(n,\gamma)Th^{233}(\beta^{-})$. This element was measured for several specimens in this study. Uranium, on the other hand, presents a somewhat more difficult problem for analysis by this technique. An attempt was made to irradiate several grams of sample and transfer the sample via a pneumatic transfer system to a BF_3 counting system to count the delayed neutrons following the methods outlined by Amiel (1962) and Hamilton (1966). Unfortunately, the counter tubes (BF_3) which have a limited lifetime appeared to be expended.

Another interesting problem would be the determination of the distribution coefficients of trace and rare-earth elements in the various phases in these rocks, in hypersthene and garnet, for example. Comparison with published data for other rock types,

especially those presumed to be from the upper mantle would provide important information regarding the effect of high temperatures and pressures on the element distributions between phases in these rocks.

BIBLIOGRAPHY

Adams, F. D. (1929) The geology of Ceylon. Canadian Jour. Research. 1, no. 6, 467-511.

Alling, H. L. (1932) The Adirondack anorthosite and its problems. Jour. Geol. 40, 193-237.

Amiel, S. (1962) Analytical applications of delayed neutron emission in fissionable elements. Anal. Chem. 34, no. 13, 1683.

Aswathanarayana, U. (1968) Precambrian geochronology of peninsular India and Ceylon: an interpretation. Bull. Geol. Soc. India. 5, no. 2, 63.

_____ (1968) Metamorphic chronology of the Precambrian provinces of South India. Canadian Jour. of Earth Sciences. 5, 591.

Bainbridge, K. T., and Nier, A. O. (1950) Relative isotopic abundances of the elements. Prelim. Rep. No. 9, Nucl. Sci. Ser. Nat. Res. Coun. U.S., Washington, D.C.

Balk, R. (1931) Structural geology of the Adirondack anorthosite. Min. Pet. Mitt. 41, 308.

_____ (1944) Comments on some eastern Adirondack problems. Jour. Geol. 52, 289.

Barron, C. N. B. (1962) Geology of the South Savannas degree square. Geol. Surv. Br. Guiana, Bull. 33, 29 pp.

Bastin, E. S. (1909) Chemical composition as a criterion in identifying metamorphosed sediments. Jour. Geol. 17, 449.

Bence, A. E. (1966) The differentiation history of the earth by rubidium-strontium isotopic relationships. Unpub. Ph.D. Thesis, Mass. Inst. Tech.

Birch, F. (1961) The V_p in rocks to 10 kb. 2, Jour. Geophys. Res. 66, 2199-2224.

Bowen, N. L. (1937) Recent high-temperature research on silicates and its significance in igneous geology. Am. Jour. Sci. 33, 1-21.

Boyd, F. R. and England, J. L. (1964) The rhombic enstatite-clinoenstatite inversion. Carnegie Inst. Yearbook, 64, 117-120.

Buddington, A. F. (1939) Adirondack igneous rocks and their metamorphism. Geol. Soc. Am. Mem. 7, 201-230.

_____ (1948) Origin of granitic rocks of the northwest Adirondacks. Geol. Soc. Am. 28.

_____ (1952) Chemical petrology of some metamorphosed Adirondack gabbroic, syenitic and quartz syenitic rocks. Am. Jour. Sci., Bowen. 37-84.

Bugge, J. A. W. (1940) Geological and petrographical investigations in the Arendal district. Norsk Geol. Tidsskr. 20, 71-112.

Cahen, L. and Snelling, N. J. (1966) The Geochronology of Equatorial Africa. North-Holland Publishing Company.

Chinner, G. A. (1960) Pelitic gneisses with varying ferrous/ferric ratios from Glen Clova, Angus, Scotland. Jour. Pet. 1, 178-217.

Christensen, J. I. (1968) Compressional wave velocities in metamorphic rocks at pressures to 10 kilobars. Jour. Geophys. Res. 24, 6147-6164.

Clifford, T. N. (1968) Radiometric dating and the pre-Silurian geology of Africa in Radiometric Dating for Geologists, Hamilton, E. I. and Farquhar, R. M. (eds.). Interscience.

Compston, W. and Pidgeon, R. T. (1962) Jour. Geophys. Res. 67, no. 9, 3493.

Crawford, A. R. (1968) Geochronology of the Precambrian rocks of peninsular India and Ceylon. Unpub. Ph.D. Thesis, Australian National University.

Dasch, E. J., Hills, F. A., and Tuekian, K. K. (1966) Strontium isotopes in deep-sea sediments. Science. 153, 295.

Doe, B. R. (1962) Relationships of lead isotopes among granites, pegmatites, and sulfide ores near Balmat, New York. Jour. Geophys. Res. 67, 2895-2906.

Dunn, J. A. (1942) Granite and magmation and metamorphism. Econ. Geol. 37, no. 3, 231-238 (discussion).

Eade, K. E., et al. (1966) Composition of crystalline shield rocks and fractionating effects of regional metamorphism. Nature. 211, no. 5055, 1245-1249.

Eskola, P. (1952) On the granulites of Lapland. Am. Jour. Sci., Bowen. 133-172.

_____ (1957) On the mineral facies of charnockites. Madras Univ. Jour., ser. B. 27, Centenary number, 101-119.

Evans, C. R., and Tarney, J. (1964) Nature. 204, 638.

Evans, C. R. (1965) Geochronology of the lewisian basement near Lochinver, Sutherland. Nature. 207, no. 4992, 54-56.

Evans, J. A. (1921) Discussion on Tilley's paper: The granite-gneisses of southern Eyre Peninsula (South Australia) and their associated amphibolites. Quart. Jour. Geol. Soc. 77, 133.

Fairbairn, H. W., et al. (1960) Age of the granitic rocks of Nova Scotia. Bull. Geol. Soc. Am. 71, 399-414.

Fairbairn, H. W., et al. (1964) Initial Sr^{87}/Sr^{86} and possible sources of granitic rocks in southern British Columbia. Jour. Geophys. Res. 69, no. 22, 4889-4893.

Faure, G., et al. (1963a) An estimate of the isotopic composition of strontium in rocks of the Precambrian shield of North America. Jour. Geophys. Res. 68, 2323.

Faure, G., et al. (1963b) The isotopic composition of strontium in oceanic and continental basalts: Application to the origin of igneous rocks. Jour. Petrol. 4, 31.

Fermor, L. L. (1938) An attempt at the correlation of the ancient schistose formations of Peninsular India. Mem. Geol. Survey of India. 70, 42.

Fleischer, M. (1965) Summary of new data on rock samples G-1 and W-1, 1962-1965. Geochim.-Cosmochim. Acta. 29, 1263-1283.

Frey, F. A., et al. (1968) Rare earth abundances in some basic rocks. Jour. Geophys. Res. 73, no. 18, 6085-6098.

Fyfe, W. S., et al. (1958) Metamorphic reactions and metamorphic facies. Geol. Soc. Am. Mem. 73.

Gast, P. W. (1960) Limitations on the composition of the upper mantle. Jour. Geophys. Res. 65, 1287-1297.

_____ (1962) Geochim.-Cosmochim. Acta. 26, 927.

Ghosh, P. K. (1941) The charnockite series of Bastar State and Western Jeypore. Rec. Geol. Surv. India. 75, Prof. Pap. 15, 1-55.

Giletti, B. J., et al. (1961) Quart. Jour. Geol. Soc., Lond. 117, 233.

Goldschmidt, V. M. (1922) Stammestypen der Eruptivgesteine. Skr. Norske Vid. Akad., Oslo. MatNat. K. 10, 12.

_____ (1933) Grundlagen der Quantitiven Geochemie. Fortschr. Mineral. Krist. Petrog. 17, 112-156.

Gordon, G. E., et al. (1968) Instrumental activation analysis of standard rocks with high-resolution -ray detectors. Geochim.-Cosmochim. Acta. 32, 369-396.

Groves, A. W. (1931) Geol. Survey Uganda Ann. Rep., 1931.

_____ (1935) The charnockite series of Uganda. Quart. Jour. Geol. Soc. (London). 91, 150.

Hamilton, E. I. (1966) The determination of uranium in rocks and minerals by the delayed neutron method. Earth and Planetary Science Letters. 1, 77-81.

Hamilton, E. I. and Farquhar, R. M. (1968) Radiometric Dating for Geologists. Interscience.

Haskin, L. A., et al. (1966) Meteoritic, solar and terrestrial rare-earth distributions in Physics and Chemistry of the Earth, 7. Pergamon.

Haskin, L. A. and Schmitt, R. A. (1967) Rare-earth distributions in Researches in Geochemistry, 2. Abelson (ed.) 234-258. Wiley.

Heath, S. A. (1967) Sr^{87}/Sr^{86} ratios in anorthosites and some associated rocks in Origin of Anorthosites--a symposium, N.Y. State Mus. and Sci. Serv., I. W. Isachsen, editor, in press.

Hedge, C. E. and Walthall, F. G. (1963) Radiogenic strontium-87 as an index of geologic processes. Science. 140, 1214.

Heier, K. S. (1960) Petrology and geochemistry of high-grade metamorphic and igneous rocks on Langøy, Northern Norway. Norg. Geol. Unders. 207, 246.

Heier, K. S., and Rogers, J. J. W. (1963) Radiometric determination of thorium, uranium and potassium in basalts and in two magnatic differentiation series. Geochim.-Cosmochim. Acta. 27, 137-154.

Heier, K. S. (1964) Rubidium/strontium and strontium-87/strontium-86 ratios in deep crustal material. Nature. 202, no. 4931, 477-478.

Heier, K. S. and Brooks, C. (1966) Geochemistry and the genesis of the Heemskirk granite, West Tasmania. Geochim.-Cosmochim. Acta. 30, 633-643.

Hepworth, J. V. (1964) Explanation of the geology of sheets 19, 20, 28 and 29 (Southern West Nile). Geological Survey of Uganda, Report No. 10.

Hoefs, J. and Wedepohl, K. H. (1968) Sr isotope studies on young volcanic rocks from Germany and Italy. Contr. Mineral. and Petrol. 19, 328-338.

Holland, T. H. (1896) On the origin and growth of garnets and of their micropegmatitic intergrowth in pyroxenic rocks. Rec. Geol. Survey of India. 29, 20-30.

Holland, T. H. (1900) The charnockite series, a group of hypersthenic rocks in peninsular India. Mem. Geol. Surv. Ind. 28, pt.2.

_____ (1901) Geology of the neighbourhood of Salem, Madras Presidency, with special reference to Leschenault de la Tour's observations. Mem. Geol. Surv. Ind. 30, 103-108.

Holmes, A. (1951) The sequence of Precambrian orogenic belts in south and central Africa. Intern. Geol. Cong. 18th Gt. Britain 1948, pt. 14. 254-269.

Howie, R. A. (1955) The geochemistry of the charnockite series of Madras India. Royal Soc. Edinburgh Trans. 62, 162-164.

Howie, R. A. and Subramaniam, A. P. (1957) The paragenesis of garnet in charnockite, enderbite, and related granulites. Min. Mag. 31, 565-586.

Howie, R. A. (1958) African charnockites and related rocks. Congo Belge Serive Geol. Bull. 8, 1-14.

Hsu, K. J. (1955) Granulites and mylonites of San Gabriel Mountains, California, Univ. Calif. Publ. Geol. Sci. 30, no.4, 223-253.

Hubbard, F. H. (1966) Myrmekite in charnockite from south-west Nigeria. Am. Min. 51, 762.

Hurley, P. M., et al. (1962) Radiogenic strontium-87 model of continent formation. Jour. Geophys. Res. 67, 5315-5334.

Hurley, P. M. and Fairbairn, H. W. (1965) Evidence from western Ontario of the isotopic composition of strontium in archean seas. M.I.T. Thirteenth Annual Progress Report. 145-147.

Krogh, T. E. and Hurley, P. M. (1968) Strontium isotope variation and whole-rock isochron studies, Grenville Province of Ontario. Jour. Geophys. Res. 73, no.22, 7107-7125.

Kulp, J. L. and Engels, J. (1963) Discordances in K:Ar and Rb:Sr isotopic ages. Radioactive dating 219-235, Proc. Symp. Intern. Atomic Energy Agency Joint Comm. Appl. Radioactivity, Athens, 1962 (Intern. Atomic Energy Agency, Vienna).

Lambert, I. B. and Heier, K. S. (1967) The vertical distribution of uranium, thorium, and potassium in the Continental Crust. Geochim.-Cosmochim. Acta. 31, 377-390.

_____ (1968) Geochemical investigations of deep-seated rocks in the Australian shield. Lithos. 1, no.1, 30-53.

Larsen, E. S. (1938) Some new variation diagrams for groups of igneous rocks. Jour. of Geology. 46, 505-520.

Ledent, D., et al. (1962) Premieres donnees sur l'age absolu des formations anciennes du "socle" du Kasai (Congo meridional) Bull. Soc. Belge Geol. 71, 223-237.

Lowden, J. A. (1961) Age determinations by the Geological Survey of Canada. Geol. Survey Canada paper 61-17, 127 pp.

Luth, W. C. (1967) Studies in the system $KAlSiO_4$-Mg_2SiO_4-SiO_2-H_2O: I, inferred phase relations and petrologic applications. Jour. Pet. 8, 372-416.

Macdonald, R. (1963) The charnockite-basement-complex in northern West Nile District Uganda, and its relation to the Western Rift. Unpub. Ph.D. Thesis, University of London.

Mason, B. (1952) Principles of Geochemistry (3rd ed.). Wiley.

Muir, I. D. and Tilley, C. E. (1958) The compositions of coexisting pyroxenes in metamorphic assemblages. Geol. Mag. 95, 403-408.

Naidu, P. R. J. (1955) Minerals from charnockites from India: Schweiz. Mineralog. Petrog. Mitt. 34, 203-279.
_____ (1963) 50th Indian Science Congress, Delhi. 1-15.

Nockolds, S. R. and Allen, R. (1953) The geochemistry of some igneous rock series. Geochim.-Cosmochim. Acta. 4, 105-142.

Pakiser, L. C. and Robinson, R. (1967) Composition of the continental crust as estimated from seismic observations in The Earth beneath the Continents. Steinhart, J. S. and Smith, T. J. (eds.) American Geophysical Union. 10, 620-626.

Papon, A. et al. (1968) Age de 2 700 millions d'années, déterminé par la méthode au strontium, pour la série charnockitique de Man, en Côte-d'Ivoire. C. R. Acad. Sc. Paris. 266, 2046-2048.

Parras, K. (1958) On the charnockites in the light of a highly metamorphic rock complex in southwestern Finland Pt. I. The charnockites-an independent problem or part of a greater whole? Bull. Comm. Géol. Finlande. 181, 1-45.

Peterman, Z. E., et al. (1967) Isotopic composition of Sr in sea water throughlut Phanerozoic time (Abstract). Program Ann. Meetings of Geol. Soc. Amer., New Orleans, 176.

Pinson, W. H. Jr., et al. (1965) Rb-Sr age of stony meteorites. Geochim.-Cosmochim. Acta. 29, 455-466.

Pitcher, W. S. and Flinn, G. W. (eds.) (1965) Controls of Metamorphism. Wiley.

Poldervaart, A. (1966) Archaean charnockitic adamellite phacoliths in the Keimoes-Kakamas region, Cape Province, South Africa. Trans. Geol. Soc. of South Africa. 69, 139-154.

Quensel, P. (1950) The charnockite series of the Varberg district on the south-western coast of Sweden. Arkiv för Mineralogi och Geologi. 1, no. 10, 229-329.

Rama, Rao, B. (1945) The charnockite rocks of Mysore (southern India). Bull. Mysore Geol. Dept. B. 18, 199p.

Ramberg, H. (1948) Econ. Geol. 43, 554.

Reesman, R. H. (1968) A rubidium-strontium isotopic investigation of the possibility of dating hydrotherman mineral deposits. Unpub. Ph.D. Thesis, Mass. Inst. Tech.

Reilly, G. and Shaw, D. M. (1967) An estimate of the composition of part of the Canadian shield in northwest Ontario. Canad. Jour. Earth Sci. 4.

Reynolds, R. C. Jr. et al. (1967) K/Rb ratios in Adirondack anorthosites and associated charnockitic rocks, and their petrogenetic implications (Abstract). Program Ann. Meetings of Geol. Soc. Amer. [Northeastern Section], Boston, 52.

Ringwood, A. E. (1961) Chemical and genetic relationships among meteorites. Geochim.-Cosmochim. Acta. 24, 159-197.

Rosenbusch, H. (1922) Elemente der Gesteinslehre. 4th ed. (edited by A. Osann) Schweitzerbart.

Schnetzler, C. C., and Philpotts, J. A. Partition coefficients of rare-earth elements and barium between igneous matrix material and rock-forming phenocrysts. Proc. Symp. Intern. Assoc. Geochem. Cosmochem. Paris (1967).

Shaw, D. M. (1968) A review of K-Rb fractionation trends by covariance analysis. Geochim.-Cosmochim. Acta. 32, 573-601.

Shields, R. et al. (1963) Survey of Rb^{85}/Rb^{87} ratios in minerals. Jour. Geophys. Res. 68, 2331-2334.

Shields, R. M. et al. (1965) The Rb^{87}-Sr^{87} age of stony meteorites. M.I.T. Thirteenth Annual Progress Report, 121-144.

Silver, L. T. (1966) Preliminary history for the crystalline complex of the Central Transverse Ranges, Los Angeles County, California (Abstract). Geol. Soc. Am. Program 1966 Annual Meeting.

Singh, S. (1966) Orthopyroxene-bearing rocks of charnockitic affinities in the South-Savanna-Kanuku complex of British Guiana. Jour. Pet. 7, no. 2, 171-194.

Spooner, C. M. (1967) Preliminary report of Sr^{87}/Sr^{86} ratios in some rocks of the granulite facies. M.I.T. Fifteenth Annual Progress Report, 125.

_____ (1968) Sr^{87}/Sr^{86} initial ratios in charnockites and pyroxene granulites. M.I.T. Sixteenth Annual Progress Report, 57-66.

Spooner, C. M. and Fairbairn, H. W. (1969) Rb-Sr initial ratios and ages of some charnockites and pyroxene granulites. Am. Geophys. Union. Program 1969 Annual Meeting.

Stillwell, F. L. (1918) The metamorphic rocks of Adelie Land, Aust. Antarctic Exp. 1911-1914. Sci. Rep. A. 3, part 1.

Subramaniam, A. P. (1959) Charnockites of the type area near Madras, -a reinterpretation. Am. Jour. Sci. 257, 321-353.

_____ (1960) Petrology of the charnockite suite of rocks from the type area around St. Thomas mount and Pallavaram, near Madras City, India: 21 st. Int. Geol. Congress Repts. 1960 Copenhagen, pt. 13, 394-403.

_____ (1962) Pyroxenes and garnets from charnockites and associated granulites. Geol. Soc. Am. Buddington Vol., 21-36.

Suter, H. (1922) Zur klassifikation der charnockit-anorthosit provinzen. Schweiz. Min. Petrogr. Mitt. 11, 307-330.

Sutton, J. and Watson, J. (1951) Quart. J. Geol. Soc. Lond. 106, 241.

Tatsumoto, M., et al. (1965) Potassium, rubidium, strontium, thorium, uranium and the ratio of Sr87 to Sr86 in oceanic tholeiitic basalt. Science. 150, 886.

Temperley, B. N. (1938) The geology of the country around Mpwapwa. Short paper, Geol. Surv. Tanganyika Territory, No. 19.

Thompson, J. B. (1947) The role of aluminum in rock-forming silicates. Bull. Geol. Soc. Am. 58, 1232.

Thornton, C. P. and Tuttle, O. F. (1960) Chemistry of igneous rocks I. differentiation index. Am. Jour. Sci. 258, 664-684.

Tilley, C. E. (1936) Enderbite, a new member of the charnockite series. Geol. Mag. 73, 312-316.

Tyrell, G. W. (1926) The Principles of Petrology. Methuen.

Urey, H. C. and Craig, H. (1953) The composition of the stone meteorites and the origin of the meteorites. Geochim.-Cosmochim. Acta. 4, 36.

Van Schmus, R. (1966) Data reduction for Sr^{84} spiked samples. M.I.T. Fourteenth Annual Progress Report, 179-181.

Venkatasubraminian, V. S., et al. (1968) Studies on the Rb-Sr and K-Ar dating of minerals from the Precambrian of India. Canad. Jour. of Earth Sciences. 5, 601.

Vredenburg, E. W. (1918) Considerations regarding a possible relationship between the charnockites and the Dharwars. J. Asiatic Soc. Bengal. N.S. 14.

Waard, D. de (1966) The biotite-cordierite-almandite subfacies of the hornblende-granulite facies. Canad. Min. 8, 481-92.

Walton, M. S. and Waard, D. de (1963) Orogenic evolution of the Precambrian in the Adirondack highlands, a new synthesis. Koninkl. Nederlandse Akad. Wetensch. Proc., ser. B, 66, 98-106.

Washington, H. S. (1916) The charnockite series of igneous rocks. Amer. J. Sci. 41, 323-338.

White, A. J. R. (1964) Clinopyroxenes from eclogites and basic granulites. Am. Min. 49, 883.

Whitney, P. R. and Hurley, P. M. (1964) The problem of inherited radiogenic strontium in sedimentary age determinations. Geochim.-Cosmochim. Acta. 28, 425.

Whitten, E. H. Timothy. (1963) Application of quantitative methods in the geochemical study of granite massifs in Studies in Analytical Geochemistry, Shaw, D. M. (ed.) University of Toronto. 76-123.

Williams, E., et al.(1967) Records of the Geological Survey of Guyana. 5.

Wilson, A. F. (1960) Co-existing pyroxenes: Some causes of variation and anomalies in the optically derived compositional tie-lines with particular reference to charnockitic rocks. Geol. Mag. 97, 1-17.

Wynne-Edwards, H. R. (1967) Westport map-area, Ontario, with special emphasis on the Precambrian rocks. Geol. Sur. Canad., Mem. 346.

_____ (1967) The Frontenac axis. Geol. Assoc. Canad. Guidebook, Geology of Parts of Eastern Ontario and Western Quebec, 73-86.

York, Derek.(1966) Least-squares fitting of a straight line. Canad. Jour. Phys. 44, 1079-1086.

BIOGRAPHICAL SKETCH

The writer was born in Ottawa, Ontario, August 18, 1940, son of Clara Joyce Spooner (née Wheeler) and Christopher Martin Spooner.

At the end of World War II, he moved to Toronto and received his primary and secondary schooling there. In his final two years of high school, he received part-time employment as a laboratory technician at the Royal Ontario Museum, Earth Science Division.

The author received his undergraduate training at McMaster University, Hamilton, Ontario, where he graduated in 1965 with a B.Sc. in Honours Geology. During his undergraduate years, he received summer employment with the Royal Ontario Museum, the Ontario Department of Mines, and the Iron Ore Company of Canada, Labrador City, Newfoundland.

The writer entered the Graduate School of the Massachusetts Institute of Technology in September of 1965 and received his S.M. degree in Geology and Geophysics in the Spring of 1967. For three years, the author received a Departmental Staff Award and was a Teaching Assistant in Petrography under Professor H. W. Fairbairn. In his final year of graduate studies, he held a research assistantship in the Geochronology Laboratory.

In June, 1969, he was elected to full membership in Sigma Xi.

He has accepted a summer post-doctoral position with Professor F. A. Frey, Massachusetts Institute of Technology, and a one year Post-Doctoral Fellowship at Kansas State University with Dr. D. G. Brookins.

In October, 1968, he was engaged to Miss Judith R. Lang of Wellesley, Massachusetts.

APPENDIX A

Petrographic Descriptions of Samples Analyzed

Charnockitic Rocks from Msagali area, Tanzania

submitted by Dr. J. V. Hepworth

R7050 (TZ 163.11B)
Charnockite
modal analysis: (500 points on slide stained for potash feldspar)
quartz 18%
potash feldspar 13%
plagioclase 48% (about An_{25-30})

biotite 8%
pyroxenes 13%
myrmekite 1-2%

Quartz shows undulatory extinction, grains have sutured boundaries and are charged with bubble trains and rutile needles. Clinopyroxene in greater abundance than hypersthene. Pronounced clustering of biotite with pyroxene. $Z \wedge c = 40°$ for clinopyroxene, $2V = \sim 60°$. Biaxial (+).

R7051 (TZ 163.30J)
Charnockite
abundance estimated:
quartz 25%
potash feldspar 25%
clinopyroxene 10%
plagioclase 40-45% ($An_{25 \pm 10}$)
biotite 5%

Clinopyroxene and biotite intimately associated (± magnetite). Specimen generally fresh with only incipient sericitization along cleavage of potash feldspars. Feldspar (potash) slightly pethitic in places. Clinopyroxene shows rough alignment of opaque mineral (magnetite ?) parallel and perpendicular to cleavage. Plagioclase rarely shows twinning and if present is usually pericline or thin albite.

R7052 (TZ 163.30R)
modal abundances estimated
Aplo-granite
quartz 45% (extreme crush texture)
potash feldspar (perthite + antiperthite) 20%
plagioclase 35% (untwinned)
myrmekite 5%
rutile
apatite
biotite

Myrmekite is present in many of the specimens adjacent to the quartz grains "growing into" the potash feldspar. Apatite and rutile

inclusions in quartz and potash feldspar. Occasional scraps ob biotite and zircon. No other mafic minerals observed. Aplitic texture.

R7053 (TZ 163.11E)
Granite (biotite) Contact Facies
modal abundances estimated:
potash feldspar 20-25%
quartz 30-35%
plagioclase 30% ($An_{10\pm5}$)
biotite 10%
amphibole 10%
rutile (as inclusions in quartz and feldspar)
apatite
zircon

Quartz sutured to saccaroidal in appearance with undulatory extinction. Potash feldspar found as irregular stringers and grains around plagioclase and quartz with about equal frequency. Amphibole (common hornblende, from pleochroism) associated with potash and plagioclase feldspars and occasionally with quartz.

R7054 (TZ 163.30N)
Biotite Gneiss
slight lineation of mafic constituents though more pronounced in hand specimen
modal estimates:
quartz 30%
anorthoclase 50%
biotite 10-12%
hornblende 10%
rutile
apatite
zorcon

Quartz forms aplitic fillings between larger grains of fledspar and quartz. Anorthoclase identified by smaller 2V = 50° Biaxial (-) and lack of staining. Incipient sericitization of feldspar parallel to cleavage. Chlorite also present as a probable alteration of an amphibole associated with potash feldspar commonly. Occasional grain of a highly pleochroic and birefringent clay mineral,perhaps celadonite (?).

R7055 (TZ 163.11F)
Biotite Gneiss
Lepidoblastic texture with porphyroblasts of quartz and plagioclase
Modal estimates:
quartz 30%
plagioclase 30% (An_{10-20})
biotite 10-15%

R7055 (TZ 163.11F) (cont.):
amphibole 8%
apatite (abundant needles in plagioclase)

R7056 (TZ 163.122) 30 miles S.W. Msagali
Charnockitic rock
Modal estimates:
quartz 30%
plagioclase 40%
potash feldspar 10-12%
biotite 15-20%
penninite 5% small 2V (Biaxial (-) Extinction 2-8°, high relief

Penninite secondary expansion cracks arising from alteration of original mafic mineral present surrounded in turn by biotite. (Expansion cracks similar to those found in troctolite where olivine has altered.) Potash feldspar in small blebs interstitial to plagioclase or plagioclase-quartz boundaries.

R7057 (TZ 163.73) 5 miles west of Msagali
biotite Gneiss
Modal estimates:
quartz 30-35%
plagioclase 20-25%
potash feldspar 10%
biotite 15%
amphibole 10% (+alteration products)
magnetite 2%
apatite

Amphibole largely altered to penninite or clinochlore (or a related chlorite group mineral)

Pyroxene Granulites from Para Mountains and Labor Serrit Area, Tanzania

Collected by: Dr. J. V. Hepworth
Institute of Geological Sciences, London

Para Mountains

R7224/TZ 73.1
Pyroxene Granulite

Description: Medium-grained granulite with large books of biotite (1-3 mm). Some hypersthene visible.

R7225/TZ 73.2
Leucocratic Granulite

Description: Alaskitic gneiss, ca. 60% potash feldspar, ca. 40% quartz.

R7230/TZ 73.15
Granulite

Description: Fine-grained granulite largely composed of dark, waxy quartz and feldspar. Has dark green appearance characteristic of this facies.

Labor Serrit

R7231/TZ 86.24
Dark Pyroxene Granulite

Description: Same as R7230/TZ 73.15

R7233/TZ 86.27
Leucocratic Granulite

Description: Garnetiferous quartzo-feldspathic gneiss. ca. 10% garnet, ca. 5% biotite.

R7236/TZ 86.32
"Nearly ultrabasic Granulite" (Amphibolite)

Description: gneissic texture

R7236/TZ 86.32 (cont.)

hornblende	65%
clinopyroxene	10%
quartz	5%
potash feldspar	20%
magnetite	1%

Charnockite Rocks from Okollo and Rakosi, West Nile District, Uganda

collected by Dr. H. W. Fairbairn

R7042/54

Mafic Charnockite

Quartz 30%	Biotite 20%
Orthoclase 5-10%	Hypersthene 1%
Plagioclase 10-15%	Clinopyroxene 1-2%
Myrmekite 5%	accessory Apatite

Slight gneissosity with bands of biotite + garnet on scale of 1 to 0.5 cm. Relatively fresh with no apparent alteration. Quartz not highly undulose, but many of the grains sutured. Biotite associated with garnet, the latter occurring in clots. Biotite within the garnet shows a radiating habit.

R7011/23

Fine-grained Leucocratic Gneiss

Quartz 35%
Potash Feldspar (+ subordinate Plagioclase) 60%
Biotite 1%
Garnet 2% (or less)

Specimen is quite fresh with only slight cloudiness of the feldspar. Pronounced gneissosity. Potash feldspar shows well-developed tatran twinning. Quartz highly undulose.

R7012/24

Leucocratic Gneiss

Quartz 60%
Potash feldspar (+ minor plagioclase) 40%
Biotite trace
Magnetite 1%

Somewhat coarser grain size than R7011/23 above (1-3mm.). Mineralogy similar with somewhat more quartz, however. Same degree of incipient alteration of feldspars.

Charnockite Rocks from Okollo and Rakosi,
West Nile District, Uganda (cont.)

R7018/30

Leucocratic Gneiss

Similar to R7012/24, though slightly larger in grain size and braid perthite more fully developed than in any of the other specimens.

R7020/32

Leucocratic Gneiss

Similar to R7012/24 above. 1-2% garnet and minor biotite. Quartz occurs in bands and in a "crush" matrix around larger grains of potash feldspar.

Indian Lake, West Canada Lakes and Blue Mountain Quadrangles

R7321/W-15(b)

Locality: Blue Mountain quadrangle

Description:

quartz	15%
potash feldspar	50-55%
amphibole	30-35%
myrmekite	1-2%
hypersthene	5%
magnetite	1-2%

Medium-grained with slight gneissosity. Potash feldspar has both patch and tartan twinning. Subhedral outline in hornblende which often surrounds grains of hypersthene. Occasional scraps of hypersthene unaltered. Quartz strained and sutured.

R7322/2(a)

Locality: Blue Mountain quadrangle

Description:

quartz	15-20%
hypersthene	10%
amphibole	15%
potash feldspar	30%
plagioclase	20%
biotite	2%

Pronounced banding of mafics, crush texture.

R7326/W-126(a)

Locality: Indian Lake quadrangle

Description:

quartz	15-20%
potash feldspar	40%
plagioclase	15-20%
pyroxene	10%
magnetite	5%

Specimen similar in mineralogy and texture to R7322. Cataclastic texture.

R7327/W-126(b)

Locality: Indian Lake quadrangle

Description:

quartz	20%
plagioclase	10-20%
potash feldspar	20%
biotite	10-15%
hornblende	15-20%
hypersthene	15%
apatite	minor

Slight gneissosity, hypersthene appears to be altered in hornblende. and magnetite is often associated with the alteration.

R7329/W-124

Locality: Indian Lake

Description:

Similar in texture and mineral proportion to R7326, slightly gneissic.

Pyroxene Granulites, Westport, Ontario

Collected by: C. M. Spooner

R7085/27

Locality: On Clear Lake road, G. S. C. Memoir 346, 1967, Westport Map area.

Description:

Plagioclase	20%
potash feldspar	40%
quartz	30%
biotite	2-3%
magnetite	1%
hornblende	8-10%

Slightly gneissic with a granular texture. Quartz slightly strained with numerous internal sutures. Potash feldspar shows varieties of rod and patch perthite. Biotite fresh but hornblende altered slightly to a mixture of a highly birefringent mineral (celadonite?) and possibly saussurite. Minor small veins of calcite and chlorite passing through all grains. Minor vein-like alteration in feldspar. Albite-Carlsbad twinning + pericline twinning common in plagioclase. Plagioclase about An_{30-40}.

R7083/25

Locality: Devil Lake road.

Description:

plagioclase } microcline }	50%
quartz	30%
biotite	10%
hornblende	10%
magnetite	2-3%
chlorite	1-2%

Granular texture with no apparent gneissosity. Relatively coarse-grained with some grains up to 3-5 mm. Potash feldspar fairly fresh, however hornblende muddy in appearance through development of chlorite (though minor). Biotite occurs in large flakes. Microcline has well-developed tartan twinning.

R7070/13

Locality: on highway north of Loon Lake.

Description:

quartz	50%
potash feldspar	40%
magnetite	1%
biotite	3%
chlorite	2%

Extreme crush texture, quartz highly strained and grains show many internal suture lines. Feldspar fairly fresh with only minor clouding.

R7090/31

Locality: Outcrop on north side of Clear Lake Road

Description:

plagioclase (An_{30})	15%
potash feldspar	45%
quartz	40%
biotite	2%

Myrmekite abundant at quartz, potash feldspar boundaries. Biotite appears to be alteration associated with minor orthopyroxene. Abundant microcline twinning and minor patch perthite.

R7112/49(1) and R7113/49(2)

Locality: Stop 4, Mineralogical Association of Canada Guidebook.

Description:

quartz	30%
hypersthene	15-20%
magnetite	5%
potash feldspar	40%

Quartz shows extreme undulatory extinction. Hypersthene associated with magnetite and slightly altered to chlorite. Slight alteration of potash feldspar to saussurite and minor carbonate.

R7061/4 and R7062/5

Locality: Road to Devil Lake.

R7061/4 and R7062/5 (cont.)

Description:

quartz	15%
potash feldspar	10-15%
biotite	10%
hornblende	60%

Largely amphibolite. Quartz strained to about same extent as in other specimens.

R7071/14

Locality: North side of highway near Loon Lake.

Description:

quartz	35%
potash feldspar	40-50%
biotite	3-5%
sericite	minor
chlorite	minor
plagioclase	15-20%
magnetite	1-2%
myrmekite	<1%
apatite	minor

Quartz shows undulose extinction, sutured grains. Numerous inclusion trains in quartz grains. Incipient sericitization in smaller feldspar grains.

Salem Area, Madras State, India

Collected by: Dr. S. Subramaniam
Government College, Salem

R7176/1
Medium-grained acid charnockite

Locality: Kullakavun Danur, west from Salem.

Description:

hypersthene	20%
quartz	35%
potash feldspar	40%
hornblende	2-5%
magnetite	1%

Incipient alteration of hypersthene to hornblende. Otherwise, specimen fresh and there is no observable gneissosity, although quartz is strained as usual.

R7178/3
Medium-grained acid charnockite and garnetiferous basic charnockite

Locality: Same as R7176

Description:

Cataclastic texture. Same mineralogy and approximate proportions as in specimen R7176.

R7180/5
Garnetiferous charnockite

Locality: Same as R7176

Description:

garnet	20%
hypersthene	5%
quartz	20%
potash feldspar	20%
sericite } carbonate }	10%
biotite	5%
plagioclase	5-10%
chlorite	10%
magnetite	1-2%

R7180/5 (cont.)

Cataclastic fine to medium grained texture. Garnet fractured and filled with birefringent alteration. Kelyphitic rims of biotite and chlorite around magnetite and hypersthene but not seen around garnet. Carbonate and carbonate + chlorite veins through specimen. Quartz highly rutilated in some grains.

R7336/14
Norite

Locality: Nagara Malai, about 6 miles north of Salem.

Description:

Hand Specimen Description: Fine-grained slightly banded granulitic rock. Melanocratic rock composed largely of hypersthene, though the quartz imparts a dark greasy aspect to the specimen.

R7337/15
Leptynite

Locality: Same as R7336

Description:

Hand Specimen Description: Fine-grained leucocratic rock with garnets about 1-3 mm. in diameter. Major phases are feldspar and quartz, the latter having the characteristic greasy lustre.

Charnockitic Rocks from Madras-Type Locality

submitted by Dr. P.R.J. Naidu

R7205/AS-12

Basic charnockite

Thin section from felsic portion of rock.

Quartz 35%
Potash feldspar 45-50%
Magnetite 1-2%
Plagioclase 5%(?)
Biotite 1%
Myrmekite 5-10%

Granoclastic texture. Specimen very fresh. Quartz strained with sutured interiors. Quartz and potash feldspar equigranular. Potash feldspar shows braid perthite with minor patch perthite. Quartz rutilated with trains of inclusions. No apatite or zircon found.

R7214/AS-85

Charnockite

Plagioclase 30%
Quartz 5%
Hornblende 20%
Hypersthene 40%
Magnetite 5%

Plagioclase shows well-developed albite and pericline twinning with an ophitic texture. Anorthite content varies from about An_{30} to An_{54}. Hornblende forming at borders of hypersthene and has a Z c angle of about 19°. Hypersthene is length slow with pale green to pink pleochroism. Upper first order birefringence. In many of these sections, hypersthene and hornblende are intimately associated and since the hornblende is pargasitic in composition, it is difficult to distinguish between the two. Therefore, the percentages of hornblende and hypersthene are likely in error.

R7215/A-95

Charnockite

Same mineral proportions as in R7214 above. Plagioclase composition by Michel-Levy method about An_{44}.

Charnockitic Rocks from Madras-Type Locality (cont.)

R7216/A-110

Charnockite

Hypersthene 20%
Garnet 25%
Hornblende 15%
Plagioclase 30%
Quartz 5-7%
Magnetite 5%

Slightly gneissic texture. Plagioclase An_{40} approximately. Garnet forms euhedral to subhedral grains which are slightly birefringent in some grains. Garnet closely associated with hypersthene. Hornblende appears to replace hypersthene. Magnetite shows skeletal outlines around the garnet.

R7217/A-115

Charnockite

Hypersthene 10%
Hornblende 50%
Plagioclase 30%
Quartz 10%

Fine-grained granoblastic texture. Hypersthene occurs as larger crystals showing exsolution lamellae and parallel extinction in appropriate sections. Hypersthene also occurs in granular aggregates with hornblende.

R7218/A-117

Charnockite

Hornblende 20%
Plagioclase 20%
Potash feldspar 10%
Magnetite 5-8%
Hypersthene 40%
Quartz 10%

Fairly pronounced gneissic to granoblastic texture. Plagioclase shows pronounced zoning in several larger crystals. Post-consolidation alteration shown by expansion cracks in feldspar adjacent to amphiboles mantling the hypersthene.

Charnockitic Rocks from Madras-Type Locality (cont.)

R7219/A-121

Charnockite

Quartz 10%
Potash Feldspar 10%
Plagioclase 30%
Hornblende 20-30%
Hypersthene 15%
Magnetite 5%

Texture is subophitic to granoblastic.

R7220/A-124

Charnockite

Quartz 15%
Potash Feldspar 5-10%
Plagioclase 20%
Hypersthene 10-15%
Hornblende 45-50%
Magnetite 3-5%

Hypersthene in fairly large crystals showing exsolution lamellae. One euhedral outline completely mantled with plagioclase. Hornblende consists of a granular aggregate with smaller grains of hypersthene. Plagioclase about An_{50} in composition.

R7221/A-126

Charnockite

Quartz 10%
Hornblende 20%
Hypersthene 10-15%
Potash feldspar 10-15%
Plagioclase 20%
Magnetite 5%

Fresh granoblastic texture with minor infilling around larger grains with a crush texture of plagioclase + quartz.

Charnockitic Rocks from Madras-Type Locality (cont.)

R7240/AS-5

Basic Charnockite

Quartz 10%
Potash Feldspar 10-15%
Plagioclase 20%
Biotite 20%
Hypersthene 30%
Magnetite 1-2%

Very fresh granoblastic texture.

R7242/AS-10

Basic charnockite (biotite-rich)

Quartz 10%
Biotite 20%
Hypersthene 30%
Plagioclase 20%
Potash Feldspar 20%
Apatite - minor
Zircon - minor

Slightly gneissic texture shown by biotite. Specimen very fresh. Plagioclase about An_{45}. Possibly two generations of biotite. Primary type shows normal pleochroism and cleavage but secondary (?) type shows brown color and no appreciable variation in pleochroism. This latter type also has numerous zircon inclusions with attendant pleochroic haloes.

Orthopyroxene-bearing Granites and Granulites from the Kanuku Complex, Guyana

submitted by J. P. Berrangé:

R7340/J.P.B. 156
Location: Map Sheet Kanuku SE, Directorate of Overseas Surveys print Laydown No. 65. (P.L.D. 65)
Lat.03°20' N, Long. 59°15' W.

Eastern Kanuku Mountains, first falls on the Maparri River, about 3 miles upstream from its confluence with the Rupununi River.

Descriptions: Medium light grey with blue tinge, medium-grained granular texture, biotite-hypersthene charnockite.

Quartz 20%
K-feldspar 50%
Biotite >10%
Hypersthene 15%
Magnetite <5%

In thin section, the specimen has a fresh appearance with no visible alteration. Nearly all grains show undulatory extinction, especially in the case of the quartz. Mafic minerals appear to be intersertal to the potash feldspar and biotite-hypersthene-magnetite are invariably associated together. The potash feldspar is essentially a patch perthite with less than 3% myrmekite at the borders of the grains. Biotite of the usual fox-red variety and strongly pleochroic.

R7341/J.P.B. 157
Location: Same locality as R7340/J.P.B. 156

Description: Same hand specimen appearance as 7340 but in thin section there is about 15% more biotite than hypersthene. Biotite shows pronounced straining and there are more numerous patches of myrmekite.

R7344/J.P.B. 177
Location: Map Sheet Kanuku SW, PLD 64
Lat. 03°17'N, Long. 59°38'W.
Western Kanuku Mountains, Moco Moco River, 1/4 mile downstream from the first falls.

Field Relations: Sample represents the most common type of gneiss found in the Kanuku Complex. The sample comes from the far north of the Kanuku Mountains where the recrystallization, mobilization, injection etc. associated with the mise in place of the South Savanna Granite is absent (see Figure in text).

R7344/J.P.B. 177 (cont.):
Description: Light grey in hand specimen with blue tinge, streaky biotite-garnet gneiss with a trifle of hypersthene. In thin section shows an extremely gneissic texture wherein biotite-garnet, and hypersthene (+ magnetite) constitute the mafic bands and individual mineral grains (hypersthene especially) are stretched in the sense of the major foliation. Locally the biotite may cut across the foliation.

Quartz 20%
Potash feldspar 40%
Biotite 15%
Hypersthene 5-8%
Garnet 10%
Magnetite 5%

Biotite associated with both garnet and hypersthene but garnet and hypersthene never found together in this section. Magnetite found with all three.

R7345/J.P.B. 177
Location: Same as R7344.

Description: Same mineralogy as R7344. More biotite (~20%). Slightly coarser in grain size for both mafic and felsic minerals. One elongated composite grain of garnet + hypersthene + biotite found with more biotite scattered in garnet than in hypersthene.

R7346/J.P.B. 216
Location: Map Sheet South Savanna NW, PLD 70.
Lat. 02°38'N, Long.59°50'W.
About one mile northeast of Raad Mountain.

Field Relations: Sample represents a large mass of pyroxene granofels that has probably been emplaced as a mantled gneiss dome into the Kanuku gneisses.

Description: Medium bluish grey, medium-grained, granulose pyroxene granofels. In thin section consists of a fine-grained,extremely granulose matrix surrounding unaltered larger grains of potash feldspar, plagioclase, and quartz (with myrmekitic borders in the larger grains). The porphyroblasts are mainly potash feldspar and plagioclase that show slight zoning but no undulose extinction. Biotite and hypersthene occur together in mafic clots that show a faint gneissosity.

R7347/J.P.B. 300
Location: Map Sheet South Savanna NE, PLD 71.

R7347/J.P.B. 300 (cont.):
Lat. 02°51'N, Long. 59°30'W.
South end of the Kurartau Mountains.

Field Relations: Same as for R7346/J.P.B. 216 but from a different body.

Description: Medium bluish grey, medium-grained, granulose, pyroxene-garnet granofels. In thin section the specimen is mineralogically similar to R7346 but for grain size which is larger in this section. There is less granulose intergranular matrix although the grains are highly undulose. Mafic minerals are mainly hypersthene and biotite and no garnet was observed. Potash feldspar mainly rod perthite although some patch perthite was also found.

APPENDIX B

Collections of Charnockites and Pyroxene Granulites

with

Rapid Analyses (Quickies) for Rubidium and Strontium

Charnockite from Msagali Charnockite Quarry and Vicinity, Tanzania

collected by Dr. J. V. Hepworth, Geological Survey of Uganda, 1967

M.I.T. #	Field #	Description	Rb	Sr	Rb/Sr
R7050	TZ163.11B	dark blue-brown charnockite (least affected by metamorphism)	59	478	0.123
R7051	TZ163.30J	dark brown charnockite	81	475	0.171
R7052	TZ163.30R	gneissose aplo-granite	93	278	0.335
R7053	TZ163.11E	contact facies	88	365	0.241
R7054	TZ163.30N	biotite gneiss	73	188	0.388
R7055	TZ163.11F	biotite gneiss	117	240	0.488
R7056	TZ163.122	dark brown charnockite near Mima, 30 miles west of Msagali	52	229	0.227
R7057	TZ163.73	charnockite, 5 miles west of Msagali	67	504	0.133

Pyroxene Granulite from Westport, Ontario

collected by C.M. Spooner, 1967

see: H.R. Wynne-Edwards, Geological Survey of Canada Memoir 346.

M.I.T.#	Field#	Description	Rb	Sr	Rb/Sr
R7058	CMS-1	alaskite gneiss, 1/2 mile s junction Hwy 42. Unit 8 of Wynne-Edwards.	139	209	0.665
R7059	2	garnet amphibolite, 1/2 mile south of locality 1	11	136	0.081
R7060	3	see map	106	298	0.356
R7061	4	charnockite (?) some hornblende	33	139	0.237
R7062	5	charnockite + pyroxenite	18	345	0.052
R7063	6	fine-grained charnockite	44	484	0.091
R7064	7	granite gneiss, Unit 8	59	156	0.378
R7065	8	on Hwy north of Bedford, see map	44	374	0.118
R7066	9	from east side of Hwy	62	151	0.411
R7067	10	from west side of Hwy	29	116	0.250
R7068	11	bluish quartzite (+ some spidote)	7	32	0.219
R7069	12	charnockite (+ some biotite)	73	272	0.268
R7070	13	charnockitic gneiss	55	417	0.132
R7071	14	charnockitic gneiss	66	212	0.311
R7072	15	charnockite (+ biotite)	70	119	0.588
R7073	16	banded gneissic granite	84	258	0.326
R7074	17	banded biotite granite	51	41	1.244
R7075	18a	hand specimen from same outcrop as 17, note tourmaline	55	70	0.786
R7076	19a	medium-fine grained biotite + px(?) gneiss + quartzite bands in same o/c	37	154	0.240

Westport, Ontario (cont.):

M.I.T.#	Field#	Description	Rb	Sr	Rb/Sr
R7077	CMS-19b	same location, about 10' away as 19a	44	165	0.267
R7078	20	roadcut, area seems sheared with bio on shear plane. Biotite poor phase collected.	118	782	0.151
R7079	21	same location as CMS-20	39	626	0.062
R7080	22	dark granulite, minor biotite	30	649	0.046
R7081	23	white granite, some epidote in o/c	137	893	0.153
R7082	24	biotite schist	33	394	0.084
R7083	25	charnockite	48	252	0.190
R7084	26	biotite gneiss, on road to Clear Lake	55	99	0.556
R7085	27	charnockitic granite	18	539	0.033
R7086	28	same as 27-note quartz	7	551	0.013
R7087	29	Clear Lake road, Unit 5 H.R.W.-E	62	99	0.626
R7088	30	pyroxene gneiss, some bio. in thin layer 6" below	92	116	0.793
R7089	18b	same locality as 18a	33	110	0.300
R7090	31	pyroxene granulite, Unit 8	37	298	0.124
R7091	32	Clear Lake road, px. granulite Unit 8	15	267	0.056
R7092	33	pyroxene granulite	6(?)		
R7093	34	pyroxene granulite			
R7094	35	hornblende, granite+sulphides	91		
R7095	36	hornblende, granite+sulphides, but less mafic material	58	272	0.213
R7096	37	pyroxene granulite	129		

Westport, Ontario (cont.):

M.I.T.#	Field#	Description	Rb	Sr	Rb/Sr
R7097	CMS-38	quartz-feldspar gneiss, + gt. Stop 13*	133	171	0.778
R7098	39(1)	amphibolite, Stop 11, p. 77 for anal.	17	76	0.224
R7099	39(2)	same outcrop as 39(1)			
R7100	40	quartz-feldspar gneiss + hyp(?) ("basement complex")	21	649	0.032
R7101	41(1)	quartz-feldspar gneiss + hyp(?) ("basement complex")	121	161	0.752
R7102	41(2)	quartz-feldspar gneiss + hyp(?) ("basement complex")	112	140	0.800
R7103	41(3)	quartz-feldspar gneiss + hyp(?) ("basement complex")	129	118	1.09
R7104	42	cordierite-sillimanite-garnet gneiss (in axial plane of syncline)	191	146	1.308
R7105	43	quartz-feldspar gneiss (minor tourmaline)	144	64	2.25
R7106	44	chondrodite marble near axial plane in syncline	nd	373	
R7107	45	garnet-quartz-feldspar gneiss	15		
R7108	46	hypersthene gneiss	73	254	0.287
R7109	47a	garnet-hypersthene gneiss	103	176	0.585
R7110	47b	Stop 4, MAC Guidebook	125	162	0.772
R7111	48	charnockite	123	185	0.665
R7112	49(1)	charnockite	73	176	0.415
R7113	49(2)	charnockite	116	142	0.817
R7114	49(3)	charnockite	63	46	1.370

*Stops designated in Mineralogical Association of Canada Guidebook, 1967.

Pyroxene Granulite from Uganda

collected by H. W. Fairbairn, 1967

Labwor Hills:

M.I.T.#	Field#	Description	Rb	Sr	Rb/Sr
R6989	1	wx. fine-gn'd biotite gneiss	29	266	0.109
R6990	2	garnet gneiss	22	232	0.094
R6991	3	coarse grained gneiss	37	278	0.133
R6992	4	quartzo-feldspathic gneiss	117	170	0.688
R6993	5	highly wx. gneiss, secondary bio.	nd	402	
R6994	6	wx. gneiss	55	193	0.284
R6995	7	medium grained hornblende granite	77	266	0.289
R6996	8	wx. charnockite	11	261	0.042

Kaabong:

R6997	9	hb (?) biotite granite gneiss	29	1377	0.021
R6998	10	hornblende granite	22	1301	0.016
R6999	11	biotite gneiss	33	1543	0.021
R7000	12	biotite granite	213	181	1.176
R7001	13	rose colored biotite granite	187	231	0.809
R7002	14	biotite gneiss, slightly wx.	29	240	0.120
R7003	15	bio. gneiss, slightly rusted	18		
R7004	16	biotite granite	11	1084	0.010

Rakosi, S.W. Nile:

R7005	17	coarse grained bio. granite (chloritized)	37	397	0.093
R7006	18	quartzo-feldspathic gneiss	139	214	0.650
R7007	19	quartzo-feldspathic gneiss	108	171	0.632
R7008	20	granite gneiss	154	106	1.452

Rakosi, S.W. Nile (cont.):

M.I.T.#	Field#	Description	Rb	Sr	Rb/Sr
R7009	21	sx. white gneiss	114	296	0.385
R7010	22	leucocratic gneiss	22	233	0.094
R7011	23	pink gneiss	199	95	2.094
R7012	24	pink gneiss	154	37	4.162
R7013	25	wx. biotite gneiss	142	481	0.295
R7014	26	coarse granite gneiss	582	29	20.06
R7015	27	wx. granite gneiss	91	499	0.182
R7016	28	rusted quartzite	nd	nd	-----
R7017	29	white granite gneiss	82	205	0.400
R7018	30	leucocratic gneiss	346	70	4.942
R7019	31	alaskitic gneiss	425	64	6.64
R7020	32	quartzo-feldspathic gneiss	267	100	2.67
R7021	33	pink granite	330	59	5.593
R7022	34	white quartzo-feldspathic gneiss	187	322	0.581
Okollo S.W. Nile:					
R7023	35	grey biotite gneiss	83	232	0.353
R7024	36	fine-grained mafic granulite	12	70	0.171
R7025	37	dark grey granulite	47	428	0.109
R7026	38	mafic gneissic granulite	31	460	0.067
R7027	39	charnockite	30	461	0.107
R7028	40	coarse-grained granite	232	97	2.391
R7029	41	granite gneiss	196	240	0.816
R7030	42	wx. biotite gneiss	47	419	0.112
R7031	43	mafic granulite	35	296	0.118
R7032	44	mafic granulite	47	507	0.092

Okollo S.W. Nile (cont.):

M.I.T.#	Field#	Description	Rb	Sr	Rb/Sr
R7033	45	fine-medium grained quartzite	67	448	0.149
R7034	46				
R7035	47	honey-colored quartzite	95	335	0.283
R7036	48	mafic granulite	50	537	0.093
R7037	49	honey-colored granulite	30	629	0.047
R7038	50	mafic granulite	20	617	0.032
R7039	51	medium-grained granulite	30	422	0.071
R7040	52	mafic granulite	25	658	0.037
R7041	53	charnockite	16	466	0.034
R7042	54	mafic granulite	80	575	0.139
R7043	55	medium-grained grey gneiss	120	586	0.204
R7044	56	fine-grained gabbro	85	741	0.114
R7045	57	charnockite	53	403	0.132
R7046	58	coarse-grained biotite gneiss	175	228	0.767
R7047	59	biotite granite gneiss	165	167	0.988
R7048	60	biotite gneiss	25	652	0.038
R7049	61	charnockite	12	392	0.031

Charnockite from Kushalnagar Area, Mysore State, India

Longitude 75° 56' 36" E, Latitude 12° 26' 45" N

collected by Dr. P.R.J. Naidu

The Mineralogical Institute, University of Mysore
Manasa Gangotri, Mysore 6, India

M.I.T.#	Field#	Description	Rb	Sr	Rb/Sr
R7209	AD/1	charnockite (dyke)	10	188	0.053
R7210	AD/2	charnockite			
R7211	AD/3	charnockite	10	249	0.040
R7212	AD/7	charnockite	10	255	0.039
R7213	A-26	charnockite (Doddabettakeri)	10	349	0.029
R7214	A-85	charnockite (Dindghad)	10	122	0.082
R7215	A-95	charnockite (Chikkamarahalli)	10	166	0.060
R7216	A-110	charnockite (Kudige-Kanive)	10	122	0.082
R7217	A-115	charnockite (Kanive Hill, left)	10	72	0.139
R7218	A-117	charnockite (Kanive-Jainkal Betta)	10	188	0.053
R7219	A-121	charnockite (Marur)	10	123	0.081
R7220	A-124	charnockite (Kanive Temple Hill, right)	10	127	0.079
R7221	A-126	charnockite (Hulse)	10	216	0.046
R7248	A-142	charnockite (near Adinadur Tribal Colony)	8	248	0.032
R7247	A-143	garnetiferous charnockite (Doddakamarahalli)	11	81	0.041
R7244	A-148	charnockite (Cauvery River bed, Hulse)	16	184	0.087
R7246	A-150	charnockite (Cauvery River bed, Shanbhoganahalli)	10	162	0.062

Charnockite from Ooty, Madras State, India

Longitude 76° 40' E, Latitude 11° 30' N

collected by Dr. P.R.J. Naidu
The Mineralogical Institute, University of Mysore
Manasa Gangotri, Mysore 6, India

M.I.T.#	Field#	Description	Rb	Sr	Rb/Sr
R7245	AS-6	Charnockite-(garnetiferous)	10	108	0.09
R7249	AS-8	intermediate gneissic charnockite	48	575	0.083
R7250	AS-9	charnockite in contact with gneiss	10	1070	0.009

Charnockite from Mettupalaiyam, Coimbatore District,

Madras State, India

Longitude 76° 40' E, Latitude 11° 15' N

collected by Dr. P.R.J. Naidu
The Mineralogical Institute, University of Mysore
Manasa Gangotri, Mysore 6, India

M.I.T.#	Field#	Description	Rb	Sr	Rb/Sr
R7206	CR-92	Charnockite	10	160	0.063
R7207	CR-84	Charnockite	10	355	0.028
R7208	CR-13	Charnockite	10	116	0.086

Charnockite from Pallavaram (type area), Madras State, India

Longitude 80° 10' E, Latitude 12° 55' N

collected by Dr. P.R.J. Naidu
The Mineralogical Institute, University of Mysore
Manasa Gangotri, Mysore 6, India

M.I.T.#	Field#	Description	Rb	Sr	Rb/Sr
R7205	AS-12	Basic charnockite (St. Thomas Mount)	157	108	1.460
R7222	AS-1	Leptynite (Rifle Range)			
R7223	AS-2	coarse-grained charnockite (intermediate) Cherimali	173	649	0.267
R7238	AS-3	Charnockite with calc-granulite vein, Trisul	10	143	0.070
R7239	AS-4	basic charnockite (hb-bio rich) Pammal	8	161	0.050
R7240	AS-5	basic charnockite (hb-bio rich) Thattangannu	73	279	0.262
R7241	AS-7	basic charnockite (hb rich)	11	89	0.128
R7242	AS-10	basic charnockite (biotite rich)	132	636	0.208
R7243	AS-11	charnockite-leptynite contact rock	186	649	0.287

Charnockite from Salem Area, Madras State, India

collected by Dr. S. Subramanian, Government College, Salem 7, Madras, India

M.I.T.#	Field#	Description	Rb	Sr	Rb/Sr
R7176	1	medium-grained acid charnockite	nd	144	-----
R7177	2	medium-grained acid charnockite with basic segregation	43	484	0.089
R7178	3	medium-grained acid charnockite and garnetiferous basic charnockite	39	358	0.109
R7179	4	metabasic variety of charnockite 1,2,3,4 collected from same o/c	nd	266	-----
R7180	5	garnetiferous charnockite	71	298	0.238
R7181	6	charnockite pegmatite			
R7182	7	coarse-grained acid charnockite	nd	591	-----
R7330	8	medium-grained acid charnockite	15	342	0.044
R7331	9	fine-grained acid charnockite	15	560	0.027
R7332	10	fine-grained acid charnockite with pseudotachylite, 8,9,10 colledted from same o/c	13	102	0.127
R7333	11	basic segregation with pyrite	10	205	0.049
R7334	12	coarse-grained charnockite	40	490	0.082
R7335	13	basic charnockite with garnet	10	690	0.014
R7336	14	norite	6	744	0.008
R7337	15	leptynite	nd	150	-----

Specimens 1 to 6 collected west of Karuppur; specimens 7 to 13 collected in the hilly region northeast of Dasinayakkanpatti. Specimens 14 and 15 collected west of Nagari Malai.

Granulite Specimens from North East Tanzania

submitted by

Dr. J. V. Hepworth, Institute of Geological Sciences, London

M.I.T.#	Field #	Description	Rb	Sr	Rb/Sr
Para Mountains, Sheet 73:					
R7224	73/1	Pyroxene granulite, dark-waxy lustre	6	890	0.007
R7225	73/2	Leucocratic granulite	62	187	0.332
R7226	73/6	"Stripped pyroxene granulite" with local anataxis, incipient agmatite	22	711	0.031
R7228	73/11	Pyroxene granulite	5.5	486	0.011
R7229	73/14	"Leucocratic granitic rock in the granulites. No distinctive granulite character and may be intrusive granite but [I am] fairly certain it is a granulitic member".	86	125	0.69
R7230	73/15	"Dark blue" granulite	26	133	0.195
Labor Serrit Area:					
R7231	86/24	Dark colored pyroxene granulite	15	1046	0.014
R7232	86/25	Pegmatoid vein with garnet	37	784	0.047
R7233	86/27	Leucocratic granulite, cataclastic texture	95	380	0.25
R7234	86/29	"Dark blue" pyroxene granulite			
R7235	86/31	Mylonite among granulites "I (J.V.H.) think this is cotectonic".	37	1291	0.029
R7236	86/32	Nearly ultrabasic granulite, but amphibolite in thin section.	11	466	0.024
R7237	86/37	Marble with graphite (phlogopite and scapolite?)	nd	134	-----

Charnockites from the Kanuku Complex, Guyana, South America

submitted by J.P. Berrangé

Exact locations and detailed descriptions are given in the text and in Appendix A.

M.I.T.#	Field#	Description	Rb	Sr	Rb/Sr
R7340/a		biotite-hypersthene charnockite	43	226	0.162
R7340/b	JPB-156	common in Kanuku Complex	34	195	0.174
R7341/a		Same location as R7340	40	200	0.200
R7341/b	JPB-157		56	181	0.309
R7342/a		biotite-hypersthene charnock-	43	245	0.176
R7342/b	JPB-157	ite with plagioclase mega- crysts.	46	250	0.184
R7343/a		same as R7342	37	243	0.152
R7343/b	JPB-157		37	248	0.149
R7344/a		biotite-garnet gneiss, common	50	200	0.250
R7344/b	JPB-177	to Kanuku Complex	62	203	0.305
R7344/c			37	205	0.180
R7345/a		same as R7344	115	162	0.710
R7345/b	JPB-177		87	131	0.664
R7345/c			99	162	0.611
R7346/a		pyroxene granofels, probably	143	195	0.733
R7346/b	JPB-216	a mantled gneiss dome intruded into Kanuku Complex	127	205	0.620
R7347/a		Same as R7346 but from a	19	210	0.090
R7347/b	JPB-300	different body	19	198	0.096

Charnockitic Rocks from Indian Lake, Blue Mountain Lake, and West Canada Lake Quadrangles

submitted by Dr. D. DeWaard, Syracuse University, New York

M.I.T.#	Field#	Description	Rb	Sr	Rb/Sr
R7320	1=W-15(a)	light medium-grained pyroxene granulite	102	350	0.29
R7321	1=W-15(b)	darker than R7320, but same grain size	71	224	0.317
R7322	5=2(a)	dark green banded granulite (sawn pieces)	60	230	0.261
R7323	5=2(b)	dark green banded granulite (sawn pieces)	98	287	0.341
R7324	5=2(c)	dark green banded granulite (sawn pieces)	187	333	0.562
R7325	5=2(d)	dark green banded granulite (sawn pieces)	156	333	0.468
R7326	3=W-126(a)	light colored pyroxene granulite	92	325	0.283
R7327	3=W-126(b)	darker but same type	23	331	0.07
R7328	2=W-142	pyroxene granulite	35	287	0.123
R7329	2=W-124	banded pyroxene granulite	60	501	0.120

Charnockite from Crane Mountain, New York

collected by Dr. P. R. Whitney

Rensselaer Polytechnic Institute, Troy, New York

M.I.T.#	Field#	Description	Rb	Sr	Rb/Sr
R7120	ACS-40	This suite forms two distinct megascopic groups - "light" and "dark"; the latter being somewhat coarser in texture.	218	136	1.603
R7121	41		214	106	2.019
R7122	42		136	170	0.800
R7123	43	In the light group are 40, 41, 43, 44a, 44b, and in the dark: 42, 45, 46, 47, 48a, 48b.	181	177	1.023
R7124	44a		172	174	0.989
R7125	44b	Additional information is given in the text (Ch.III)	153	153	1.000
R7126	45		121	190	0.637
R7127	46		114	189	0.603
R7128	47		110	192	0.573
R7129	48a		110	211	0.521
R7130	48b		123	186	0.661

Charnockite from Indian Lake, New York

collected by C.M. Spooner, 1967

M.I.T.#	Field#	Description	Rb	Sr	Rb/Sr
R7115	CMS-50	Mangerite-Charnockite, near bench mark, and 50' north, route 30	52	233	0.233
R7116	51	north of spec. locality 50, near bench mark, charnockite gneiss	54	488	0.111
R7117	52	east side of route 30, charnockite	72	283	0.254
R7118	53	east side of route 30, charnockite	69	345	0.200
R7119	54	west of route 30, charnockite	58	289	0.201

APPENDIX C

IBM/OS 360 Program for Least Squares Regression

(after York, 1966)

```
      $JOB          SPOONER,KP#26,TIME#10,PAGES#100
    1       DIMENSION X(50),Y(50),U(50),V(50),P(50),Q(50),W(50),SQW(50),
           1RESX(50),RESY(50)
    2   100 READ(5,1)B,N,(X(I),Y(I),P(I),Q(I),I=1,N)
    3     1 FORMAT(F15.8, I10/%2F15.7,2E15.5<<
    4       SUMW=0.
    5       SUMA=0.
    6       SUMB=0.
    7       SUMC=0.
    8       SUMD=0.
    9       SUME=0.
   10       SUMS=0.
   11       SUMT=0.
   12       XBAR=0.
   13       YBAR=0.
   14       DO 2 I=1,N
   15       W(I)=P(I)*Q(I)/(B*B*Q(I)+P(I))
   16       SQW(I)=W(I)**2
   17     2 SUMW=SUMW+W(I)
   18       DO 3 I=1,N
   19       XBAR=XBAR+W(I)*X(I)/SUMW
   20     3 YBAR=YBAR+W(I)*Y(I)/SUMW
   21       DO 4 I=1,N
   22       U(I)=X(I)-XBAR
   23       V(I)=Y(I)-YBAR
   24       SUMA=SUMA+SQW(I)*(U(I)**2)/P(I)
   25       SUMB=SUMB+SQW(I)*U(I)*V(I)/P(I)
   26       SUMC=SUMC+SQW(I)*(V(I)**2)/P(I)
   27       SUMD=SUMD+W(I)*(U(I)**2)
   28     4 SUME=SUME+W(I)*U(I)*V(I)
   29       COA=0.6666667*SUMB/SUMA
   30       COB=(SUMC-SUMD)/(3.0*SUMA)
   31       COC=-SUME/SUMA
   32       CPHI=(COA**3-1.5*COA*COB+0.5*COC)/(COA**2-COB)**1.5
   33       IF(CPHI**2-1.0)6,6,10
   34     6 ALPHA=(SQRT(1.0-CPHI**2))/CPHI
   35       IF(-ALPHA)7,7,8
   36     7 PHI=ATAN(ALPHA)
   37       GO TO 9
   38     8 PHI=3.1415927+ATAN(ALPHA)
   39     9 SLOPEA=COA+2.0*SQRT(COA**2-COB)*COS(PHI/3.0)
   40       SLOPEB=COA+2.0*SQRT(COA**2-COB)*COS((PHI+6.283185)/3.0)
   41       SLOPEC=COA+2.0*SQRT(COA**2-COB)*COS((PHI+12.56637)/3.0)
   42       GO TO 30
   43    10 A=3.0*(COB-COA**2)
   44       C=-2.0*(COA**3)+3.0*COA*COB-COC
   45       Z=(-C/2.0+SQRT((C**2)/4.0+(A**3)/27.0))**(1.0/3.0)
   46       T=(-C/2.0-SQRT((C**2)/4.0+(A**3)/27.0))**(1.0/3.0)
   47       SLOPEA=Z+T+COA
   48       SLOPEB=0.00000000
   49       SLOPEC=0.00000000
   50    30 AINT=YBAR-SLOPEA*XBAR
   51       BINT=YBAR-SLOPEB*XBAR
   52       CINT=YBAR-SLOPEC*XBAR
   53       DO 31 I=1,N
```

```
      SUMS=SUMS+W(I)*(SLOPEC*U(I)-V(I))**2
      SUMT=SUMT+W(I)*(X(I)**2)
      RESX(I)=-(SLOPEC)*W(I)*(CINT+SLOPEC*X(I)-Y(I))/(P(I)*X(I))
   31 RESY(I)=W(I)*(CINT+SLOPEC*X(I)-Y(I))/(Q(I)*Y(I))
      AN=N
      SIGMAB=SQRT(SUMS/((AN-2.0)*SUMD))
      SIGMAA=SIGMAB*SQRT(SUMT/SUMW)
      WRITE(6,5)SLOPEA,AINT,SLOPEB,BINT,SLOPEC,CINT,XBAR,YBAR,SIGMAA,
     1SIGMAB,B
    5 FORMAT(10X, 8HSLOPEA# ,F15.8,5X,6HAINT# ,F15.8//10X, 8HSLOPEB# ,
     1F15.8,5X,6HBINT# ,F15.8//10X,8HSLOPEC# ,F15.8,5X,6HCINT# ,F15.8/
     210X, 8H  XBAR# ,F15.8,5X,6HYBAR# ,F15.8//10X, 8HSIGMAA# ,F15.8,
     33X, 8HSIGMAB# ,F15.8//10X, 8H     B# ,F15.8<
      WRITE(6,20)(RESX(I),RESY(I),I=1,N)
   20 FORMAT(10X,28HRESX                          RESY//%9X,F11.8,13X,F11.8<
      WRITE(6,21)(X(I),P(I),Y(I),Q(I),I=1,N)
   21 FORMAT(56H      X                P                    Y
     1//%F15.7,2X,E15.5,2X,F15.7,2X,E15.5<<
      AGE=ALOG(1.0+SLOPEC)*1.0E11/1.39
      ERAGE=(AGE*SIGMAB)/SLOPEC
      WRITE(6,29)
      WRITE(6,35) AGE,ERAGE
   29 FORMAT(10X,@AGE AND ERROR IN AGE FOR LAMBDA#1.39 X10E-11@<
   35 FORMAT(10X, 5HAGE= ,E14.6,12X,7HERAGE= ,E12.4)
*WARNING**    CC-6
      WRITE(6,99)
   99 FORMAT(1H1<
      GO TO 100
      END
```

APPENDIX D

IBM/OS 360 Program for C.I.P.W. Norm Calculation

```
$JOB            LUTH,KP=29,TIME=10,PAGES=20
C CIPW NORM-DINESS AND LUTH-REVISED MAR 6/68 BY C. M. SPOONER,M.I.T.
C     DATA CARD SPECIFICATIONS                                  COLUMNS
C     1. 2A5  10 CHARACTERS FOR IDENTIFICATION                    1-10
C     I2  2 CHAR. IF NA CARB CALC    (NA)                        11-12
C     I2  2 CHAR. IF CA CARB TO BE CALC.          (IC)           13-14
C     11F6.3  SIO2,AL2O3,FE2O3,FEO,MGO,CAO,NA2O,K2O,TIO2,P2O5,MNO
C     2.  12F6.3 ZRO2,CO2,SO3,CL,F,S,CR2O3,NIO,COO,BAO,SRO,LI2O
C THE NORM CALCULATED IS THE ORIGINAL CIPW NORM MODIFIED ONLY IN THAT
C LI2O IS ADDED TO MGO AND THENARDITE IS CALC WHEN SO3 REPORTED
C THE MGO/FEO RATIO IN THE DIOPSIDE,HYPERSTHENE AND OLIVINE IS PRINTED.
C  AS A SEPARATE SUBROUTINE ARE REPORTED
C     1. AB/AB+OR+Q,OR/AB+OR+Q ,Q/AB+OR+Q
C     2. AB/AB+OR+AN,... ETC.
C     3. (-C) THE WEIGHT AMOUNT OF AL2O3 REQUIRED TO FORM AL2O3
C     SATURATED NORMATIVE MINERALS FROM ACMITE, NA MS, K MS, DIOPSIDE,
C     WOLLASTONITE,AND CA OS.
C     4. AB,OR,LC,NE,KALIOPHYLLITE, AND Q ARE RECALC. TO NE,KS,AND Q
C     FURTHER RECALCULATED TO 1.000 AND PRINTED
C     59 OL,PX, AND FP ARE CALC. AS FOLLOWS
C     A.  OL= (CA OS + OL) NORMATIVE
C     B.  PYROXENE = ( ACMITE + DI + WO + HYPERSTHENE) NORMATIVE
C     C. FELDSPAR = (AB + OR + AN)
C     D. THESE ARE RECALCULATED TO 1.000 AND PRINTED
C     THE OXIDATION RATIO ( CHINNER, J. PET.,1960) IS CALC AND PRINTED
C  THE DIFFERENTIATION INDEX ( THORNTON AND TUTTLE) IS CALC AND PRINTED
C     CIPW NORM CALCULATION  MAIN PROGRAMME
1           DIMENSION N(2)
2           COMMON N,NA,IC,SIO,ALO,FEO3,FEO2,AMGO,CAO,ANAO,AKO,TIO,PO,AMNO,ZRO
           1,CO,CL,F,S,CRO,ANIO,COO,SRO,ALIO,SIO1,ALO1,FEO31,FEO21,AMGO1,CAO1,
           2ANAO1,AKO1,TIO1,PO1,AMNO1,ZRO1,CO1,SO1,CL1,F1,S1,CRO1,ANIO1,COO1,
           3SRO1,ALIO1,AP,HL,TH,PR,CM,AIL,FR,ANC,CC,Z,OR,AKS,AB,AN,C,AC,ANS,AN
           4I,HM,SP,RU,R,SS,SS1,HY,AMWDI,AMWHY,AMWOL,WO,DI,OL,SIOC,PF,ANE,AB1,
           5OR1,CS,DI1,OL1,ALC,SALG,FEMG,ALC1,SO,SIOC1,BAO,BAO1,AKP,Q,SUM,CDI,
           6BQ,BAB,BOR,CQ,CNE,CKP,DQ,DNE,DKP,DCAC,DCNS,DCKS,DCDI,DCWO,DCCS,DC,
           7DAB,DOR,DAN,FPY,FOL,FFS,SFPY,SFOL,SFFS,RATIO
3         1 CALL ACESS
4           IF (N(2)) 2222,2222,2
5         2 CALL FELD
6           CALL FERO
7           IF(SIO1-SIOC1)73,1118,1118
8        73 CALL DEF
9      1118 SUM= SIO+ALO+FEO3+AMGO+CAO+ANAO+AKO+TIO+PO+AMNO+ZRO+CO+SO+
           1CL+F+CRO+ANIO+COO+BAO+SRO+ALIO+S+FEO2
10          SALG=Q+C+Z+OR+AB+AN+ALC+ANE+AKP+HL+TH+ANC
11          FEMG=AC+ANS+AKS+DI+WO+HY+OL+CS+AMT+CM+HM+AIL+SP+PF+RU+AP+FR+
           1PR+CC
12          CDI=Q+OR+AB+ANE+AKP+ALC
13          CALL CALC
14          CALL PRINT
15       3333 GO TO 1
16       2222 STOP
17          END
```

```
      SUBROUTINE ACESS
      DIMENSION N(2)
      COMMON N,NA,IC,SIO,ALO,FEO3,FEO2,AMGO,CAO,ANAO,AKO,TIO,PO,AMNO,ZRO
     1,CO,CL,F,S,CRO,ANIO,COO,SRO,ALIO,SIO1,ALO1,FEO31,FEO21,AMGO1,CAO1,
     2ANAO1,AKO1,TIO1,PO1,AMNO1,ZRO1,CO1,SO1,CL1,F1,S1,CRO1,ANIO1,COO1,
     3SRO1,ALIO1,AP,HL,TH,PR,CM,AIL,FR,ANC,CC,Z,OR,AKS,AB,AN,C,AC,ANS,AP
     4T,HM,SP,RO,R,SS,SS1,HY,AMWOI,AMWHY,AMWOL,WO,DI,OL,SIOC,PF,ANE,AB1,
     5OR1,CS,DI1,OL1,ALC,SALG,FEMG,ALC1,SO,SIOC1,BAO,BAO1,AKP,Q,SUM,CDI,
     6BQ,BAB,BOR,CQ,CNE,CKP,DQ,DNE,DKP,DCAC,DCNS,DCKS,DCDI,DCWO,DCCS,DC,
     7DAB,DOR,DAN,FPY,FOL,FFS,SFPY,SFOL,SFFS,RATIO
      READ(5,1) N(1),N(2),NA,IC,SIO,ALO,FEO3,FEO2,AMGO,CAO,ANAO,AKO,TIO,
     1PO,AMNO,ZRO,CO,SO,CL,F,S,CRO,ANIO,COO,BAO,SRO,ALIO
    1 FORMAT (2A5,2I2,11F6.0,/12F6.0)
      IF (N(2)) 2222,2222,2221
 2222 STOP
 2221 SIO1=SIO/60.
      ALO1=ALO/102.
      FEO31=FEO3/160.
      FEO21=FEO2/72.
      IF(FEO31) 500,500,501
  501 RATIO=(2.*FEO31/(2.*FEO31+FEO21))*100.
  500 CONTINUE
      AMGO1=AMGO/40.
      CAO1=CAO/56.
      ANAO1=ANAO/62.
      AKO1=AKO/94.
      TIO1=TIO/80.
      PO1=PO/142.
      AMNO1=AMNO/71.
      ZRO1=ZRO/123.
      CO1=CO/44.
      SO1=SO/80.
      CL1=CL/71.
      F1=F/38.
      S1=S/32.
      CRO1=CRO/152.
      ANIO1=ANIO/75.
      COO1=COO/75.
      BAO1=BAO/153.5
      SRO1=SRO/103.5
      ALIO1=ALIO/30.
      FEO21=AMNO1+ANIO1+FEO21
      CAO1=CAO1+SRO1+BAO1
      AMGO1=AMGO1+ALIO1
      IF (PO1-.002) 3,3,4
    4 IF (F1-.002) 141,141,142
  141 AP=PO1*310.
      CAO1=CAO1-3.*PO1
      GO TO 5
  142 AP=PO1*336.
      CAO1= CAO1-3.3333*PO1
      F1=F1-.3333*PO1
      GO TO 5
    3 AP=0.
    5 IF (CL1-.002) 6,6,7
```

```
      6 HL=0.
        GO TO 8
      7 HL=2.*CL1*117.
        ANA01=ANA01-CL1
      8 IF(SO1-.002)9,9,10
     10 TH=SO1*142.
        ANA01=ANA01-SO1
        GO TO 11
      9 TH=0.
     11 IF(S1-.002) 12,12,13
     13 PR=S1*60.
        FE021=FE021-.5*S1
        GO TO 14
     12 PR=0.
     14 IF(CR01-.002) 15,15,16
     16 CM=CR01*224.
        FE021=FE021-CR01
        GO TO 17
     15 CM=0.
     17 IF(TI01-.002) 18,18,19
     18 AIL=0.
        GO TO 20
     19 IF(FE021-TI01)21,22,22
     21 AIL=FE021*152.
        TI01=TI01-FE021
        FE021=0.
        GO TO 20
     22 AIL=TI01*152.
        FE021=FE021-TI01
        TI01=0.
     20 IF(F1-.002) 23,23,24
     23 FR=0.
        GO TO 25
     24 FR=F1*78.
        CA01=CA01-F1
     25 IF (NA) 26,26,27
     27 ANC=C01*106.
        ANA01=ANA01-C01
        CC=0.
        GO TO 28
     26 ANC=0.
        IF(IC) 29,29,30
     30 CC=C01*100.
        CA01=CA01-C01
        GO TO 28
     29 CC=0.
     28 IF(ZR01-0.002)31,31,32
     31 Z=0.
        GO TO 33
     32 Z=ZR01*183.
     33 RETURN
        END
```

```
      SUBROUTINE FELD
      DIMENSION N(2)
      COMMON N,NA,IC,SIO,ALO,FEO3,FEO2,AMGO,CAO,ANAO,AKO,TIO,PO,AMNO,ZR
     1,CO,CL,F,S,CRO,ANIO,COO,SRO,ALIO,SIO1,ALO1,FEO31,FEO21,AMGO1,CAO1
     2ANAO1,AKO1,TIO1,PO1,AMNO1,ZRO1,CO1,SO1,CL1,F1,S1,CRO1,ANIO1,COO1,
     3SRO1,ALIO1,AP,HL,TH,PR,CM,AIL,FR,ANC,CC,Z,OR,AKS,AB,AN,C,AC,ANS,A
     4I,HM,SP,RU,R,SS,SS1,HY,AMWOI,AMWHY,AMWOL,WO,DI,OL,SIOC,PF,ANE,AB1
     5OR1,CS,DI1,OL1,ALC,SALG,FEMG,ALC1,SO,SIOC1,BAO,BAO1,AKP,Q,SUM,CDI
     6BQ,BAB,BOR,CQ,CNE,CKP,DQ,DNE,DKP,DCAC,DCNS,DCKS,DCDI,DCWO,DCCS,DC
     7DAB,DOR,DAN,FPY,FOL,FFS,SFPY,SFOL,SFFS,RATIO
   33 IF(AKO1-.002)34,34,35
   34 OR=0.
      AKS=0.
      GO TO 36
   35 IF(ALO1-AKO1) 37,37,38
   37 OR=ALO1*556.
      AKS=(AKO1-ALO1)*154.
      ALO1=0.
      GO TO 36
   38 AKS=0.
      OR=AKO1*556.
      ALO1=ALO1-AKO1
   36 IF(ALO1-.002) 39,39,40
   40 IF(ALO1-ANAO1) 41,41,42
   41 AB=ALO1*524.
      ANAO1=ANAO1-ALO1
      AN=0.
      C=0.
      GO TO 49
   42 AB=ANAO1*524.
      ALO1=ALO1-ANAO1
      ANAO1=0.
      IF(ALO1-.002) 43,43,44
   43 AN=0.
      C=0.
   46 AC=0.
      ANS=0.
      GO TO 45
   44 IF(ALO1-CAO1) 47,47,48
   47 AN=ALO1*278.
      CAO1=CAO1-ALO1
      C=0.
      GO TO 46
   48 AN=CAO1*278.
      C=(ALO1-CAO1)*102.
      CAO1=0.
      GO TO 46
   39 AB=0.
      AN=0.
      C=0.
   49 IF(FEO31-.002) 50,50,51
   51 IF(FEO31-ANAO) 521,521,531
  531 AC=ANAO1*462.
      FEO31=FEO31-ANAO1
      ANS=0.
```

```
      ANAO1=0.
      GO TO 45
  521 AC=FEO31*462.
      ANAO1=ANAO1-FEO31
      FEO31=0.
      ANS=ANAO1*122.
      GO TO 45
   50 ANS= ANAO1*122.
      AC=0.
      ANAO1=0.
   45 IF(FEO31-.002) 54,54,55
   54 AMT=0.
      HM=0.
      GO TO 56
   55 IF(FEO21-FEO31)57,58,58
   57 AMT=FEO21*232.
      HM=(FEO31-FEO21)*160.
      FEO21=0.
      GO TO 56
   58 AMT=FEO31*232.
      HM=0.
      FEO21=FEO21-FEO31
   56 IF(CAO1-.002)581,581,571
  571 IF(TIO1-CAO1) 60,60,59
   59 SP=CAO1*196.
   63 RU=(TIO1-CAO1)*80.
      CAO1=0.
      GO TO 64
   60 SP=TIO1*196.
      RU=0.
      CAO1=CAO1-TIO1
      GO TO 64
  581 SP=0.
      IF(TIO1-.002) 62,62,63
   62 RU=0.
      CAO1=0.
      GO TO 64
   64 RETURN
      END
```

```
      SUBROUTINE FERO
      DIMENSION N(2)
      COMMON N,NA,IC,SIO,ALO,FEO3,FEO2,AMGO,CAO,ANAO,AKO,TIO,PO,AMNO,ZRO
     1,CO,CL,F,S,CRO,ANIO,COO,SRO,ALIO,SIO1,ALO1,FEO31,FEO21,AMGO1,CAO1,
     2ANAO1,AKO1,TIO1,PO1,AMNO1,ZRO1,CO1,SO1,CL1,F1,S1,CRO1,ANIO1,COO1,
     3SRO1,ALIO1,AP,HL,TH,PR,CM,AIL,FR,ANC,CC,Z,OR,AKS,AB,AN,C,AC,ANS,AM
     4T,HM,SP,RU,R,SS,SS1,HY,AMWDI,AMWHY,AMWOL,WO,DI,OL,SIOC,PF,ANE,AB1,
     5OR1,CS,DI1,OL1,ALC,SALG,FEMG,ALC1,SO,SIOC1,BAO,BAO1,AKP,Q,SUM,CO1,
     6BQ,BAB,BOR,CQ,CNE,CKP,DQ,DNE,DKP,DCAC,DCNS,DCKS,DCDI,DCWO,DCCS,DC,
     7DAB,DOR,DAN,FPY,FOL,FFS,SFPY,SFOL,SFFS,RATIO
   64 IF(AMGO1-.002)643,643,644
  644 R=AMGO1/FEO21
      IF(FEO21) 641,641,642
  641 AMWDI=216.
      AMWHY=100.
      AMWOL=140.
      F1=-1.
      SS=AMGO1
      GO TO 645
  643 AMWDI=248.
      AMWHY=132.
      F1=-2.
      SS=FEO21
      AMWOL=204.
      GO TO 645
  642 AMWDI=56.+2.*60.+(40.*R+72.)/(R+1.)
      AMWHY=(40.*R+72.)/(R+1.)+60.
      AMWOL=2.*(40.*R+72.)/(R+1.)+60.
      F1=0.
      SS=AMGO1+FEO21
  645 IF(CAO1-.002) 66,66,65
   65 IF(CAO1-SS)68,68,67
   67 DI=SS*AMWDI
      HY=0.
      SS1=0.
      CAO1=CAO1-SS
      WO=CAO1*116.
      GO TO 69
   68 DI=CAO1*AMWDI
  671 SS1=SS-CAO1
      HY=SS1*AMWHY
      CAO1=0.
      WO=0.
      GO TO 69
   66 WO=0.
      DI=0.
      GO TO 671
   69 SIOC=Z/183.+SP/196.+4.*AC/462.+AKS/154.+ANS/122.+6.*OR/556.+6.*A
     1B/524.+2.*AN/278.+2.*DI/AMWDI+WO/116.+HY/AMWHY
      SIOC1=SIOC
   71 IF(SIO1-SIOC1)73,72,72
   72 Q=(SIO1-SIOC1)*60.
      OL=0.
      PF=0.
      ANE=0.
```

```
      ALC=0.
      CS=0.
      AKP=0.
   73 RETURN
      END
```

```
      SUBROUTINE DEF
      DIMENSION N(2)
      COMMON N,NA,IC,SIO,ALO,FEO3,FEO2,AMGO,CAO,ANAO,AKO,TIO,PO,AMNO,ZRO
     1,CO,CL,F,S,CRO,ANIO,COO,SRO,ALIO,SIO1,ALO1,FEO31,FEO21,AMGO1,CAO1,
     2ANAO1,AKO1,TIO1,PO1,AMNO1,ZRO1,CO1,SO1,CL1,F1,S1,CRO1,ANIO1,COO1,
     3SRO1,ALIO1,AP,HL,TH,PR,CM,AIL,FR,ANC,CC,Z,OR,AKS,AB,AN,C,AC,ANS,AM
     41,HM,SP,RU,R,SS,SS1,HY,AMWDI,AMWHY,AMWOL,WO,DI,OL,SIOC,PF,ANE,AB1,
     5OR1,CS,DI1,OL1,ALC,SALG,FEMG,ALC1,SO,SIOC1,BAO,BAO1,AKP,Q,SUM,CDI,
     6BQ,BAB,BOR,CQ,CNE,CKP,DQ,DNE,DKP,DCAC,DCNS,DCKS,DCDI,DCWO,DCCS,DC,
     7DAB,DOR,DAN,FPY,FOL,FFS,SFPY,SFOL,SFFS,RATIO
   73 Q=0.
      SIOC1=SIOC1-HY/AMWHY
      IF(SIO1-SIOC1)74,75,75
   75 IF(SIO1-SIOC1-.5*SS1) 74,74,76
   76 HY1=(2.*(SIO1-SIOC1)-SS1)*AMWHY
      OL=(SS1-HY1/AMWHY)*AMWOL/2.
      HY=HY1
      GO TO 1113
   74 HY=0.
      OL=SS1*AMWOL/2.
      PF=136.*SP/196.
      SIOC1=SIOC1-SP/196.
      SP=0.
      SIOC1=SIOC1-6.*AB/524.+OL/AMWOL
      IF(SIO1-SIOC1) 77,77,78
   78 IF(SIO1-SIOC1-2.*AB/524.)77,79,79
   79 AB1=((SIO1-SIOC1-2.*AB/524.)/4.)*524.
      ANE=(AB/524.-AB1/524.)*284.
      AB=AB1
      GO TO 1115
   77 ANE=(AB/524.)*284.
      AB=0.
      SIOC1=SIOC1-6.*OR/556.+2.*ANE/284.
      IF(SIO1-SIOC1) 80,80,81
   81 IF(SIO1-SIOC1-4.*OR/556.) 80,82,82
   82 OR1=(SIO1-SIOC1-4.*OR/556.)/2.
      ALC=(OR/556.-OR1/556.)*436.
      OR=OR1*556.
      GO TO 1116
   80 ALC=436.*OR/556.
      OR=0.
      SIOC1=SIOC1-WO/116.+4.*ALC/436.
      IF(SIO1-SIOC1) 83,83,841
  841 IF(WO/116.-(SIO1-SIOC1))83,84,84
   84 CS=(WO/116.-(SIO1-SIOC1))*172.
      WO=(WO/116.-(2.*CS/172.))*116.
      GO TO 1117
   83 SIOC1=SIOC1-2.*DI/AMWDI
   86 DI1=(2.*(SIO1-SIOC1)-DI/AMWDI-(DI/AMWDI+WO/116.))/2.
      OL1=((DI/AMWDI-DI1)/2.)*AMWOL
      CS=(DI/AMWDI+WO/116.-DI1)/2.
      CS=CS*172.
      ZA=2.*DI1+2.*CS/172.+2.*OL1/AMWOL-2.*(SIO1-SIOC1)
      IF(ZA) 87,87,85
   87 OL=OL+OL1
```

```
      WO=0.
      DI=DI1*AMWDI
      GO TO 1117
   85 OL=OL+AMWOL*DI/(2.*AMWDI)
      CS=172.*DI/(2.*AMWDI) + 172.*WO/(2.*116.)
      DI=0.
      WO=0.
      SIOC1=Z/183.+4.*AC/462.+AKS/154.+ANS/122.+2.*AN/278.+OL/AMWOL+
     1CS/172.+2.*ANE/284.
      SIOC1=SIO1-SIOC1
      ALC1=((SIOC1-2.*ALC/436.)/2.)*436.
      AKP=((4.*ALC/436.-SIOC1)/2.)*256.
      ALC=ALC1
      GO TO 1118
 1113 PF=0.
 1114 ANE=0.
 1115 ALC=0.
 1116 CS=0.
 1117 AKP=0.
 1118 RETURN
      END
```

```
      SUBROUTINE CALC
      DIMENSION N(2)
      COMMON N,NA,IC,SIO,ALO,FEO3,FEO2,AMGO,CAO,ANAO,AKO,TIO,PO,AMNO,ZRO
     1,CO,CL,F,S,CRO,ANIO,COO,SRO,ALIO,SIO1,ALO1,FEO31,FEO21,AMGO1,CAO1,
     2ANAO1,AKO1,TIO1,PO1,AMNO1,ZRO1,CO1,SO1,CL1,F1,S1,CRO1,ANIO1,COO1,
     3SRO1,ALIO1,AP,HL,TH,PR,CM,AIL,FR,ANC,CC,Z,OR,AKS,AB,AN,C,AC,ANS,AM
     4T,HM,SP,RO,R,SS,SS1,HY,AMWO1,AMWHY,AMWOL,WO,DI,OL,SIOC,PF,ANE,AB1,
     5OR1,CS,DI1,OL1,ALC,SALG,FEMG,ALC1,SO,SIOC1,BAO,BAO1,AKP,Q,SUM,CDI,
     6BQ,BAB,BOR,CQ,CNE,CKP,DQ,DNE,DKP,DCAC,DCNS,DCKS,DCDI,DCWO,DCCS,DC,
     7DAB,DOR,DAN,FPY,FOL,FFS,SFPY,SFOL,SFFS,RATIO
  100 BQ=Q/(AB+OR+Q)
      BAB=AB/(AB+OR+Q)
      BOR=OR/(AB+OR+Q)
  101 CQ=Q+.458*AB+.432*OR+.275*ALC
      CNE=ANE+.542*AB
      CKP=AKP+.568*OR+.725*ALC
  102 DQ=CQ/(CQ+CNE+CKP)
      DNE=CNE/(CQ+CNE+CKP)
      DKP=CKP/(CQ+CNE+CKP)
  103 DCAC=.221*AC
      DCNS=.836*ANS
      DCKS=.662*AKS
      DCDI=.440*DI
      DCWO=.879*WO
      DCCS=1.186*CS
  104 DC=DCAC+DCNS+DCKS+DCDI+DCWO+DCCS
  105 DAB=AB/(AB+AN+OR)
      DOR=OR/(AB+AN+OR)
      DAN=AN/(AB+AN+OR)
  106 FPY=AC+DI+WO+HY
      FOL=CS+OL
      FFS=AB+AN+OR
  107 SFPY=FPY/(FPY+FOL+FFS)
      SFOL=FOL/(FPY+FOL+FFS)
      SFFS=FFS/(FPY+FOL+FFS)
  108 RETURN
      END
```

```
      SUBROUTINE PRINT
      DIMENSION N(2)
      COMMON N,NA,TC,SIO,ALO,FEO3,FEO2,AMGO,CAO,ANAO,AKO,TIO,PO,AMNO,ZRO
     1,CO,CL,F,S,CRO,ANIO,COO,SRO,ALIO,SIO1,ALO1,FEO31,FEO21,AMGO1,CAO1,
     2ANAO1,AKO1,TIO1,PO1,AMNO1,ZRO1,CO1,SO1,CL1,F1,S1,CRO1,ANIO1,COO1,
     3SRO1,ALIO1,AP,HL,TH,PR,CM,AIL,FR,ANC,CC,Z,OR,AKS,AB,AN,C,AC,ANS,AM
     4T,HM,SP,RU,R,SS,SSI,HY,AMWOI,AMWHY,AMWOL,WO,DI,OL,SIOC,PF,ANE,AB1,
     5OR1,CS,DI1,OL1,ALC,SALG,FEMG,ALC1,SO,SIOC1,BAO,BAO1,AKP,Q,SUM,CDI,
     6BQ,BAB,BOR,CQ,CNE,CKP,DQ,DNE,DKP,DCAC,DCNS,DCKS,DCDI,DCWO,DCCS,DC,
     7DAB,DOR,DAN,FPY,FOL,FFS,SFPY,SFOL,SFFS,RATIO
      WRITE(6,1119) N(1),N(2),SIO,Q,BQ,ALO,C,DC,FEO3,Z,FEO2,OR,
     1BOR,DOR,AMGO,AB,BAB,DAB,CAO,AN,DAN,ANAO,ALC,AKO,AKP
 1119 FORMAT(1H1,10X,18HCHEMICAL ANALYSIS,3X,2A5,10X,9HCIPW NORM/48X,
     116H(WEIGHT PERCENT)///50X,11HSALIC GROUP/
     210X,4HSIO2,12X,F6.3,10X,6HQUARTZ,20X,F6.3,5X,F6.3/
     310X,5HAL2O3,11X,F6.3,10X,8HCORUNDUM,18X,F6.3,2X,3H(-),F6.3/
     410X,5HFE2O3,11X,F6.3,10X,6HZIRCON,20X,F6.3/
     510X,3HFEO,13X,F6.3,10X,10HORTHOCLASE,16X,F6.3,5X,F6.3,5X,F6.3/
     o10X,3HMGO,13X,F6.3,10X,6HALBITE,20X,F6.3,5X,F6.3,5X,F6.3/
     710X,3HCAO,13X,F6.3,10X,9HANORTHITE,17X,F6.3,16X,F6.3/
     810X,4HNA2O,12X,F6.3,10X,7HLEUCITE,19X,F6.3/
     910X,3HK2O,13X,F6.3,10X,12HKALIOPHYLITE,14X,F6.3)
      WRITE(6,1120) TIO,ANE,PO,TH,AMNO,ANC,ZRO,HL,CO,SALG,SO,CL,F,S,CRO
     1,AC,DCAC,ANIO,ANS,DCNS,COO,AKS,DCKS
 1120 FORMAT(     10X,4HTIO2,12X,F6.3,10X,9HNEPHELINE,17X,F6.3/
     110X,4HP2O5,12X,F6.3,10X,10HTHENARDITE,16X,F6.3/
     210X,3HMNO,13X,F6.3,10X,16HSODIUM CARBONATE,10X,F6.3/
     310X,4HZRO2,12X,F6.3,10X,6HHALITE,20X,F6.3/
     410X,3HCO2,13X,F6.3,22X,3HSUM,2X,F7.3/
     510X,3HSO3,13X,F6.3,/10X,3HCL2,13X,F6.3,/10X,2HF2,14X,F6.3/
     610X,1HS,15X,F6.3,21X,11HFEMIC GROUP,18X,4H(-C)/
     710X,5HCR2O3,11X,F6.3,10X,6HACMITE,20X,F6.3,5X,F6.3/
     810X,3HNIO,13X,F6.3,10X,19HSODIUM METASILICATE,7X,F6.3,5X,F6.3/
     910X,3HCOO,13X,F6.3,10X,22HPOTASSIUM METASILICATE,4X,F6.3,5X,F6.3)
      WRITE(6,1122)BAO,DI,DCDI,SRO,WO,DCWO,ALIO,HY,OL,SUM,CS,DCCS,AMT,
     1DQ,HM,DNE,AIL,DKP,SP,PF,RU
 1122 FORMAT(     10X,3HBAO,13X,F6.3,10X,8HDIOPSIDE,18X,F6.3,5X,F6.3/
     110X,3HSRO,13X,F6.3,10X,12HWOLLASTONITE,14X,F6.3,5X,F6.3/
     210X,4HLI2O,12X,F6.3,10X,11HHYPERSTHENE,15X,F6.3/
     342X,7HOLIVINE,19X,F6.3/
     410X,3HSUM,12X,F7.3,10X,21HCALCIUM ORTHOSILICATE,5X,F6.3,5X,F6.3/
     542X,9HMAGNETITE,17X,F6.3,/10X,6HQUARTZ,10X,F6.3,10X,8HHEMATITE,
     618X,F6.3/10X,9HNEPHELINE,7X,F6.3,10X,8HILMENITE,18X,F6.3/
     710X,9HKALSILITE,7X,F6.3,10X,6HSPHENE,20X,F6.3/
     842X,10HPEROVSKITE,16X,F6.3/42X,6HRUTILE,20X,F6.3)
      WRITE(6,1123)SFOL,AP,SFPY,FR,SFFS,PR,CC,CM,FEMG
 1123 FORMAT(     10X,7HOLIVINE,9X,F6.3,10X,7HAPATITE,19X,F6.3/
     110X,8HPYROXENE,8X,F6.3,10X,8HFLUORITE,18X,F6.3/
     210X,8HFELDSPAR,8X,F6.3,10X,6HPYRITE,20X,F6.3/
     342X,7HCALCITE,19X,F6.3/42X,8HCHROMITE,18X,F6.3//
     454X,3HSUM,12X,F7.3)
      WRITE(6,1124) RATIO
 1124 FORMAT(1H /1H /10X,42HOXIDATION RATIO MOL(2FE2O3/2FE2O3+FEO)X100,
     1F7.3)
      IF(1.+F1)1129,1127,1126
```

```
      1126 WRITE(6,1131) K
      1131 FORMAT(1H /1H /10X,'RATIO MGO/FEO IN HYPERSTHENE DIOPSIDE AND
     1OLIVINE = ',1PE12.4)
           GO TO 3333
      1127 WRITE(6,1128)
      1128 FORMAT (1H /1H /10X,43HNO IRON IN HYPERSTHENE DIOPSIDE AND OLIVIN
     1)
           GO TO 3333
      1129 WRITE(6,1130)
      1130 FORMAT(1H /1H /10X,48HNO MAGNESIUM IN HYPERSTHENE DIOPSIDE AND OL
     1VINE)
      3333 WRITE(6,3334)CDI
      3334 FORMAT(1H /1H /10X,24HDIFFERENTIATION INDEX = ,F7.3)
      3335 RETURN
           END
```

N.O

APPENDIX E

C.I.P.W. Norm Calculations for Charnockite Analyses from the Literature

COMPILATION OF ANALYSES OF THE CHARNOCKITE SERIES

P. Quensel (1950) Arkiv för Mineralog och Geologi, Band 1, No. 10.

Q-1 Basic charnockite, Lassabacka, Varberg.

Q-2 Basic charnockite, Högaballa, Träslövsläge.

Q-3 Basic charnockite (hornblende norite) St. Thomas Mt., Madras, H. S. Washington, Am. Jour. Sci., 1916, 41, p. 330.

Q-4 Basic charnockite (basic garnetiferous norite) Niapa Hill, Uganda (A. W. Groves, Quart. Jour., Vol. 91, 1935, p. 170).

Q-5 Basic charnockite (garnetiferous orthoclase-norite) on the road, Colombo-Ratapura. (F. D. Adams, Canadian Jour. of Res., 1929, I, p. 482).

Q-6 Intermediate charnockite (previously named 'Varberg granite') Apeluiken, south of Varberg (A. E. Törnebohm, S. G. U. Ser. Ba., No. 6, 1910, p. 20).

Q-7 Intermediate charnockite, Fästningsberget, Varberg. Ibid.

Q-8 Sub-acid charnockite, Traneberg, Varberg.

Q-9 Coarse-grained leucocratic charnockite, Träslövsläge.

Q-10 Fine-grained dark charnockite, between Björka and Trönninge (silicified basic charnockite).

Q-11 Felsic charnockite, Himle.

Q-12 Gneiss of the surrounding formation.

Q-13 Typical orthogneiss surrounding the charnockite mass of Mt. Wati, Uganda.

Q-14 Intermediate charnockite, Mt. Wati, Uganda.

Q-15 Basic charnockite, Lassabacka, Varberg.

Q-16 Garnetiferous amphibolite, Getterö Island, Varberg.

R. A. Howie (1955) Trans. Roy. Soc. Edin., Vol. LXII, pt. III.

HOWIE-1 Charnockite, Pallavaram, Madras, Anal. J. H. Scoon.

HOWIE-2 Charnockite, Trisul Hill, Meanambakam, Madras, Anal. J. H. Scoon.

HOWIE-3 Charnockite, Magazine Hill, St. Thomas' Mount, Madras, Anal. J. H. Scoon.

HOWIE-4 As above, Anal. H. S. Washington (1916, A.J.S. 41, p. 323).

HOWIE-5 Charnockite, St. Thomas' Mount, Madras, Anal. T. L. Walker (Holland, 1900, Mem. Geol. Survey of India, 28, pt.2, p. 142).

HOWIE-6 Charnockite, same locality, Anal. P. C. Roy (Holland, Ibid.).

HOWIE-7 MSt./56, same locality, Anal. C. Rajagopalan (1948) Proc. Indian Acad. Sci. 24, 315 and 26, 237.

HOWIE-8 MSt./29, same locality, see HOWIE-7.

HOWIE-9 "Acid charnockite", Pallavaram, Anal. R. D. Sundaram, M.Sc. Thesis, 1947 (Pichamuthu (1953) Mysore Geol. Assoc.).

HOWIE-10 "Granodiorite", St. Thomas' Mount, MSt./38, Madras, Anal. C. Rajagopalan (1947).

HOWIE-11 Enderbite, Pallavaram, Madras, Anal., R. A. Howie

HOWIE-12 Enderbite, Proclamation Island, Enderby Land, Anal. C. E. Tilley (1937) B.A.N.Z. Anarctic Res. Exp. Rep. Ser. A, 2 pt. 1.

HOWIE-13 Garnetiferous leptynite, Anal. R. A. Howie.

HOWIE-14 Garnet granulite, Proclamation Island, Enderby Land, Anal. C. E. Tilley (1937).

HOWIE-15 Acid intermediate rock, Nambran Paramba, Tinnevelly district, Madras, Anal. R. A. Howie.

HOWIE-16 Intermediate rock, Ambagamudam Pothai, Tinnevelly district, Madras, Anal. R. A. Howie.

HOWIE-17 Intermediate rock, Miladampari, Palni Town, Madura, Anal. R. A. Howie.

HOWIE-18 Shevaroy Hills, Madras, Anal. J. H. Scoon.

HOWIE-19 Intermediate rock, Valegan Pothai, near Tenkor, Tinnevelly district, Anal. R. A. Howie.

HOWIE-20 Intermediate rock, Salem, Madras, Anal. J. H. Scoon.

HOWIE-21 Intermediate rock, Vercaud, Shevaroy Hills, Madras, Anal. H. S. Washington (1916), A.J.S., 41, p. 328.

HOWIE-22 Same locality, Anal. T. L. Walker (Holland, 1900, p. 151).

HOWIE-23 Hypersthene diorite of the charnockite series, Pallavaram, Madras Anal. J. H. Scoon.

HOWIE-24 Norite, Nagarmalai, Salem, Madras, Anal. R. A. Howie

HOWIE-25 Augite-Norite, North-East side of Magazine Hill, St. Thomas' Mount, Madras, Anal. H. S. Washington (1916, p. 328).

HOWIE-26 Same locality, Anal. T. L. Walker (Holland, 1900, p. 156).

HOWIE-27 "Norite", St. Thomas' Mount, Madras, Anal. C. Rajagopalan (1947) p. 238.

HOWIE-28 "Hypersthene Gabbro", same locality, Anal. C. Rajagopalan (1947) p. 238.

HOWIE-29 "Hornblende Norite", same locality, Anal. C. Rajagopalan (1947) p. 238.

HOWIE-30 Pyroxenite dyke, Pammal, Madras, Anal. J. H. Scoon.

HOWIE-31 Pyroxenite, Pammal Hill, Pallavasa, Madras, Anal. J. H. Scoon.

HOWIE-32 "Bahiaite", Pammal Hill, Madras, Anal. H. S. Washington (1916) p. 332.

HOWIE-33 Pyroxenite, Pallavaram, Madras, Anal. T. L. Walker, Holland (1900) p. 166.

HOWIE-34 Average of 46 pyroxenites (S. R. Nockolds, 1954, Bull. Geol. Soc. Am., 66, 1022).

R. A. Howie (1965) The Indian Mineralogist, 6, p. 67-76.

R.A.H.-1 Charnockite, Pangnirtung, east coast of Baffin Island, Northwest Territories, Canada. Anal. R. A. Howie.

R.A.H.-2 Enderbite, Dadanawa, South Savannas, Guyana, Anal. R. A. Howie

R.A.H.-3 Enderbitic charnockite, Musefu, Lulau, Congo, Anal. R. C. Tyler

R.A.H.-4 Intermediate charnockite, Bahia, Brazil, Anal. R. A. Howie

R.A.H.-5 Intermediate charnockite, Mt. Wati West Nile district, Uganda, Groves (1935) Anal. A. W. Groves.

CHEMICAL ANALYSIS. Q-1

SIO2	44.700
AL203	14.390
FE203	5.740
FEO	11.670
MGO	5.900
CAO	8.740
NA2O	2.150
K2O	1.370
TIO2	5.130
P2O5	0.0
MNO	0.200
ZRO2	0.0
CO2	0.0
SO3	0.0
CL2	0.0
F2	0.0
S	0.0
CR2O3	0.0
NIO	0.0
COO	0.0
BAO	0.0
SRO	0.0
LI2O	0.0
SUM	99.990
QUARTZ	0.450
NEPHELINE	0.375
KALSILITE	0.175
CLIVINE	0.021
PYROXENE	0.347
FELDSPAR	0.632

CIPW NORM
(WEIGHT PERCENT)

SALIC GROUP		
QUARTZ	0.0	0.0
CORUNDUM	0.0	(-) 6.382
ZIRCON	0.0	
ORTHOCLASE	8.103	0.308
ALBITE	18.171	0.692
ANORTHITE	25.528	
LEUCITE	0.0	
KALIOPHYLITE	0.0	
NEPHELINE	0.0	
THENARDITE	0.0	
SODIUM CARBONATE	0.0	
HALITE	0.0	
SUM	51.802	

FEMIC GROUP		(-C)
ACMITE	0.0	0.0
SODIUM METASILICATE	0.0	0.0
POTASSIUM METASILICATE	0.0	0.0
DIOPSIDE	14.505	6.382
WOLLASTONITE	0.0	0.0
HYPERSTHENE	13.891	
OLIVINE	1.725	
CALCIUM ORTHOSILICATE	0.0	0.0
MAGNETITE	8.323	
HEMATITE	0.0	
ILMENITE	9.747	
SPHENE	0.0	
PEROVSKITE	0.0	
RUTILE	0.0	
APATITE	0.0	
FLUORITE	0.0	
PYRITE	0.0	
CALCITE	0.0	
CHROMITE	0.0	
SUM	48.191	

OXIDATION RATIO MOL(2FE203/2FE203+FEO) X100= 30.684

RATIO MGO/FEO IN HYPERSTHENE DIOPSIDE AND CLIVINE = 2.2727E 00

DIFFERENTIATION INDEX = 26.274

CHEMICAL ANALYSIS, Q-2

SIO2	45.090
AL2O3	16.650
FE2O3	6.060
FEO	8.990
MGO	7.250
CAO	9.520
NA2O	2.770
K2O	0.950
TIO2	2.400
P2O5	0.0
MNO	0.310
ZRO2	0.0
CO2	0.0
SO3	0.0
CL2	0.0
F2	0.0
S	0.0
CR2O3	0.0
NIO	0.0
COO	0.0
BAO	0.0
SRO	0.0
LI2O	0.0
SUM	99.990
QUARTZ	0.444
NEPHELINE	0.444
KALSILITE	0.112
CLIVINE	0.164
PYROXENE	0.160
FELDSPAR	0.676

CIPW NORM
(WEIGHT PERCENT)

SALIC GROUP		
QUARTZ	0.0	0.0
CORUNDUM	0.0	(-) 6.069
ZIRCON	0.0	
ORTHOCLASE	5.619	0.201
ALBITE	22.398	0.799
ANORTHITE	30.149	
LEUCITE	0.0	
KALIOPHYLITE	0.0	
NEPHELINE	0.549	
THENARDITE	0.0	
SODIUM CARBONATE	0.0	
HALITE	0.0	
SUM	58.716	

FEMIC GROUP		(-C)
ACMITE	0.0	0.0
SODIUM METASILICATE	0.0	0.0
POTASSIUM METASILICATE	0.0	0.0
DIOPSIDE	13.793	6.069
WOLLASTONITE	0.0	0.0
HYPERSTHENE	0.0	
OLIVINE	14.139	
CALCIUM ORTHOSILICATE	0.0	0.0
MAGNETITE	8.787	
HEMATITE	0.0	
ILMENITE	4.560	
SPHENE	0.0	
PEROVSKITE	0.0	
RUTILE	0.0	
APATITE	0.0	
FLUORITE	0.0	
PYRITE	0.0	
CALCITE	0.0	
CHROMITE	0.0	
SUM	41.278	

OXIDATION RATIO MOL(2FE2O3/2FE2O3+FEO) X100= 37.760

RATIO MGO/FEO IN HYPERSTHENE DIOPSIDE AND CLIVINE = 2.9543E 00

DIFFERENTIATION INDEX = 28.566

CHEMICAL ANALYSIS, Q-3

SIO2	50.220
AL2O3	11.690
FE2O3	2.640
FEO	15.820
MGO	5.600
CAO	7.920
NA2O	3.090
K2O	0.890
TIO2	1.940
P2O5	0.200
MNO	0.0
ZRO2	0.0
CO2	0.0
SO3	0.0
CL2	0.0
F2	0.0
S	0.0
CR2O3	0.0
NIO	0.0
COO	0.0
BAO	0.0
SRO	0.0
LI2O	0.0
SUM	100.010
QUARTZ	0.454
NEPHELINE	0.451
KALSILITE	0.095
OLIVINE	0.066
PYROXENE	0.428
FELDSPAR	0.507

CIPW NORM
(WEIGHT PERCENT)

SALIC GROUP		
QUARTZ	0.0	0.0
CORUNDUM	0.0	(-) 8.866
ZIRCON	0.0	
ORTHOCLASE	5.264	0.168
ALBITE	26.115	0.832
ANORTHITE	15.374	
LEUCITE	0.0	
KALIOPHYLITE	0.0	
NEPHELINE	0.0	
THENARDITE	0.0	
SODIUM CARBONATE	0.0	
HALITE	0.0	
SUM 46.753		
FEMIC GROUP		(-C)
ACMITE	0.0	0.0
SODIUM METASILICATE	0.0	0.0
POTASSIUM METASILICATE	0.0	0.0
DIOPSIDE	20.150	8.866
WOLLASTONITE	0.0	0.0
HYPERSTHENE	19.316	
OLIVINE	6.076	
CALCIUM ORTHOSILICATE	0.0	0.0
MAGNETITE	3.828	
HEMATITE	0.0	
ILMENITE	3.686	
SPHENE	0.0	
PEROVSKITE	0.0	
RUTILE	0.0	
APATITE	0.0	
FLUORITE	0.0	
PYRITE	0.0	
CALCITE	0.0	
CHROMITE	0.0	
SUM	53.057	

OXIDATION RATIO MOL(2FE2O3/2FE2O3+FEO) X100= 13.058

RATIO MGO/FEO IN HYPERSTHENE DIOPSIDE AND CLIVINE = 7.8224E-01

DIFFERENTIATION INDEX = 31.380

CHEMICAL ANALYSIS, Q-4

		CIPW NORM (WEIGHT PERCENT)		
SIO2	47.250			
AL2O3	15.670	SALIC GROUP		
FE2O3	1.300	QUARTZ	0.0	0.0
FEO	10.330	CORUNDUM	0.0	(-)12.107
MGO	8.930	ZIRCON	0.0	
CAO	13.820	ORTHOCLASE	0.0	0.0
NA2O	1.710	ALBITE	14.452	1.000
K2O	0.070	ANORTHITE	35.041	
TIO2	0.690	LEUCITE	0.0	
P2O5	0.070	KALIOPHYLITE	0.0	
MNO	0.150	NEPHELINE	0.0	
ZRO2	0.0	THENARDITE	0.0	
CO2	0.0	SODIUM CARBONATE	0.0	
SO3	0.0	HALITE	0.0	
CL2	0.0	SUM 49.493		
F2	0.0			
S	0.0			
CR2O3	0.0			
NIO	0.0	FEMIC GROUP		(-C)
COO	0.0	ACMITE	0.0	0.0
BAO	0.0	SODIUM METASILICATE	0.0	0.0
SRO	0.010	POTASSIUM METASILICATE	0.0	0.0
LI2O	0.0	DIOPSIDE	27.515	12.107
		WOLLASTONITE	0.0	0.0
SUM	100.000	HYPERSTHENE	2.821	
		OLIVINE	16.832	
QUARTZ	0.458	CALCIUM ORTHOSILICATE	0.0	0.0
NEPHELINE	0.542	MAGNETITE	1.885	
KALSILITE	0.0	HEMATITE	0.0	
		ILMENITE	1.311	
		SPHENE	0.0	
OLIVINE	0.174	PEROVSKITE	0.0	
PYROXENE	0.314	RUTILE	0.0	
FELDSPAR	0.512	APATITE	0.0	
		FLUORITE	0.0	
		PYRITE	0.0	
		CALCITE	0.0	
		CHROMITE	0.0	
		SUM	50.364	

OXIDATION RATIO MOL(2FE2O3/2FE2O3+FEO) X100= 10.174

RATIO MGO/FEO IN HYPERSTHENE DIOPSIDE AND OLIVINE = 1.7328E 00

DIFFERENTIATION INDEX = 14.452

CHEMICAL ANALYSIS, Q-5

		CIPW NORM (WEIGHT PERCENT)		
SIO2	50.950			
AL2O3	19.630			
FE2O3	5.070			
FEO	6.340	SALIC GROUP		
MGO	2.630	QUARTZ	0.762	0.017
CAO	7.480	CORUNDUM	0.0 (-)	0.933
NA2O	3.380	ZIRCON	0.0	
K2O	2.630	ORTHOCLASE	15.556	0.347
TIO2	0.940	ALBITE	28.566	0.636
P2O5	0.680	ANORTHITE	30.568	
MNO	0.140	LEUCITE	0.0	
ZRO2	0.0	KALICPHYLITE	0.0	
CO2	0.0	NEPHELINE	0.0	
SO3	0.0	THENARDITE	0.0	
CL2	0.0	SODIUM CARBONATE	0.0	
F2	0.0	HALITE	0.0	
S	0.0	SUM 75.452		
CR2O3	0.130			
NIO	0.0			
COO	0.0			
BAO	0.0	FEMIC GROUP		(-C)
SRO	0.0	ACMITE	0.0	0.0
LI2O	0.0	SODIUM METASILICATE	0.0	0.0
		POTASSIUM METASILICATE	0.0	0.0
SUM	100.000	DIOPSIDE	2.121	0.933
		WOLLASTONITE	0.0	0.0
QUARTZ	0.458	HYPERSTHENE	11.677	
NEPHELINE	0.345	OLIVINE	0.0	
KALSILITE	0.197	CALCIUM ORTHOSILICATE	0.0	0.0
		MAGNETITE	7.351	
		HEMATITE	0.0	
OLIVINE	0.0	ILMENITE	1.786	
PYROXENE	0.156	SPHENE	0.0	
FELDSPAR	0.844	PEROVSKITE	0.0	
		RUTILE	0.0	
		APATITE	1.485	
		FLUORITE	0.0	
		PYRITE	0.0	
		CALCITE	0.0	
		CHROMITE	0.0	
		SUM	24.420	

OXIDATION RATIO MOL(2FE2O3/2FE2O3+FEO) X100= 41.851

RATIO MGO/FEO IN HYPERSTHENE DIOPSIDE AND OLIVINE = 1.4113E 00

DIFFERENTIATION INDEX = 44.884

CHEMICAL ANALYSIS, Q-6

SIO2	54.550
AL2O3	16.150
FE2O3	2.790
FEO	6.230
MGO	1.600
CAO	5.880
NA2O	4.230
K2O	3.760
TIO2	2.480
P2O5	1.870
MNO	0.270
ZRO2	0.0
CO2	0.0
SO3	0.0
CL2	0.0
F2	0.0
S	0.0
CR2O3	0.0
NIO	0.0
COO	0.0
BAO	0.0
SRO	0.190
LI2O	0.0
SUM	100.000
QUARTZ	0.481
NEPHELINE	0.314
KALSILITE	0.205
CLIVINE	0.0
PYROXENE	0.138
FELDSPAR	0.862

CIPW NORM
(WEIGHT PERCENT)

SALIC GROUP		
QUARTZ	3.629	0.059
CORUNDUM	0.0	(-) 1.761
ZIRCON	0.0	
ORTHOCLASE	22.240	0.361
ALBITE	35.750	0.580
ANORTHITE	13.930	
LEUCITE	0.0	
KALIOPHYLITE	0.0	
NEPHELINE	0.0	
THENARDITE	0.0	
SODIUM CARBONATE	0.0	
HALITE	0.0	
SUM	75.549	

FEMIC GROUP		(-C)
ACMITE	0.0	0.0
SODIUM METASILICATE	0.0	0.0
POTASSIUM METASILICATE	0.0	0.0
DIOPSIDE	4.002	1.761
WOLLASTONITE	0.0	0.0
HYPERSTHENE	7.526	
OLIVINE	0.0	
CALCIUM ORTHOSILICATE	0.0	0.0
MAGNETITE	4.045	
HEMATITE	0.0	
ILMENITE	4.712	
SPHENE	0.0	
PEROVSKITE	0.0	
RUTILE	0.0	
APATITE	4.082	
FLUORITE	0.0	
PYRITE	0.0	
CALCITE	0.0	
CHROMITE	0.0	
SUM	24.367	

OXIDATION RATIO MOL(2FE2O3/2FE2O3+FEO) X100= 28.727

RATIO MGO/FEO IN HYPERSTHENE DIOPSIDE AND CLIVINE = 9.5481E-01

DIFFERENTIATION INDEX = 61.619

CHEMICAL ANALYSIS, Q-7

		CIPW NORM (WEIGHT PERCENT)		
SIO2	60.540			
AL2O3	16.750			
FE2O3	2.210	SALIC GROUP		
FEO	4.820	QUARTZ	7.017	0.097
MGO	0.820	CORUNDUM	0.0	(-) 1.187
CAO	3.780	ZIRCON	0.0	
NA2O	4.760	ORTHOCLASE	25.316	0.349
K2O	4.280	ALBITE	40.230	0.554
TIO2	0.960	ANORTHITE	11.651	
P2O5	0.770	LEUCITE	0.0	
MNO	0.100	KALIOPHYLITE	0.0	
ZRO2	0.0	NEPHELINE	0.0	
CO2	0.0	THENARDITE	0.0	
SO3	0.0	SODIUM CARBONATE	0.0	
CL2	0.0	HALITE	0.0	
F2	0.0	SUM 84.213		
S	0.0			
CR2O3	0.0			
NIO	0.0			
COO	0.0	FEMIC GROUP		(-C)
BAO	0.0	ACMITE	0.0	0.0
SRO	0.210	SODIUM METASILICATE	0.0	0.0
LI2O	0.0	POTASSIUM METASILICATE	0.0	0.0
		DIOPSIDE	2.697	1.187
SUM	100.000	WOLLASTONITE	0.0	0.0
		HYPERSTHENE	6.285	
QUARTZ	0.501	OLIVINE	0.0	
NEPHELINE	0.300	CALCIUM ORTHOSILICATE	0.0	0.0
KALSILITE	0.198	MAGNETITE	3.204	
		HEMATITE	0.0	
		ILMENITE	1.824	
OLIVINE	0.0	SPHENE	0.0	
PYROXENE	0.104	PEROVSKITE	0.0	
FELDSPAR	0.896	RUTILE	0.0	
		APATITE	1.681	
		FLUORITE	0.0	
		PYRITE	0.0	
		CALCITE	0.0	
		CHROMITE	0.0	
		SUM	15.692	

OXIDATION RATIO MOL(2FE2O3/2FE2O3+FEO) X100= 29.211

RATIO MGO/FEO IN HYPERSTHENE DIOPSIDE AND OLIVINE = 4.8190E-01

DIFFERENTIATION INDEX = 72.563

CHEMICAL ANALYSIS, Q-8

		CIPW NORM (WEIGHT PERCENT)		
SIO2	62.170			
AL2O3	17.650			
FE2O3	1.250			
FEO	4.050	SALIC GROUP		
MGO	1.880	QUARTZ	11.876	0.185
CAO	5.030	CORUNDUM	0.0 (-)	1.481
NA2O	4.020	ZIRCON	0.0	
K2O	3.100	ORTHOCLASE	18.336	0.286
TIO2	0.800	ALBITE	33.975	0.529
P2O5	0.0	ANORTHITE	20.912	
MNO	0.060	LEUCITE	0.0	
ZRO2	0.0	KALICPHYLITE	0.0	
CO2	0.0	NEPHELINE	0.0	
SO3	0.0	THENARDITE	0.0	
CL2	0.0	SODIUM CARBONATE	0.0	
F2	0.0	HALITE	0.0	
S	0.0	SUM 85.099		
CR2O3	0.0			
NIO	0.0			
COO	0.0			
BAO	0.0	FEMIC GROUP		(-C)
SRO	0.0	ACMITE	0.0	0.0
LI2O	0.0	SODIUM METASILICATE	0.0	0.0
		POTASSIUM METASILICATE	0.0	0.0
SUM	100.010	DIOPSIDE	3.366	1.481
		WOLLASTONITE	0.0	0.0
QUARTZ	0.551	HYPERSTHENE	8.213	
NEPHELINE	0.287	OLIVINE	0.0	
KALSILITE	0.162	CALCIUM ORTHOSILICATE	0.0	0.0
		MAGNETITE	1.812	
		HEMATITE	0.0	
OLIVINE	0.0	ILMENITE	1.520	
PYROXENE	0.137	SPHENE	0.0	
FELDSPAR	0.863	PEROVSKITE	0.0	
		RUTILE	0.0	
		APATITE	0.0	
		FLUORITE	0.0	
		PYRITE	0.0	
		CALCITE	0.0	
		CHROMITE	0.0	
		SUM	14.911	

OXIDATION RATIO MOL(2FE2O3/2FE2O3+FEO) X100= 21.739

RATIO MGO/FEO IN HYPERSTHENE DIOPSIDE AND OLIVINE = 1.1965E 00

DIFFERENTIATION INDEX = 64.188

CHEMICAL ANALYSIS, Q-9

SIO2	62.380
AL2O3	18.590
FE2O3	1.660
FEO	1.510
MGO	0.870
CAO	2.050
NA2O	4.510
K2O	7.730
TIO2	0.600
P2O5	0.0
MNO	0.080
ZRO2	0.0
CO2	0.0
SO3	0.0
CL2	0.0
F2	0.0
S	0.0
CR2O3	0.0
NIO	0.0
COO	0.0
BAO	0.0
SRO	0.0
LI2O	0.0
SUM	99.980
QUARTZ	0.452
NEPHELINE	0.243
KALSILITE	0.305
OLIVINE	0.0
PYROXENE	0.040
FELDSPAR	0.960

CIPW NORM
(WEIGHT PERCENT)

SALIC GROUP

QUARTZ	1.197	0.014
CORUNDUM	0.0	(-) 0.908
ZIRCON	0.0	
ORTHOCLASE	45.722	0.538
ALBITE	38.117	0.448
ANORTHITE	7.584	
LEUCITE	0.0	
KALIOPHYLITE	0.0	
NEPHELINE	0.0	
THENARDITE	0.0	
SODIUM CARBONATE	0.0	
HALITE	0.0	
SUM	92.619	

FEMIC GROUP

		(-C)
ACMITE	0.0	0.0
SODIUM METASILICATE	0.0	0.0
POTASSIUM METASILICATE	0.0	0.0
DIOPSIDE	2.063	0.908
WOLLASTONITE	0.0	0.0
HYPERSTHENE	1.751	
OLIVINE	0.0	
CALCIUM ORTHOSILICATE	0.0	0.0
MAGNETITE	2.407	
HEMATITE	0.0	
ILMENITE	1.140	
SPHENE	0.0	
PEROVSKITE	0.0	
RUTILE	0.0	
APATITE	0.0	
FLUORITE	0.0	
PYRITE	0.0	
CALCITE	0.0	
CHROMITE	0.0	
SUM	7.362	

OXICATION RATIO MOL(2FE2O3/2FE2O3+FEO) X100= 49.734

RATIO MGO/FEO IN HYPERSTHENE DIOPSIDE AND OLIVINE = 5.1492E 00

DIFFERENTIATION INDEX = 85.036

CHEMICAL ANALYSIS, Q-10

SIO2	51.780
AL2O3	20.030
FE2O3	7.080
FEO	3.610
MGO	3.050
CAO	10.480
NA2O	1.810
K2O	0.500
TIO2	1.000
P2O5	0.500
MNO	0.160
ZRO2	0.0
CO2	0.0
SO3	0.0
CL2	0.0
F2	0.0
S	0.0
CR2O3	0.0
NIO	0.0
COO	0.0
BAO	0.0
SRO	0.0
LI2O	0.0
SUM	100.000
QUARTZ	0.695
NEPHELINE	0.253
KALSILITE	0.051
OLIVINE	0.0
PYROXENE	0.129
FELDSPAR	0.871

CIPW NORM
(WEIGHT PERCENT)

SALIC GROUP		
QUARTZ	14.474	0.442
CORUNDUM	0.0	(-) 1.399
ZIRCON	0.0	
ORTHOCLASE	2.957	0.090
ALBITE	15.297	0.467
ANORTHITE	44.997	
LEUCITE	0.0	
KALIOPHYLITE	0.0	
NEPHELINE	0.0	
THENARDITE	0.0	
SODIUM CARBONATE	0.0	
HALITE	0.0	
SUM	77.726	

FEMIC GROUP		(-C)
ACMITE	0.0	0.0
SODIUM METASILICATE	0.0	0.0
POTASSIUM METASILICATE	0.0	0.0
DIOPSIDE	3.179	1.399
WOLLASTONITE	0.0	0.0
HYPERSTHENE	6.153	
OLIVINE	0.0	
CALCIUM ORTHOSILICATE	0.0	0.0
MAGNETITE	9.255	
HEMATITE	0.697	
ILMENITE	1.900	
SPHENE	0.0	
PEROVSKITE	0.0	
RUTILE	0.0	
APATITE	1.092	
FLUORITE	0.0	
PYRITE	0.0	
CALCITE	0.0	
CHROMITE	0.0	
SUM	22.276	

OXIDATION RATIO MOL(2FE2O3/2FE2O3+FEO) X100= 63.835

NO IRON IN HYPERSTHENE DIOPSIDE AND OLIVINE

DIFFERENTIATION INDEX = 32.729

CHEMICAL ANALYSIS, Q-11

SIO2	73.930
AL2O3	13.620
FE2O3	0.600
FEO	1.120
MGO	0.140
CAO	1.040
NA2O	2.440
K2O	6.890
TIO2	0.200
P2O5	0.0
MNO	0.020
ZRO2	0.0
CO2	0.0
SO3	0.0
CL2	0.0
F2	0.0
S	0.0
CR2O3	0.0
NIO	0.0
COO	0.0
BAO	0.0
SRO	0.0
LI2O	0.0
SUM	100.000
QUARTZ	0.626
NEPHELINE	0.122
KALSILITE	0.252
OLIVINE	0.0
PYROXENE	0.024
FELDSPAR	0.976

CIPW NORM
(WEIGHT PERCENT)

SALIC GROUP		
QUARTZ	30.361	0.331
CORUNDUM	0.235	(-) 0.0
ZIRCON	0.0	
ORTHOCLASE	40.754	0.444
ALBITE	20.622	0.225
ANORTHITE	5.163	
LEUCITE	0.0	
KALIOPHYLITE	0.0	
NEPHELINE	0.0	
THENARDITE	0.0	
SODIUM CARBONATE	0.0	
HALITE	0.0	
SUM	97.135	

FEMIC GROUP		(-C)
ACMITE	0.0	0.0
SODIUM METASILICATE	0.0	0.0
POTASSIUM METASILICATE	0.0	0.0
DIOPSIDE	0.0	0.0
WOLLASTONITE	0.0	0.0
HYPERSTHENE	1.616	
OLIVINE	0.0	
CALCIUM ORTHOSILICATE	0.0	0.0
MAGNETITE	0.870	
HEMATITE	0.0	
ILMENITE	0.380	
SPHENE	0.0	
PEROVSKITE	0.0	
RUTILE	0.0	
APATITE	0.0	
FLUORITE	0.0	
PYRITE	0.0	
CALCITE	0.0	
CHROMITE	0.0	
SUM	2.866	

OXIDATION RATIO MOL(2FE2O3/2FE2O3+FEO) X100= 32.530

RATIO MGO/FEO IN HYPERSTHENE DIOPSIDE AND CLIVINE = 3.6507E-01

DIFFERENTIATION INDEX = 91.737

CHEMICAL ANALYSIS, Q-12

SIO2	72.840
AL2O3	14.560
FE2O3	1.250
FEO	0.670
MGO	0.330
CAO	1.790
NA2O	3.410
K2O	4.960
TIO2	0.160
P2O5	0.0
MNO	0.020
ZRO2	0.0
CO2	0.0
SO3	0.0
CL2	0.0
F2	0.0
S	0.0
CR2O3	0.0
NIO	0.0
CGO	0.0
BAO	0.0
SRO	0.0
LI2O	0.0
SUM	99.990
QUARTZ	0.632
NEPHELINE	0.178
KALSILITE	0.190
OLIVINE	0.0
PYROXENE	0.016
FELDSPAR	0.984

CIPW NORM
(WEIGHT PERCENT)

SALIC GROUP		
QUARTZ	29.607	0.337
CORUNDUM	0.308	(-) 0.0
ZIRCON	0.0	
ORTHOCLASE	29.338	0.334
ALBITE	28.820	0.328
ANORTHITE	8.886	
LEUCITE	0.0	
KALIOPHYLITE	0.0	
NEPHELINE	0.0	
THENARDITE	0.0	
SODIUM CARBONATE	0.0	
HALITE	0.0	
SUM	96.958	

FEMIC GROUP		(-C)
ACMITE	0.0	0.0
SODIUM METASILICATE	0.0	0.0
POTASSIUM METASILICATE	0.0	0.0
DIOPSIDE	0.0	0.0
WOLLASTONITE	0.0	0.0
HYPERSTHENE	1.059	
OLIVINE	0.0	
CALCIUM ORTHOSILICATE	0.0	0.0
MAGNETITE	1.812	
HEMATITE	0.0	
ILMENITE	0.0	
SPHENE	0.0	
PEROVSKITE	0.0	
RUTILE	0.0	
APATITE	0.0	
FLUORITE	0.0	
PYRITE	0.0	
CALCITE	0.0	
CHROMITE	0.0	
SUM	2.872	

OXIDATION RATIO MOL(2FE2O3/2FE2O3+FEO) X100= 62.674

RATIO MGO/FEO IN HYPERSTHENE DIOPSIDE AND OLIVINE = 4.6486E 00

DIFFERENTIATION INDEX = 87.765

CHEMICAL ANALYSIS, Q-13

SIO2	68.250
AL2O3	15.190
FE2O3	1.480
FEO	1.690
MGO	0.730
CAO	2.400
NA2O	2.860
K2O	6.800
TIO2	0.300
P2O5	0.240
MNO	0.050
ZRO2	0.0
CO2	0.0
SO3	0.0
CL2	0.0
F2	0.0
S	0.0
CR2O3	0.0
NIO	0.0
COO	0.0
BAO	0.0
SRO	0.0
LI2O	0.0
SUM	99.990
QUARTZ	0.571
NEPHELINE	0.156
KALSILITE	0.273
OLIVINE	0.0
PYROXENE	0.061
FELDSPAR	0.939

CIPW NORM
(WEIGHT PERCENT)

SALIC GROUP		
QUARTZ	19.437	0.232
CORUNDUM	0.0	(-) 1.245
ZIRCON	0.0	
ORTHOCLASE	40.221	0.480
ALBITE	24.172	0.288
ANORTHITE	8.466	
LEUCITE	0.0	
KALIOPHYLITE	0.0	
NEPHELINE	0.0	
THENARDITE	0.0	
SODIUM CARBONATE	0.0	
HALITE	0.0	
SUM 92.295		

FEMIC GROUP		(-C)
ACMITE	0.0	0.0
SODIUM METASILICATE	0.0	0.0
POTASSIUM METASILICATE	0.0	0.0
DIOPSIDE	2.830	1.245
WOLLASTONITE	0.0	0.0
HYPERSTHENE	1.909	
OLIVINE	0.0	
CALCIUM ORTHOSILICATE	0.0	0.0
MAGNETITE	2.146	
HEMATITE	0.0	
ILMENITE	0.570	
SPHENE	0.0	
PEROVSKITE	0.0	
RUTILE	0.0	
APATITE	0.0	
FLUORITE	0.0	
PYRITE	0.0	
CALCITE	0.0	
CHROMITE	0.0	
SUM	7.455	

OXIDATION RATIO MOL(2FE2O3/2FE2O3+FEO) X100= 44.077

RATIO MGO/FEO IN HYPERSTHENE DIOPSIDE AND OLIVINE = 1.6329E 00

DIFFERENTIATION INDEX = 83.830

CHEMICAL ANALYSIS, Q-14

SIO2	68.570
AL2O3	15.030
FE2O3	0.990
FEO	2.250
MGO	1.130
CAO	2.580
NA2O	3.040
K2O	5.870
TIO2	0.300
P2O5	0.240
MNO	0.100
ZRO2	0.0
CO2	0.0
SO3	0.0
CL2	0.0
F2	0.0
S	0.0
CR2O3	0.0
NIO	0.0
COO	0.0
BAO	0.0
SRO	0.0
LI2O	0.0
SUM	100.100
QUARTZ	0.584
NEPHELINE	0.172
KALSILITE	0.244
CLIVINE	0.0
PYROXENE	0.091
FELDSPAR	0.909

CIPW NORM
(WEIGHT PERCENT)

SALIC GROUP		
QUARTZ	20.463	0.253
CORUNDUM	0.0	(-) 1.033
ZIRCON	0.0	
ORTHOCLASE	34.720	0.429
ALBITE	25.693	0.318
ANORTHITE	9.973	
LEUCITE	0.0	
KALIOPHYLITE	0.0	
NEPHELINE	0.0	
THENARDITE	0.0	
SODIUM CARBONATE	0.0	
HALITE	0.0	
SUM	90.849	

FEMIC GROUP		(-C)
ACMITE	0.0	0.0
SODIUM METASILICATE	0.0	0.0
POTASSIUM METASILICATE	0.0	0.0
DIOPSIDE	2.348	1.033
WOLLASTONITE	0.0	0.0
HYPERSTHENE	4.659	
OLIVINE	0.0	
CALCIUM ORTHOSILICATE	0.0	0.0
MAGNETITE	1.435	
HEMATITE	0.0	
ILMENITE	0.570	
SPHENE	0.0	
PEROVSKITE	0.0	
RUTILE	0.0	
APATITE	0.0	
FLUORITE	0.0	
PYRITE	0.0	
CALCITE	0.0	
CHROMITE	0.0	
SUM	9.013	

OXIDATION RATIO MOL(2FE2O3/2FE2O3+FEO) X100= 28.367

RATIO MGO/FEO IN HYPERSTHENE DIOPSIDE AND CLIVINE = 1.2433E 00

DIFFERENTIATION INDEX = 80.876

CHEMICAL ANALYSIS, Q-15

SIO2	46.450
AL2O3	16.050
FE2O3	7.650
FEO	6.770
MGO	6.310
CAO	8.590
NA2O	2.760
K2O	3.530
TIO2	1.500
P2O5	0.0
MNO	0.400
ZRO2	0.0
CO2	0.0
SO3	0.0
CL2	0.0
F2	0.0
S	0.0
CR2O3	0.0
NIO	0.0
COO	0.0
BAO	0.0
SRO	0.0
LI2O	0.0
SUM	100.010
QUARTZ	0.377
NEPHELINE	0.322
KALSILITE	0.302
CLIVINE	0.106
PYROXENE	0.216
FELDSPAR	0.678

CIPW NORM
(WEIGHT PERCENT)

SALIC GROUP		
QUARTZ	0.0	0.0
CORUNDUM	0.0	(-) 7.614
ZIRCON	0.0	
ORTHOCLASE	20.880	0.622
ALBITE	12.662	0.378
ANORTHITE	20.929	
LEUCITE	0.0	
KALIOPHYLITE	0.0	
NEPHELINE	5.780	
THENARDITE	0.0	
SODIUM CARBONATE	0.0	
HALITE	0.0	
SUM	60.251	
FEMIC GROUP		(-C)
ACMITE	0.0	0.0
SODIUM METASILICATE	0.0	0.0
POTASSIUM METASILICATE	0.0	0.0
DIOPSIDE	17.305	7.614
WOLLASTONITE	0.0	0.0
HYPERSTHENE	0.0	
OLIVINE	8.517	
CALCIUM ORTHOSILICATE	0.0	0.0
MAGNETITE	11.092	
HEMATITE	0.0	
ILMENITE	2.850	
SPHENE	0.0	
PEROVSKITE	0.0	
RUTILE	0.0	
APATITE	0.0	
FLUORITE	0.0	
PYRITE	0.0	
CALCITE	0.0	
CHROMITE	0.0	
SUM	39.765	

OXIDATION RATIO MOL(2FE2O3/2FE2O3+FEO) X100= 50.421

RATIO MGO/FEO IN HYPERSTHENE DIOPSIDE AND OLIVINE = 4.7660E 00

DIFFERENTIATION INDEX = 39.322

CHEMICAL ANALYSIS, Q-16

SIO2	46.650
AL2O3	13.780
FE2O3	3.370
FEO	12.900
MGO	6.910
CAO	10.640
NA2O	0.690
K2O	2.500
TIO2	2.420
P2O5	0.0
MNO	0.140
ZRO2	0.0
CO2	0.0
SO3	0.0
CL2	0.0
F2	0.0
S	0.0
CR2O3	0.0
NIO	0.0
COO	0.0
BAO	0.0
SRO	0.0
LI2O	0.0
SUM	100.000
QUARTZ	0.439
NEPHELINE	0.153
KALSILITE	0.407
CLIVINE	0.072
PYROXENE	0.401
FELDSPAR	0.527

CIPW NORM
(WEIGHT PERCENT)

SALIC GROUP		
QUARTZ	0.0	0.0
CORUNDUM	0.0	(-) 9.363
ZIRCON	0.0	
ORTHOCLASE	14.787	0.717
ALBITE	5.832	0.283
ANORTHITE	27.070	
LEUCITE	0.0	
KALIOPHYLITE	0.0	
NEPHELINE	0.0	
THENARDITE	0.0	
SODIUM CARBONATE	0.0	
HALITE	0.0	
SUM	47.689	

FEMIC GROUP		(-C)
ACMITE	0.0	0.0
SODIUM METASILICATE	0.0	0.0
POTASSIUM METASILICATE	0.0	0.0
DIOPSIDE	21.279	9.363
WOLLASTONITE	0.0	0.0
HYPERSTHENE	15.053	
OLIVINE	6.497	
CALCIUM ORTHOSILICATE	0.0	0.0
MAGNETITE	4.886	
HEMATITE	0.0	
ILMENITE	4.598	
SPHENE	0.0	
PEROVSKITE	0.0	
RUTILE	0.0	
APATITE	0.0	
FLUORITE	0.0	
PYRITE	0.0	
CALCITE	0.0	
CHROMITE	0.0	
SUM	52.313	

OXIDATION RATIO MOL(2FE2O3/2FE2O3+FEO) X100= 19.036

RATIO MGO/FEO IN HYPERSTHENE DIOPSIDE AND CLIVINE = 1.3306E 00

DIFFERENTIATION INDEX = 20.619

CHEMICAL ANALYSIS, HOWI -1

SIO2	77.530
AL203	9.840
FE203	0.410
FEO	3.340
MGO	1.210
CAO	1.140
NA20	1.940
K20	3.880
TIO2	0.560
P205	0.110
MNO	0.030
ZRO2	0.0
CO2	0.0
SO3	0.0
CL2	0.0
F2	0.0
S	0.0
CR203	0.0
NIO	0.0
COO	0.0
BAO	0.0
SRO	0.0
LI20	0.0
SUM	99.990
QUARTZ	0.740
NEPHELINE	0.105
KALSILITE	0.155
OLIVINE	0.0
PYROXENE	0.150
FELDSPAR	0.850

CIPW NORM
(WEIGHT PERCENT)

SALIC GROUP			
QUARTZ	44.913		0.533
CORUNDUM	0.362	(-)	0.0
ZIRCON	0.0		
ORTHOCLASE	22.950		0.272
ALBITE	16.396		0.195
ANORTHITE	5.659		
LEUCITE	0.0		
KALIOPHYLITE	0.0		
NEPHELINE	0.0		
THENARDITE	0.0		
SODIUM CARBONATE	0.0		
HALITE	0.0		
SUM	90.280		

FEMIC GROUP		(-C)
ACMITE	0.0	0.0
SODIUM METASILICATE	0.0	0.0
POTASSIUM METASILICATE	0.0	0.0
DIOPSIDE	0.0	0.0
WOLLASTONITE	0.0	0.0
HYPERSTHENE	7.942	
OLIVINE	0.0	
CALCIUM ORTHOSILICATE	0.0	0.0
MAGNETITE	0.594	
HEMATITE	0.0	
ILMENITE	1.064	
SPHENE	0.0	
PEROVSKITE	0.0	
RUTILE	0.0	
APATITE	0.0	
FLUORITE	0.0	
PYRITE	0.0	
CALCITE	0.0	
CHROMITE	0.0	
SUM	9.600	

OXIDATION RATIO MOL(2FE203/2FE203+FEO) X100= 9.949

RATIO MGO/FEO IN HYPERSTHENE DIOPSIDE AND OLIVINE = 8.1210E-01

DIFFERENTIATION INDEX = 84.259

CHEMICAL ANALYSIS, HOWI -2

SIO2	72.560
AL2O3	13.410
FE2O3	1.300
FEO	2.320
MGO	0.580
CAO	2.120
NA2O	2.800
K2O	4.270
TIO2	0.400
P2O5	0.140
MNO	0.040
ZRO2	0.0
CO2	0.0
SO3	0.0
CL2	0.0
F2	0.0
S	0.0
CR2O3	0.0
NIO	0.0
COO	0.0
BAO	0.0
SRO	0.0
LI2O	0.0
SUM	99.940
QUARTZ	0.670
NEPHELINE	0.156
KALSILITE	0.174
OLIVINE	0.0
PYROXENE	0.064
FELDSPAR	0.936

CIPW NORM
(WEIGHT PERCENT)

SALIC GROUP		
QUARTZ	33.356	0.405
CORUNDUM	0.309	(-) 0.0
ZIRCON	0.0	
ORTHOCLASE	25.257	0.307
ALBITE	23.665	0.288
ANORTHITE	10.524	
LEUCITE	0.0	
KALIOPHYLITE	0.0	
NEPHELINE	0.0	
THENARDITE	0.0	
SODIUM CARBONATE	0.0	
HALITE	0.0	
SUM 93.110		

FEMIC GROUP		(-C)
ACMITE	0.0	0.0
SODIUM METASILICATE	0.0	0.0
POTASSIUM METASILICATE	0.0	0.0
DIOPSIDE	0.0	0.0
WOLLASTONITE	0.0	0.0
HYPERSTHENE	4.045	
OLIVINE	0.0	
CALCIUM ORTHOSILICATE	0.0	0.0
MAGNETITE	1.885	
HEMATITE	0.0	
ILMENITE	0.760	
SPHENE	0.0	
PEROVSKITE	0.0	
RUTILE	0.0	
APATITE	0.0	
FLUORITE	0.0	
PYRITE	0.0	
CALCITE	0.0	
CHROMITE	0.0	
SUM	6.690	

OXIDATION RATIO MOL(2FE2O3/2FE2O3+FEO) X100= 33.524

RATIO MGO/FEO IN HYPERSTHENE DIOPSIDE AND OLIVINE = 7.3752E-01

DIFFERENTIATION INDEX = 82.277

CHEMICAL ANALYSIS, HOWI -3

SIO2	71.170
AL203	15.200
FE203	0.810
FEO	1.540
MGO	0.530
CAO	2.680
NA2O	3.010
K2O	4.720
TIO2	0.460
P2O5	0.080
MNO	0.020
ZRO2	0.0
CO2	0.0
SO3	0.0
CL2	0.0
F2	0.0
S	0.0
CR2O3	0.0
NIO	0.0
COO	0.0
BAO	0.0
SRO	0.0
LI2O	0.0
SUM	100.220
QUARTZ	0.638
NEPHELINE	0.169
KALSILITE	0.194
OLIVINE	0.0
PYROXENE	0.040
FELDSPAR	0.960

CIPW NORM
(WEIGHT PERCENT)

SALIC GROUP		
QUARTZ	28.427	0.348
CORUNDUM	0.245	(-) 0.0
ZIRCON	0.0	
ORTHOCLASE	27.918	0.341
ALBITE	25.439	0.311
ANORTHITE	13.304	
LEUCITE	0.0	
KALIOPHYLITE	0.0	
NEPHELINE	0.0	
THENARDITE	0.0	
SODIUM CARBONATE	0.0	
HALITE	0.0	
SUM 95.333		

FEMIC GROUP		(-C)
ACMITE	0.0	0.0
SODIUM METASILICATE	0.0	0.0
POTASSIUM METASILICATE	0.0	0.0
DIOPSIDE	0.0	0.0
WOLLASTONITE	0.0	0.0
HYPERSTHENE	2.758	
OLIVINE	0.0	
CALCIUM ORTHOSILICATE	0.0	0.0
MAGNETITE	1.174	
HEMATITE	0.0	
ILMENITE	0.874	
SPHENE	0.0	
PEROVSKITE	0.0	
RUTILE	0.0	
APATITE	0.0	
FLUORITE	0.0	
PYRITE	0.0	
CALCITE	0.0	
CHROMITE	0.0	
SUM	4.807	

OXIDATION RATIO MOL(2FE203/2FE203+FEO) X100= 32.129

RATIO MGO/FEO IN HYPERSTHENE DIOPSIDE AND OLIVINE = 1.2203E 00

DIFFERENTIATION INDEX = 81.784

CHEMICAL ANALYSIS, HOWI -4

SIO2	77.280
AL2O3	10.970
FE2O3	1.040
FEO	2.020
MGO	0.430
CAO	1.020
NA2O	2.850
K2O	4.130
TIO2	0.260
P2O5	0.0
MNO	0.0
ZRO2	0.0
CO2	0.0
SO3	0.0
CL2	0.0
F2	0.0
S	0.0
CR2O3	0.0
NIO	0.0
COO	0.0
BAO	0.0
SRO	0.0
LI2O	0.0
SUM	100.000
QUARTZ	0.699
NEPHELINE	0.146
KALSILITE	0.155
OLIVINE	0.0
PYROXENE	0.061
FELDSPAR	0.939

CIPW NORM
(WEIGHT PERCENT)

SALIC GROUP		
QUARTZ	41.054	0.458
CORUNDUM	0.0	(-) 0.0
ZIRCON	0.0	
ORTHOCLASE	24.428	0.273
ALBITE	24.087	0.269
ANORTHITE	4.905	
LEUCITE	0.0	
KALIOPHYLITE	0.0	
NEPHELINE	0.0	
THENARDITE	0.0	
SODIUM CARBONATE	0.0	
HALITE	0.0	
SUM 94.475		
FEMIC GROUP		(-C)
ACMITE	0.0	0.0
SODIUM METASILICATE	0.0	0.0
POTASSIUM METASILICATE	0.0	0.0
DIOPSIDE	0.0	0.0
WOLLASTONITE	0.0	0.0
HYPERSTHENE	3.491	
OLIVINE	0.0	
CALCIUM ORTHOSILICATE	0.0	0.0
MAGNETITE	1.508	
HEMATITE	0.0	
ILMENITE	0.494	
SPHENE	0.0	
PEROVSKITE	0.0	
RUTILE	0.0	
APATITE	0.0	
FLUORITE	0.0	
PYRITE	0.0	
CALCITE	0.0	
CHROMITE	0.0	
SUM	5.493	

OXIDATION RATIO MOL(2FE2O3/2FE2O3+FEO) X100= 31.664

RATIO MGO/FEO IN HYPERSTHENE DIOPSIDE AND OLIVINE = 5.8725E-01

DIFFERENTIATION INDEX = 89.569

CHEMICAL ANALYSIS, HOWI -5

SIO2	74.940
AL203	13.640
FE203	4.950
FEO	0.0
MGO	0.680
CAO	0.930
NA20	1.540
K20	3.310
TIO2	0.0
P205	0.0
MNO	0.0
ZRO2	0.0
CO2	0.0
SO3	0.0
CL2	0.0
F2	0.0
S	0.0
CR203	0.0
NIO	0.0
COO	0.0
BAO	0.0
SRO	0.0
LI20	0.0
SUM	99.990
QUARTZ	0.781
NEPHELINE	0.085
KALSILITE	0.134
OLIVINE	0.0
PYROXENE	0.044
FELDSPAR	0.956

CIPW NORM
(WEIGHT PERCENT)

SALIC GROUP		
QUARTZ	50.309	0.607
CORUNDUM	5.821	(-) 0.0
ZIRCON	0.0	
ORTHOCLASE	19.578	0.236
ALBITE	13.015	0.157
ANORTHITE	4.617	
LEUCITE	0.0	
KALIOPHYLITE	0.0	
NEPHELINE	0.0	
THENARDITE	0.0	
SODIUM CARBONATE	0.0	
HALITE	0.0	
SUM 93.340		

FEMIC GROUP		(-C)
ACMITE	0.0	0.0
SODIUM METASILICATE	0.0	0.0
POTASSIUM METASILICATE	0.0	0.0
DIOPSIDE	0.0	0.0
WOLLASTONITE	0.0	0.0
HYPERSTHENE	1.700	
OLIVINE	0.0	
CALCIUM ORTHOSILICATE	0.0	0.0
MAGNETITE	0.0	
HEMATITE	4.950	
ILMENITE	0.0	
SPHENE	0.0	
PEROVSKITE	0.0	
RUTILE	0.0	
APATITE	0.0	
FLUORITE	0.0	
PYRITE	0.0	
CALCITE	0.0	
CHROMITE	0.0	
SUM	6.650	

OXIDATION RATIO MOL(2FE203/2FE203+FEO) X100= 100.000

NO IRON IN HYPERSTHENE DIOPSIDE AND OLIVINE

DIFFERENTIATION INDEX = 82.902

CHEMICAL ANALYSIS, HOWI -6

SIO2	74.530
AL2O3	11.280
FE2O3	5.340
FEO	0.0
MGO	0.590
CAO	0.740
NA2O	0.440
K2O	6.070
TIO2	0.0
P2O5	0.0
MNO	0.0
ZRO2	0.0
CO2	0.0
SO3	0.0
CL2	0.0
F2	0.0
S	0.0
CR2O3	0.0
NIO	0.0
COO	0.0
BAO	0.0
SRO	0.0
LI2O	0.0
SUM	98.990
QUARTZ	0.739
NEPHELINE	0.023
KALSILITE	0.237
OLIVINE	0.0
PYROXENE	0.033
FELDSPAR	0.967

CIPW NORM
(WEIGHT PERCENT)

SALIC GROUP		
QUARTZ	46.258	0.539
CORUNDUM	2.622	(-) 0.0
ZIRCON	0.0	
ORTHOCLASE	35.903	0.418
ALBITE	3.719	0.043
ANORTHITE	3.674	
LEUCITE	0.0	
KALIOPHYLITE	0.0	
NEPHELINE	0.0	
THENARDITE	0.0	
SODIUM CARBONATE	0.0	
HALITE	0.0	
SUM 92.175		

FEMIC GROUP		(-C)
ACMITE	0.0	0.0
SODIUM METASILICATE	0.0	0.0
POTASSIUM METASILICATE	0.0	0.0
DIOPSIDE	0.0	0.0
WOLLASTONITE	0.0	0.0
HYPERSTHENE	1.475	
OLIVINE	0.0	
CALCIUM ORTHOSILICATE	0.0	0.0
MAGNETITE	0.0	
HEMATITE	5.340	
ILMENITE	0.0	
SPHENE	0.0	
PEROVSKITE	0.0	
RUTILE	0.0	
APATITE	0.0	
FLUORITE	0.0	
PYRITE	0.0	
CALCITE	0.0	
CHROMITE	0.0	
SUM	6.815	

OXIDATION RATIO MOL(2FE2O3/2FE2O3+FEO) X100= 100.000

NO IRON IN HYPERSTHENE DIOPSIDE AND OLIVINE

DIFFERENTIATION INDEX = 85.880

CHEMICAL ANALYSIS, HOWI -7

SIO2	75.160
AL203	13.680
FE203	4.970
FEO	0.0
MGO	0.690
CAO	0.940
NA2O	1.540
K2O	3.320
TIO2	0.0
P2O5	0.0
MNO	0.0
ZRO2	0.0
CO2	0.0
SO3	0.0
CL2	0.0
F2	0.0
S	0.0
CR2O3	0.0
NIO	0.0
COO	0.0
BAO	0.0
SRO	0.0
LI2O	0.0
SUM	100.300
QUARTZ	0.781
NEPHELINE	0.085
KALSILITE	0.134
OLIVINE	0.0
PYROXENE	0.044
FELDSPAR	0.956

CIPW NORM
(WEIGHT PERCENT)

SALIC GROUP			
QUARTZ	50.454		0.607
CORUNDUM	5.832	(-)	0.0
ZIRCON	0.0		
ORTHOCLASE	19.637		0.236
ALBITE	13.015		0.157
ANORTHITE	4.666		
LEUCITE	0.0		
KALIOPHYLITE	0.0		
NEPHELINE	0.0		
THENARDITE	0.0		
SODIUM CARBONATE	0.0		
HALITE	0.0		
SUM 93.605			

FEMIC GROUP		(-C)
ACMITE	0.0	0.0
SODIUM METASILICATE	0.0	0.0
POTASSIUM METASILICATE	0.0	0.0
DIOPSIDE	0.0	0.0
WOLLASTONITE	0.0	0.0
HYPERSTHENE	1.725	
OLIVINE	0.0	
CALCIUM ORTHOSILICATE	0.0	0.0
MAGNETITE	0.0	
HEMATITE	4.970	
ILMENITE	0.0	
SPHENE	0.0	
PEROVSKITE	0.0	
RUTILE	0.0	
APATITE	0.0	
FLUORITE	0.0	
PYRITE	0.0	
CALCITE	0.0	
CHROMITE	0.0	
SUM	6.695	

OXIDATION RATIO MOL(2FE203/2FE203+FEO) X100= 100.000

NO IRON IN HYPERSTHENE DIOPSIDE AND OLIVINE

DIFFERENTIATION INDEX = 83.107

CHEMICAL ANALYSIS, HOWI -8

SIO2	71.460
AL2O3	14.700
FE2O3	1.050
FEO	1.330
MGO	0.440
CAO	2.610
NA2O	4.440
K2O	3.270
TIO2	0.620
P2O5	0.0
MNO	0.080
ZRO2	0.0
CO2	0.0
SO3	0.0
CL2	0.0
F2	0.0
S	0.0
CR2O3	0.0
NIO	0.0
COO	0.0
BAO	0.0
SRO	0.0
LI2O	0.0
SUM	100.000
QUARTZ	0.627
NEPHELINE	0.242
KALSILITE	0.131
OLIVINE	0.0
PYROXENE	0.040
FELDSPAR	0.960

CIPW NORM
(WEIGHT PERCENT)

SALIC GROUP		
QUARTZ	27.119	0.323
CORUNDUM	0.0	(-) 0.886
ZIRCON	0.0	
ORTHOCLASE	19.342	0.230
ALBITE	37.525	0.447
ANORTHITE	10.485	
LEUCITE	0.0	
KALIOPHYLITE	0.0	
NEPHELINE	0.0	
THENARDITE	0.0	
SODIUM CARBONATE	0.0	
HALITE	0.0	
SUM 94.472		

FEMIC GROUP		(-C)
ACMITE	0.0	0.0
SODIUM METASILICATE	0.0	0.0
POTASSIUM METASILICATE	0.0	0.0
DIOPSIDE	2.013	0.886
WOLLASTONITE	0.0	0.0
HYPERSTHENE	0.817	
OLIVINE	0.0	
CALCIUM ORTHOSILICATE	0.0	0.0
MAGNETITE	1.522	
HEMATITE	0.0	
ILMENITE	1.178	
SPHENE	0.0	
PEROVSKITE	0.0	
RUTILE	0.0	
APATITE	0.0	
FLUORITE	0.0	
PYRITE	0.0	
CALCITE	0.0	
CHROMITE	0.0	
SUM	5.530	

OXIDATION RATIO MOL(2FE2O3/2FE2O3+FEO) X100= 41.538

RATIO MGO/FEO IN HYPERSTHENE DIOPSIDE AND OLIVINE = 2.0808E 00

DIFFERENTIATION INDEX = 83.986

CHEMICAL ANALYSIS, HOWI -9

SIO2	72.150
AL2O3	10.140
FE2O3	0.170
FEO	3.090
MGO	2.050
CAO	5.670
NA2O	4.920
K2O	1.370
TIO2	0.430
P2O5	0.0
MNO	0.0
ZRO2	0.0
CO2	0.0
SO3	0.0
CL2	0.0
F2	0.0
S	0.0
CR2O3	0.0
NIO	0.0
COO	0.0
BAO	0.0
SRO	0.0
LI2O	0.0
SUM	99.990
QUARTZ	0.644
NEPHELINE	0.295
KALSILITE	0.060
OLIVINE	0.0
PYROXENE	0.293
FELDSPAR	0.707

CIPW NORM
(WEIGHT PERCENT)

SALIC GROUP		
QUARTZ	26.604	0.349
CORUNDUM	0.0	(-) 9.679
ZIRCON	0.0	
ORTHOCLASE	8.103	0.106
ALBITE	41.582	0.545
ANORTHITE	1.524	
LEUCITE	0.0	
KALIOPHYLITE	0.0	
NEPHELINE	0.0	
THENARDITE	0.0	
SODIUM CARBONATE	0.0	
HALITE	0.0	
SUM	77.813	

FEMIC GROUP		(-C)
ACMITE	0.0	0.0
SODIUM METASILICATE	0.0	0.0
POTASSIUM METASILICATE	0.0	0.0
DIOPSIDE	20.380	8.967
WOLLASTONITE	0.809	0.711
HYPERSTHENE	0.0	
OLIVINE	0.0	
CALCIUM ORTHOSILICATE	0.0	0.0
MAGNETITE	0.0	
HEMATITE	0.0	
ILMENITE	0.817	
SPHENE	0.0	
PEROVSKITE	0.0	
RUTILE	0.0	
APATITE	0.0	
FLUORITE	0.0	
PYRITE	0.0	
CALCITE	0.0	
CHROMITE	0.0	
SUM	22.006	

OXIDATION RATIO MOL(2FE2O3/2FE2O3+FEO) X100= 4.718

RATIO MGO/FEO IN HYPERSTHENE DIOPSIDE AND OLIVINE = 1.365IE 00

DIFFERENTIATION INDEX = 76.289

CHEMICAL ANALYSIS, H 10

SIO2	69.170
AL2O3	14.620
FE2O3	1.400
FEO	4.630
MGO	1.970
CAO	2.330
NA2O	4.250
K2O	0.830
TIO2	0.740
P2O5	0.0
MNO	0.060
ZRO2	0.0
CO2	0.0
SO3	0.0
CL2	0.0
F2	0.0
S	0.0
CR2O3	0.0
NIO	0.0
COO	0.0
BAO	0.0
SRO	0.0
LI2O	0.0
SUM	100.000
QUARTZ	0.688
NEPHELINE	0.273
KALSILITE	0.039
OLIVINE	0.0
PYROXENE	0.175
FELDSPAR	0.825

CIPW NORM
(WEIGHT PERCENT)

SALIC GROUP		
QUARTZ	30.537	0.428
CORUNDUM	2.483	(-) 0.0
ZIRCON	0.0	
ORTHOCLASE	4.909	0.069
ALBITE	35.919	0.503
ANORTHITE	11.567	
LEUCITE	0.0	
KALIOPHYLITE	0.0	
NEPHELINE	0.0	
THENARDITE	0.0	
SODIUM CARBONATE	0.0	
HALITE	0.0	
SUM 85.416		
FEMIC GROUP		(-C)
ACMITE	0.0	0.0
SODIUM METASILICATE	0.0	0.0
POTASSIUM METASILICATE	0.0	0.0
DIOPSIDE	0.0	0.0
WOLLASTONITE	0.0	0.0
HYPERSTHENE	11.149	
OLIVINE	0.0	
CALCIUM ORTHOSILICATE	0.0	0.0
MAGNETITE	2.030	
HEMATITE	0.0	
ILMENITE	1.406	
SPHENE	0.0	
PEROVSKITE	0.0	
RUTILE	0.0	
APATITE	0.0	
FLUORITE	0.0	
PYRITE	0.0	
CALCITE	0.0	
CHROMITE	0.0	
SUM	14.585	

OXIDATION RATIO MOL(2FE2O3/2FE2O3+FEO) X100= 21.392

RATIO MGO/FEO IN HYPERSTHENE DIOPSIDE AND OLIVINE = 1.0445E 00

DIFFERENTIATION INDEX = 71.366

CHEMICAL ANALYSIS, H 11

SIO2	78.500
AL2O3	12.490
FE2O3	0.530
FEO	0.610
MGO	0.260
CAO	2.380
NA2O	3.780
K2O	1.330
TIO2	0.090
P2O5	0.030
MNO	0.010
ZRO2	0.0
CO2	0.0
SO3	0.0
CL2	0.0
F2	0.0
S	0.0
CR2O3	0.0
NIO	0.0
COO	0.0
BAO	0.0
SRO	0.0
LI2O	0.0
SUM	100.010
QUARTZ	0.745
NEPHELINE	0.203
KALSILITE	0.052
OLIVINE	0.0
PYROXENE	0.025
FELDSPAR	0.975

CIPW NORM
(WEIGHT PERCENT)

SALIC GROUP		
QUARTZ	45.650	0.534
CORUNDUM	0.493	(-) 0.0
ZIRCON	0.0	
ORTHOCLASE	7.867	0.092
ALBITE	31.947	0.374
ANORTHITE	11.815	
LEUCITE	0.0	
KALIOPHYLITE	0.0	
NEPHELINE	0.0	
THENARDITE	0.0	
SODIUM CARBONATE	0.0	
HALITE	0.0	
SUM 97.772		

FEMIC GROUP		(-C)
ACMITE	0.0	0.0
SODIUM METASILICATE	0.0	0.0
POTASSIUM METASILICATE	0.0	0.0
DIOPSIDE	0.0	0.0
WOLLASTONITE	0.0	0.0
HYPERSTHENE	1.350	
OLIVINE	0.0	
CALCIUM ORTHOSILICATE	0.0	0.0
MAGNETITE	0.768	
HEMATITE	0.0	
ILMENITE	0.0	
SPHENE	0.0	
PEROVSKITE	0.0	
RUTILE	0.0	
APATITE	0.0	
FLUORITE	0.0	
PYRITE	0.0	
CALCITE	0.0	
CHROMITE	0.0	
SUM	2.118	

OXIDATION RATIO MOL(2FE2O3/2FE2O3+FEO) X100= 43.882

RATIO MGO/FEO IN HYPERSTHENE DIOPSIDE AND OLIVINE = 1.2263E 00

DIFFERENTIATION INDEX = 85.464

CHEMICAL ANALYSIS, H 12

SIO2	75.810
AL203	13.980
FE203	0.480
FEO	1.170
MGO	0.520
CAO	3.550
NA2O	3.650
K2O	0.740
TIO2	0.080
P2O5	0.0
MNO	0.0
ZRO2	0.0
CO2	0.0
SO3	0.0
CL2	0.0
F2	0.0
S	0.0
CR203	0.0
NIO	0.0
COO	0.0
BAO	0.0
SRO	0.0
LI2O	0.0
SUM	99.980
QUARTZ	0.753
NEPHELINE	0.215
KALSILITE	0.032
OLIVINE	0.0
PYROXENE	0.055
FELDSPAR	0.945

CIPW NORM
(WEIGHT PERCENT)

SALIC GROUP		
QUARTZ	42.600	0.547
CORUNDUM	0.706	(-) 0.0
ZIRCON	0.0	
ORTHOCLASE	4.377	0.056
ALBITE	30.848	0.396
ANORTHITE	17.623	
LEUCITE	0.0	
KALIOPHYLITE	0.0	
NEPHELINE	0.0	
THENARDITE	0.0	
SODIUM CARBONATE	0.0	
HALITE	0.0	
SUM	96.155	
FEMIC GROUP		(-C)
ACMITE	0.0	0.0
SODIUM METASILICATE	0.0	0.0
POTASSIUM METASILICATE	0.0	0.0
DIOPSIDE	0.0	0.0
WOLLASTONITE	0.0	0.0
HYPERSTHENE	3.049	
OLIVINE	0.0	
CALCIUM ORTHOSILICATE	0.0	0.0
MAGNETITE	0.696	
HEMATITE	0.0	
ILMENITE	0.0	
SPHENE	0.0	
PEROVSKITE	0.0	
RUTILE	0.0	
APATITE	0.0	
FLUORITE	0.0	
PYRITE	0.0	
CALCITE	0.0	
CHROMITE	0.0	
SUM	3.745	

OXIDATION RATIO MOL(2FE203/2FE203+FEO) X100= 26.966

RATIO MGO/FEO IN HYPERSTHENE DIOPSIDE AND OLIVINE = 9.8113E-01

DIFFERENTIATION INDEX = 77.826

CHEMICAL ANALYSIS, H 13

SIO2	78.140
AL2O3	10.680
FE2O3	0.990
FEO	2.510
MGO	0.180
CAO	0.400
NA2O	2.200
K2O	4.550
TIO2	0.310
P2O5	0.0
MNO	0.040
ZRO2	0.0
CO2	0.0
SO3	0.0
CL2	0.0
F2	0.0
S	0.0
CR2O3	0.0
NIO	0.0
COO	0.0
BAO	0.0
SRO	0.0
LI2O	0.0
SUM	100.000
QUARTZ	0.721
NEPHELINE	0.111
KALSILITE	0.168
OLIVINE	0.0
PYROXENE	0.074
FELDSPAR	0.926

CIPW NORM
(WEIGHT PERCENT)

SALIC GROUP		
QUARTZ	45.291	0.499
CORUNDUM	1.395	(-) 0.0
ZIRCON	0.0	
ORTHOCLASE	26.913	0.296
ALBITE	18.594	0.205
ANORTHITE	1.986	
LEUCITE	0.0	
KALIOPHYLITE	0.0	
NEPHELINE	0.0	
THENARDITE	0.0	
SODIUM CARBONATE	0.0	
HALITE	0.0	
SUM 94.178		
FEMIC GROUP		(-C)
ACMITE	0.0	0.0
SODIUM METASILICATE	0.0	0.0
POTASSIUM METASILICATE	0.0	0.0
DIOPSIDE	0.0	0.0
WOLLASTONITE	0.0	0.0
HYPERSTHENE	3.798	
OLIVINE	0.0	
CALCIUM ORTHOSILICATE	0.0	0.0
MAGNETITE	1.435	
HEMATITE	0.0	
ILMENITE	0.589	
SPHENE	0.0	
PEROVSKITE	0.0	
RUTILE	0.0	
APATITE	0.0	
FLUORITE	0.0	
PYRITE	0.0	
CALCITE	0.0	
CHROMITE	0.0	
SUM	5.822	

OXIDATION RATIO MOL(2FE2O3/2FE2O3+FEO) X100= 26.198

RATIO MGO/FEO IN HYPERSTHENE DIOPSIDE AND OLIVINE = 1.7743E-01

DIFFERENTIATION INDEX = 90.798

CHEMICAL ANALYSIS, H 14

SIO2	74.290
AL2O3	14.140
FE2O3	0.0
FEO	1.560
MGO	0.410
CAO	0.0
NA2O	1.660
K2O	2.740
TIO2	5.110
P2O5	0.090
MNO	0.0
ZRO2	0.0
CO2	0.0
SO3	0.0
CL2	0.0
F2	0.0
S	0.0
CR2O3	0.0
NIO	0.0
COO	0.0
BAO	0.0
SRO	0.0
LI2O	0.0
SUM	100.000
QUARTZ	0.799
NEPHELINE	0.091
KALSILITE	0.110
OLIVINE	0.0
PYROXENE	0.033
FELDSPAR	0.967

CIPW NORM
(WEIGHT PERCENT)

SALIC GROUP		
QUARTZ	53.543	0.639
CORUNDUM	8.436	(-) 0.0
ZIRCON	0.0	
ORTHOCLASE	16.207	0.193
ALBITE	14.030	0.167
ANORTHITE	0.0	
LEUCITE	0.0	
KALIOPHYLITE	0.0	
NEPHELINE	0.0	
THENARDITE	0.0	
SODIUM CARBONATE	0.0	
HALITE	0.0	
SUM 92.215		
FEMIC GROUP		(-C)
ACMITE	0.0	0.0
SODIUM METASILICATE	0.0	0.0
POTASSIUM METASILICATE	0.0	0.0
DIOPSIDE	0.0	0.0
WOLLASTONITE	0.0	0.0
HYPERSTHENE	1.025	
OLIVINE	0.0	
CALCIUM ORTHOSILICATE	0.0	0.0
MAGNETITE	0.0	
HEMATITE	0.0	
ILMENITE	3.293	
SPHENE	0.0	
PEROVSKITE	0.0	
RUTILE	3.377	
APATITE	0.0	
FLUORITE	0.0	
PYRITE	0.0	
CALCITE	0.0	
CHROMITE	0.0	
SUM	7.695	

OXIDATION RATIO MOL(2FE2O3/2FE2O3+FEO) X100= 26.198

NO IRON IN HYPERSTHENE DIOPSIDE AND OLIVINE

DIFFERENTIATION INDEX = 83.779

CHEMICAL ANALYSIS, H 15

SIO2	67.510
AL203	15.800
FE203	1.630
FEO	1.700
MGO	0.680
CAO	2.330
NA2O	3.800
K2O	5.870
TIO2	0.400
P2O5	0.230
MNO	0.400
ZRO2	0.0
CO2	0.0
SO3	0.0
CL2	0.0
F2	0.0
S	0.0
CR2O3	0.0
NIO	0.0
COO	0.0
BAO	0.0
SRO	0.0
LI2O	0.0
SUM	100.350
QUARTZ	0.556
NEPHELINE	0.208
KALSILITE	0.236
OLIVINE	0.0
PYROXENE	0.059
FELDSPAR	0.941

CIPW NORM
(WEIGHT PERCENT)

SALIC GROUP		
QUARTZ	16.735	0.200
CORUNDUM	0.0	(-) 1.059
ZIRCON	0.0	
ORTHOCLASE	34.720	0.415
ALBITE	32.116	0.384
ANORTHITE	8.664	
LEUCITE	0.0	
KALIOPHYLITE	0.0	
NEPHELINE	0.0	
THENARDITE	0.0	
SODIUM CARBONATE	0.0	
HALITE	0.0	
SUM 92.235		

FEMIC GROUP		(-C)
ACMITE	0.0	0.0
SODIUM METASILICATE	0.0	0.0
POTASSIUM METASILICATE	0.0	0.0
DIOPSIDE	2.407	1.059
WOLLASTONITE	0.0	0.0
HYPERSTHENE	2.360	
OLIVINE	0.0	
CALCIUM ORTHOSILICATE	0.0	0.0
MAGNETITE	2.363	
HEMATITE	0.0	
ILMENITE	0.760	
SPHENE	0.0	
PEROVSKITE	0.0	
RUTILE	0.0	
APATITE	0.0	
FLUORITE	0.0	
PYRITE	0.0	
CALCITE	0.0	
CHROMITE	0.0	
SUM	7.890	

OXIDATION RATIO MOL(2FE203/2FE203+FEO) X100= 46.321

RATIO MGO/FEO IN HYPERSTHENE DIOPSIDE AND OLIVINE = 1.2093E 00

DIFFERENTIATION INDEX = 83.571

CHEMICAL ANALYSIS, H 16

SIO2	65.620
AL2O3	15.480
FE2O3	1.940
FEO	3.130
MGO	1.390
CAO	3.260
NA2O	3.430
K2O	4.650
TIO2	0.770
P2O5	0.280
MNO	0.040
ZRO2	0.0
CO2	0.0
SO3	0.0
CL2	0.0
F2	0.0
S	0.0
CR2O3	0.0
NIO	0.0
COO	0.0
BAO	0.0
SRO	0.0
LI2O	0.0
SUM	99.990
QUARTZ	0.580
NEPHELINE	0.210
KALSILITE	0.209
OLIVINE	0.0
PYROXENE	0.100
FELDSPAR	0.900

CIPW NORM
(WEIGHT PERCENT)

SALIC GROUP		
QUARTZ	18.162	0.243
CORUNDUM	0.0	(-) 1.130
ZIRCON	0.0	
ORTHOCLASE	27.504	0.368
ALBITE	28.989	0.388
ANORTHITE	13.059	
LEUCITE	0.0	
KALIOPHYLITE	0.0	
NEPHELINE	0.0	
THENARDITE	0.0	
SODIUM CARBONATE	0.0	
HALITE	0.0	
SUM	87.714	

FEMIC GROUP		(-C)
ACMITE	0.0	0.0
SODIUM METASILICATE	0.0	0.0
POTASSIUM METASILICATE	0.0	0.0
DIOPSIDE	2.568	1.130
WOLLASTONITE	0.0	0.0
HYPERSTHENE	5.152	
OLIVINE	0.0	
CALCIUM ORTHOSILICATE	0.0	0.0
MAGNETITE	2.813	
HEMATITE	0.0	
ILMENITE	1.463	
SPHENE	0.0	
PEROVSKITE	0.0	
RUTILE	0.0	
APATITE	0.0	
FLUORITE	0.0	
PYRITE	0.0	
CALCITE	0.0	
CHROMITE	0.0	
SUM	11.997	

OXIDATION RATIO MOL(2FE2O3/2FE2O3+FEO) X100= 35.808

RATIO MGO/FEO IN HYPERSTHENE DIOPSIDE AND OLIVINE = 1.5593E 00

DIFFERENTIATION INDEX = 74.655

CHEMICAL ANALYSIS, H 17

SIO2	65.090
AL2O3	15.260
FE2O3	3.060
FEO	3.400
MGO	1.160
CAO	2.880
NA2O	4.010
K2O	3.960
TIO2	0.890
P2O5	0.190
MNO	0.090
ZRO2	0.0
CO2	0.0
SO3	0.0
CL2	0.0
F2	0.0
S	0.0
CR2O3	0.0
NIO	0.0
COO	0.0
BAO	0.0
SRO	0.0
LI2O	0.0
SUM	99.990
QUARTZ	0.580
NEPHELINE	0.243
KALSILITE	0.176
OLIVINE	0.0
PYROXENE	0.084
FELDSPAR	0.916

CIPW NORM
(WEIGHT PERCENT)

SALIC GROUP		
QUARTZ	18.152	0.241
CORUNDUM	0.0	(-) 0.867
ZIRCON	0.0	
ORTHOCLASE	23.423	0.310
ALBITE	33.891	0.449
ANORTHITE	11.899	
LEUCITE	0.0	
KALIOPHYLITE	0.0	
NEPHELINE	0.0	
THENARDITE	0.0	
SODIUM CARBONATE	0.0	
HALITE	0.0	
SUM 87.365		

FEMIC GROUP		(-C)
ACMITE	0.0	0.0
SODIUM METASILICATE	0.0	0.0
POTASSIUM METASILICATE	0.0	0.0
DIOPSIDE	1.970	0.867
WOLLASTONITE	0.0	0.0
HYPERSTHENE	4.338	
OLIVINE	0.0	
CALCIUM ORTHOSILICATE	0.0	0.0
MAGNETITE	4.437	
HEMATITE	0.0	
ILMENITE	1.691	
SPHENE	0.0	
PEROVSKITE	0.0	
RUTILE	0.0	
APATITE	0.0	
FLUORITE	0.0	
PYRITE	0.0	
CALCITE	0.0	
CHROMITE	0.0	
SUM	12.436	

OXIDATION RATIO MOL(2FE2O3/2FE2O3+FEO) XIOO= 44.751

RATIO MGO/FEO IN HYPERSTHENE DIOPSIDE AND OLIVINE = 1.5899E 00

DIFFERENTIATION INDEX = 75.466

CHEMICAL ANALYSIS, H 18

SIO2	60.220
AL203	14.940
FE203	2.220
FEO	7.060
MGO	4.340
CAO	4.270
NA2O	3.910
K2O	1.400
TIO2	0.970
P2O5	0.230
MNO	0.130
ZRO2	0.0
CO2	0.0
SO3	0.300
CL2	0.0
F2	0.0
S	0.0
CR2O3	0.0
NIO	0.0
COO	0.0
BAO	0.0
SRO	0.0
LI2O	0.0
SUM	99.990
QUARTZ	0.594
NEPHELINE	0.318
KALSILITE	0.089
OLIVINE	0.0
PYROXENE	0.262
FELDSPAR	0.738

CIPW NORM
(WEIGHT PERCENT)

SALIC GROUP		
QUARTZ	13.651	0.258
CORUNDUM	0.0	(-) 0.402
ZIRCON	0.0	
ORTHOCLASE	8.281	0.156
ALBITE	31.081	0.586
ANORTHITE	20.089	
LEUCITE	0.0	
KALIOPHYLITE	0.0	
NEPHELINE	0.0	
THENARDITE	0.532	
SODIUM CARBONATE	0.0	
HALITE	0.0	
SUM 73.634		

FEMIC GROUP		(-C)
ACMITE	0.0	0.0
SODIUM METASILICATE	0.0	0.0
POTASSIUM METASILICATE	0.0	0.0
DIOPSIDE	0.913	0.402
WOLLASTONITE	0.0	0.0
HYPERSTHENE	20.153	
OLIVINE	0.0	
CALCIUM ORTHOSILICATE	0.0	0.0
MAGNETITE	3.219	
HEMATITE	0.0	
ILMENITE	1.843	
SPHENE	0.0	
PEROVSKITE	0.0	
RUTILE	0.0	
APATITE	0.0	
FLUORITE	0.0	
PYRITE	0.0	
CALCITE	0.0	
CHROMITE	0.0	
SUM	26.128	

OXIDATION RATIO MOL(2FE203/2FE203+FEO) X100= 22.058

RATIO MGO/FEO IN HYPERSTHENE DIOPSIDE AND OLIVINE = 1.4685E 00

DIFFERENTIATION INDEX = 53.013

CHEMICAL ANALYSIS, H 19

SIO2	59.360
AL2O3	15.580
FE2O3	2.040
FEO	5.420
MGO	2.950
CAO	5.700
NA2O	4.230
K2O	3.200
TIO2	0.990
P2O5	0.470
MNO	0.060
ZRO2	0.0
CO2	0.0
SO3	0.0
CL2	0.0
F2	0.0
S	0.0
CR2O3	0.0
NIO	0.0
COO	0.0
BAO	0.0
SRO	0.0
LI2O	0.0
SUM	100.000
QUARTZ	0.508
NEPHELINE	0.317
KALSILITE	0.176
OLIVINE	0.0
PYROXENE	0.216
FELDSPAR	0.784

CIPW NORM
(WEIGHT PERCENT)

SALIC GROUP		
QUARTZ	6.519	0.107
CORUNDUM	0.0	(-) 4.171
ZIRCON	0.0	
ORTHOCLASE	18.928	0.309
ALBITE	35.750	0.584
ANORTHITE	14.033	
LEUCITE	0.0	
KALIOPHYLITE	0.0	
NEPHELINE	0.0	
THENARDITE	0.0	
SODIUM CARBONATE	0.0	
HALITE	0.0	
SUM	75.229	

FEMIC GROUP		(-C)
ACMITE	0.0	0.0
SODIUM METASILICATE	0.0	0.0
POTASSIUM METASILICATE	0.0	0.0
DIOPSIDE	9.479	4.171
WOLLASTONITE	0.0	0.0
HYPERSTHENE	9.427	
OLIVINE	0.0	
CALCIUM ORTHOSILICATE	0.0	0.0
MAGNETITE	2.958	
HEMATITE	0.0	
ILMENITE	1.881	
SPHENE	0.0	
PEROVSKITE	0.0	
RUTILE	0.0	
APATITE	1.026	
FLUORITE	0.0	
PYRITE	0.0	
CALCITE	0.0	
CHROMITE	0.0	
SUM	24.772	

OXIDATION RATIO MOL(2FE2O3/2FE2O3+FEO) X100= 25.303

RATIO MGO/FEO IN HYPERSTHENE DIOPSIDE AND OLIVINE = 1.4461E 00

DIFFERENTIATION INDEX = 61.197

CHEMICAL ANALYSIS, H 20

SIO2	54.530
AL2O3	15.680
FE2O3	4.010
FEO	6.010
MGO	4.410
CAO	7.180
NA2O	4.400
K2O	1.550
TIO2	1.630
P2O5	0.450
MNO	0.150
ZRO2	0.0
CO2	0.0
SO3	0.0
CL2	0.0
F2	0.0
S	0.0
CR2O3	0.0
NIO	0.0
COO	0.0
BAO	0.0
SRO	0.0
LI2O	0.0
SUM	100.000
QUARTZ	0.485
NEPHELINE	0.409
KALSILITE	0.106
OLIVINE	0.0
PYROXENE	0.257
FELDSPAR	0.743

CIPW NORM
(WEIGHT PERCENT)

SALIC GROUP		
QUARTZ	2.923	0.059
CORUNDUM	0.0	(-) 5.181
ZIRCON	0.0	
ORTHOCLASE	9.168	0.186
ALBITE	37.187	0.755
ANORTHITE	18.423	
LEUCITE	0.0	
KALIOPHYLITE	0.0	
NEPHELINE	0.0	
THENARDITE	0.0	
SODIUM CARBONATE	0.0	
HALITE	0.0	
SUM 67.701		

FEMIC GROUP		(-C)
ACMITE	0.0	0.0
SODIUM METASILICATE	0.0	0.0
POTASSIUM METASILICATE	0.0	0.0
DIOPSIDE	11.775	5.181
WOLLASTONITE	0.0	0.0
HYPERSTHENE	10.633	
OLIVINE	0.0	
CALCIUM ORTHOSILICATE	0.0	0.0
MAGNETITE	5.814	
HEMATITE	0.0	
ILMENITE	3.097	
SPHENE	0.0	
PEROVSKITE	0.0	
RUTILE	0.0	
APATITE	0.982	
FLUORITE	0.0	
PYRITE	0.0	
CALCITE	0.0	
CHROMITE	0.0	
SUM	32.301	

OXIDATION RATIO MOL(2FE2O3/2FE2O3+FEO) X100= 37.520

RATIO MGO/FEO IN HYPERSTHENE DIOPSIDE AND OLIVINE = 2.7461E 00

DIFFERENTIATION INDEX = 49.278

CHEMICAL ANALYSIS, H 21

SIO2	64.050
AL2O3	14.920
FE2O3	2.330
FEO	5.090
MGO	3.300
CAO	4.490
NA2O	3.730
K2O	1.090
TIO2	0.830
P2O5	0.080
MNO	0.050
ZRO2	0.0
CO2	0.0
SO3	0.150
CL2	0.0
F2	0.0
S	0.0
CR2O3	0.0
NIO	0.0
COO	0.0
BAO	0.0
SRO	0.0
LI2O	0.040
SUM	100.150
QUARTZ	0.649
NEPHELINE	0.289
KALSILITE	0.062
OLIVINE	0.0
PYROXENE	0.205
FELDSPAR	0.795

CIPW NORM
(WEIGHT PERCENT)

SALIC GROUP		
QUARTZ	21.118	0.357
CORUNDUM	0.0	(-) 0.566
ZIRCON	0.0	
ORTHOCLASE	6.447	0.109
ALBITE	31.525	0.534
ANORTHITE	20.716	
LEUCITE	0.0	
KALIOPHYLITE	0.0	
NEPHELINE	0.0	
THENARDITE	0.0	
SODIUM CARBONATE	0.0	
HALITE	0.0	
SUM 79.806		

FEMIC GROUP		(-C)
ACMITE	0.0	0.0
SODIUM METASILICATE	0.0	0.0
POTASSIUM METASILICATE	0.0	0.0
DIOPSIDE	1.287	0.566
WOLLASTONITE	0.0	0.0
HYPERSTHENE	13.885	
OLIVINE	0.0	
CALCIUM ORTHOSILICATE	0.0	0.0
MAGNETITE	3.378	
HEMATITE	0.0	
ILMENITE	1.577	
SPHENE	0.0	
PEROVSKITE	0.0	
RUTILE	0.0	
APATITE	0.0	
FLUORITE	0.0	
PYRITE	0.0	
CALCITE	0.0	
CHROMITE	0.0	
SUM	20.128	

OXIDATION RATIO MOL[2FE2O3/2FE2O3+FEO] X100= 29.178

RATIO MGO/FEO IN HYPERSTHENE DIOPSIDE AND OLIVINE = 1.8044E 00

DIFFERENTIATION INDEX = 59.090

CHEMICAL ANALYSIS, H 22

SIO2	63.770
AL2O3	16.300
FE2O3	7.490
FEO	0.0
MGO	2.490
CAO	6.330
NA2O	3.680
K2O	1.210
TIO2	0.0
P2O5	0.0
MNO	0.0
ZRO2	0.0
CO2	0.0
SO3	0.0
CL2	0.0
F2	0.0
S	0.0
CR2O3	0.0
NIO	0.0
COO	0.0
BAO	0.0
SRO	0.0
LI2O	0.0
SUM	101.270
QUARTZ	0.653
NEPHELINE	0.280
KALSILITE	0.067
OLIVINE	0.0
PYROXENE	0.128
FELDSPAR	0.872

CIPW NORM
(WEIGHT PERCENT)

SALIC GROUP		
QUARTZ	21.996	0.365
CORUNDUM	0.0	(-) 2.420
ZIRCON	0.0	
ORTHOCLASE	7.157	0.119
ALBITE	31.102	0.516
ANORTHITE	24.346	
LEUCITE	0.0	
KALIOPHYLITE	0.0	
NEPHELINE	0.0	
THENARDITE	0.0	
SODIUM CARBONATE	0.0	
HALITE	0.0	
SUM 84.602		

FEMIC GROUP		(-C)
ACMITE	0.0	0.0
SODIUM METASILICATE	0.0	0.0
POTASSIUM METASILICATE	0.0	0.0
DIOPSIDE	5.499	2.420
WOLLASTONITE	0.0	0.0
HYPERSTHENE	3.679	
OLIVINE	0.0	
CALCIUM ORTHOSILICATE	0.0	0.0
MAGNETITE	0.0	
HEMATITE	7.490	
ILMENITE	0.0	
SPHENE	0.0	
PEROVSKITE	0.0	
RUTILE	0.0	
APATITE	0.0	
FLUORITE	0.0	
PYRITE	0.0	
CALCITE	0.0	
CHROMITE	0.0	
SUM	16.668	

OXIDATION RATIO MOL(2FE2O3/2FE2O3+FEO) X100= 100.000

NO IRON IN HYPERSTHENE DIOPSIDE AND OLIVINE

DIFFERENTIATION INDEX = 60.255

CHEMICAL ANALYSIS, H 23

SIO2	51.640
AL2O3	13.880
FE2O3	4.510
FEO	11.650
MGO	8.720
CAO	9.510
NA2O	2.020
K2O	0.340
TIO2	1.120
P2O5	0.230
MNO	0.230
ZRO2	0.0
CO2	0.0
SO3	0.0
CL2	0.0
F2	0.0
S	0.0
CR2O3	0.0
NIO	0.0
COO	0.0
BAO	0.0
SRO	0.0
LI2O	0.0
SUM	103.850
QUARTZ	0.506
NEPHELINE	0.439
KALSILITE	0.054
OLIVINE	0.0
PYROXENE	0.496
FELDSPAR	0.504

CIPW NORM
(WEIGHT PERCENT)

SALIC GROUP		
QUARTZ	1.975	0.094
CORUNDUM	0.0	(-) 7.002
ZIRCON	0.0	
ORTHOCLASE	2.011	0.095
ALBITE	17.072	0.811
ANORTHITE	27.767	
LEUCITE	0.0	
KALIOPHYLITE	0.0	
NEPHELINE	0.0	
THENARDITE	0.0	
SODIUM CARBONATE	0.0	
HALITE	0.0	
SUM 48.825		

FEMIC GROUP		(-C)
ACMITE	0.0	0.0
SODIUM METASILICATE	0.0	0.0
POTASSIUM METASILICATE	0.0	0.0
DIOPSIDE	15.914	7.002
WOLLASTONITE	0.0	0.0
HYPERSTHENE	30.216	
OLIVINE	0.0	
CALCIUM ORTHOSILICATE	0.0	0.0
MAGNETITE	6.539	
HEMATITE	0.0	
ILMENITE	2.128	
SPHENE	0.0	
PEROVSKITE	0.0	
RUTILE	0.0	
APATITE	0.0	
FLUORITE	0.0	
PYRITE	0.0	
CALCITE	0.0	
CHROMITE	0.0	
SUM	54.798	

OXIDATION RATIO MOL(2FE2O3/2FE2O3+FEO) X100= 25.839

RATIO MGO/FEO IN HYPERSTHENE DIOPSIDE AND OLIVINE = 1.7744E 00

DIFFERENTIATION INDEX = 21.059

CHEMICAL ANALYSIS, H 24

SIO2	48.840
AL2O3	14.980
FE2O3	2.400
FEO	11.560
MGO	8.720
CAO	9.510
NA2O	2.020
K2O	0.540
TIO2	1.190
P2O5	0.210
MNO	0.230
ZRO2	0.0
CO2	0.0
SO3	0.0
CL2	0.0
F2	0.0
S	0.0
CR2O3	0.0
NIO	0.0
COO	0.0
BAO	0.0
SRO	0.0
LI2O	0.0
SUM	100.200
QUARTZ	0.454
NEPHELINE	0.457
KALSILITE	0.090
OLIVINE	0.081
PYROXENE	0.384
FELDSPAR	0.535

CIPW NORM
(WEIGHT PERCENT)

SALIC GROUP		
QUARTZ	0.0	0.0
CORUNDUM	0.0	(-) 6.153
ZIRCON	0.0	
ORTHOCLASE	3.194	0.158
ALBITE	17.072	0.842
ANORTHITE	30.173	
LEUCITE	0.0	
KALIOPHYLITE	0.0	
NEPHELINE	0.0	
THENARDITE	0.0	
SODIUM CARBONATE	0.0	
HALITE	0.0	
SUM 50.440		
FEMIC GROUP		(-C)
ACMITE	0.0	0.0
SODIUM METASILICATE	0.0	0.0
POTASSIUM METASILICATE	0.0	0.0
DIOPSIDE	13.984	6.153
WOLLASTONITE	0.0	0.0
HYPERSTHENE	22.231	
OLIVINE	7.598	
CALCIUM ORTHOSILICATE	0.0	0.0
MAGNETITE	3.480	
HEMATITE	0.0	
ILMENITE	2.261	
SPHENE	0.0	
PEROVSKITE	0.0	
RUTILE	0.0	
APATITE	0.0	
FLUORITE	0.0	
PYRITE	0.0	
CALCITE	0.0	
CHROMITE	0.0	
SUM	49.554	

OXIDATION RATIO MOL(2FE2O3/2FE2O3+FEO) X100= 15.743

RATIO MGO/FEO IN HYPERSTHENE DIOPSIDE AND OLIVINE = 1.6278E 00

DIFFERENTIATION INDEX = 20.266

CHEMICAL ANALYSIS, H 26

SIO2	53.780
AL2O3	19.380
FE2O3	0.0
FEO	15.390
MGO	2.790
CAO	7.680
NA2O	0.0
K2O	0.0
TIO2	0.0
P2O5	0.0
MNO	0.0
ZRO2	0.0
CO2	0.0
SO3	0.0
CL2	0.0
F2	0.0
S	0.0
CR2O3	0.0
NIO	0.0
COO	0.0
BAO	0.0
SRO	0.0
LI2O	0.0
SUM	99.020
QUARTZ	1.000
NEPHELINE	0.0
KALSILITE	0.0
OLIVINE	0.0
PYROXENE	0.480
FELDSPAR	0.520

CIPW NORM
(WEIGHT PERCENT)

SALIC GROUP			
QUARTZ	20.313		1.000
CORUNDUM	5.391	(-)	0.0
ZIRCON	0.0		
ORTHOCLASE	0.0		0.0
ALBITE	0.0		0.0
ANORTHITE	38.126		
LEUCITE	0.0		
KALIOPHYLITE	0.0		
NEPHELINE	0.0		
THENARDITE	0.0		
SODIUM CARBONATE	0.0		
HALITE	0.0		
SUM 63.830			

FEMIC GROUP		(-C)
ACMITE	0.0	0.0
SODIUM METASILICATE	0.0	0.0
POTASSIUM METASILICATE	0.0	0.0
DIOPSIDE	0.0	0.0
WOLLASTONITE	0.0	0.0
HYPERSTHENE	35.190	
OLIVINE	0.0	
CALCIUM ORTHOSILICATE	0.0	0.0
MAGNETITE	0.0	
HEMATITE	0.0	
ILMENITE	0.0	
SPHENE	0.0	
PEROVSKITE	0.0	
RUTILE	0.0	
APATITE	0.0	
FLUORITE	0.0	
PYRITE	0.0	
CALCITE	0.0	
CHROMITE	0.0	
SUM	35.190	

OXIDATION RATIO MOL(2FE2O3/2FE2O3+FEO) X100= 13.058

RATIO MGO/FEO IN HYPERSTHENE DIOPSIDE AND OLIVINE = 3.2632E-01

DIFFERENTIATION INDEX = 20.313

CHEMICAL ANALYSIS, H 27

SIO2	52.720
AL203	16.640
FE203	0.780
FEO	11.340
MGO	4.240
CAO	8.890
NA20	3.500
K20	0.570
TIO2	1.020
P205	0.360
MNO	0.450
ZRO2	0.0
CO2	0.0
SO3	0.0
CL2	0.0
F2	0.0
S	0.0
CR203	0.0
NIO	0.0
COO	0.0
BAO	0.0
SRO	0.0
LI2O	0.0
SUM	100.510
QUARTZ	0.455
NEPHELINE	0.487
KALSILITE	0.058
OLIVINE	0.001
PYROXENE	0.369
FELDSPAR	0.630

CIPW NORM
(WEIGHT PERCENT)

SALIC GROUP		
QUARTZ	0.0	0.0
CORUNDUM	0.0	(-) 5.214
ZIRCON	0.0	
ORTHOCLASE	3.371	0.102
ALBITE	29.581	0.898
ANORTHITE	27.973	
LEUCITE	0.0	
KALIOPHYLITE	0.0	
NEPHELINE	0.0	
THENARDITE	0.0	
SODIUM CARBONATE	0.0	
HALITE	0.0	
SUM 60.925		

FEMIC GROUP		(-C)
ACMITE	0.0	0.0
SODIUM METASILICATE	0.0	0.0
POTASSIUM METASILICATE	0.0	0.0
DIOPSIDE	11.850	5.214
WOLLASTONITE	0.0	0.0
HYPERSTHENE	23.815	
OLIVINE	0.072	
CALCIUM ORTHOSILICATE	0.0	0.0
MAGNETITE	1.131	
HEMATITE	0.0	
ILMENITE	1.938	
SPHENE	0.0	
PEROVSKITE	0.0	
RUTILE	0.0	
APATITE	0.786	
FLUORITE	0.0	
PYRITE	0.0	
CALCITE	0.0	
CHROMITE	0.0	
SUM	39.591	

OXIDATION RATIO MOL(2FE203/2FE203+FEO) X100= 5.830

RATIO MGO/FEO IN HYPERSTHENE DIOPSIDE AND OLIVINE = 7.2497E-01

DIFFERENTIATION INDEX = 32.952

CHEMICAL ANALYSIS, H 28

SIO2	50.090
AL2O3	16.520
FE2O3	1.970
FEO	11.350
MGO	5.880
CAO	9.030
NA2O	2.640
K2O	0.510
TIO2	1.490
P2O5	0.350
MNO	0.450
ZRO2	0.0
CO2	0.0
SO3	0.0
CL2	0.0
F2	0.0
S	0.0
CR2O3	0.0
NIO	0.0
COO	0.0
BAO	0.0
SRO	0.0
LI2O	0.0
SUM	100.280
QUARTZ	0.455
NEPHELINE	0.477
KALSILITE	0.068
OLIVINE	0.002
PYROXENE	0.391
FELDSPAR	0.608

CIPW NORM
(WEIGHT PERCENT)

SALIC GROUP		
QUARTZ	0.0	0.0
CORUNDUM	0.0	(-) 4.059
ZIRCON	0.0	
ORTHOCLASE	3.017	0.119
ALBITE	22.312	0.881
ANORTHITE	31.679	
LEUCITE	0.0	
KALIOPHYLITE	0.0	
NEPHELINE	0.0	
THENARDITE	0.0	
SODIUM CARBONATE	0.0	
HALITE	0.0	
SUM 57.008		
FEMIC GROUP		(-C)
ACMITE	0.0	0.0
SODIUM METASILICATE	0.0	0.0
POTASSIUM METASILICATE	0.0	0.0
DIOPSIDE	9.225	4.059
WOLLASTONITE	0.0	0.0
HYPERSTHENE	27.422	
OLIVINE	0.179	
CALCIUM ORTHOSILICATE	0.0	0.0
MAGNETITE	2.856	
HEMATITE	0.0	
ILMENITE	2.831	
SPHENE	0.0	
PEROVSKITE	0.0	
RUTILE	0.0	
APATITE	0.764	
FLUORITE	0.0	
PYRITE	0.0	
CALCITE	0.0	
CHROMITE	0.0	
SUM	43.278	

OXIDATION RATIO MOL[2FE2O3/2FE2O3+FEO] X100= 13.511

RATIO MGO/FEO IN HYPERSTHENE DIOPSIDE AND OLIVINE = 1.1049E 00

DIFFERENTIATION INDEX = 25.329

CHEMICAL ANALYSIS, H 29

SIO2	49.050
AL2O3	12.820
FE2O3	2.760
FEO	14.500
MGO	4.550
CAO	10.060
NA2O	3.120
K2O	0.910
TIO2	2.010
P2O5	0.360
MNO	0.350
ZRO2	0.0
CO2	0.0
SO3	0.0
CL2	0.0
F2	0.0
S	0.0
CR2O3	0.0
NIO	0.0
COO	0.0
BAO	0.0
SRO	0.0
LI2O	0.0
SUM	100.490
QUARTZ	0.454
NEPHELINE	0.450
KALSILITE	0.096
OLIVINE	0.112
PYROXENE	0.344
FELDSPAR	0.544

CIPW NORM
(WEIGHT PERCENT)

SALIC GROUP		
QUARTZ	0.0	0.0
CORUNDUM	0.0	(-)10.992
ZIRCON	0.0	
ORTHOCLASE	5.383	0.170
ALBITE	26.369	0.830
ANORTHITE	18.260	
LEUCITE	0.0	
KALIOPHYLITE	0.0	
NEPHELINE	0.0	
THENARDITE	0.0	
SODIUM CARBONATE	0.0	
HALITE	0.0	
SUM 50.011		

FEMIC GROUP		(-C)
ACMITE	0.0	0.0
SODIUM METASILICATE	0.0	0.0
POTASSIUM METASILICATE	0.0	0.0
DIOPSIDE	24.982	10.992
WOLLASTONITE	0.0	0.0
HYPERSTHENE	6.595	
OLIVINE	10.300	
CALCIUM ORTHOSILICATE	0.0	0.0
MAGNETITE	4.002	
HEMATITE	0.0	
ILMENITE	3.819	
SPHENE	0.0	
PEROVSKITE	0.0	
RUTILE	0.0	
APATITE	0.786	
FLUORITE	0.0	
PYRITE	0.0	
CALCITE	0.0	
CHROMITE	0.0	
SUM	50.483	

OXIDATION RATIO MOL(2FE2O3/2FE2O3+FEO) X100= 14.626

RATIO MGO/FEO IN HYPERSTHENE DIOPSIDE AND OLIVINE = 6.9384E-01

DIFFERENTIATION INDEX = 31.752

CHEMICAL ANALYSIS, H 30

SIO2	48.590
AL203	8.850
FE203	4.380
FEO	12.430
MGO	19.980
CAO	7.310
NA2O	0.170
K2O	0.020
TIO2	1.330
P2O5	0.130
MNO	0.220
ZRO2	0.0
CO2	0.0
SO3	0.0
CL2	0.0
F2	0.0
S	0.0
CR203	0.0
NIO	0.0
COO	0.0
BAO	0.0
SRO	0.0
LI2O	0.0
SUM	103.410
QUARTZ	0.458
NEPHELINE	0.542
KALSILITE	0.0
OLIVINE	0.085
PYROXENE	0.652
FELDSPAR	0.263

CIPW NORM
(WEIGHT PERCENT)

SALIC GROUP		
QUARTZ	0.0	0.0
CORUNDUM	0.0	(-) 4.557
ZIRCON	0.0	
ORTHOCLASE	0.0	0.0
ALBITE	1.437	1.000
ANORTHITE	23.358	
LEUCITE	0.0	
KALIOPHYLITE	0.0	
NEPHELINE	0.0	
THENARDITE	0.0	
SODIUM CARBONATE	0.0	
HALITE	0.0	
SUM 24.795		
FEMIC GROUP		(-C)
ACMITE	0.0	0.0
SODIUM METASILICATE	0.0	0.0
POTASSIUM METASILICATE	0.0	0.0
DIOPSIDE	10.357	4.557
WOLLASTONITE	0.0	0.0
HYPERSTHENE	51.195	
OLIVINE	8.038	
CALCIUM ORTHOSILICATE	0.0	0.0
MAGNETITE	6.351	
HEMATITE	0.0	
ILMENITE	2.527	
SPHENE	0.0	
PEROVSKITE	0.0	
RUTILE	0.0	
APATITE	0.0	
FLUORITE	0.0	
PYRITE	0.0	
CALCITE	0.0	
CHROMITE	0.0	
SUM	78.468	

OXIDATION RATIO MOL(2FE203/2FE203+FEO) X100= 24.078

RATIO MGO/FEO IN HYPERSTHENE DIOPSIDE AND OLIVINE = 3.7916E 00

DIFFERENTIATION INDEX = 1.437

CHEMICAL ANALYSIS, H 31

SIO2	45.190
AL2O3	8.850
FE2O3	4.380
FEO	12.430
MGO	19.980
CAO	7.310
NA2O	0.170
K2O	0.020
TIO2	1.330
P2O5	0.130
MNO	0.220
ZRO2	0.0
CO2	0.0
SO3	0.0
CL2	0.0
F2	0.0
S	0.0
CR2O3	0.0
NIO	0.0
COO	0.0
BAO	0.0
SRO	0.0
LI2O	0.0
SUM	100.010
QUARTZ	0.458
NEPHELINE	0.542
KALSILITE	0.0
OLIVINE	0.184
PYROXENE	0.544
FELDSPAR	0.273

CIPW NORM
(WEIGHT PERCENT)

SALIC GROUP		
QUARTZ	0.0	0.0
CORUNDUM	0.0	(-) 4.557
ZIRCON	0.0	
ORTHOCLASE	0.0	0.0
ALBITE	1.437	1.000
ANORTHITE	23.358	
LEUCITE	0.0	
KALIOPHYLITE	0.0	
NEPHELINE	0.0	
THENARDITE	0.0	
SODIUM CARBONATE	0.0	
HALITE	0.0	
SUM 24.795		
FEMIC GROUP		(-C)
ACMITE	0.0	0.0
SODIUM METASILICATE	0.0	0.0
POTASSIUM METASILICATE	0.0	0.0
DIOPSIDE	10.357	4.557
WOLLASTONITE	0.0	0.0
HYPERSTHENE	39.104	
OLIVINE	16.728	
CALCIUM ORTHOSILICATE	0.0	0.0
MAGNETITE	6.351	
HEMATITE	0.0	
ILMENITE	2.527	
SPHENE	0.0	
PEROVSKITE	0.0	
RUTILE	0.0	
APATITE	0.0	
FLUORITE	0.0	
PYRITE	0.0	
CALCITE	0.0	
CHROMITE	0.0	
SUM	75.068	

OXIDATION RATIO MOL(2FE2O3/2FE2O3+FEO) X100= 24.078 %

RATIO MGO/FEO IN HYPERSTHENE DIOPSIDE AND OLIVINE = 3.7916E 00

DIFFERENTIATION INDEX = 1.437 %

CHEMICAL ANALYSIS, H 32

SIO2	48.110
AL2O3	5.440
FE2O3	3.170
FEO	12.600
MGO	20.240
CAO	7.710
NA2O	0.480
K2O	0.100
TIO2	1.290
P2O5	0.270
MNO	0.150
ZRO2	0.0
CO2	0.0
SO3	0.0
CL2	0.0
F2	0.0
S	0.0
CR2O3	0.0
NIO	0.070
COO	0.0
BAO	0.0
SRO	0.0
LI2O	0.0
SUM	99.630
QUARTZ	0.458
NEPHELINE	0.542
KALSILITE	0.0
OLIVINE	0.127
PYROXENE	0.692
FELDSPAR	0.181

CIPW NORM
(WEIGHT PERCENT)

SALIC GROUP		
QUARTZ	0.0	0.0
CORUNDUM	0.0	(-) 9.036
ZIRCON	0.0	
ORTHOCLASE	0.0	0.0
ALBITE	4.057	1.000
ANORTHITE	12.674	
LEUCITE	0.0	
KALIOPHYLITE	0.0	
NEPHELINE	0.0	
TI NARDITE	0.0	
SODIUM CARBONATE	0.0	
HALITE	0.0	
SUM	16.731	
FEMIC GROUP		(-C)
ACMITE	0.0	0.0
SODIUM METASILICATE	0.0	0.0
POTASSIUM METASILICATE	0.0	0.0
DIOPSIDE	20.537	9.036
WOLLASTONITE	0.0	0.0
HYPERSTHENE	43.238	
OLIVINE	11.706	
CALCIUM ORTHOSILICATE	0.0	0.0
MAGNETITE	4.596	
HEMATITE	0.0	
ILMENITE	2.451	
SPHENE	0.0	
PEROVSKITE	0.0	
RUTILE	0.0	
APATITE	0.0	
FLUORITE	0.0	
PYRITE	0.0	
CALCITE	0.0	
CHROMITE	0.0	
SUM	82.528	

OXIDATION RATIO MOL(2FE2O3/2FE2O3+FEO) X100= 18.462

RATIO MGO/FEO IN HYPERSTHENE DIOPSIDE AND OLIVINE = 3.5607E 00

DIFFERENTIATION INDEX = 4.057

CHEMICAL ANALYSIS, H 33

SIO2	46.550
AL2O3	9.740
FE2O3	16.240
FEO	0.0
MGO	17.960
CAO	9.510
NA2O	0.0
K2O	0.0
TIO2	0.0
P2O5	0.0
MNO	0.0
ZRO2	0.0
CO2	0.0
SO3	0.0
CL2	0.0
F2	0.0
S	0.0
CR2O3	0.0
NIO	0.0
COO	0.0
BAO	0.0
SRO	0.0
LI2O	0.0
SUM	100.000
QUARTZ	1.000
NEPHELINE	0.0
KALSILITE	0.0
OLIVINE	0.0
PYROXENE	0.668
FELDSPAR	0.332

CIPW NORM
(WEIGHT PERCENT)

SALIC GROUP		
QUARTZ	3.691	I.000
CORUNDUM	0.0	(-) 7.064
ZIRCON	0.0	
ORTHOCLASE	0.0	0.0
ALBITE	0.0	0.0
ANORTHITE	26.546	
LEUCITE	0.0	
KALIOPHYLITE	0.0	
NEPHELINE	0.0	
THENARDITE	0.0	
SODIUM CARBONATE	0.0	
HALITE	0.0	
SUM 30.238		
FEMIC GROUP		(-C)
ACMITE	0.0	0.0
SODIUM METASILICATE	0.0	0.0
POTASSIUM METASILICATE	0.0	0.0
DIOPSIDE	16.056	7.064
WOLLASTONITE	0.0	0.0
HYPERSTHENE	37.467	
OLIVINE	0.0	
CALCIUM ORTHOSILICATE	0.0	0.0
MAGNETITE	0.0	
HEMATITE	16.240	
ILMENITE	0.0	
SPHENE	0.0	
PEROVSKITE	0.0	
RUTILE	0.0	
APATITE	0.0	
FLUORITE	0.0	
PYRITE	0.0	
CALCITE	0.0	
CHROMITE	0.0	
SUM	69.762	

OXIDATION RATIO MOL(2FE2O3/2FE2O3+FEO) X100= 100.000

NO IRON IN HYPERSTHENE DIOPSIDE AND OLIVINE

DIFFERENTIATION INDEX = 3.691

CHEMICAL ANALYSIS. H 34

SIO2	50.740
AL2O3	4.120
FE2O3	2.450
FEO	7.400
MGO	21.810
CAO	12.060
NA2O	0.450
K2O	0.210
TIO2	0.530
P2O5	0.090
MNO	0.130
ZRO2	0.0
CO2	0.0
SO3	0.0
CL2	0.0
F2	0.0
S	0.0
CR2O3	0.0
NIO	0.0
COO	0.0
BAO	0.0
SRO	0.0
LI2O	0.0
SUM	99.990
QUARTZ	0.452
NEPHELINE	0.409
KALSILITE	0.140
OLIVINE	0.133
PYROXENE	0.724
FELDSPAR	0.143

CIPW NORM
(WEIGHT PERCENT)

SALIC GROUP		
QUARTZ	0.0	0.0
CORUNDUM	0.0	(-)17.873
ZIRCON	0.0	
ORTHOCLASE	1.242	0.246
ALBITE	3.803	0.754
ANORTHITE	8.590	
LEUCITE	0.0	
KALIOPHYLITE	0.0	
NEPHELINE	0.0	
THENARDITE	0.0	
SODIUM CARBONATE	0.0	
HALITE	0.0	
SUM 13.636		
FEMIC GROUP		(-C)
ACMITE	0.0	0.0
SODIUM METASILICATE	0.0	0.0
POTASSIUM METASILICATE	0.0	0.0
DIOPSIDE	40.620	17.873
WOLLASTONITE	0.0	0.0
HYPERSTHENE	28.402	
OLIVINE	12.685	
CALCIUM ORTHOSILICATE	0.0	0.0
MAGNETITE	3.552	
HEMATITE	0.0	
ILMENITE	1.007	
SPHENE	0.0	
PEROVSKITE	0.0	
RUTILE	0.0	
APATITE	0.0	
FLUORITE	0.0	
PYRITE	0.0	
CALCITE	0.0	
CHROMITE	0.0	
SUM	86.266	

OXIDATION RATIO MOL(2FE2O3/2FE2O3+FEO) X100= 22.957

RATIO MGO/FEO IN HYPERSTHENE DIOPSIDE AND OLIVINE = 6.5954E 00

DIFFERENTIATION INDEX = 5.045

CHEMICAL ANALYSIS, .A.H -1

SIO2	70.820				
AL2O3	13.890	CIPW NORM			
FE2O3	1.470	(WEIGHT PERCENT)			
FEO	2.480				
MGO	0.510				
CAO	3.110	SALIC GROUP			
NA2O	2.620	QUARTZ	30.696		0.389
K2O	4.400	CORUNDUM	0.0	(-)	0.872
TIO2	0.550	ZIRCON	0.0		
P2O5	0.100	ORTHOCLASE	26.026		0.330
MNO	0.040	ALBITE	22.143		0.281
ZRO2	0.0	ANORTHITE	13.097		
CO2	0.0	LEUCITE	0.0		
SO3	0.0	KALIOPHYLITE	0.0		
CL2	0.0	NEPHELINE	0.0		
F2	0.0	THENARDITE	0.0		
S	0.0	SODIUM CARBONATE	0.0		
CR2O3	0.0	HALITE	0.0		
NIO	0.0	SUM 91.961			
COO	0.0				
BAO	0.0				
SRO	0.0				
LI2O	0.0	FEMIC GROUP			(-C)
		ACMITE	0.0		0.0
SUM	99.990	SODIUM METASILICATE	0.0		0.0
		POTASSIUM METASILICATE	0.0		0.0
QUARTZ	0.660	DIOPSIDE	1.981		0.872
NEPHELINE	0.152	WOLLASTONITE	0.0		0.0
KALSILITE	0.187	HYPERSTHENE	2.772		
		OLIVINE	0.0		
		CALCIUM ORTHOSILICATE	0.0		0.0
OLIVINE	0.0	MAGNETITE	2.131		
PYROXENE	0.072	HEMATITE	0.0		
FELDSPAR	0.928	ILMENITE	1.045		
		SPHENE	0.0		
		PEROVSKITE	0.0		
		RUTILE	0.0		
		APATITE	0.0		
		FLUORITE	0.0		
		PYRITE	0.0		
		CALCITE	0.0		
		CHROMITE	0.0		
		SUM	7.930		

OXIDATION RATIO MOL(2FE2O3/2FE2O3+FEO) X100= 34.788

RATIO MGO/FEO IN HYPERSTHENE DIOPSIDE AND OLIVINE = 6.7299E-01

DIFFERENTIATION INDEX = 78.864

CHEMICAL ANALYSIS, .A.H -3

SIO2	69.930
AL2O3	12.760
FE2O3	1.610
FEO	4.490
MGO	1.840
CAO	3.440
NA2O	3.290
K2O	1.670
TIO2	0.700
P2O5	0.170
MNO	0.700
ZRO2	0.0
CO2	0.0
SO3	0.0
CL2	0.0
F2	0.0
S	0.0
CR2O3	0.0
NIO	0.0
COO	0.0
BAO	0.0
SRO	0.0
LI2O	0.0
SUM	100.600
QUARTZ	0.701
NEPHELINE	0.218
KALSILITE	0.081
OLIVINE	0.0
PYROXENE	0.191
FELDSPAR	0.809

CIPW NORM
(WEIGHT PERCENT)

SALIC GROUP		
QUARTZ	31.525	0.456
CORUNDUM	0.0	(-) 0.735
ZIRCON	0.0	
ORTHOCLASE	9.878	0.143
ALBITE	27.806	0.402
ANORTHITE	15.086	
LEUCITE	0.0	
KALIOPHYLITE	0.0	
NEPHELINE	0.0	
THENARDITE	0.0	
SODIUM CARBONATE	0.0	
HALITE	0.0	
SUM 84.295		

FEMIC GROUP		(-C)
ACMITE	0.0	0.0
SODIUM METASILICATE	0.0	0.0
POTASSIUM METASILICATE	0.0	0.0
DIOPSIDE	1.670	0.735
WOLLASTONITE	0.0	0.0
HYPERSTHENE	10.811	
OLIVINE	0.0	
CALCIUM ORTHOSILICATE	0.0	0.0
MAGNETITE	2.334	
HEMATITE	0.0	
ILMENITE	1.330	
SPHENE	0.0	
PEROVSKITE	0.0	
RUTILE	0.0	
APATITE	0.0	
FLUORITE	0.0	
PYRITE	0.0	
CALCITE	0.0	
CHROMITE	0.0	
SUM	16.145	

OXIDATION RATIO MOL(2FE2O3/2FE2O3+FEO) X100= 24.398

RATIO MGO/FEO IN HYPERSTHENE DIOPSIDE AND OLIVINE = 8.6130E-01

DIFFERENTIATION INDEX = 69.208

CHEMICAL ANALYSIS, .A.H -4

SIO2	68.740
AL203	16.380
FE203	1.750
FEO	1.250
MGO	1.120
CAO	2.090
NA20	4.490
K20	3.690
TIO2	0.380
P205	0.090
MNO	0.030
ZRO2	0.0
CO2	0.0
SO3	0.0
CL2	0.0
F2	0.0
S	0.0
CR203	0.0
NIO	0.0
COO	0.0
BAO	0.0
SRO	0.0
LI20	0.0
SUM	100.010
QUARTZ	0.598
NEPHELINE	0.251
KALSILITE	0.151
OLIVINE	0.0
PYROXENE	0.042
FELDSPAR	0.958

CIPW NORM
(WEIGHT PERCENT)

SALIC GROUP			
QUARTZ	22.253		0.271
CORUNDUM	1.182	(-)	0.0
ZIRCON	0.0		
ORTHOCLASE	21.826		0.266
ALBITE	37.948		0.463
ANORTHITE	10.375		
LEUCITE	0.0		
KALIOPHYLITE	0.0		
NEPHELINE	0.0		
THENARDITE	0.0		
SODIUM CARBONATE	0.0		
HALITE	0.0		
SUM 93.584			

FEMIC GROUP		(-C)
ACMITE	0.0	0.0
SODIUM METASILICATE	0.0	0.0
POTASSIUM METASILICATE	0.0	0.0
DIOPSIDE	0.0	0.0
WOLLASTONITE	0.0	0.0
HYPERSTHENE	3.077	
OLIVINE	0.0	
CALCIUM ORTHOSILICATE	0.0	0.0
MAGNETITE	2.537	
HEMATITE	0.0	
ILMENITE	0.722	
SPHENE	0.0	
PEROVSKITE	0.0	
RUTILE	0.0	
APATITE	0.0	
FLUORITE	0.0	
PYRITE	0.0	
CALCITE	0.0	
CHROMITE	0.0	
SUM	6.336	

OXIDATION RATIO MOL(2FE203/2FE203+FEO) X100= 55.752

RATIO MGO/FEO IN HYPERSTHENE DIOPSIDE AND OLIVINE = 1.3358E 01

DIFFERENTIATION INDEX = 82.026

CHEMICAL ANALYSIS, .A.H -5

SIO2	63.100
AL2O3	16.620
FE2O3	3.580
FEO	3.510
MGO	1.770
CAO	4.050
NA2O	2.680
K2O	3.370
TIO2	0.790
P2O5	0.450
MNO	0.070
ZRO2	0.0
CO2	0.0
SO3	0.0
CL2	0.0
F2	0.0
S	0.0
CR2O3	0.0
NIO	0.0
COO	0.0
BAO	0.0
SRO	0.0
LI2O	0.0
SUM	99.990

QUARTZ	0.642
NEPHELINE	0.186
KALSILITE	0.172
OLIVINE	0.0
PYROXENE	0.101
FELDSPAR	0.895

CIPW NORM
(WEIGHT PERCENT)

SALIC GROUP			
QUARTZ	23.390		0.355
CORUNDUM	2.147	(-)	0.0
ZIRCON	0.0		
ORTHOCLASE	19.933		0.302
ALBITE	22.650		0.343
ANORTHITE	17.462		
LEUCITE	0.0		
KALIOPHYLITE	0.0		
NEPHELINE	0.0		
THENARDITE	0.0		
SODIUM CARBONATE	0.0		
HALITE	0.0		
SUM 85.583			

FEMIC GROUP		(-C)
ACMITE	0.0	0.0
SODIUM METASILICATE	0.0	0.0
POTASSIUM METASILICATE	0.0	0.0
DIOPSIDE	0.0	0.0
WOLLASTONITE	0.0	0.0
HYPERSTHENE	6.733	
OLIVINE	0.0	
CALCIUM ORTHOSILICATE	0.0	0.0
MAGNETITE	5.191	
HEMATITE	0.0	
ILMENITE	1.501	
SPHENE	0.0	
PEROVSKITE	0.0	
RUTILE	0.0	
APATITE	0.982	
FLUORITE	0.0	
PYRITE	0.0	
CALCITE	0.0	
CHROMITE	0.0	
SUM	14.408	

OXIDATION RATIO MOL(2FE2O3/2FE2O3+FEO) X100= 47.861

RATIO MGO/FEO IN HYPERSTHENE DIOPSIDE AND OLIVINE = 2.5306E 00

DIFFERENTIATION INDEX = 65.974

CHEMICAL ANALYSIS, .A.H -6

SIO2	61.170
AL2O3	17.770
FE2O3	0.620
FEO	5.840
MGO	1.620
CAO	4.780
NA2O	3.790
K2O	2.480
TIO2	1.520
P2O5	0.310
MNO	0.100
ZRO2	0.0
CO2	0.0
SO3	0.0
CL2	0.0
F2	0.0
S	0.0
CR2O3	0.0
NIO	0.0
COO	0.0
BAO	0.0
SRO	0.0
LI2O	0.0
SUM	100.000
QUARTZ	0.578
NEPHELINE	0.285
KALSILITE	0.137
OLIVINE	0.0
PYROXENE	0.148
FELDSPAR	0.852

CIPW NORM
(WEIGHT PERCENT)

SALIC GROUP			
QUARTZ	14.200		0.233
CORUNDUM	0.805	(-)	0.0
ZIRCON	0.0		
ORTHOCLASE	14.669		0.241
ALBITE	32.032		0.526
ANORTHITE	21.909		
LEUCITE	0.0		
KALIOPHYLITE	0.0		
NEPHELINE	0.0		
THENARDITE	0.0		
SODIUM CARBONATE	0.0		
HALITE	0.0		
SUM 83.615			

FEMIC GROUP		(-C)
ACMITE	0.0	0.0
SODIUM METASILICATE	0.0	0.0
POTASSIUM METASILICATE	0.0	0.0
DIOPSIDE	0.0	0.0
WOLLASTONITE	0.0	0.0
HYPERSTHENE	11.923	
OLIVINE	0.0	
CALCIUM ORTHOSILICATE	0.0	0.0
MAGNETITE	0.899	
HEMATITE	0.0	
ILMENITE	2.888	
SPHENE	0.0	
PEROVSKITE	0.0	
RUTILE	0.0	
APATITE	0.677	
FLUORITE	0.0	
PYRITE	0.0	
CALCITE	0.0	
CHROMITE	0.0	
SUM	16.387	

OXIDATION RATIO MOL(2FE2O3/2FE2O3+FEO) X100= 8.721

RATIO MGO/FEO IN HYPERSTHENE DIOPSIDE AND OLIVINE = 6.7902E-01

DIFFERENTIATION INDEX = 60.901